



DOCTORAL DISSERTATION

The role of atmospheric moisture transport in major drought episodes

Milica Stojanovic

2018

Universidade de Vigo

International Doctoral School

Milica Stojanovic

DOCTORAL DISSERTATION

**The role of atmospheric moisture transport in major drought
episodes**

Supervised by:

Luis Gimeno Presa, PhD

Anita Rodrigues de Moraes Drumond, PhD

2018

Universidade de Vigo

International Doctoral School

Luis Gimeno Presa y Anita Rodrigues de Moraes Drumond

DECLARES that the present work, entitled “*The role of atmospheric moisture transport in major drought episodes*”, submitted by Milica Stojanovic to obtain the title of Doctor, was carried out under his/her supervision in the PhD programme “Applied Physics”.

Ourense, 28 October 2018

The supervisor(s),

Dr. Luis Gimeno Presa

Dra. Anita Rodrigues de Moraes Drumond

Agradecimientos / Acknowledgements

Este trabajo no se habría podido realizar sin colaboración de muchas personas, a quienes agradezco su ayuda y apoyo a lo largo de estos años de estudio.

Quedo especialmente agradecida del Dr. Luis Gimeno y la Dra. Anita Drumond por darme oportunidad de comenzar el Doctorado bajo de su tutoría, por sus orientaciones, confianza en mí y ayuda incondicional durante todo el periodo de doctorado.

Me gustaría agradecer a la Dra. Raquel Nieto, por estar siempre disponible para resolver cualquier duda y por sus consejos.

Agradezco a todos mis compañeros, con quienes he compartido cada día en la Universidad: Rogert, Marta, Zeinab, Danica, Dejanira, Iago, Lucía, Juliet, Elena, Jorge, Elham, Mojtaba, Moha, y Aleksandar. Por su ayuda en muchas ocasiones, por las conversaciones y los buenos momentos de amistad que hemos tenido. Han sido unos compañeros muy especiales que han hecho mi estancia inolvidable.

Doy gracias a Gloria, Antonio, Jorge e Iván, mis vecinos, por el cariño y la atención que me brindaron durante mi estancia en España.

No podría dejar de dar las gracias a mis padres y mi hermano, quienes me han apoyado siempre que lo he necesitado y que sin duda han contribuido a que haya llegado hasta aquí. A mis primos, amigos y a todas las personas que han estado a mi lado.

Este trabajo se ha ejecutado gracias al financiamiento recibido de la Comisión Europea a través del proyecto Erasmus Mundus Green-Tech-WB: Tecnologías inteligentes y verdes para sociedades innovadoras y sostenibles en los Balcanes Occidentales (551984-EM-1-2014-1-ES-ERA Mundus -EMA2).

CONTENTS

ABSTRACT	XIII
LIST OF FIGURES	XV
LIST OF TABLES	XVI
LIST OF ACRONYMS	XVII
1. INTRODUCTION	1
1.1 Background on Drought	1
1.2 The hydrological cycle: moisture transport.....	4
1.3 Linkage between moisture transport and drought	7
1.4 Scope of this thesis	8
2. OBJECTIVES	10
3. METHODOLOGY	12
3.1 Overview of drought indices and the identification and characterization of drought episodes.....	12
3.1.1 The Standardised Precipitation Evapotranspiration Index (SPEI).....	15
3.1.2 Identification and characterization of meteorological drought episodes	16
3.2 Methods for establishing source-sink relationships: The Lagrangian approach.....	17
3.2.1 Brief review of the Lagrangian approach FLEXPART	20
3.2.2 Identification of moisture sources and sinks using FLEXPART	21
3.3 Statistical analyses	23

3.4 Datasets	23
3.5 Defining the regions of interest for drought analysis.....	25
4. COLLECTION OF PUBLICATIONS	27
5. SUMMARY, CONCLUSIONS, AND FURTHER RESEARCH	107
APPENDIX A: SUPPLEMENTARY MATERIAL.....	113
REFERENCES.....	116

RESUMEN

La sequía es un fenómeno natural y complejo que ocurre cuando la disponibilidad de agua está por debajo de los niveles normales durante un largo período y no puede satisfacer la demanda existente. Se diferencia de otros peligros naturales en muchos aspectos, especialmente porque es difícil definir cuándo empieza una sequía o cuando termina, por tanto, es complicado definir y cuantificar su impacto. Los efectos de la sequía se acumulan lentamente durante un período sustancial de tiempo y se extienden a un área geográfica más grande. Esto puede afectar a todos los componentes del ciclo hidrológico. Debido a su desarrollo a largo plazo, el carácter progresivo de sus impactos y los límites espaciales difusos, la sequía es uno de los peligros naturales más complejos para identificar, analizar, monitorear y controlar.

Como resultado del cambio climático, principalmente como consecuencia de la disminución de la precipitación, pero también debido al aumento de la evaporación, se proyecta que las sequías serán más intensas y severas en el futuro. Por lo tanto, es importante examinar los mecanismos responsables de los déficits en la precipitación, o los mecanismos relacionados con cualquier reducción en la evaporación de la fuente que causa la sequía en ciertas regiones. El transporte de humedad de las fuentes a los continentes circundantes representa una parte importante del ciclo hidrológico, y sus déficits o cambios pueden jugar un papel crucial en la justificación de las sequías. Teniendo en cuenta este importante papel que tiene el transporte de humedad en el desarrollo de las sequías, comprender la relación entre las fuentes y los sumideros de humedad en el ciclo hidrológico es uno de los retos más importantes al cual actualmente se enfrenta la comunidad científica.

Para comprender la relación entre el transporte de humedad y las sequías, se investigó en este trabajo el transporte de humedad y sus anomalías durante los episodios de sequía meteorológica más severos en todo mundo durante el periodo comprendido

entre 1980 y 2015, ambos incluidos. El estudio está motivado por los recientes cambios observados, que tienen una importante implicación en la rama atmosférica del ciclo hidrológico.

El análisis inicial se centró en una perspectiva regional, y luego la investigación se expandió hacia una escala global. Los resultados y explicaciones más detalladas para cada región analizada se pueden encontrar en los manuscritos.

El *corpus* de esta tesis consiste en un total de tres artículos publicados y uno de ellos enviado (y en estos momentos bajo revisión) a revistas especializadas incluidas en la lista de *Journal Citation Reports* (JCR).

El conjunto de resultados obtenidos como parte del trabajo de investigación desarrollado durante la realización de esta tesis doctoral se organizó de la siguiente manera: la Sección 1 describe el trasfondo de la investigación, incluyendo un breve resumen de la definición y caracterización de las sequías, el transporte de humedad en la atmósfera y la importancia de esta investigación. También se revisaron algunos hallazgos sobre el vínculo entre el transporte de humedad y las sequías que se han reportado en otros estudios. La Sección 2 proporciona una visión general de las tareas de investigación realizadas a lo largo del periodo de la tesis. En la Sección 3 se incluye una revisión detallada de los métodos y técnicas de investigación utilizada para la identificación de episodios de sequía y fuentes y sumideros de humedad. La Sección 4 incluye el compendio de los cuatro manuscritos que conforman la parte esencial de este documento. Finalmente, la Sección 5 presenta un resumen y las principales conclusiones extraídas de la investigación realizada. También se presentan recomendaciones para trabajos futuros y limitaciones del estudio.

El estudio puede considerarse como una aplicación del método Lagrangiano para la estimación del transporte de humedad, ampliamente utilizado por el Laboratorio de Física Ambiental (EPhysLab, por sus siglas en inglés) en estudios de sequías, ya que varios trabajos relacionados con el cambio climático han señalado cambios importantes

en la estructura de fenómenos climáticos extremos en muchas regiones, y estos cambios pueden estar relacionados con variaciones en las fuentes de humedad.

El análisis inicial de las anomalías en el transporte de humedad durante los episodios de sequías meteorológicas más severos que ocurrieron en el período 1980-2015 se enfocó primero en una perspectiva regional, estudiando la cuenca del río Danubio (DRB, por sus siglas en inglés), luego los análisis se extendieron a escala continental, analizando las sequías ocurridas en la región de Europa Central (CEU, por sus siglas en inglés) y Mediterránea (MED, por sus siglas en inglés). Finalmente, se estudiaron las 27 regiones de referencia (RRs) especificadas en el 5° Reporte de Evaluación (AR5, por sus siglas en inglés) del Panel Intergubernamental sobre el Cambio Climático (IPCC), elevando así la investigación a una escala global.

Además del análisis de anomalías en el transporte de humedad, un análisis del aporte de humedad desde la cuenca del Mar Mediterráneo durante los episodios de sequías meteorológicas detectadas en CEU, proporcionó una perspectiva climatológica de cómo el déficit de transporte de humedad desde el Mar Mediterráneo es asociable a la aparición de episodios de sequía en CEU. Se realizó, además, un estudio de los indicadores de la sequía sobre CEU en base a su severidad, duración, intensidad y valor máximo.

En primer lugar, para todos los trabajos realizados, se identificaron los episodios de sequía que ocurrieron en las regiones de interés a través del Índice Estandarizado de Precipitación-Evapotranspiración (SPEI, por sus siglas en inglés). El SPEI se basa en el procedimiento original utilizado para calcular el Índice de Precipitación Estandarizado (SPI, por sus siglas en inglés), pero en lugar de centrarse únicamente en la precipitación, se basa en el balance hidroclimático (precipitación menos evapotranspiración) calculado en diferentes escalas temporales. La escala de tiempo en la que se acumula el déficit de agua es extremadamente importante y separa funcionalmente la sequía meteorológica, agrícola e hidrológica. Se considera que la sequía meteorológica es la causa principal de sequías, mientras que los otros tipos describen los efectos secundarios de un déficit de

precipitación a largo plazo en medidas como la humedad del suelo, los flujos de los ríos y/o los sectores económicos. En comparación con otros índices de sequía ampliamente utilizados, la ventaja crucial de SPEI es que combina características multiescalares con la posibilidad de incluir la temperatura en el análisis de sequía, esto permite representar de manera más realista las condiciones de sequía bajo la influencia de calentamiento climático. Diversos estudios indican que durante el siglo pasado el planeta ha experimentado un aumento en la temperatura global, y que esto continuará en las próximas décadas. Se ha encontrado, además, que las temperaturas más altas afectan la severidad de las sequías. A la luz de este hecho, el uso de índices de sequía que consideran los datos de temperatura parece ser mejor que utilizar índices sin información de datos de temperatura para identificar la influencia de la sequía en diferentes sistemas ecológicos, hidrológicos y agrícolas en escenarios de cambio climático. El SPEI que corresponde al balance hidroclimático de un mes (SPEI-1), fue elegido para la identificación de episodios de sequía en diversas regiones del planeta a lo largo de este estudio, ya que esta escala de tiempo está estrechamente relacionada con las sequías meteorológicas, sobre las cuales fue enfocado esta investigación. Indicadores de sequía como la severidad (el valor absoluto de la suma de todos los valores de SPEI durante el episodio), la duración (el número de meses entre el primer y el último mes del episodio), la intensidad (severidad dividida por la duración) y el valor máximo durante el episodio también fueron calculados.

Usando el SPEI es posible comparar diferentes características del episodio detectado con el propósito de conocer la evolución espacial y temporal sobre las regiones continentales a estudiar. Los análisis separados de las sequías meteorológicas en tres regiones de Europa (DRB, CEU y MED) revelaron el impacto del episodio de sequía meteorológica de 2003 en todo el continente, proporcionando información sobre la extensión espacial de las áreas afectadas, así como su evolución temporal e impactos. De los 50 episodios de sequía ocurridos en la cuenca del río Danubio durante 1980-2014, el episodio que ocurrió de febrero a agosto de 2003 fue el más severo durante la temporada

de primavera/verano. Extendiendo los análisis hacia una escala continental, los episodios de sequías meteorológicas más severos durante el período 1980-2015 fueron de febrero a junio de 2003 para Europa Central, y de mayo a agosto de 2003 para la región Mediterránea. El inicio de la sequía se verificó primero en Europa Central y en la cuenca del río Danubio (febrero de 2003) y parece que las condiciones de sequía se extendieron hacia el sur, ocurriendo el fin de la sequía en la región del Mediterráneo. Al comparar los indicadores de sequía asociados con cada una de las tres regiones, los resultados muestran que el episodio fue más severo y más largo en la cuenca del río Danubio.

Respecto al valor máximo, el SPEI-1 alcanzó los valores mayores en la región del Danubio y el Mediterráneo. En concreto, para el episodio de febrero a junio de 2003 en Europa Central se alcanzó un valor de -1.86 , que pertenece a la categoría severa; mientras que sobre la cuenca del río Danubio el episodio de febrero a agosto de 2003 mostró un valor máximo de -2.09 , y en la región Mediterránea de mayo a agosto de 2003 marcó un valor de -2.71 , ambos incluidos en la categoría de sequía extrema. Para las tres regiones, junio de 2003 fue el mes en que el SPEI-1 alcanzó su valor máximo.

Después de la identificación de los episodios de sequía y su caracterización, se realizó un análisis del transporte de humedad y sus anomalías desde sus fuentes de humedad, tanto oceánicas como continentales, para verificar la posible influencia de estos cambios en la ocurrencia de los episodios de sequías meteorológica más severos identificado en el período de 1980 a 2015.

Los análisis del transporte de humedad se realizaron utilizando un método Lagrangiano que utilizando las salidas globales del modelo de dispersión de partículas FLEXPART (FLEXible PARTicle dispersion model) permite rastrear parcelas de masa de aire con el objetivo de localizar aquellas regiones donde las partículas reciben o pierden humedad. Este modelo y metodología ha aplicado en varios estudios para estimar los cambios de humedad a lo largo de trayectorias e identificar fuentes de humedad y sumideros en diferentes regiones del mundo; sin embargo, no se había realizado un análisis sistemático de las sequías meteorológicas y el transporte de humedad asociado.

Para rastrear los cambios en la humedad atmosférica a lo largo de las trayectorias, el modelo FLEXPART se implementa con datos de reanálisis ERA-Interim del Centro Europeo para Previsiones Meteorológicas a Plazo Medio (ECMWF, por sus siglas en inglés), que tienen una resolución horizontal de 1° en 61 niveles verticales de 0.1 a 1000 hPa, estando disponible en un intervalo de tiempo de 6 horas.

Así pues, en este trabajo, como se ha comentado, se ha utilizado las salidas de un experimento con el modelo FLEXPART ejecutado en escala global, en el que la atmósfera se divide homogéneamente en una gran cantidad de partículas de aire (aproximadamente 2 millones) a las que se le supone de masa constante. Las partículas se advectaron utilizando un campo de viento tridimensional (3D) y para cada parcela de aire se registraron, entre otras variables, la humedad específica (q) y la posición de las partículas (latitud, longitud y altitud). Con estas variables es posible calcular a lo largo de las trayectorias el cambio de la humedad específica, y finalmente obtener el balance de agua dulce E-P (evaporación (E) menos precipitación (P)) en una columna atmosférica dada, con el propósito de encontrar dónde las partículas ganan humedad (la evaporación neta supera a la precipitación) o dónde la pierden (la precipitación neta es mayor que la evaporación).

La principal ventaja del método Lagrangiano es que permite el seguimiento de las masas de aire (partículas) hacia atrás y hacia adelante en el tiempo. Así, el análisis hacia atrás en el tiempo, permite la identificación de las principales fuentes de humedad para una región de estudio específica (llamada sumidero). Las fuentes de humedad son aquellas regiones en las que $(E - P)$ es positivo ($E - P > 0$), lo que indica que las partículas de aire obtienen humedad en lugar de perderla a lo largo de sus trayectorias hacia el sumidero. Por el contrario, al usar el análisis hacia adelante en el tiempo, las regiones en las que prevaleció la pérdida de humedad, valores negativos de E-P ($E - P < 0$) se consideran sumideros de humedad. En este trabajo, se aplicó un umbral definido mediante la imposición de un percentil a los promedios anuales de los valores positivos de $E - P$ para delimitar la extensión espacial de cada fuente de humedad. Una vez

delimitadas las fuentes de humedad se dividieron en oceánicas y continentales. Se utilizó el percentil 90 para definir las fuentes de humedad en el estudio de cuenca del río Danubio (DRB), y el percentil 95 para las fuentes en los estudios para Europa Central (CEU), región Mediterránea (MED) y para las 27 RRs del IPCC. Una vez que se definieron las principales fuentes de humedad para cada región de estudio, las masas de aire sobre cada una de las fuentes se rastrearon hacia adelante en el tiempo con el propósito de calcular las anomalías en la contribución de humedad sobre las regiones analizadas durante los episodios de sequías meteorológicas más severas.

Como se indicó anteriormente a través del análisis hacia atrás en el tiempo se identificó la ubicación de las principales fuentes climatológicas de humedad. Los resultados mostraron que las principales fuentes de humedad que aparecen como fuentes comunes para tres regiones de Europa (DRB, CEU, MED) son: el Mar Mediterráneo, el Océano Atlántico Norte, el Mar Caspio, el Mar Negro y las fuentes de humedad terrestre que rodean a cada una de las tres regiones. Una vez que se identificaron las fuentes, se realizó un análisis hacia adelante en el tiempo desde cada una de estas fuentes identificadas para determinar la contribución de humedad que saliendo de esas fuentes genera precipitación sobre los sumideros (DRB, CEU, MED). Así, los resultados climatológicos a escala anual revelaron que la contribución de humedad para las tres regiones provino principalmente del Mar Mediterráneo y de las fuentes de humedad terrestres que rodean la región junto con las propias regiones. En este análisis se detectó una clara variabilidad estacional, mostrándose que durante los meses de verano las principales fuentes de humedad fueron las propias regiones y sus fuentes de humedad terrestres, mientras que durante los meses de invierno es el Mar Mediterráneo el que ejerce el papel de fuente de humedad principal.

El análisis de las anomalías de transporte de humedad desde cada fuente mostró que durante el episodio de sequía de 2003 para Europa Central y la región Mediterránea la reducción más intensa en la contribución de humedad se debió a un descenso en el transporte desde el Mar Mediterráneo, mientras que para la cuenca del río Danubio,

además del Mar Mediterráneo, el descenso de humedad precedente desde la región circundante terrestre fue también importante.

Además, durante estos episodios de sequía se observaron anomalías en otras variables, como un claro aumento de la subsidencia, un aumento de la evapotranspiración y una reducción en la precipitación. Los mapas de las anomalías mensuales del flujo de humedad integrado en la vertical (VIMF, por sus siglas en inglés) y su divergencia durante 2003 también se calcularon como información complementaria para evaluar las condiciones dinámicas en la atmósfera. Los mapas mostraron que una circulación anticiclónica anómala localizada en Europa inhibió el transporte de humedad desde el mar Mediterráneo hacia las regiones analizadas.

Teniendo en cuenta la importancia que tiene el Mar Mediterráneo para la región europea como fuente de humedad para su precipitación, se examinaron las variaciones en esta contribución durante todos los episodios de sequías meteorológicas (detectadas mediante SPEI-1) en la región de Europa Central (CEU). La detección de las sequías que ocurrieron en CEU se realizó para el período de 1980 a 2015, encontrando 51 episodios de sequía, 29 episodios tuvieron inicio en invierno (octubre-marzo) y 22 episodios en verano (abril-septiembre). Para estos eventos se calculó el aporte de humedad desde el Mar Mediterráneo y sus anomalías. Luego, se realizó un análisis de regresión lineal para verificar los posibles vínculos entre las variaciones en la contribución de humedad del Mar Mediterráneo y los diferentes indicadores de sequía para los episodios seleccionados. Se aplicó la prueba t-Student con un nivel de significación del 95% para confirmar la importancia estadística del coeficiente de regresión. Los resultados mostraron la existencia de una relación significativa entre la severidad, la duración, el valor máximo (durante la temporada de invierno) y las anomalías del aporte de humedad desde el Mar Mediterráneo. Esto implica que los episodios que fueron más largos, más severos y que tenían un valor máximo mayor (durante la temporada de invierno), podrían asociarse con la intensificación en el déficit de contribución de humedad desde Mar Mediterráneo durante los episodios de sequía analizados. El mayor valor de coeficiente de

determinación (R^2) se encontró entre la severidad del episodio de sequía y las anomalías de humedad desde el Mar Mediterráneo, lo que significa que la variabilidad en la severidad de los episodios de sequía podría estar modulada por las variaciones en la contribución de humedad desde el Mar Mediterráneo. Sin embargo, no se determinó una relación lineal entre la intensidad y el valor máximo (el período completo, la temporada de verano) de los episodios de sequía y las anomalías del aporte de humedad del mar Mediterráneo.

Finalmente, y pasando a un análisis sistemático de los procesos de transporte de humedad que desencadenan episodios de sequía a escala global, se realiza un estudio en profundidad para cada una de las 27 RRs del IPCC, proporcionando un catálogo en el cual se identificaron los episodios de sequía en todo el mundo para 1980-2015, y se analizan algunos de los componentes del balance de humedad durante los episodios de sequías meteorológicas más severos en cada una de las regiones. El catálogo estará disponible gratuitamente en el enlace <http://ephyslab.uvigo.es/seth/> y contiene elementos que pueden ser útiles para interpretar el clima actual relacionado con las variaciones en el transporte de humedad. El propósito de este catálogo descrito en esta tesis es contribuir a una comprensión más profunda de las sequías en las regiones climáticas definidas en el IPCC y consideradas como referencia, en particular en los estudios del cambio climático, por parte de la comunidad científica.

ABSTRACT

Droughts are projected to become more intense and severe in the future as the result of increased evaporation and reduced precipitation. The transport of moisture from the sources to surrounding continents represents an important part of the hydrological cycle and deficits or changes in transport can play a crucial role in determining drought. Because of the important role of moisture transport in the development of drought, understanding the connections between the sources and sinks of moisture in the hydrological cycle is one of the most important challenges that humanity is currently facing. This thesis can be considered as an innovative application of the Lagrangian method used by the Environmental Physics Laboratory group (EPhysLab) in studies of droughts, since several studies concerning climate change have reported important changes in the structure of extreme weather phenomena in many regions and these changes may be related to variations in sources of moisture.

In order to investigate the relationship between moisture transport and drought, anomalies in moisture transport during the most severe meteorological drought episodes around the world were investigated. The initial drought analysis was regional and focused on the Danube River Basin (DRB); the analysis was then extended to a continental scale, analysing Central Europe (CEU) and the Mediterranean region (MED). Finally, the 27 Reference Regions (RRs) specified in the 5th Assessment Report (AR5) of the Intergovernmental Panel on Climate Change (IPCC) were studied in order to expand the investigation to a global scale.

First, the multiscalar Standardised Precipitation Evapotranspiration Index (SPEI) was used to identify drought episodes that occurred in the analysed regions. Separate analysis of meteorological droughts over three regions in Europe (DRB, CEU, MED) revealed the impact of the 2003 meteorological drought episodes across the continent. After

identifying the drought episodes, anomalies in moisture transport were analysed in order to determine whether there were variations in moisture transport from the sources to the analysed regions during severe episodes of drought. Anomalies in moisture transport were investigated with the Lagrangian FLEXible PARTicle (FLEXPART) dispersion model, which was used to track air masses and locate regions where the particles gain or lose humidity.

The climatological moisture sources for the analysed regions were characterized using Lagrangian backward tracking and the main moisture sources that serve as common sources for all three regions were determined to be the Mediterranean Sea, the North Atlantic Ocean, the Caspian Sea, the Black Sea, and terrestrial moisture sources surrounding the area. Once these sources were identified, forward tracking was performed in order to analyse anomalies in moisture contribution to the analysed areas during the most severe episodes of drought. This study determined that a decrease in moisture contribution and precipitation occurred along with the appearance of the 2003 drought episodes, while the episodes ended when primarily Mediterranean Sea (MDS), began to provide moisture to all three regions in Europe.

Besides the analysis of anomalies in the transport of moisture, an analysis of moisture contribution from the MDS during meteorological drought episodes over CEU provided a climatological perspective of how moisture transport from a major moisture source may be linked to drought indicators and the occurrence of drought episodes.

Finally, by analysing anomalous moisture transport and drought episodes in the 27 IPCC RRs, this study provides an in-depth systematic analysis of the moisture transport processes that trigger drought episodes at the global scale, which is necessary for understanding the driving factors of extreme weather events.

LIST OF FIGURES

Figure 1. Sequence of drought occurrence and impacts of each drought type. Figure from WMO, [2006] and Zargar et al. [2011].	3
Figure 2. Schematic representation of hydrological cycle from [Mdee, et al. 2018].	5
Figure 3. Geographical location of the Danube River Basin (DRB), delimited by the black contour line. The shades of green illustrate the elevation of the region in meters. Figure from Stojanovic et al. [2017].	25
Figure 4. Set of 27 Continental Reference Regions (RRs) based on the geographical domains defined in the AR5 by the IPCC. The definition of each RR acronym can be found at: http://www.ipcc-data.org/guidelines/pages/ar5_regions.html	26

LIST OF TABLES

Table 1. A brief description of the strengths and limitations of the most common drought indices. Adapted from Zargar et al. [2011].	13
Table 2. Drought categories based on the SPEI values, according to the categories given by McKee et al. [1993], which were applied to the SPI.	17
Table 3. Summary of the advantages and limitations of methods used to investigate sources and sinks of moisture. Adapted from Gimeno et al. [2012].	18
Table 4. Collection of datasets, sources, period, and spatial resolution.....	25
Table 5. List of articles within this thesis.....	29
Table 6. A brief description of the journals listed in Table 5 and a summary of their quality indices.....	30

LIST OF ACRONYMS

The following abbreviations are used in this manuscript:

AR5	5th Assessment Report
CEU	Central Europe
CRU	Climate Research Unit
DRB	Danube River Basin
E	Evaporation
EA	East Atlantic
ECMWF	European Center for Medium-Range Weather Forecast
ENSO	El Niño Southern Oscillation
EPhysLAB	Environmental Physics Laboratory
FLEXPART	FLEXible PARTicle dispersion model
GFC	Global Forecast System
GLEAM	Global Land Evaporation Amsterdam Model
IPCC	Intergovernmental Panel on Climate Change
MDS	Mediterranean Sea
MED	Mediterranean
NAO	North Atlantic Oscillation
OAFLEX	Objectively Analyzed air-sea Fluxes
PDSI	Palmer Drought Severity Index
PET	Potential Evapotranspiration
PRE	Precipitation
RDI	Reconnaissance Drought Index
RRs	Reference Regions
SDI	Streamflow Drought Index
SPEI	Standardised Precipitation Evapotranspiration Index
SPI	Standardised Precipitation Index

SSA	South-eastern South America
SSI	Standardised Streamflow Index
TS	Time-Series
VIMF	Vertically Integrated Moisture Flux
WRF	Weather Research and Forecasting Model

1

Introduction

1.1 Background on Drought

Drought is a complex phenomenon that occurs when water availability is significantly less than regular levels for an extended period and the available water cannot satisfy the demand [Redmond, 2002; Mishra and Singh, 2010; Dai, 2010; Trenberth et al., 2014]. Drought differs from other natural disasters in many ways; for example, it is particularly difficult to define when a drought begins and when a drought is finished [McKee et al., 1993; Wilhite, 2000; Lloyd-Hughes, 2013; Leelaruban and Padmanabhan, 2017; Wang et al., 2018]. Thus, it is difficult to define and quantify the impacts of droughts [Wilhite and Glantz, 1985; Wilhite et al., 2014; Otkin et al., 2017; Naumann et al., 2018]. The effects of droughts accumulate slowly, over a substantial amount of time, and expand over large geographical regions, which can influence all stages of the atmosphere water cycle [Tallaksen et al., 2004; Ionita et al., 2017]. Because they take a long time to develop, droughts are one of the most complicated natural disasters to identify, examine, monitor, and manage.

Due to the complexity of droughts and the numerous sectors affected by them, four major categories of drought have been defined: meteorological, agricultural, hydrological, and socioeconomic droughts [Wilhite and Glantz, 1985; WMO, 2006; Mishra and Singh, 2010]. A meteorological drought is defined as below average amounts of precipitation for a certain period of time and may be combined with an increased

potential evapotranspiration [Hanel et al., 2018] It represents the principal cause of droughts, and the three other types of drought occur as a result of meteorological drought [Khalili et al., 2011, Spinoni et al., 2016; Wang et al., 2017]. Agricultural drought signifies a period with decreasing soil moisture, which affects agricultural through water stress in plants, reduced biomass, and reduced crop yield. Hydrological drought refers to a period when the water content of groundwater aquifers, reservoirs, streams, and lakes is below average. Socioeconomic drought occurs when the demand for an economic good surpasses its supply because of insufficient water supply during that time [Wilhite and Glantz, 1985; Heim, 2002; WMO, 2006; Smathkin and Schipper, 2008; Nalbantis and Tsakiris, 2009; Mishra and Singh, 2010; Lloyd-Hughes, 2013]. Therefore, efficient monitoring of meteorological droughts is necessary in order to provide early warnings and perform risk management in areas with water resources and agricultural production. The relationship between the four types of drought and their impacts are summarised in Figure 1.

Although a precipitation deficit represents the principal cause of drought, other causes can also generate or increase droughts, such as more intense but less frequent precipitation or extremely high temperatures [Dai et al., 2010; Vicente-Serrano et al., 2012]. These climate extremes can lead to major natural disasters and socioeconomic impacts, particularly when they appear concurrently [Zscheischler and Seneviratne. 2017; Hao et al., 2013; Mazdiyasi and AghaKouchak, 2015; Zscheischler et al., 2018; Naumann et al., 2018].

The progressive intensification and expansion of climate extremes is considered to be among the most serious effects of climate change on society according to the IPCC [IPCC, 2013, 2014a]. Some studies have observed that droughts have already become unusually frequent and serious worldwide, such as in the Mediterranean region [Hoerling et al., 2012; Vicente-Serrano et al., 2014; Naumann et al., 2015], West Africa [Sheffield et al., 2012; Dai, 2013; Masih et al., 2014], and China [Qian et al., 2011; Yu et al., 2013; Wang et al., 2017].

As for the European continent, global warming is projected to significantly modify the water balance across Europe, which will lead to temperature increases, changes in spatio-temporal allocation of precipitation, and ultimately more serious and permanent droughts [Beniston et al., 2007; Briffa et al., 2009; Spinoni et al., 2013; Forzieri et al., 2014; Spinoni et al., 2015a; Gudmundsson and Seneviratne, 2015]. Heat waves are also predicted to rise in frequency and duration, which climate models principally attribute to land–atmosphere coupling [Seneviratne et al., 2006; Fischer et al., 2007; Miralles et al., 2014; Donat et al., 2017; Miralles et al., 2018].

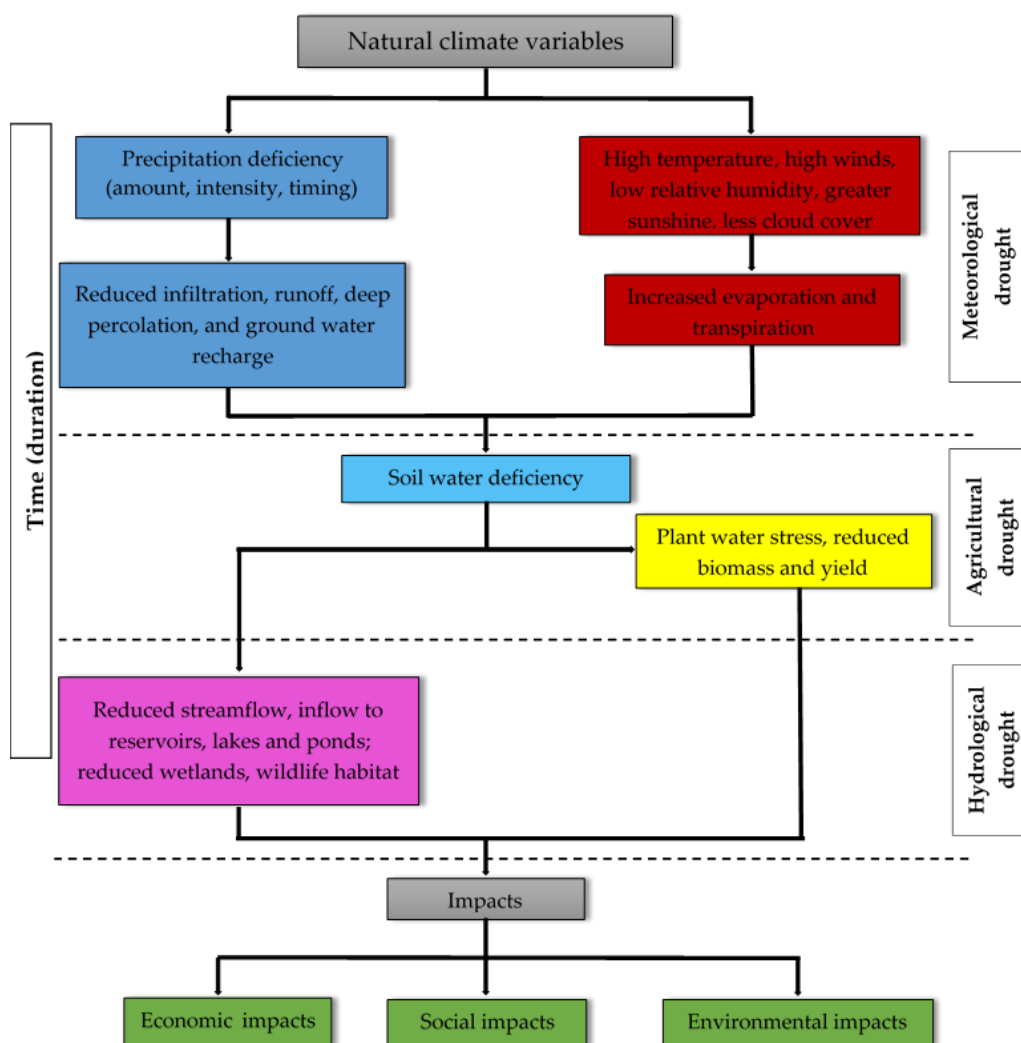


Figure 1. Sequence of drought occurrence and impacts of each drought type. Figure from WMO, [2006] and Zargar et al. [2011].

As a consequence of global warming during recent decades, the climate has generally exhibited drier conditions [Trenberth et al., 2014] and more occurrences of extreme weather events [Trenberth, 2011; Dai, 2013; Cook et al., 2015; Trenberth et al., 2015]. Based on these trends, there have been various global assessments of future drought conditions [e.g., Burke and Brown, 2008; Sheffield and Wood, 2008; Touma et al., 2015; Zhao and Dai, 2016]. Developing estimates of accessible water resources, identifying their spatio-temporal distribution, and investigating drought risks are necessary in order to preserve the world's economic, social, and environmental systems [Wilhite, 1993; Hao et al., 2017].

1.2 The hydrological cycle: moisture transport

Water plays a crucial role in all aspects of life on Earth and because of that, scientists are very interested in understanding the basic components of the water cycle [Kuchment, 2004]. Because of the nature of the water cycle and its potential to cause significant social impacts, such as drought, understanding the water cycle and its fluctuations over time is the most significant topic of current research into climate variability and assessment of climate change. The hydrological cycle represents the continuous movement of water from one reservoir to another by the physical processes of evaporation, condensation, precipitation, infiltration, surface swelling, and underground flow [WMO, 2012]. Schematic representation of the hydrological cycle is represent on Figure 2.

The basic principle of the hydrological cycle is that evaporation from one area contributes to moisture transport and precipitation, either within the same area or in other areas. The movement of water begins with the evaporation of water, principally from the

surface of the ocean. In oceanic regions, evaporation generally exceeds precipitation. Every year, 90% of this evaporated water is returned to the oceans by way of precipitation and the remaining 10% is transported over landmasses, where precipitation exceeds evapotranspiration [Oki, 2005]. As a result of precipitation, surface water enters rivers and other water bodies that return to the ocean, ending the cycle [Lehner et al., 2006; Gimeno et al., 2010; Gimeno et al., 2012].

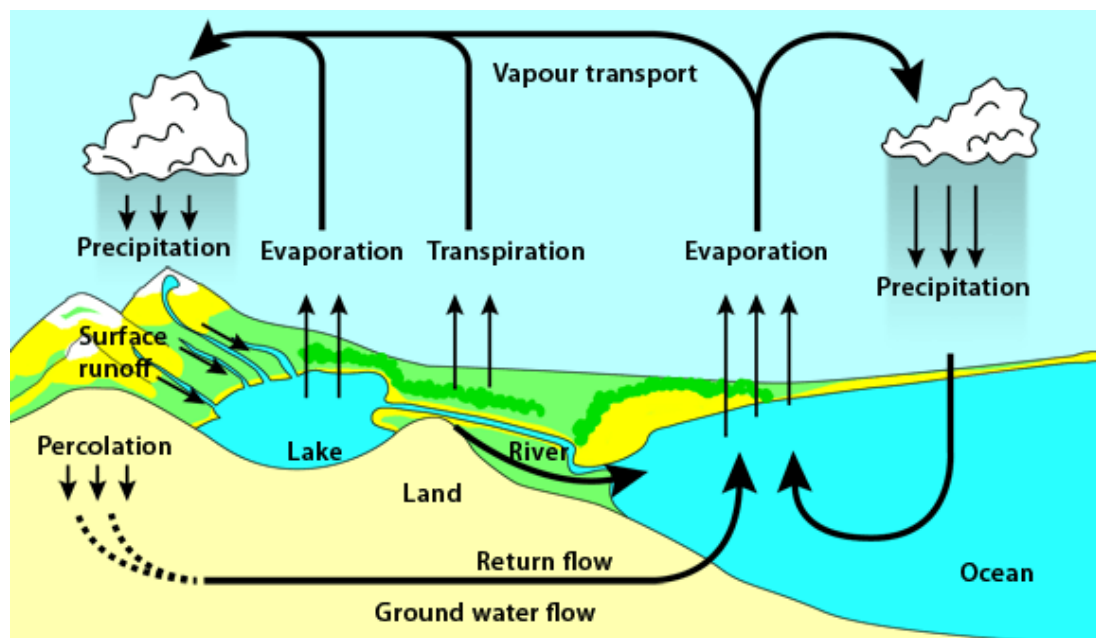


Figure 2. Schematic representation of hydrological cycle from [Mdee, et al. 2018].

In the hydrological cycle, atmospheric moisture transport is considered to be the link between ocean evaporation and continental precipitation. Understanding moisture transport is crucial in order to diagnose and predict precipitation variability. Thus, there is a great concern among scientists to comprehend the sources of moisture and precipitation that occur over a specified area because variations in the precipitation of one area could be related to variations in the sources of moisture [Trenberth and Guillemot, 1998; Bisselink et al., 2008; García-Ruiz et al., 2011; Gómez-Hernández et al., 2013]. In fact,

investigating the impact of moisture sources' contributions to the occurrence of extreme weather events like droughts and floods has become a significant research area.

Many previous studies have focused on investigating moisture sources for diverse areas of the world using different methodologies. In North America, Domínguez et al., [2009] determined the moisture sources responsible for the onset of the North American monsoon and Duran-Quesada et al. [2010] did similar work for Central America. Both studies highlighted the importance of the moisture that comes from the Caribbean Sea and also indicated that moisture from the equatorial Pacific area is important for Central America. Studies have also attempted to identify the sources of moisture that affect South America; a study by Drumond et al. [2008] investigated the origin of moisture reaching the central region of Brazil and the La Plata River basin and demonstrated the significance of the Atlantic Ocean on moisture in South America.

In Africa, Nieto et al. [2006] determined that moisture recycling accounted for a significant fraction of the moisture sources in the Sahel during 2000-2004, with the North Atlantic, Mediterranean Sea, and Red Sea also serving as moisture sources. Dirmeyer et al. [2009] also found that terrestrial sources of moisture prevailed in this area. In Asia, Drumond et al. [2011] determined the main summertime moisture sources in China, as well as the variations to these sources in both wetter and drier years.

There have also been studies that have identified moisture sources in Iceland, Greenland, and the Antarctic. Nieto et al. [2007] determined the regions where moisture is gained or lost in Iceland, which obtains its moisture from the Baltic Sea and the western North Atlantic. Sodemann et al. [2008] identified the sources in Greenland during the winter season in order to determine the origin of precipitation in this region and Nieto et al. [2010] did the same for the Antarctic.

With regard to the Mediterranean region, Mariotti et al. [2002] performed a budget analysis that analysed contributions to the freshwater flux in the Mediterranean Sea (MDS), which included atmospheric and river release inputs, and demonstrated the importance of the MDS to the region. Schicker et al. [2010] and Nieto et al. [2010] both

tracked air masses from the Mediterranean Basin in order to determine the principal sources of moisture; likewise, they calculated the contribution of moisture from this area to the surrounding terrestrial areas. Drumond et al. [2011] continued the study of Nieto et al. [2010] by focusing on variations in moisture sources during each season in the diverse Mediterranean areas. Long-term variations in the principal moisture sources of the Mediterranean Basin were explored by Gómez-Hernández et al. [2013] over eight areas.

Previous studies have also highlighted the role of the MDS as a moisture source for various areas in Europe. For instance, Sodemann and Zubler [2010] examined variations in the moisture sources in the Alps during the period from 1995–2002 and determined that the Mediterranean moisture source has the main influence on the Southern Alps. Bisselink and Dolman [2008] analysed the contribution of the different moisture sources over Europe and showed that during the winter, moisture mainly comes from the MDS, while local evaporation plays a significant role during the summer.

Moisture sources have also been studied on a global scale; for example, Gimeno et al. [2013] investigated the land and oceanic sources of continental precipitation. They reported that the Indian Ocean and South Pacific were the main moisture sources in Australia and Indonesia, the MDS was the main source in Europe and North Africa, and the Northern Atlantic Ocean was the main source in Mexico, the South American continent, and portions of Eurasia.

1.3 Linkage between moisture transport and drought

The transport of water vapour is an important factor in drought development. According to Liu et al. [2017], the occurrence of meteorological drought may be associated with the variability of water vapour transport. Variations in moisture transport over an area are usually related to a precipitation deficit and, in some cases, to the occurrence of drought [Liu et al., 2017]. Many studies have determined that the drought in several European regions has become more serious in the last few decades

[Tsiourtis, 2001; Levison and Waple, 2004; Luterbacher et al., 2004; Lelieveld et al., 2012; Trigo et al., 2013; IPCC, 2014; Ionita et al., 2015; Spinoni et al., 2016; Naumann et al., 2018]. Despite a number of studies investigating moisture transport, relatively few studies have examined the contribution of moisture sources and moisture transport to drought episodes at the regional scale [e.g. Drumond et al., 2016; Drumond et al., 2017; Salah et al., 2018]. Drumond et al. [2016] investigated the role of moisture transport using a case study from the 2012 drought events that occurred over the Central United States. Drumond et al. [2017] determined when hydrological drought conditions, observed in the climatological moisture sinks of the MDS throughout the winter and summer seasons, were related to variations in moisture transport. Salah et al. [2018] identified the principal moisture sources in the Fertile Crescent throughout the wet season (October to May) and examined the variations in principal sources during severe drought episodes that occurred between 1998–2000 and 2007–2009.

At the global scale, no studies have reported an in-depth analysis of the contributions of moisture sources and moisture transport processes to drought episodes. Considering this, the need for a better understanding of the role of moisture transport on the meteorological droughts is evident. In order to address the numerous challenges linked to the water cycle, the transport of atmospheric moisture and the relationship between sources and sinks must be specifically investigated because of the role of moisture transport in the onset of drought [Hoeling and Kumar, 2003; Lehner et al., 2006; Seneviratne et al., 2006; Gimeno et al., 2012; Gimeno et al., 2013; Trigo et al., 2013; Gimeno et al., 2016].

1.4 Scope of this thesis

Climate change is the main danger facing the 21st century and one of the primary causes of rising temperatures and extreme weather events [Lehner et al., 2006; Trenberth

et al., 2015]. As the result of global warming, the frequency and severity of droughts are expected to increase in the future, mostly due to reduced precipitation and increased evaporation [Dai, 2010; Sheffield and Wood, 2008; Trenberth, 2011; Seneviratne et al., 2012; Sheffield et al., 2012; Trenberth et al., 2014]. As stated above, drought is a natural disaster that occurs around the world [Vicente-Serrano et al., 2014; Naumann et al., 2015; Sori et al., 2017; Wang et al., 2017; Salah et al., 2018]. Previous studies have indicated that a lack of moisture transport plays a main role in the occurrence of drought [Redmond, 2002; Seneviratne et al., 2006; Trigo et al., 2013; Gimeno et al., 2016].

Although regional investigations focused on different types of droughts have suggested that droughts are strongly affected by anomalies in a region's moisture sources, a systematic analysis of meteorological droughts, which are the principal type of drought, and associated moisture transport is still missing. Therefore, a global assessment of these processes is necessary in order to determine drought mechanisms and develop early warning systems, monitoring, and forecasting.

2

Objectives

The main objective of this thesis was to study **anomalies in moisture contribution during the most severe meteorological drought episodes around the world** using a Lagrangian method. In order to better comprehend the mechanisms evolved in moisture transport and droughts, the analysis method was first applied to a regional case study of the 2003 meteorological drought episode in the DRB. The analysis of this episode was extended to a continental scale by analysing its evolution over the CEU and MED regions. An analysis of moisture contribution from the MDS during meteorological drought episodes over CEU provided a climatological perspective of how moisture transport from a major moisture source may be associated with the occurrence of drought events. Finally, a drought analysis of the 27 RRs identified in the AR5 of the IPCC provided some information about how moisture transport anomalies may vary during significant meteorological drought episodes in different areas of the globe.

In order to achieve this principal aim, a set of specific objectives was applied in three of the four articles that make up the body of this thesis: “Moisture Transport Anomalies over the Danube River Basin during Two Drought Events: A Lagrangian Analysis,” published in the journal *Atmosphere* in 2017; “Anomalies in Moisture Supply during the 2003 Drought Event in Europe: A Lagrangian Analysis,” published in the journal *Water* in 2018; and “Bridging Anomalous Moisture Transport and Drought Episodes in the IPCC Reference Regions,” submitted to the journal *Bulletin of the American Meteorological Society (BAMS)* in 2018. The specific objectives are:

- 1) Identification and characterization of the meteorological drought episodes in order to select the most severe episode;
- 2) Climatological determination of the principal sources of moisture to the drought region;
- 3) Analysis of moisture transport anomalies from the identified sources to the region during the most severe meteorological drought episode.

A fourth objective was also achieved in the article “Variations in Moisture Supply from the Mediterranean Sea during Meteorological Drought Episodes over Central Europe”, published in the journal *Atmosphere* in 2018:

- 4) Analysis of the relationship between anomalies in moisture contribution from the MDS and different drought indicators (duration, severity, intensity, and peak values).

3

Methodology

3.1 Overview of drought indices and the identification and characterization of drought episodes

Drought indices are used to detect, monitor, and evaluate drought events. Because of the difficulties in predicting the development of droughts, considerable effort has been put towards developing a drought indicator that is appropriate for drought monitoring. Diverse indices have been developed for drought quantification, investigation, and monitoring, such as the Palmer Drought Severity Index (PDSI) [Palmer, 1965; Wells et al., 2004], Deciles [Gibbs and Maher, 1967], Reconnaissance Drought Index (RDI) [Tsakiris and Vangelis, 2005], Streamflow Drought Index (SDI), [Nalbantis and Tsakiris, 2009], Standardised Precipitation Index (SPI) [McKee et al., 1993; WMO, 2012], Standardised Precipitation Evapotranspiration Index (SPEI) [Vicente-Serrano et al., 2010a; Vicente-Serrano et al., 2010b]. Table 1 provides a brief description of these drought indices, as well as their main advantages and limitations.

The majority of studies linked to drought analysis have employed the PDSI based on the soil-water balance equation [Palmer, 1965; Wells et al., 2004] and the SPI based on precipitation probabilistic approach [McKee et al., 1993; WMO, 2012], respectively. The SPEI was created to overcome the deficiencies of the PDSI and the SPI and was based on a climatic water balance: precipitation (PRE) minus potential evapotranspiration (PET) [Vicente-Serrano et al., 2010a; Vicente-Serrano et al., 2010b]. The crucial

advantage of the SPEI over other widely used indices is that it combines multiscalar characteristics and temperature data in the analysis of drought, which can help to determine drought conditions in the analysed area more accurately. The SPEI is discussed in detail in Section 3.1.1.

Table 1. A brief description of the strengths and limitations of the most common drought indices. Adapted from Zargar et al. [2011].

Indices	Brief description	Advantages	Limitations
Deciles [Gibbs and Maher, 1997]	The cumulative frequency distribution of precipitation is obtained by ranking long-term monthly rainfall data from highest to lowest and dividing the data into 10 equal parts (deciles).	Provides precise statistical measure of precipitation; The methodology is simple and the computation is easy.	Requires long-term precipitation data; Does not consider evaporation; Does not provide information about when the drought begins or when it ends.
Palmer Drought Severity Index (PDSI) [Palmer, 1965]	Estimates relative dryness using precipitation and temperature data.	Widely used to detect agricultural drought; Considers impact of evapotranspiration on drought;	Treats all forms of precipitation as rain; Uses a fixed time scale.
Reconnaissance Drought Index (RDI) [Tsakiris and Vangelis, 2005]	Based on the ratio between precipitation and potential evapotranspiration.	Successfully relates agricultural and hydrological drought.	Cannot identify all drought episodes that may occur throughout the year using data from short time periods; Calculation of potential evapotranspiration requires access to many parameters and data collected over long time periods.

<p>Standardised Precipitation Index (SPI) [McKee et al., 1993]</p>	<p>Each component of a water resources system responds to scarcity in precipitation over diverse time scales.</p>	<p>Can be computed on diverse time scales; Less complex than PDSI; Use of diverse time scales enables the effects of precipitation deficiency on diverse water components (groundwater, soil moisture) to be estimated.</p>	<p>Requires a long time series of precipitation data; Only accounts for precipitation and does not consider temperature data.</p>
<p>Standardised Precipitation Evapotranspiration Index (SPEI) [Vicente-Serrano et al., 2010a]</p>	<p>Considers both precipitation and potential evapotranspiration based on climatic water balance calculated at diverse time scales.</p>	<p>Combines multiscale aspects of the SPI with information about evapotranspiration, making it more useful for climate change studies; Considers the influence of temperature on drought assessment; Can identify different types of drought.</p>	<p>Requires baseline data collected over a long period to precisely calculate the index; Has more data requirements than the precipitation SPI.</p>
<p>Streamflow Drought Index (SDI) [Nalbantis and Tsakiris, 2009]</p>	<p>Utilizes monthly streamflow data to create a drought index.</p>	<p>Easy to calculate using the SPI program; Can examine different time scales; Result precision increases streamflow data sets from longer time periods.</p>	<p>Only considers streamflow data for drought monitoring without exploring other influences.</p>

3.1.1 The Standardised Precipitation Evapotranspiration Index (SPEI)

The SPEI proposed by Vicente-Serrano et al. [2010a] is based on the procedure originally used to compute the SPI, which only focuses on precipitation; however, the SPEI considers the climatic water balance that may be computed at diverse time scales. The difference, Di , between PRE and PET for the time period i is computed according to equation 1 and difference values are calculated over different time scales.

$$Di = PREi - PETi \quad (1)$$

To calculate the SPEI over diverse time scales, a log-logistic probability distribution was used to transform the calculated values to standardised units, in which dry conditions are represented by negative values and wet conditions are represented by positive values. Other probability distributions could be applied, but the SPEI designers recommended the log-logistic probability distribution because it offers better SPEI time series results than other distributions [Vicente-Serrano et al., 2010a].

The SPEI is a broadly used drought index because it has a multiscalar nature and considers both precipitation and temperature [Vicente-Serrano et al., 2012; Vicente-Serrano et al., 2015; WMO, 2012]. The fundamental advantage of the SPEI is that it includes temperature data, which is an important factor in the study of droughts and climate change. Diverse studies have reported that global temperatures increased throughout the previous century [Jones and Moberg, 2003], and are expected to continue increasing over the coming decades [Solomon et al., 2007]. Higher temperatures have been found to affect the severity of droughts [Beniston, et al., 2007; Dai, 2010; Dai, 2013; Potop, 2011; Sheffield and Wood, 2008; Vicente-Serrano et al., 2010a]. In light of this fact, drought indices that consider temperature data are likely to be more accurate than indices without temperature information for identifying the influence of drought on

diverse ecological, hydrological, and agricultural systems during climate changes scenarios.

Several studies have used the SPEI to study drought variability and the influences of climate change on drought conditions. From the time that it was created [Vicente-Serrano et al., 2010a], the SPEI has been broadly used in Americas [Sordo-Ward et al., 2017; Meza, 2013; Vicente-Serrano et al., 2016; Drumond et al., 2016; Sori et al., 2018], Asia [Homdee et al., 2016; Mathbout et al., 2018; Wang et al., 2018; Gao et al., 2017; Ayantobo et al., 2017; Tan et al., 2015], Africa [Salah et al., 2018; Sori et al., 2017; Hassanein et al., 2013], and Europe [Potop et al., 2013; Spinoni et al., 2015a; Paulo et al., 2012].

The One Month Standardised Precipitation Evapotranspiration Index (SPEI-1) was used in the studies of meteorological drought episodes and moisture transport reported in this thesis.

3.1.2 Identification and characterization of meteorological drought episodes

The SPEI-1, which represents the water balance of one month, was used to identify drought episodes because of its approximate association with meteorological droughts [Liu et al., 2017]. Drought episodes were identified according to the criteria of McKee et al. [1993]: an episode begins when the SPEI-1 is less than or equal to zero (included) and ends when the SPEI-1 returns to a positive value (greater than zero, not included).

When a drought episode was identified, the peak values, duration, severity, and intensity of episode were calculated [Spinoni et al., 2014; 2018; Tan et al., 2015]. The peak values of a drought episode are the largest magnitude negative recorded values. Duration indicates the number of months between the first and last months of the drought, severity is calculated as the sum of all SPEI values (absolute values) during the episode, and intensity is computed as the ratio between severity and duration. The peak values recorded throughout the episodes may be grouped into four categories based on the

categories that McKee et al. [1993] developed for the SPI (given in Table 2); the same categories can be used because the computations of the SPI and the SPEI are similar.

Table 2. Drought categories based on the SPEI values, according to the categories given by McKee et al. [1993], which were applied to the SPI.

SPEI Values	Drought Category
$-1.0 < \text{SPEI} < 0$	Mild
$-1.5 < \text{SPEI} \leq -1.0$	Moderate
$-2.0 < \text{SPEI} \leq -1.5$	Severe
$\text{SPEI} \leq -2.0$	Extreme

3.2 Methods for establishing source-sink relationships: The Lagrangian approach

Three principal methods are used to investigate source and sink relationships: “analytical and box models”, “physical water vapour tracers,” and “numerical water vapour tracers” (Lagrangian and Eulerian methods) [Gimeno et al., 2012]. A summary of the main strengths and limitations of each method is given in Table 3.

Box models do not offer information about the origin of moisture nor the physical processes that take place inside the box itself and physical tracers rely on the strength of isotopic signals. Lagrangian and Eulerian techniques use numerical water vapour tracers. Eulerian techniques are widely applied to identify reference points in a gridded system that monitors pressure, temperature, and the chemical concentration of tracers in time. The Lagrangian model is based on following the path of water-containing particles in order to provide information about the trajectories of air masses and the variability of their physical properties, such as moisture content.

Unlike Lagrangian models, which track the trajectories of air masses to establish source-sink connections, Eulerian models concentrate on identifying the locations through which moisture travels as time passes. The Eulerian methodology is widely used because of its simplicity; however, it is not easy to establish the connection between the precipitation that occurs in a certain area and the regions where moisture evaporated. Although each of the aforementioned methodologies offer useful information about moisture transport, the Lagrangian method was selected for use in this thesis because it can be used to establish the connection between moisture sources and sinks.

The Lagrangian method used in this thesis is described in detail in Stohl and James (2004, 2005); it is based on the FLEXPART dispersion model with input from the Era-Interim dataset. The Lagrangian method has been successfully used to analyse moisture trajectories in a long list of articles studying the sources and sinks of moisture in diverse areas around the world: e.g., Nieto et al., 2006; Stohl et al., 2008; Drumond et al., 2008; Schicker et al., 2010; Gimeno et al., 2010; Duran-Quesada et al., 2010; Sorí et al., 2017; Vázquez et al., 2017; Salah et al., 2018; Ciric et al., 2018. A brief explanation of the FLEXPART dispersion model is presented in Section 3.2.1 and the approach used to identify sources and sinks of moisture is discussed in Section 3.2.2.

Table 3. Summary of the advantages and limitations of methods used to investigate sources and sinks of moisture. Adapted from Gimeno et al. [2012].

Type	Strengths	Limitations	References
Analytical and box models	Simple, requires few parameters.	Do not provide information about the processes that happen inside the box.	Budyko [1974]; Brubaker et al. [1993]; Dominguez et al. [2006].

Physical water vapour tracers	Transport processes used in models may be validated by comparing the modeled and measured isotopic composition of precipitation and adding isotopic processes to the analytical and numerical models.	The use of models makes the method very sensitive to mistakes in the simulation of the hydrological cycle; Using isotopes relies on the strength of the isotopic signal; Validation depends on the availability of data.	Gat and Carmil [1970]; Salati et al. [1979]; Rozanski et al. [1982]; Coplen et al. [2008].
Numerical water vapour tracers	Eulerian Able to quantify inflows and outflows of moisture in a region; Computes the moisture transport between predetermined source and sink regions.	Not capable of geographical identification of moisture sources.	Starr and Peixoto [1958]; Peixoto and Oort [1992]; Joussaume et al. [1984]; Koster et al. [1986]; Bosilovich and Schubert [2002].
	Lagrangian Provides moisture source diagnostics; Determines the areas where particles gain and lose moisture by using the particles information; Suitable for establishing the connection between moisture sources and sinks using backward and forward tracking.	Unable to make separate calculations of evaporation and precipitation; thus, results should always be considered as the balance between them; Results are highly dependent on the input data quality.	D'Abreton and Tyson [1995]; Wernli [1997]; Massacand et al. [1998]; Dirmeyer and Brubaker [1999]; Brubaker et al. [2001]; Dirmeyer and Brubaker [2006]; Stohl and James [2004, 2005].

3.2.1 Brief review of the Lagrangian approach FLEXPART

The FLEXPART dispersion model was initially created for computing the long-term and mesoscale dispersion of air pollutants from point sources [Stohl et al., 1998]. Since its creation, FLEXPART has undergone various changes and progressed as a tool for atmospheric transport modeling and analysis. Applications of FLEXPART have diversified from air pollution analysis to other analyses where the transport of moisture plays an important role: e.g., interchange between the stratosphere and troposphere [Stohl et al., 2003] or the global water cycle [Stohl et al., 2004; Gimeno et al., 2012]. The model can be fed with reanalysis datasets from the European Centre for Medium-Range Weather Forecast (ECMWF) or the Global Forecast System (GFS), or outputs from other models such as the Weather Research and Forecasting Model (WRF).

The FLEXPART model requires three-dimensional fields and two-dimensional fields as input data. The three-dimensional fields include temperature data, horizontal and vertical wind components, and data for specific humidity; the two-dimensional fields include total cloud cover, large-scale and convective precipitation, the surface pressure, horizontal wind components at 10 meters, temperature at 2 meters, sensible heat flux, dew point temperature, solar radiation, topography, east/west and north/south surface stress, land sea mask and the sub-grid standard deviation of topography [Stohl et al., 2005]. The model also includes parametrizations for the atmospheric boundary layer, the turbulent movements for the wind components, wind fluctuations [Hanna, 1982], mesoscale velocity fluctuations, and convective transport [Emanuel and Zivkovic-Rothman, 1999]. More information about the FLEXPART dispersion model can be found in Stohl et al. [2004, 2005] and on the following webpage: <https://www.flexpart.eu/>.

3.2.2 Identification of moisture sources and sinks using FLEXPART

The Lagrangian datasets analysed in this thesis are from a global simulation run by the FLEXPART v9.0 model [Stohl and James, 2004, 2005], which was fed with the global ERA-Interim reanalysis data set for the period 1980-2015 [Dee et al., 2011]. The input ERA-Interim dataset is available at 1° horizontal resolution on 61 vertical levels from 0.1 to 1000 hPa.

The method operates by homogeneously dividing the atmosphere into a great number of air particles (approximately 2.0 million in this simulation), while maintaining a constant mass. The particles were transported by a 3-dimensional wind field and the specific humidity (q), latitude, longitude, and altitude of the particles were recorded for each air parcel.

Fluctuations in the specific humidity (q) of the particles can be calculated at 6 h intervals using equation 2:

$$(e - p) = m \left(\frac{dq}{dt} \right) \quad (2)$$

where m represents the mass of a particle and $(e - p)$ represents evaporation minus precipitation, which is the freshwater flux of the particle. Changes in specific humidity allow us to detect which particles lose moisture through precipitation (p) or gain moisture through evaporation (e) as they travel across their trajectory. By summing the freshwater flux $(e - p)$ of all particles present in the atmospheric column over an area A , the total freshwater flux $(E - P)$ can be determined using equation 3:

$$(E - P) \approx \frac{\sum_{k=1}^k (e-p)}{A} \quad (3)$$

where E represents the total evaporation, P represents the total precipitation, and K represents the number of particles over the area A .

By tracking $(E - P)$ backward and forward in time, it is possible to determine whether the atmosphere in a region gains $(E - P > 0)$ or loses $(E - P < 0)$ moisture. Backward tracking identifies the principal moisture sources of the given region. Those

areas where $(E - P > 0)$ indicate that air particles obtain humidity rather than lose it along their trajectories towards the target region, were treated as moisture sources. Conversely, using forward tracking, areas where $(E - P < 0)$ correspond to areas where particle's predominantly lose moisture and thus are treated as moisture sinks. In the analyses discussed in this thesis, the tracking period was restricted to 10 days because this is the mean water vapour lifetime in the atmosphere [Numaguti, 1999].

Once the target area has been defined, the area's climatological sources of moisture were identified through backward tracking and a percentile criterion [Drumond et al., 2014]. A percentile criterion of the positive magnitudes of the annual average of $(E - P)$ was applied to determine a threshold that would limit the spatial girth of moisture sources. The 90th percentile was used for the DRB and the 95th percentile was used for the CEU, the MED, and the 27 IPCC RRs; these percentiles define the areas where air masses were likely to take up a large quantity of moisture as they travel towards the target area. In different words, the 90th percentile criterion will indicate the 10% of grid points with the highest positive $(E - P)$ values on the map (in the case of 95th percentile, 5%).

Forward tracking air masses travelling from identified moisture sources to the target area allows their moisture contribution and variations during a drought episode to be determined. The monthly anomaly was calculated as the difference between the monthly mean and the corresponding monthly climatological mean.

The role of the IPCC RRs as sources of moisture for remote continental areas was also examined. The identification of remote moisture sinks is based on tracking air masses over the RRs forward in time. The 99th percentile considering only the negative values of the annual mean of $(E - P)$, defined the spatial extent of these sinks and identified regions where air masses lose a great amount of moisture as they travel away from the RRs.

3.3 Statistical analyses

The Pearson correlation coefficient was used to analyse the relationship between anomalies in contribution of moisture from the sources to the analysed regions and the SPEI-1 time series in order to detect linear variability [Wilks, 2011]. The Pearson correlation coefficient may be considered as a measure of the strength and direction of the linear connection between two variables. The statistical significance of the correlation coefficient was evaluated using a Student's t-test at a 99.9% significance level for the DRB, CEU, and MED regions and at 99% significance level for the 27 IPCC RRs.

A linear regression analysis was also performed to determine when fluctuations in the moisture supply from the MDS to CEU could influence different drought indicators (severity, duration, intensity, peak value). The coefficient of determination (R^2), which represents the percentage of the variance in the dependent variable that is predictable with respect to the independent variable, was used to define the representativeness of this study. The result of the regression analysis was corroborated by the Spearman's rank correlation coefficient [Zar, 1972]. The Spearman's rank correlation coefficient is a non-parametric measure of degree of dependence between two variables and it is based on the ranked values. The significance of the coefficient of regression was evaluated using the Student's t-test at a 95% significance level.

3.4 Datasets

The analyses were performed for the period from 1980 to 2014 for the DRB and from 1980 to 2015 for CEU, the MED, and the 27 IPCC RRs.

The SPEI was calculated using the monthly PRE and PET datasets (original resolution = 0.5 degrees) from the Climate Research Unit (CRU) Time-Series (TS) Version 3.23 and 3.24.01 [Harris et al., 2014], which are available at: <http://www.cru.uea.ac.uk/data>.

The Lagrangian model (FLEXPART) was run using the ERA-Interim reanalysis datasets (original resolution = 1 degree) from the European Centre for Medium-Range Weather Forecasts (ECMWF) [Dee et al., 2011]. The dataset is available at: <https://www.ecmwf.int/en/forecasts/datasets/archive-datasets/reanalysis-datasets/era-interim>.

Additional datasets were used for different purposes throughout this work:

- Datasets of the vertical integral of the eastward and northward water vapour flux from the ERA-Interim reanalysis were used to calculate the Vertically Integrated Moisture Flux (VIMF) and its divergence. The VIMF values identify moisture transport in the atmosphere, as well as moisture sources and sinks, by assessing the divergence of this flux from a Eulerian perspective [Trenberth and Guillemot, 1998; Gimeno et al., 2010].
- Evaporation rate data was obtained from the Objectively Analysed air-sea Heat Fluxes (OAFLUX) for maritime regions [Yu et al., 2008] (<http://oaflux.whoi.edu/>) and from the Global Land Evaporation Amsterdam Model (GLEAM v3.1a) for terrestrial areas [Miralles et al., 2011] (<https://www.gleam.eu/>).
- Vertical velocity (ω , Ω) at 500 hPa, obtained from ERA-Interim, was used to diagnose the stability of the atmosphere [e.g. Salah et al., 2018].

Table 4 lists the sources, periods, and spatial resolution of the datasets used in this study. All datasets were interpolated to a 1 degree resolution (in some cases, they were originally available in a different resolution) before proceeding with the calculations.

Table 4. Collection of datasets, sources, period, and spatial resolution.

Datasets	Sources	Periods	Original horizontal spatial resolution (long x lat)
Precipitation	CRU 3.23; 3.2401	1980-2014; 1980-2015	0.5° x 0.5°
Potential Evapotranspiration	CRU 3.23; 3.2401	1980-2014; 1980-2015	0.5° x 0.5°
Vertical integral of eastward and northward water vapour flux	ERA-Interim	1980-2014; 1980-2015	1° x 1°
Ocean evaporation	OAFflux	1980-2015	1° x 1°
Land evaporation	GLEAM 3.1a	1980-2015	0.25° x 0.25°
Vertical velocity (omega) at 500 hPa	ERA-Interim	1980-2014; 1980-2015	1° x 1°

3.5 Defining the regions of interest for drought analysis

The area of the DRB was defined using data from the HydroSHEDS project, which provides hydrological data and maps based on shuttle elevation derivatives at multiple levels [Lehner and Grill, 2013]; the HydroSHEDS project is accessible online at: <https://hydrosheds.cr.usgs.gov/dataavail.php>. The DRB area is shown in Figure 3.

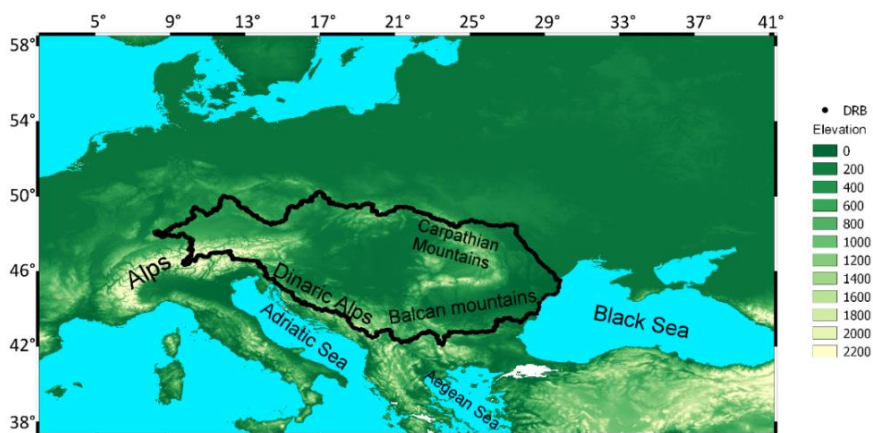


Figure 3. Geographical location of the Danube River Basin (DRB), delimited by the black contour line. The shades of green illustrate the elevation of the region in meters. Figure from Stojanovic et al. [2017].

In the following articles the spatial domains of the areas of interest are based on the RRs defined in the AR5 of the IPCC (http://www.ipcc-data.org/guidelines/pages/ar5_regions.html) and areas in CEU and the MED have been investigated in two articles. The 27 RRs considered for the elaboration of the drought catalogue are shown in Figure 4. These regions represent different climatic regimes (homogeneous climate) and were selected based on projected changes in extreme temperature and precipitation [IPCC, 2014a; IPCC, 2014b].

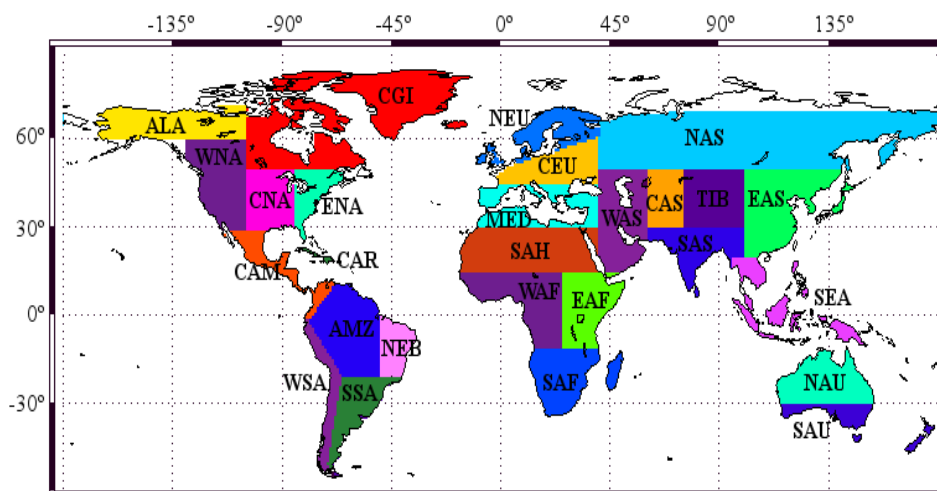


Figure 4. Set of 27 Continental Reference Regions (RRs) based on the geographical domains defined in the AR5 by the IPCC. The definition of each RR acronym can be found at: http://www.ipcc-data.org/guidelines/pages/ar5_regions.html.

4

Collection of publications

In the future, drought is projected to increase in severity and frequency as a consequence of reduced precipitation and increased evaporation. Hence, it is important to study mechanisms responsible for reduced precipitation and mechanisms associated with changes in evaporation from moisture sources that trigger drought in different areas. Understanding the connection between moisture sources and sinks is crucial because of the important role that they have in extreme weather events. Anomalies in the transport of atmospheric moisture represent one of the processes that requires further investigation.

This thesis provides an analysis of anomalies in moisture transport during severe meteorological drought episodes around the world using a Lagrangian method. From regional to a global scale, drought analysis was initially conducted for the Danube River Basin (DRB), subsequently extended to Europe (CEU and MED RRs), and finally extended across the whole world through drought analysis of the 27 RRs defined by the IPCC.

This chapter summarises the principal results of this research and the four scientific articles published in specialized journals. Table 5 provides basic information about each paper (title, authors, year of publication, and journal) and Table 6 briefly describes each journal.

The first article, **“Moisture Transport Anomalies over the Danube River Basin during Two Drought Events: A Lagrangian Analysis”** by M. Stojanovic, A. Drumond,

R. Nieto and L. Gimeno, was published in the journal *Atmosphere* in 2017. In this article, a Lagrangian analysis of anomalies in moisture transport during two drought episodes (1989/1990 and 2003) located over the DRB region was provided on a regional scale.

The second article in this thesis, “**Anomalies in Moisture Supply during the 2003 Drought Event in Europe: A Lagrangian Analysis**” by M. Stojanovic, A. Drumond, R. Nieto and L. Gimeno, was published in the journal *Water* in 2018. This article used the same methodology as the preceding article to study anomalous conditions during most severe meteorological drought episodes, specifically to investigate the expansion of the 2003 drought conditions across Europe. The study considered two spatial domains, CEU and the MED, in order to investigate anomalies in moisture contribution over CEU and the MED during the 2003 meteorological drought episode, which was the most severe episode registered over either region during 1980-2015.

The third article in this thesis, “**Variations in Moisture Supply from the Mediterranean Sea during Meteorological Drought Episodes over Central Europe**” by M. Stojanovic, A. Drumond, R. Nieto and L. Gimeno, was published in the journal *Atmosphere* in 2018. This article aimed to determine some connection between diverse drought indicators and variations in moisture transport from the MDS, which was identified as the principal moisture source for the surrounding continental areas in previous articles.

Finally, the article entitled “**Bridging Anomalous Moisture Transport and Drought Episodes in the IPCC Reference Regions**” by A. Drumond, M. Stojanovic, R. Nieto, S.M. Vicente-Serrano and L. Gimeno was submitted to the journal *Bulletin of the American Meteorological Society (BAMS)* in 2018. This article analyses anomalies in atmospheric moisture transport during the most severe meteorological drought episodes recorded in each one of the 27 RRs defined in the AR5 of the IPCC. This article applies the same methodology of drought analysis at a global scale. Because this article analyses a large number of regions, the outcomes will be presented to the scientific community in an online catalogue. In order to illustrate the content that will be provided in the catalogue,

this article analyses the South-eastern South America (SSA) region in detail. The results for all the regions will be provided here: <http://ephyslab.uvigo.es/seth/>.

Table 5. List of articles within this thesis.

Title	Authors	Year	Journal
“Moisture Transport Anomalies over the Danube River Basin during Two Drought Events: A Lagrangian Analysis”	Milica Stojanovic, Anita Drumond, Raquel Nieto and Luis Gimeno	2017	<i>Atmosphere</i>
“Anomalies in Moisture Supply during the 2003 Drought Event in Europe: A Lagrangian Analysis”	Milica Stojanovic, Anita Drumond, Raquel Nieto and Luis Gimeno	2018	<i>Water</i>
“Variations in Moisture Supply from the Mediterranean Sea during Meteorological Drought Episodes over Central Europe”	Milica Stojanovic, Anita Drumond, Raquel Nieto and Luis Gimeno	2018	<i>Atmosphere</i>
“Bridging Anomalous Moisture Transport and Drought Episodes in the IPCC Reference Regions”	Anita Drumond, Milica Stojanovic, Raquel Nieto, Sergio Martin Vicente-Serrano and Luis Gimeno	2018	<i>Bulletin of the American Meteorological Society (BAMS)</i> <i>In review</i>

Table 6. A brief description of the journals listed in Table 5 and a summary of their quality indices.

Journal	Description	Quality indices (October 2018)
<i>Atmosphere</i>	<i>Atmosphere</i> is an international, peer-reviewed, open access journal of scientific research related to the atmosphere and it is published online monthly by MDPI.	<ul style="list-style-type: none"> - Current Impact Factor: 1.704 - 5-year Impact Factor: 1.775 - 1,047 articles published so far - Total cites in 2017: 561 - Cite Score 2017 (Scopus): (Q2) in the category “<i>Environmental Science</i>” - ISSN: 2073-4433
<i>Water</i>	<i>Water</i> is a peer-reviewed, open access journal on water science and technology, including the ecology and management of water resources, and it is published online monthly by MDPI.	<ul style="list-style-type: none"> - Current Impact Factor: 2.069 - 5-year Impact Factor: 2.250 - 3,781 articles published so far - Total cites in 2017: 2588 - Cite Score 2017 (Scopus): (Q1) in the category “<i>Water Science and Technology</i>” and “<i>Aquatic Science</i>” - ISSN: 2073-4441
<i>Bulletin of the American Meteorological Society (BAMS)</i>	<i>The Bulletin of the American Meteorological Society (BAMS)</i> is the flagship magazine of the AMS and publishes articles of interest and significance for the weather, water, and climate community.	<ul style="list-style-type: none"> - Current Impact Factor 2017/2018: 7.804 - Total articles published in 2017/2018: 126 - Total cites in 2017: 2965 - Cite Score 2017 (Scopus): (Q1) in the category “<i>Atmospheric Science</i>” - Journal ISSN: 1520-0477, 0003-0007

Article

Moisture Transport Anomalies over the Danube River Basin during Two Drought Events: A Lagrangian Analysis

Milica Stojanovic ^{1,*} , Anita Drumond ¹ , Raquel Nieto ^{1,2}  and Luis Gimeno ¹

¹ Environmental Physics Laboratory (EPhysLab), Facultad de Ciencias, Universidad de Vigo, 32004 Ourense, Spain; anitadru@uvigo.es (A.D.); rnieto@uvigo.es (R.N.); l.gimeno@uvigo.es (L.G.)

² Department of Atmospheric Sciences, Institute of Astronomy, Geophysics, and Atmospheric Sciences, University of São Paulo, São Paulo 05508-090, Brazil

* Correspondence: smilica@alumnos.uvigo.es; Tel.: +34-988-387-208

Received: 10 August 2017; Accepted: 28 September 2017; Published: 3 October 2017

Abstract: In this paper, we provide a Lagrangian analysis of the anomalies in the moisture transport during two important drought events (1989/1990 and 2003) configured over the Danube River Basin (DRB) region. Firstly, we identified the drought episodes that occurred over the DRB in the period of 1980–2014 through the Standardized Precipitation Evapotranspiration Index (SPEI). SPEI was calculated using monthly Climatic Research Unit (CRU) Time-Series (TS) Version 3.23 precipitation and potential evapotranspiration (PET) datasets with a spatial resolution of 0.5 degrees. The monthly SPEI-1 index was applied to identify the drought episodes and their respective indicators, including duration, severity, and intensity. Two significant drought events were selected: 1989/1990 (presenting dry conditions during October 1989–March 1990) and 2003 (presenting dry conditions during April 2003–September 2003). These events were associated with the two most severe SPEI-1 episodes identified over the DRB during 1980–2014. Then, an analysis of anomalies in the moisture transport was conducted in order to verify possible changes in the moisture supply from the climatological sources for the DRB during these episodes. The moisture transport analysis was performed through a Lagrangian approach, which uses the outputs of the FLEXiblePARTicle dispersion model FLEXPART integrated with one of the reanalysis produced by the European Centre for Medium-Range Weather Forecasts (ECMWF): the ECMWF Re-Analysis (ERA)-Interim dataset. The DRB receives moisture from seven different moisture source regions: the North Atlantic Ocean (NATL), North Africa (NAF), the Mediterranean Sea (MED), the Black Sea (BS), the Caspian Sea (CS), the DRB, and Central and Eastern Europe (Rest of Land (RestL)). The analysis of drought events shows that the precipitation and moisture supply from the selected sources weakened mainly during both drought events. Anomalous subsidence and an increased PET also prevailed over the DRB during these SPEI-1 episodes. RestL and MED registered the most intensive reduction in the moisture supply over the DRB during both periods.

Keywords: Danube River Basin; drought; Standardized Precipitation Evapotranspiration Index; Lagrangian analysis

1. Introduction

Water is very important for life on Earth and because of that, there is a huge interest among meteorologists and hydrologists to understand the basic elements of the hydrological cycle [1–3]. The main drivers of variability in the water balance are precipitation and evaporation. Climate change is one of the major threats of the 21st century, and according to the Intergovernmental Panel on Climate Change (IPCC) reports (IPCC, 2013), the mean surface temperature will rise globally, which will have

consequences for the global hydrological cycle, and it will contribute to water scarcity. Previous studies on precipitation variability have shown decreasing trends in Central and Southeastern Europe and increasing trends in Northern Europe in the last few years [4,5]. Evaporation is projected to increase in Central and Southeastern Europe, and it can have an impact on the soil moisture, water balance, river runoff, and groundwater resources [6].

Rivers constitute an important part of the global hydrological cycle. They have multiple functions, serving as a source of energy and natural resources for transportation, agriculture, and industry, and they have a significant role in the ecological balance [4,7,8]. River flows are highly sensitive, especially to changes in precipitation and evaporation, and information about the potential effects of climate change on river flows is needed for long-term planning and adaptation [9].

The Danube is one of the most important European waterways, and has a very large drainage area of 817,000 km² extending from Central to Southeastern Europe (Figure 1). It is one of the most international river basins. From the Schwarzwald Mountains in Germany to the Black Sea in Romania, the Danube river flows through 19 countries (Germany, Austria, Slovakia, Hungary, Croatia, Serbia, Montenegro, Romania, Bulgaria, Moldova, Ukraine, Poland, Czech Republic, Switzerland, Italy, Slovenia, Bosnia-Herzegovina, Albania, and Macedonia) [10]. The Danube has a manifold importance in the ecological balance of the region and a significant socio-economic role in industry activity, agriculture, and domestic fresh water supplies [8,10]. It is characterized by a diverse topography. The region is divided into three characteristic morphological and climatic regions: the southern Dinaric–Balkan mountain chains, the western Alps, and the eastern Carpathian mountain bow (Figure 1). These mountain chains receive the highest annual precipitation of about 2000 mm per year. In contrast, the plains (the Vienna basin, Pannonian basin, and the Romanian and Prut low plains) are extremely dry and receive about 500 mm per year. Evaporation is also very significant for the water balance in the Danube drainage area, especially in the lowlands where the mean annual evaporation is estimated to be between 450 and 650 mm per year, and water and moisture from rivers in the wet mountains can help to balance the evaporation deficits [10].

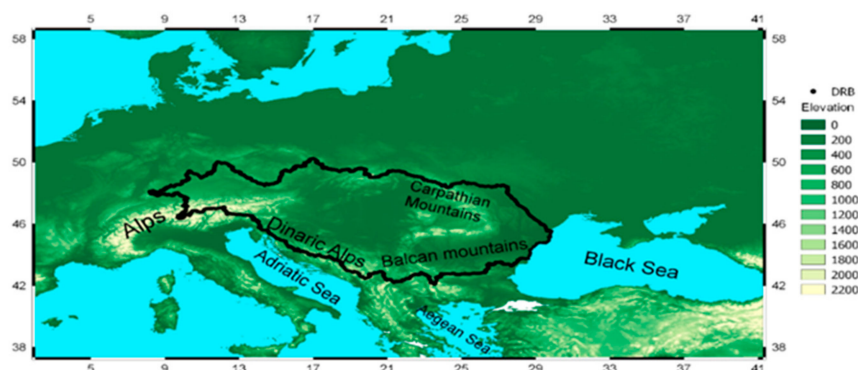


Figure 1. The black contour line indicates the Danube river basin (DRB) area. In colors is indicated the elevation of the region (units in meters). Data from the Hydrosheds project (Available online: <https://hydrosheds.cr.usgs.gov/dataavail.php>).

Many studies have pointed out the effect of precipitation and temperature changes on the Danube flow regime and the possible impacts on water resources and extreme hydrological events, such as floods and droughts, which will be more intensive and more frequent in the Danube River Basin (DRB) [11,12]. During the twentieth century, the climate in Central and Eastern Europe has been characterized by an overall temperature increase, and the beginning of the 21st century is marked by the occurrence of severe and prolonged drought episodes [13]. One of the causes for the occurrence of drought could be the anomalies in the moisture transport, and because of that, understanding the source–sink relationships in the atmospheric water cycle is very important due to the role that they play in extreme meteorological events [14].

Ciric et al. [7] presented the climatology of the major sources of moisture for the DRB during the period of 1980–2014 using a Lagrangian approach and data from the reanalysis produced by the European Centre for Medium-Range Weather Forecasts (ECMWF): the ECMWF Re-Analysis (ERA)-Interim. The DRB receives moisture from seven major moisture source regions: the North Atlantic Ocean (NATL), North Africa (NAF), the Mediterranean Sea (MED), the Black Sea (BS), the Caspian Sea (CS), the DRB, and Central and Eastern Europe (Rest of Land (RestL)) (Figure 2). They also found that the main moisture source during the winter (October–March) for the DRB is the Mediterranean Sea, while during summer (April–September) the principal source of moisture is the DRB itself. The importance of the Mediterranean Sea as a moisture source for the region has been pointed out in previous Lagrangian studies. Using a previous version of the Lagrangian approach applied by Ciric et al. [7] and the ECMWF analysis data, Drumond et al. [15] investigated the seasonal variations in moisture sources for different Mediterranean target regions for 2000–2004, showing that the Mediterranean Sea is the main moisture source for the Balkan Peninsula. Gomez-Hernandez et al. [16] extended Drumond et al. [15] for a 21-year period (using the ERA-40 reanalysis data set) and identified the main moisture sources and sinks over the Mediterranean region, pointing out the role of the Central Mediterranean Sea as the dominant moisture source for the Balkan Peninsula during the winter season. Applying a different Lagrangian approach integrated with data from the ERA-40 reanalysis from 1995 to 2002, Sodemann et al. [17] showed the major importance of the Mediterranean as a moisture source for precipitation events in the Southern Alps.

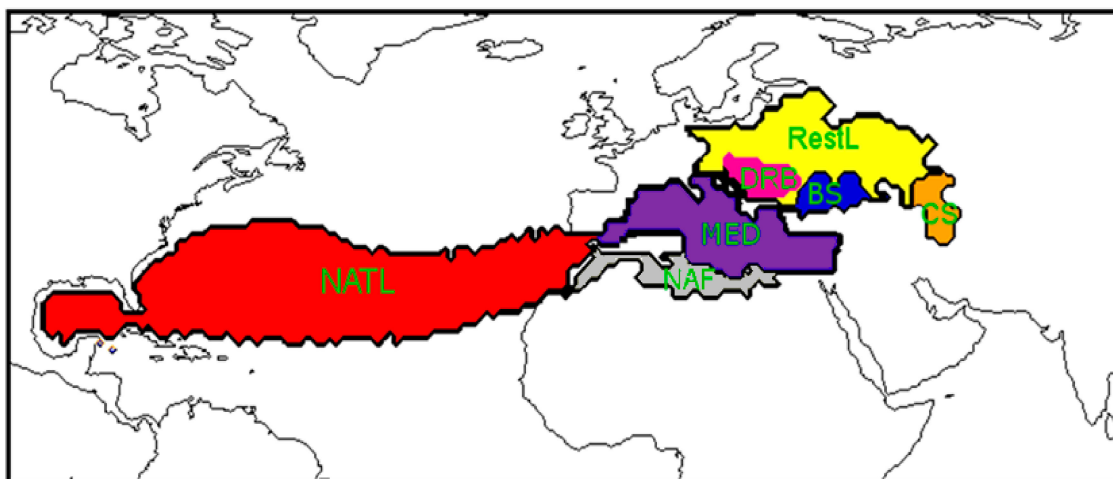


Figure 2. Moisture sources (Evaporation minus Precipitation) (E–P) for the Danube River Basin according to the Ciric et al. [7]. The black contour line indicates the sources: NATL (North Atlantic Ocean) red color, MED (Mediterranean Sea) violet color, NAF (North Africa) grey color, DRB (Danube River Basin) pink color, BS (Black Sea) blue color, CS (Caspian Sea) orange color, and RestL (Central and Eastern Europe) yellow color.

The main objectives of this study are (1) to rank meteorological drought events over the DRB that occurred in the period of 1980–2014 through the standardized precipitation evapotranspiration index (SPEI) [18] and (2) to analyse anomalies in the moisture supply for the two most severe meteorological drought events over the DRB using a Lagrangian approach [19,20]. In Section 2, the data and methodology are explained; Section 3 presents the results and discussion; Section 4 summarizes the conclusions.

2. Data and Method

2.1. Using SPEI-1 (One-Month Standardized Precipitation Evapotranspiration Index) to Identify Meteorological Drought Events over the DRB

Generally, drought may be defined as a natural hazard related to a prolonged lack of precipitation, which can have impacts on different types of systems (economy, ecology, agriculture, forestry, etc.) [21]. There is no universally accepted definition of drought. It is possible to define drought in meteorological terms (the magnitude of a precipitation shortfall and the duration of this shortfall event), agricultural terms (referring to a period with low soil moisture, which leads to reduced crop production and plant growth), hydrological terms (low river flows and low water levels in rivers, lakes, and groundwater) and socioeconomic terms (based on the process of the supply and demand of some economic good with elements of meteorological, hydrological, and agricultural drought) [21–26]. Meteorological drought can be considered as the primary cause of a drought, while the other types of drought describe secondary effects of a prolonged rainfall deficit on specific compartments (e.g., soil moisture, river flows, reservoirs, and economic sectors) [27]. Drought is a concealed phenomenon, and because of its hidden effects, it is very difficult to determine when it begins and also when it is over. Quantitative evaluation of the likelihood of occurrence and expected severity of drought is of key importance for the understanding, monitoring, and mitigation of the system.

Given the difficulty in predicting the evolution of droughts and to quantify drought in terms of its duration, severity, and intensity due to its essential nature, much effort has been invested to develop a drought indicator appropriate for drought monitoring [18–22,28].

A large number of studies related to the analysis and monitoring of drought has been conducted using either the Palmer drought severity index (PDSI), based on a soil-water balance equation [29], or the standardized precipitation index (SPI), a multi-scaling indicator based on a precipitation probabilistic approach. At present, the SPI is applied by the World Meteorological Organization (WMO) to monitor droughts, and its different timescales correspond to different accumulation periods of anomalous precipitation, which can be associated with different drought types, such as 1 month SPI for meteorological drought, 1–6-month SPI for agricultural drought, and 6–24-month SPI or more for hydrological drought [30].

The recently developed SPEI [20] follows the same conceptual approach of SPI, but it is based on a monthly climatic water balance (precipitation (PRE) minus potential evapotranspiration (PET)). The role of temperature through PET is considered one of the crucial advantages of the SPEI over the most widely used drought indexes. For example, it is known that meteorological drought conditions can be aggravated by high temperatures and low relative humidity [27]. The climatic water balance may be computed at various time scales (i.e., accumulation periods), and the resulting values are fit to a log-logistic probability distribution to transform the original values to standardized units that are comparable in space and time and at different SPEI time scales. The time scale over which the water deficit accumulates becomes extremely important and functionally separates hydrological, agricultural, and other types of drought. Therefore, SPEI multi-scalar characteristics also enable the identification of different drought types and impacts in the context of global warming [18,31–33].

In this paper, we analyze changes in the moisture supply into the DRB during the two most severe meteorological drought episodes observed in the period of 1980–2014. We have chosen the SPEI to identify the meteorological drought episodes because it relies on PRE and PET. The SPEI-1 corresponds to the water balance conditions accumulated during one month. This time scale was selected because we are interested in investigating variations in the moisture transport, which is closely related to meteorological drought [34]. The index was calculated using monthly Climatic Research Unit (CRU) Time-Series (TS) Version 3.23 precipitation and the PET dataset available at a spatial resolution of 0.5 degrees [35].

According to McKee et al. [36], a drought episode was defined as a period of one month (or more) starting with a negative SPEI value followed by a value of -1 or less and ending when SPEI returns

again to positive values [36,37]. The respective episode indicators, including duration (the number of months between the start (included) and the last month (not included)), severity (the absolute value of the sum of all SPEI values during the episode), and intensity (severity divided by duration), were calculated [37,38]. The peak monthly values of SPEI registered during the episodes identified were then classified into four categories based on the classification of McKee et al. [36] for the SPI (shown in Table 1), because of the similarity in the calculation principles between SPI and SPEI.

Table 1. Drought classification based on the monthly standardized precipitation evapotranspiration index (SPEI) values, according to the classification proposed by McKee et al. [36].

SPEI Values	Drought Category
0; −0.99	Mild
−1.00; −1.49	Moderate
−1.50; −1.99	Severe
≤ −2.0	Extreme

2.2. Lagrangian Analysis of the Anomalies in the Moisture Supply during Drought Events

In the present study, we analyze anomalous moisture transport into the DRB during two severe drought events. For this purpose, we applied a Lagrangian approach [19,20] based on the FLEXiblePARTicle dispersion model FLEXPART V9.0 integrated with the ERA-Interim reanalysis data from the ECMWF [39]. This dataset has a 1° spatial resolution on 60 vertical levels from 1000 to 0.1 hPa. We have chosen the ERA-Interim data set because its performance in reproducing the hydrological cycle and the water balance closure is considered better than the other reanalysis products available, such as the ERA-40, the Modern Era Retrospective-Analysis for Research and Applications (MERRA), and the Climate Forecast System Reanalysis (CFSR) [40,41]. In addition, because the FLEXPART model requires high-quality data for wind and humidity, its application in periods prior to the significant improvement seen in the measurements in 1979 following the inclusion of satellite data should, therefore, be avoided.

A detailed comparison of different approaches applied in moisture transport analysis and the main advantages and disadvantages of the methodology applied here were discussed by Gimeno et al. [42]. Briefly mentioning some of them, one advantage is that the Lagrangian approach is suitable for establishing moisture source–sink relationships. Nevertheless, the method is mostly limited by the use of a time derivative of the humidity (unrealistic fluctuations in humidity could be considered as moisture fluxes). Such numerical errors may be minimized given the large number of particles found in each atmospheric column.

In this Lagrangian approach, the changes in specific humidity are diagnosed along trajectories, which enable the identification of the sources and sinks of moisture. The method has been supported by a long list of publications [43–47], and consists of dividing the global atmosphere homogeneously into finite elements of volume (for this study, nearly 2.0 million "particles") with constant mass (m), which are moved using a three-dimensional wind field. The longitude, latitude, and altitude of the particles and specific humidity (q) are registered at 6-hour intervals. The time change in specific humidity ($e-p = m dq/dt$) over each particle trajectory helps us to identify those particles that obtain moisture through evaporation (e) from the environment or lose it through precipitation (p). The total surface freshwater flux ($E-P$) associated with the tracked particles is obtained by adding up ($e-p$) for all of the particles existing in the atmosphere over a given area. (E) and (P) represent the rates of evaporation and precipitation per unit area, respectively. All of the particles were tracked for a period of 10 days, which is the average residence time of water vapor in the atmosphere [48].

The trajectory of the particles can be traced using a backward in time analysis with the aim to determine the moisture sources for the target area (regions where the particles gained humidity, $E - P > 0$). We can also conduct a forward in time analysis with the aim of identifying the sinks of the

moisture transported by particles leaving a given source (sinks are the regions where the particles lost humidity $E - P < 0$). The reader may read [49] (and the references therein) for examples of analysis.

The climatological moisture sources for the DRB during the period of 1980–2014 were previously identified by Ciric et al. [7] through a backward experiment. In the present work, we make use of forward analyses from those sources to analyze the respective moisture supply for precipitation into the DRB. The water vapor condensed over the DRB (i.e., the moisture supply) can be then converted into surface precipitation depending on favorable dynamical conditions.

The analysis for the anomalous contribution from the moisture sources to the DRB during the drought events was achieved by calculating monthly anomalies of forward analysis for each source averaged over the DRB. In this way, we can compare the relative importance of the anomalous supply for the DRB associated with each selected moisture source. We also calculate the standardized anomaly of precipitation and PET from the CRU and the standardized anomaly of vertical velocity (ω) at 500 hPa from the ERA-Interim reanalysis, all of them averaged over the DRB area. Maps of the vertically integrated moisture flux (VIMF) and its divergence from ERA-Interim were also plotted. The VIMF is useful for illustrating the anomalous moisture flux conditions observed over the DRB region during the drought episodes.

3. Results and Discussion

3.1. Selection of the Meteorological Drought Events over DRB in the Period of 1980–2014

We identified the meteorological drought episodes over the DRB during 1980–2014 through the time scale SPEI-1, as shown in Figure 3. We identified 50 drought episodes.

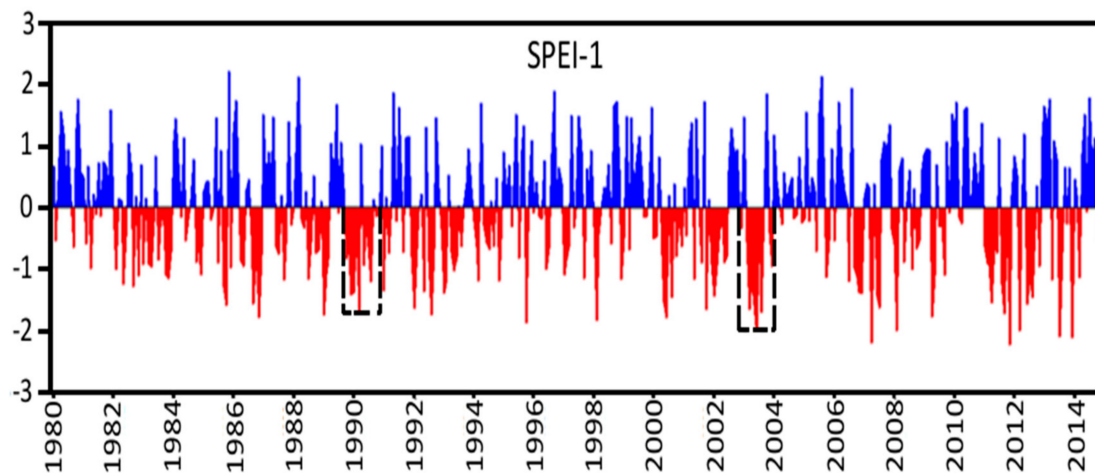


Figure 3. Time series of standardized precipitation evapotranspiration index for 1 month (SPEI-1) averaged over the Danube River Basin (DRB) during 1980–2014. Positive values are in blue and negative in red. The black rectangles show the development of the drought events in 1989/1990 and 2003.

Following the criteria of the identification of episodes of McKee et al. [36], Table 2 represents the top five most severe drought episodes that occurred over the DRB in the period 1980–2014 on the SPEI-1. The characteristics of the episodes, such as their duration, severity, intensity, and the peak values, are also shown in Table 2.

We selected two drought events to study in this paper, one during 2003 and another one during 1989/1990 based on the characteristics of the episodes. These events were the two most severe SPEI-1 episodes identified over the DRB during 1980–2014: from February to August 2003 (7 months) and from October 1989 to March 1990 (6 months).

The SPEI-1 for the episode 1989/1990 reached a peak of -1.72 , belonging to the category severe drought, while the peak registered during the episode of 2003 exceeded -2.0 , which is associated with

the category extreme. Among all of the drought episodes that occurred in period 1980–2014 on the SPEI-1, the longest and the most severe was the February 2003–August 2003 episode. The episode October 1989–March 1990 on SPEI-1 was the second most severe drought episode.

Table 2. Top five most severe drought episodes occurring over the DRB on SPEI-1 in the period 1980–2014.

Five Most Severe Drought Episodes Occurring on SPEI-1	Severity	Duration	Intensity	Peak Month of Each Episode
February 2003–August 2003	8.80	7	1.25	June 2003 −2.09
October 1989–March 1990	6.12	6	1.02	March 1990 −1.72
December 2001–June 2002	5.51	7	0.78	January 2002 −1.44
January 2011–June 2011	5.39	6	0.89	April 2011 −1.55
August 2011–November 2011	5.30	4	1.32	November 2011 −2.22

3.2. Anomalous Patterns Configured during the Drought Events in 1989–1990 and 2003

3.2.1. Drought Event in 1989/1990

The drought event in 1989/1990 has been investigated by previous studies [50–52]. This event, which affected Southern Europe and the Mediterranean region, received considerable attention because of the impact that it had on agriculture, losses in crop yield, and water supply [50].

Standardized monthly anomalies of PET, PRE, and omega at 500 hPa are shown in Figure 4a. Monthly anomalies of the moisture supply ($E - P < 0$) over the DRB by the particles leaving the sources obtained via the forward experiment during the 1989/1990 event are shown in Figure 4b together with the precipitation anomalies accumulated during the SPEI-1 episode (AA-1) defined in Table 2. The bars shown in Figure 4b (left axis) represent the monthly anomalies of the moisture supply by the seven different moisture sources (the North Atlantic Ocean (NATL) (red), North Africa (NAF) (grey), the Mediterranean Sea (MED) (violet), the Black Sea (BS) (blue), the Caspian Sea (CS) (brown), DRB (pink), and Central and Eastern Europe (Rest of Land (RestL) (yellow bars)). For each month, the bars for each source region are superimposed to avoid cluttering. The height of each color bar (computed through the difference between the top and the bottom values of the rectangle read in the left y-axis) represents the magnitude of the anomalous contribution from the respective source. This means that larger color squares are associated with a more intensive anomalous contribution. The superimposition of the anomalous moisture supply allows us to estimate the accumulated anomalies in the moisture contribution from all the studied sources in a given month. For example, in August 1989, the highest positive anomaly was registered for RestL (yellow rectangle, 1.31 mm/day), followed by the DRB (the second largest rectangle, 0.59 mm/day), and that by the NATL was the third contribution (0.22 mm/day), reaching when they were accumulated 2.12 mm/day. On the other hand, the accumulated negative anomalies reached the value of -0.8 mm/day, and the total budget from the seven sources is 1.32 mm/day, indicating, in this particular month, a final positive anomalous support of moisture over the DRB.

From Figure 4, we can see that from September 1989 to February 1990, the moisture supply from all of the selected sources is reduced (except from the North Atlantic in November 1989 and January 1990), which is associated with negative anomalies of PRE and positive ones of omega. From March 1990 to May 1990, there is some increase in the moisture contribution from North Africa (NAF), from other terrestrial sources (RestL), and from the Danube itself. We can notice a small increase in precipitation during April 1990, but it seems that the contribution of these sources is not sufficient

to maintain the positive anomaly of precipitation. It seems that the SPEI-1 episode was associated with the increasing of the negative AA-1 precipitation anomalies (brown line in Figure 4b). Anomalous subsidence also prevailed during this SPEI-1 episode (positive values of omega anomalies in Figure 4a, yellow line).

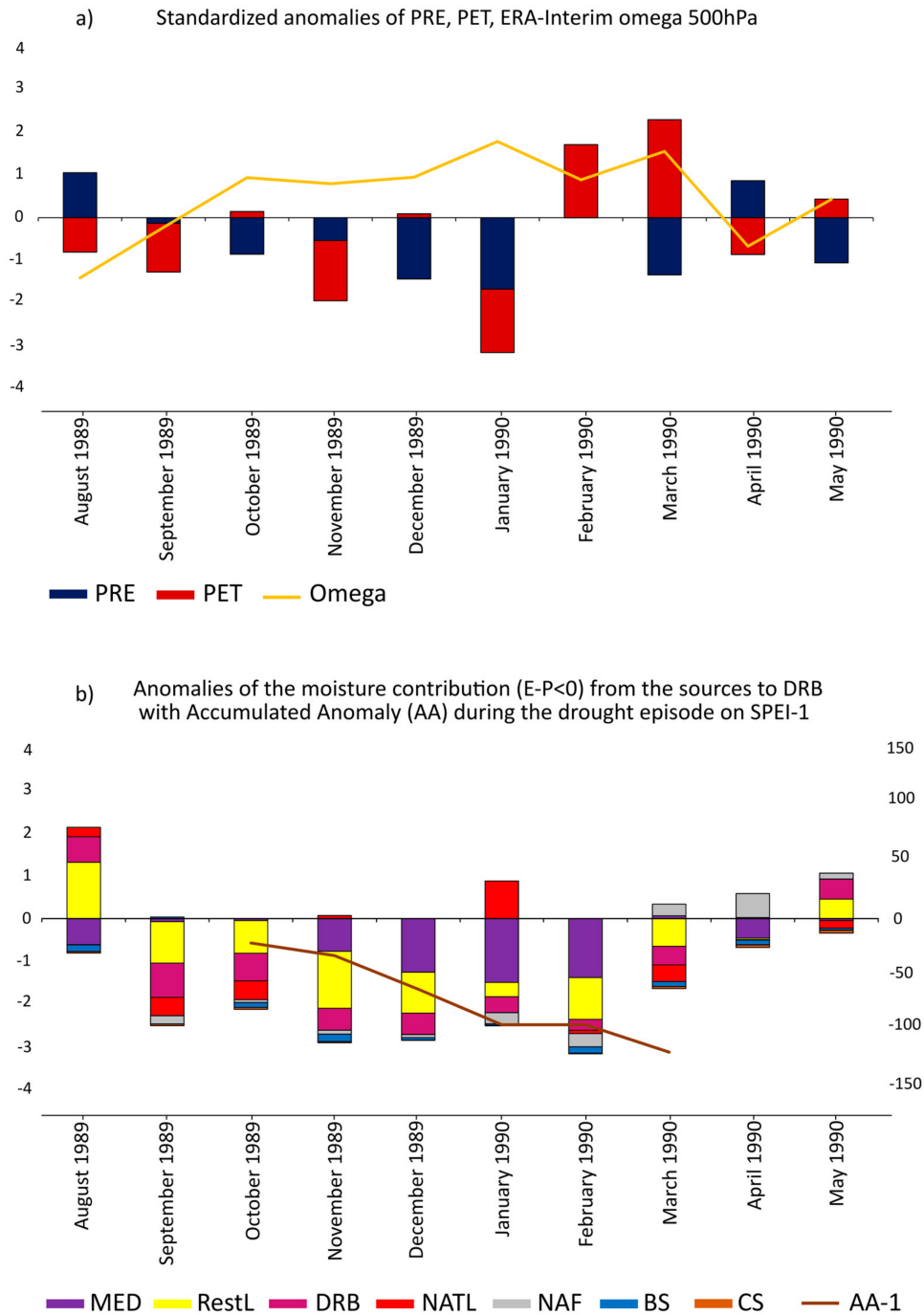


Figure 4. (a) Standardized anomalies of the precipitation (PRE, blue bars), potential evapotranspiration (PET, red bars) (data from Climatic Research Unit (CRU) Time Series (TS) 3.23), and ECMWF Re-Analysis (ERA)-Interim omega at 500 hPa (omega 500, yellow line), and (b) Anomalies in the moisture supply ($E - P < 0$) (accumulated bars) by each source over the DRB obtained via the forward FLEXPART experiment (left axis, in mm/day) and the accumulated precipitation anomalies (brown line AA-1) (right axis, in mm/month) for the 1989–1990 event.

The anomalies in the moisture supply by the sources for the DRB accumulated along the SPEI-1 episode are presented in Table 3, summarizing the exclusive effect of each source. In general, Table 3 shows that a reduction in the moisture supply by the studied sources prevailed during the episode, with the exception of the North Atlantic. When comparing the accumulated values from the selected sources, the results indicate that the Rest of Land source (RestL) registered the most intensive negative anomalies accumulated, followed by the Mediterranean (MED) (−4.98, and −4.85 mm/day, respectively).

Table 3. Anomalies of the moisture supply from the sources over DRB accumulated during the drought episode that occurred on SPEI-1 associated with the event 1989/1990 (in mm/day).

Scale	Drought Episode	MED	RestL	DRB	NATL	NAF	BS	CS
SPEI-1	October 1989–March 1990	−4.85	−4.98	−2.71	0.04	−0.52	−0.65	−0.15

Figure 5 shows the map of the anomalies of the VIMF and its divergence configured over the Mediterranean and North Atlantic regions during the episode. The reader can notice that divergent conditions of VIMF (reddish colors) prevailed over Europe and the Mediterranean, suggesting the inhibition of precipitation over this large spatial domain during the event. Drumond et al. [53] also identified this episode in their analysis of the driest winter conditions verified over the moisture sinks of the MED, which reveals not only that drier conditions have been extended over southeastern Europe during the 1989/1990 winter, but also that the anomalous moisture supply from the MED favored these conditions.

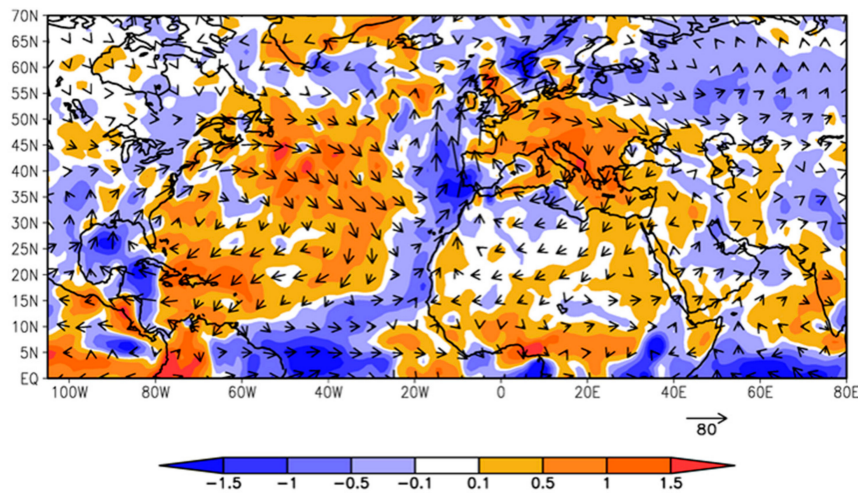


Figure 5. Anomalies of ERA-Interim vertically integrated moisture flux (vector, kg/m/s) and its respective divergence (shaded, mm/day) averaged for the 1989/1990 episode.

An anomalous anticyclonic circulation localized over central Europe confirms the Lagrangian results concerning the inhibition of the moisture transport from the MED to the DRB, as well as from central/North Europe (including the RestL area). This anticyclonic anomaly may be related to the second prominent mode of climate variability that affects the North Atlantic region and Europe, the East Atlantic (EA) pattern [54]. During its positive phase, this pattern consists in a north–south dipole of 500 hPa geopotential anomalies with enhanced positive anomalies spanning from the western North Atlantic to eastern Europe, and it is also associated with negative anomalies over southern Europe and the eastern Mediterranean [55]. During the drought episode analyzed here, the index of EA remains positive with a mean value of 0.37, but it is higher during the last four months of the period, reaching 1.12. So, this condition favors the drought.

A vector analysis indicates that the moisture transport from the Atlantic Ocean and Mediterranean Sea that converged over the eastern Atlantic are associated with a moisture flux northwards.

3.2.2. Drought Event in 2003

This drought event is the longest and the most severe of all the drought events that occurred over the DRB on the SPEI-1 in the period of 1980–2014. It seems that this event may be associated with the heat waves registered over Europe in the summer of 2003. These heat waves received substantial attention because of the impacts that they had on river flow, central European glaciers, and losses in crop yield, as well as other serious consequences, which have been the focus of many studies [56–59]. Fink et al. [56] analyzed the synoptic situation and the impacts of the hot, dry 2003 European summer heatwaves. They found that the summer of 2003 was the warmest since 1864, and the impacts of its dryness were intensified by high evaporation rates and the drought conditions during the previous period. They also mentioned that summer heatwaves in 2003 not only affected Central Europe, but also the Mediterranean region, which is in agreement with our results for the DRB.

Similar to Figure 4, Figure 6a shows the standardized anomaly of PET, PRE, and omega at 500 hPa, while Figure 6b shows the anomalies of the moisture supply over the DRB from the sources obtained via the forward experiment for this drought event. It includes the AA-1 precipitation anomalies accumulated during the SPEI-1 episode shown in Table 2.

From Figure 6b, we can see that during the period previous to the event, there were positive anomaly contributions from the Mediterranean Sea until January 2003, while anomalies of PRE are positive and anomalies of omega and PET are negative (Figure 6a).

From February 2003, the onset of the drought event, to August 2003, the contribution from the sources to precipitation predominantly weakened (Figure 6b). The positive anomalies of PET and omega (indicating subsidence), which reached their peak in June 2003, and the most intense negative accumulated anomaly for precipitation in August 2003, on SPEI-1 are associated with the negative anomaly of precipitation during the 2003 summer season that is associated with a reduction in moisture supply from almost all of the sources. The SPEI-1 episode finished in August 2003, and an intensified contribution from the Mediterranean and Black Seas occurred in September 2003 (Figure 6b). In October 2003, when all of the sources show a positive anomaly contribution, the anomaly of PRE registered positive values. Our findings are also in agreement with Ciais et al. [57] and Rebetz et al. [58], which show that precipitation was below normal during the whole of 2003 in Europe with the exception of October 2003. The anomalous subsidence over the DRB persisted in all periods from February 2003 to September 2003.

The anomalies in the moisture supply from the sources over the DRB accumulated during the 2003 episode are shown in Table 4. Table 4 shows a predominance of reduced moisture supply from the studied sources. When we compare the accumulated values from the sources, the results indicate that the RestL and MED registered the most intensive negative anomalies accumulated during the 2003 episode (−5.38, and −4.79 mm/day, respectively).

Table 4. Same as Table 3, but for the 2003 event.

Scale	Drought Episode	MED	RestL	DRB	NATL	NAF	BS	CS
SPEI-1	February 2003–August 2003	−4.79	−5.38	−2.90	−1.97	−0.78	−0.60	−0.002

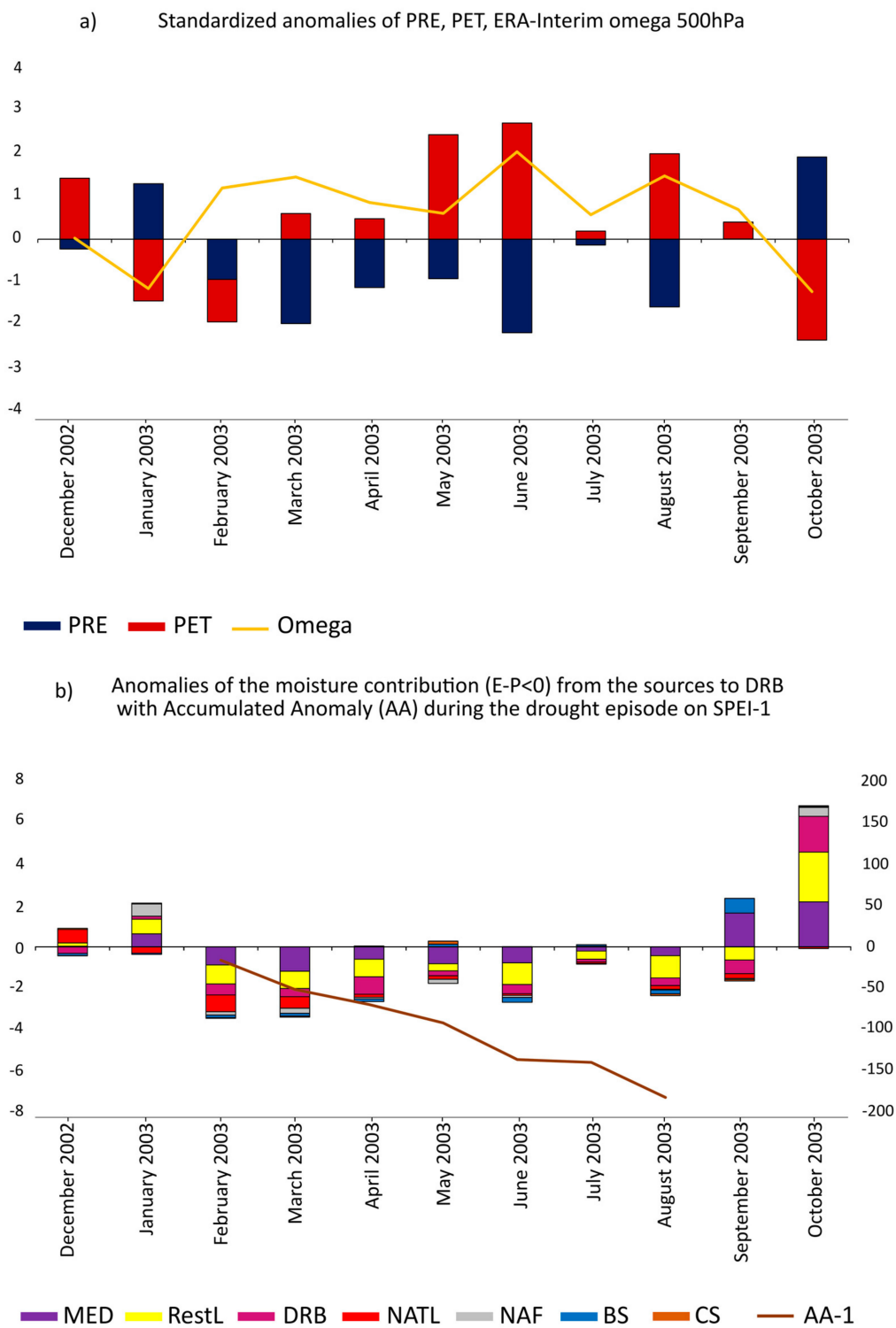


Figure 6. (a) Standardized anomalies of the precipitation (PRE, blue bars), potential evapotranspiration (PET, red bars) (data from Climatic Research Unit (CRU) Time Series (TS) 3.23), and ECMWF Re-Analysis ERA-Interim omega at 500hPa (omega 500, yellow line), and (b) Anomalies in the moisture supply ($E - P < 0$) (accumulated bars) by each source over the DRB obtained via the forward FLEXPART experiment (left axis, in mm/day) and the accumulated precipitation anomalies (brown line AA-1) (right axis, in mm/month) for the 2003 drought event.

Figure 7 shows the map of the anomalies of the VIMF and its divergence configured over the Mediterranean and North Atlantic regions during the 2003 episode. Quite similar to the 1989/90 event, divergent conditions of VIMF and an anomalous anticyclonic circulation localized over central Europe (the East Atlantic index is also positive during the entire period and during the last four months (0.38 and 0.14, respectively)) inhibited moisture supply from both the MED and RestL to the DRB. This drought episode has also been identified by Drumond et al. [53] between the driest summer conditions verified over the moisture sinks of the MED, which reveals that dry conditions extended over southern and western Europe during 2003. It is also interesting to observe an anomalous VIMF convergence over northwestern Africa, favoring precipitation over the region, which agrees with the study of Wolter et al. [60]. According to these authors, during the European spring season, mature El Niño events tend to create anomalies over the northern Atlantic that are associated with below-normal rainfall over the western Mediterranean and with the intensification and the northward displacement of precipitation over northwestern Africa. These anomalous patterns lead to drier 2003 European conditions.

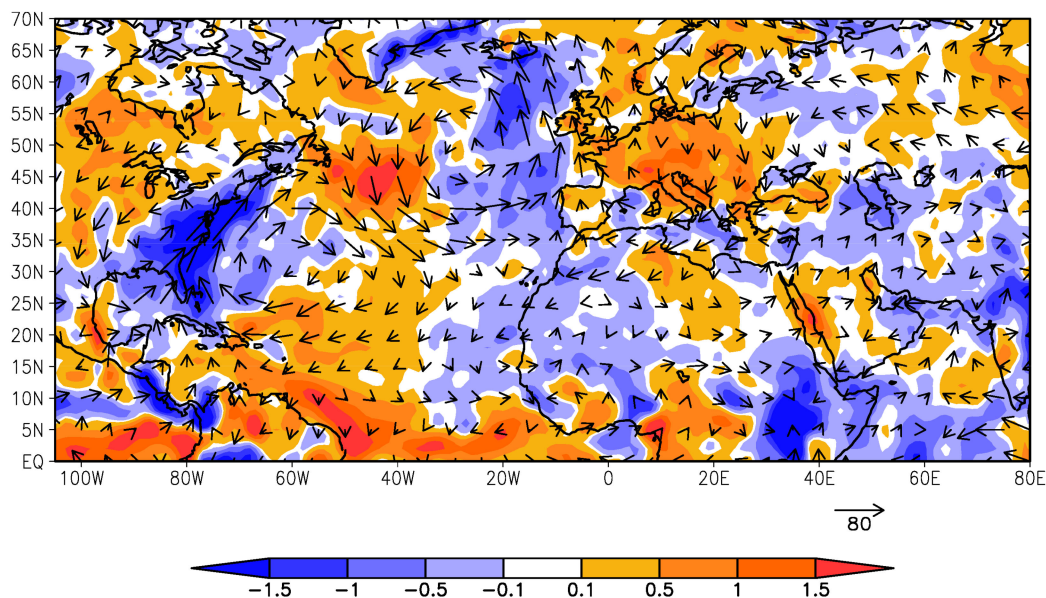


Figure 7. Anomalies of ERA-Interim vertically integrated moisture flux (vector, kg/m/s) and its respective divergence (shaded, mm/day) averaged for the 2003 episode.

3.3. Variations in the Moisture Supply from the Moisture Sources for the DRB and Meteorological Drought Conditions over the Basin during 1980–2014

The analyses for the 1989/1990 and 2003 episodes performed in the previous sections revealed that the RestL and MED were the sources presenting the most intensive reduction in the moisture supply over the DRB during both periods, independently of their occurrence in different seasons: 1989/90 during the winter and 2003 in the summer. Although these results cannot be conclusive because they refer to only two episodes and an analysis of all events would be exhaustive, in this section our aim is to provide some climatological perspective of the relationship between the occurrence of meteorological dry conditions over the DRB and the moisture supply from the studied sources.

Table 5 shows the Pearson correlation coefficients between the anomalies in the moisture supply from the sources to the DRB and SPEI-1 time series in an attempt to reveal some joint linear variability. Although all values are positive, it is worth mentioning that the RestL and MED show the highest annual correlation values (exceeding 0.5). It indicates that an enhanced (inhibited) moisture supply from these sources was linearly associated with moist (dry) conditions over the DRB on the SPEI-1 scale. These results support the case studies suggesting the relative importance of the moisture supply

particularly from the RestL, MED, and DRB sources, which are the major sources of moisture for the DRB [7].

Table 5. Pearson correlation coefficients between the anomalies in the moisture supply from the sources to the DRB and SPEI-1 time series. Except for CS, all the values are significant at 99.9% according to the Student's *t*-test.

Moisture Sources	Correlation Coefficient
RestL	0.56
MED	0.53
DRB	0.46
NAF	0.41
BS	0.37
NATL	0.34
CS	0.19

4. Conclusions

In this paper, we investigated the anomalies in the moisture transport observed during two significant drought events over the Danube River Basin (DRB) (1989–1990 and 2003) through a Lagrangian approach. We calculated the standardized precipitation evapotranspiration index (SPEI) to identify the drought episodes that occurred over the DRB in the period of 1980–2014. SPEI was obtained using the monthly CRU (TS3.23) precipitation and potential evapotranspiration dataset, available at a spatial resolution of 0.5 degree. The monthly values of SPEI were classified into four categories (mild, moderate, severe, and extreme) based on the classification of McKee et al. [36]. The monthly SPEI-1 index was used to identify the drought episodes and to calculate their respective indicators, including duration, severity, and intensity. A Lagrangian approach was then applied using data from ERA-Interim in order to analyze the variation in moisture supply into the DRB during the selected drought events. The main conclusions of the study are summarized as follows.

The two most severe drought episodes that occurred during 1980–2014 on the timescale of SPEI-1 were the episodes October 1989–March 1990 and February 2003–August 2003.

Anomalous subsidence (positive anomalies of omega at 500 hPa) and reduced precipitation predominated during the episode October 1989–March 1990. The event was associated with reduced moisture supply from almost all of the sources investigated (except the North Atlantic in November 1989 and January 1990).

For 2003, the results show that the reduction in the moisture supply and PRE over the DRB occurred together with the onset of the episode. The SPEI-1 episode lasted up to August 2003, being characterized by anomalous subsidence, increased PET, and reduced PRE over the DRB associated with the predominance of reduced moisture supply from the selected sources. From September 2003, the dismissal of the SPEI-1 episode and the weakening of the anomalous subsidence and PET are associated with increasing PRE and moisture supply from the analyzed sources.

Concerning the PET and the SPEI-1 episodes, the 1989/1990 episode was the only one presenting negative anomalies of PET, although these were weaker than the negative anomalies of PRE, which results in $PRE - PET < 0$ and in negative SPEI values.

The analysis for the drought episodes identified on SPEI-1 (October 1989–March 1990 and February 2003–August 2003) shows that the RestL and MED were the sources presenting the most intensive reduction in the moisture supply over the DRB during both periods. Also, the RestL and MED present the highest correlation values between the anomalies in the moisture supply from the sources to the DRB and SPEI-1 time series.

Acknowledgments: Thanks for the funding by the Spanish Government and FEDER through the SETH (CGL2014-60849-JIN) project. M. Stojanovic's Ph.D. fellowship is supported by European Commission under the Erasmus Mundus project Green-Tech-WB: Smart and Green technologies for innovative and sustainable societies

in Western Balkans (551984-EM-1-2014-1-ES-ERA Mundus-EMA2). R. Nieto also acknowledges the support of the CNPq Grant 314734/2014-7 by the Brazilian government. We also thank the IMDROFLOOD project financed by the Water Works 2014 co-funded call of the European Commission. We acknowledge both anonymous referees for their comments that have improved this paper.

Author Contributions: M. Stojanovic, A. Drumond, and L. Gimeno conceived of and designed the experiments. M. Stojanovic performed the experiments and M. Stojanovic, A. Drumond, and L. Gimeno analyzed the data. M. Stojanovic, A. Drumond, R. Nieto, and L. Gimeno wrote the paper.

Conflicts of Interest: The authors declare no conflict of interest. The founding sponsors had no role in the design of the study; in the collection, analyses or interpretation of data; in the writing of the manuscript; nor in the decision to publish the results.

References

1. Kuchment, L.S. The Hydrological Cycle and Human Impact on It. 2004. Available online: <http://www.biodiversity.ru/programs/ecoservices/library/functions/water/doc/Kuchment.pdf> (accessed on 10 May 2017).
2. Christensen, J.H.; Christensen, O.B. Severe summertime flooding in Europe. *Nature* **2003**, *421*, 805–806. [[CrossRef](#)] [[PubMed](#)]
3. Schär, C.; Vidale, P.L.; Lüthi, D.C.; Frei, C.; Häberli, C.; Liniger, M.A.; Appenzeller, C. The role of increasing temperature variability in European summer heatwaves. *Nature* **2004**, *427*, 332–336. [[CrossRef](#)] [[PubMed](#)]
4. Nikolova, N.; Vassilev, S. Variability of summer-time precipitation in Danube plain, Bulgaria. *J. Geogr. Inst. “Jovan Cvijic” SASA* **2005**, *54*, 19–32. [[CrossRef](#)]
5. García-Ruiz, J.M.; López-Moreno, J.I.; Vicente-Serrano, S.M.; Lasanta-Martínez, T.; Beguería, S. Mediterranean water resources in a global change scenario. *Earth. Sci. Rev.* **2011**, *105*, 121–139. [[CrossRef](#)]
6. Bates, B.C.; Kundzewicz, Z.W.; Wu, S.; Palutikof, J.P. Technical Paper of the Intergovernmental Panel on Climate Change: Climate Change Water. 2008. Available online: <https://www.ipcc.ch/pdf/technical-papers/climate-change-water-en.pdf> (accessed on 10 May 2017).
7. Ciric, D.; Stojanovic, M.; Drumond, A.; Nieto, R.; Gimeno, L. Tracking the Origin of Moisture over the Danube River Basin Using a Lagrangian Approach. *Atmosphere* **2016**, *7*, 162. [[CrossRef](#)]
8. Gibson, J.J.; Aggarwal, P.; Hogan, J.; Herczeg, A. Isotope studies in large river basins: A new global research focus. *Eos, Trans. Am. Geophys. Union* **2002**, *83*, 613–617. [[CrossRef](#)]
9. Stagl, C.J.; Hattermann, F.F. Impacts of climate change on the hydrological regime of the Danube River and its tributaries using an ensemble of climate scenarios. *Water* **2015**, *7*, 6139–6172. [[CrossRef](#)]
10. Rîmbu, N.; Boroneanț, C.; Buță, C.; Dima, M. Decadal variability of the Danube river flow in the lower basin and its relation with the North Atlantic Oscillation. *Int. J. Climatol.* **2002**, *22*, 1169–1179. [[CrossRef](#)]
11. Pistocchi, A.; Beck, H.; Bisselink, B.; Gelati, E.; Lavallo, C.; Feher, J. Water Scenarios for the Danube River Basin: Elements for the Assessment of the Danube Agriculture-Energy-Water Nexus. 2015. Available online: <https://ec.europa.eu/jrc/en/publication/water-scenarios-danube-river-basin-elements-assessment-danube-agriculture-energy-water-nexus> (accessed on 10 May 2017).
12. Mishra, A.K.; Singh, V.P. A review of drought concepts. *J. Hydrol.* **2010**, *391*, 202–216. [[CrossRef](#)]
13. Popova, Z. Drought vulnerability estimated based on crop-yield models. In *Drought Management Centre for South-East Europe -DMCSEE—Summary of Project Results*; Slovenian Environmental Agency: Ljubljana, Slovenia, 2012; pp. 39–54. [[CrossRef](#)]
14. Seneviratne, S.I.; Lüthi, D.; Litschi, M.; Schär, C. Land-atmosphere coupling and climate change in Europe. *Nature* **2006**, *443*, 205–209. [[CrossRef](#)] [[PubMed](#)]
15. Drumond, A.; Nieto, R.; Hernández, E.; Gimeno, L. A Lagrangian analysis of the variation in moisture sources related to drier and wetter conditions in regions around the Mediterranean basin. *Nat. Hazards Earth Sys. Sci.* **2011**, *11*, 2307–2320. [[CrossRef](#)]
16. Gómez-Hernández, M.; Drumond, A.; Gimeno, L.; Garcia-Herrera, R. Variability of moisture sources in the Mediterranean region during the period 1980–2000. *Water Resour. Res.* **2013**, *49*, 6781–6794. [[CrossRef](#)]
17. Sodemann, H.; Zuber, E. Seasonal and inter-annual variability of the moisture sources for Alpine precipitation during 1995–2002. *Int. J. Climatol.* **2010**, *30*, 947–961. [[CrossRef](#)]
18. Vicente-Serrano, S.M.; Beguería, S.; Lopez-Moreno, A.J. A multiscalar drought index sensitive to global warming: The standardized precipitation evapotranspiration index. *J. Clim.* **2010**, *23*, 1696–1718. [[CrossRef](#)]

19. Stohl, A.; James, P. A Lagrangian Analysis of the Atmospheric Branch of the Global Water Cycle. Part I: Method Description, Validation, and Demonstration for the August 2002 Flooding in Central Europe. *J. Hydrometeorol.* **2004**, *5*, 656–678. [[CrossRef](#)]
20. Stohl, A.; James, P. A Lagrangian analysis of the atmospheric branch of the global water cycle: Part II: Moisture Transports between Earth's Ocean Basins and River Catchments. *J. Hydrometeorol.* **2005**, *6*, 948–961. [[CrossRef](#)]
21. World Meteorological Organization. Drought Monitoring and Early Warning: Concepts, Progress and Future Challenges. 2006. Available online: <http://www.wamis.org/agm/pubs/brochures/WMO1006e.pdf> (accessed on 11 May 2017).
22. Wilhite, D.A.; Glantz, M.H. Understanding the Drought Phenomenon: The Role of Definitions. *Water Int.* **1985**, *10*, 111–120. [[CrossRef](#)]
23. Panu, U.S.; Sharma, T.C. Challenges in drought research: Some perspectives and future directions. *Hydrol. Sci. J.* **2002**, *47*, S19–S30. [[CrossRef](#)]
24. Urama, K.C.; Ozor, N. Impacts of Climate Change on Water Resources in Africa: The Role of Adaptation. African Technology Policy Studies Network (ATPS), 2010. Available online: http://www.ourplanet.com/climate-adaptation/Urama_Ozorv.pdf (accessed on 11 May 2017).
25. Dai, A. Drought under global warming: A review. *WIREs Clim. Chang.* **2010**, *2*, 45–65. [[CrossRef](#)]
26. Zlatanovic, N.; Stojkovic, M. Assessment and monitoring of droughts in Southeastern Europe: A Review. *Water Res. Man.* **2016**, *6*, 11–18.
27. Spinoni, J.; Naumann, G.; Vogt, J.; Barbosa, P. Meteorological Droughts in Europe: Events and Impacts: Past Trends and Future Projections. 2016. Available online: http://www.droughtmanagement.info/literature/EC-JRC_Report%20on%20Droughts%20in%20Europe_2016.pdf (accessed on 15 September 2017).
28. Rahmat, S.N. Methodology for Development of Drought Severity-Duration-Frequency (SDF) Curves. Ph.D. Thesis, RMIT University, Melbourne, Australia, 28 August 2014.
29. Palmer, W.C. Meteorological Drought. 1965. Available online: <https://www.ncdc.noaa.gov/temp-and-precip/drought/docs/palmer.pdf> (accessed on 11 May 2017).
30. World Meteorological Organization. Standardized Precipitation Index User Guide. 2012. Available online: http://www.wamis.org/agm/pubs/SPI/WMO_1090_EN.pdf (accessed on 15 September 2017).
31. Vicente-Serrano, S.M.; Gouveira, C.; Camarero, J.J.; Beguería, S.; Trigo, R.; LúpezMoreno, J.I.; Azorin-Molina, C.; Pasho, E.; Lorenzo-Lacruz, J.; Revuelto, J.; et al. Drought Impacts on Vegetation Activity, Growth and Primary Production in Humid and Arid Ecosystems. 2012. Available online: http://digital.csic.es/bitstream/10261/62153/1/BegueriaS_Drought_CongSal-AEC_2012.pdf (accessed on 11 May 2017).
32. Begueria, S.; Vicente-Serrano, S.M.; Reig, F.; Latorre, B. Standardized precipitation evapotranspiration index (SPEI) revisited: Parameter fitting, evapotranspiration models, tools, datasets and drought monitoring. *Int. J. Climatol.* **2013**, *34*, 3001–3023. [[CrossRef](#)]
33. Potop, V.; Boroneanț, C.; Možný, M.; Štěpánek, P.; Skalák, P. Observed spatiotemporal characteristics of drought on various time scales over the Czech Republic. *Theor. Appl. Climatol.* **2014**, *115*, 563–581. [[CrossRef](#)]
34. Liu, Z.; Lu, G.; He, H.; Wu, Z.; He, J. Anomalous Features of Water Vapor Transport during Severe Summer and Early Fall Droughts in Southwest China. *Water* **2017**, *9*, 244. [[CrossRef](#)]
35. Harris, I.; Jones, P.D.; Osborn, T.J.; Lister, D.H. Updated high-resolution grids of monthly climatic observations—The CRU TS3.10 Dataset. *Int. J. Climatol.* **2014**, *34*, 623–642. [[CrossRef](#)]
36. McKee, T.B.; Doesken, N.J.; Kleist, J. The relationship of drought frequency and duration to time scales. In Proceedings of the Eighth Conference on Applied Climatology, Anaheim, CA, USA, 17–22 January 1993; pp. 179–184.
37. Tan, C.; Yang, J.; Li, M. Temporal-Spatial Variation of Drought Indicated by SPI and SPEI in Ningxia Hui Autonomous Region, China. *Atmosphere* **2015**, *6*, 1399–1421. [[CrossRef](#)]
38. Spinoni, J.; Naumann, G.; Carrao, H.; Barbosa, P.; Vogt, J. World drought frequency, duration, and severity for 1951–2010. *Int. J. Climatol.* **2014**, *34*, 2792–2804. [[CrossRef](#)]
39. Dee, D.P.; Uppala, S.M.; Simmons, A.J.; Berrisford, P.; Poli, P.; Kobayashi, S.; Andrae, U.; Balmaseda, M.A.; Balsamo, G.; Bauer, P.; et al. The ERA-Interim reanalysis: Configuration and performance of the data assimilation system. *Q. J. R. Meteorol. Soc.* **2001**, *137*, 553–597. [[CrossRef](#)]

40. Trenberth, K.E.; Fasullo, J.T.; Mackaro, J. Atmospheric moisture transports from ocean to land and global energy flows in reanalyses. *J. Clim.* **2011**, *24*, 4907–4924. [[CrossRef](#)]
41. Lorenz, C.; Kunstmann, H. The hydrological cycle in three state-of-the-art reanalyses: Intercomparison and performance analysis. *J. Hydrometeorol.* **2012**, *13*, 1397–1420. [[CrossRef](#)]
42. Gimeno, L.; Stohl, A.; Trigo, R.M.; Dominguez, F.; Yoshimura, K.; Yu, L.; Drumond, A.; Duran-Quesada, A.M.; Nieto, R. Oceanic and terrestrial sources of continental precipitation. *Rev. Geophys.* **2012**, *50*, 1–41. [[CrossRef](#)]
43. Nieto, R.; Gallego, D.; Trigo, R.M.; Ribera, P.; Gimeno, L. Dynamic identification of moisture sources in the Orinoco basin in equatorial South America. *Hydrol. Sci. J.* **2008**, *53*, 602–617. [[CrossRef](#)]
44. Drumond, A.; Nieto, R.; Gimeno, L.; Ambrizzi, T. A Lagrangian identification of major sources of moisture over Central Brazil and La Plata Basin. *J. Geophys. Res. Atmos.* **2008**, *113*. [[CrossRef](#)]
45. Huang, Y.; Cui, X. Moisture sources of an extreme precipitation event in Sichuan, China, based on the Lagrangian method. *Atmos. Sci. Lett.* **2015**, *16*, 177–183. [[CrossRef](#)]
46. Viste, E.; Sorteberg, A. The effect of moisture transport variability on Ethiopian summer precipitation. *Int J. Climatol.* **2012**, *33*, 3106–3123. [[CrossRef](#)]
47. Stohl, A.; Forster, C.; Sodemann, H. Remote sources of water vapor forming precipitation on the Norwegian west coast at 60° N—A tale of hurricanes and an atmospheric river. *J. Geophys. Res. Atmos.* **2008**, *113*. [[CrossRef](#)]
48. Numaguti, A. Origin and recycling processes of precipitating water over the Eurasian continent: Experiments using an atmospheric general circulation model. *J. Geophys. Res. Atmos.* **1999**, *104*, 1957–1972. [[CrossRef](#)]
49. Vázquez, M.; Nieto, R.; Drumond, A.; Gimeno, L. Extreme Sea Ice Loss over the Arctic: An Analysis Based on Anomalous Moisture Transport. *Atmosphere* **2017**, *8*, 32. [[CrossRef](#)]
50. Spinoni, J.; Naumann, G.; Vogt, V.V.; Barbosa, P. The biggest drought events in Europe from 1950–2012. *J. Hydrol.* **2015**, *3*, 509–524. [[CrossRef](#)]
51. Tselepidaki, I.; Zarifis, B.; Asimakopoulos, D.N. Low precipitation over Greece during 1989–1990. *Theor. Appl. Climatol.* **1992**, *46*, 115–121. [[CrossRef](#)]
52. Tsakiris, G.; Vangelis, H. Establishing a drought index incorporating evapotranspiration. *Eur. Water* **2005**, *9*, 3–11.
53. Drumond, A.; Gimeno, L.; Nieto, R.; Trigo, R.M.; Vicente-Serrano, S.M. Drought episodes in the climatological sinks of the Mediterranean moisture source: The role of moisture transport. *Global Planet. Change* **2017**, *151*, 4–14. [[CrossRef](#)]
54. Barnston, A.G.; Livezey, R.E. Classification, seasonality and persistence of low-frequency atmospheric circulation patterns. *Mon. Wea. Rev.* **1987**, *115*, 1083–1126. [[CrossRef](#)]
55. Trigo, R.; Xoplaki, E.; Zorita, E.; Luterbacher, J.; Kricak, S.O.; Albert, P.; Jacobeit, J.; Sáenz, J.; Fernández, J.; Glonzález-Rouco, F.; et al. Relations between Variability in the Mediterranean Region and Mid-latitude Variability. *Dev. Earth Environ. Sci.* **2006**, *4*, 179–226.
56. Fink, A.H.; Brücher, T.; Krüger, A.; Leckebusch, G.C.; Pinto, J.G.; Ulbrich, U. The 2003 European summer heatwaves and drought-synoptic diagnosis and impacts. *Weather* **2004**, *59*, 209–216. [[CrossRef](#)]
57. Ciais, P.; Reichstein, M.; Viovy, N.; Granier, A.; Ogée, J.; Allard, V.; Aubinet, M.; Buchmann, N.; Bernhofer, C.; Carrara, A.; et al. Europe-wide reduction in primary productivity caused by the heat and drought in 2003. *Nature* **2005**, *437*, 529–533. [[CrossRef](#)] [[PubMed](#)]
58. Rebetez, M.; Mayer, H.; Dupont, O.; Schindler, D.; Gartner, K.; Kropp, J.P.; Menzel, A. Heat and drought 2003 in Europe: A climate synthesis. *Ann. For. Sci.* **2006**, *63*, 569–577. [[CrossRef](#)]
59. Chase, T.N.; Wolter, K.; Pielke, R.A.; Rasool, I. Was the 2003 European heat wave unusual in a global context? *Geophys. Res. Lett.* **2006**, *33*. [[CrossRef](#)]
60. Wolter, K.; Baldi, M.; Chase, T.N.; Otterman, J.; Pielke, R.A.; Rasool, I. Possible Causes of the South-Central European Heat Wave of 2003 a Diagnostic Perspective. 2005. Available online: <https://meetings.copernicus.org/www.cosis.net/abstracts/EGU05/10447/EGU05-J-10447.pdf> (accessed on 17 September 2017).



Article

Anomalies in Moisture Supply during the 2003 Drought Event in Europe: A Lagrangian Analysis

Milica Stojanovic, Anita Drumond , Raquel Nieto  and Luis Gimeno *

Environmental Physics Laboratory (EPHysLab), Facultade de Ciencias, Universidade de Vigo, 32004 Ourense, Spain; smilica@alumnos.uvigo.es (M.S.); anitadru@uvigo.es (A.D.); rnieto@uvigo.es (R.N.)

* Correspondence: l.gimeno@uvigo.es; Tel.: +34-988-387-208

Received: 2 March 2018; Accepted: 10 April 2018; Published: 12 April 2018



Abstract: In the last few decades, many studies have identified an increasing number of natural hazards associated with extreme precipitation and drought events in Europe. During the 20th century, the climate in Central Europe and the Mediterranean region was characterised by an overall temperature increase, and the beginning of the 21st century has been marked by severe and prolonged drought events. The aim of this study is to analyse variations in the moisture supply during the 2003 drought episode that affected large portions of Europe. In order to better characterise the evolution of the episodes across the continent, separate analyses were performed for two spatial domains: Central Europe and the Mediterranean region. These regions were defined according to the 5th Intergovernmental Panel on Climate Change Assessment Report. For both regions, this drought episode was most severe from 1980 to 2015, according to the one-month Standardised Precipitation Evapotranspiration Index (SPEI-1) analysis, which was conducted using monthly precipitation and potential evapotranspiration data from the Climate Research Unit. Analyses of precipitation, potential evapotranspiration, pressure velocity at 500 hPa, and vertically integrated moisture flux were conducted to characterise the anomalous patterns over the regions during the event. A Lagrangian approach was then applied in order to investigate possible continental-scale changes in the moisture supply over the Central European and Mediterranean regions during 2003. This approach is based on the FLEXible PARTicle (FLEXPART) dispersion model, integrated with data from the European Centre for Medium-Range Weather Forecasts (ECMWF): the ECMWF Re-Analysis ERA-Interim. The results indicate that anomalous subsidence, increased evapotranspiration, and reduced precipitation predominated over both regions during the episode. The most intense reduction in the moisture supply over Central Europe was registered for the Mediterranean Sea (MDS) and the Central European region, while for the Mediterranean region, most intense reduction in the moisture supply was observed in the MDS and—in minor-scale—Gibraltar regions.

Keywords: drought; Mediterranean region; Central Europe; Lagrangian method; Standardised Precipitation Evapotranspiration Index

1. Introduction

Climate change is one of the major causes of global temperature increases and the variability of extreme events, including droughts [1]. During the 20th century, the climate in Central Europe and the Mediterranean region was characterised by an overall temperature increase, and the beginning of 21st century has been marked by severe and prolonged drought events [2–6].

Droughts are part of the natural climate cycle. They commonly affect large areas, and are related to a prolonged lack of precipitation. A drought is a complex phenomenon that has an impact on different types of systems (environment, economy, society, agriculture, etc.); it is generally accepted that it is one of the costliest natural hazards [7,8]. Therefore, it is possible to define a drought in

meteorological (rainfall for a specified period is below the normal amount), agricultural (there is not enough soil moisture to satisfy the needs of crop production at a particular time), and hydrological terms (there are deficiencies in surface water supply based on measurements of stream flow and lake, reservoir, and groundwater levels) [7,9–11]. Meteorological droughts represent the primary cause of droughts, while the other types describe the secondary effects of a long-term precipitation deficit on measures such as soil moisture, river flows, and/or economic sectors [5]. Droughts are often considered as concealed phenomena due to the difficulty in estimating when they begin and when they end. The effects of a drought often accumulate slowly, and can last from several months up to years. This can impact all of the components of the hydrological cycle. A precipitation deficit, which typically leads to a drought, combined with high evapotranspiration losses, can cause a deficit in soil moisture [7,8,12]. For this reason, a quantitative assessment of the likelihood of occurrence and expected strength of a drought is crucial for understanding, monitoring, and mitigating the drought. Given the difficulty in predicting the evolution of droughts and their quantification in terms of duration, severity, and intensity, there have been many efforts to develop a drought indicator that is suitable for their monitoring [7,9,13].

In this study, we focus on the 2003 meteorological drought event that occurred in Europe, mainly affecting the Central European region (CEU) and the Mediterranean region (MED) (Figure 1). As a result of its unique geographic location, the MED is particularly vulnerable to climate variability and climate change. This region is located in the transition zone between the African climate regime (hot and dry) in the south and the European climate regime (mild and humid) in the north, thus experiencing large climate variation [14]. In the last few decades, the climate extremes registered in the MED and CEU displayed a relative increase in the duration of heat waves and a relative decrease in precipitation [8,15–19]. The year 2003 was characterised by one of the worst droughts recorded in Europe [15,20,21]. According to Levinson and Waple [15], the annual mean surface temperature in 2003 was above average throughout Europe. The primary reason for the 2003 drought in Europe was the increase in the frequency of warm temperature extremes; the global surface temperature was among the three highest temperatures ever recorded, estimated to be 0.46 °C above the 1961–1990 mean temperature [16,22]. The European heat waves of 2003 have been investigated in previous studies [2,8,23–28]. These heat waves, which represented the combination of anomalously high temperatures across most of the continent, induced a number of health, ecological, societal, and economic impacts. These impacts included forest fires, increased pollution, wilted crops, and excessive mortality of elderly individuals recorded in several countries across Europe [29,30].

A precipitation deficit occurring over an area may also be related to changes in moisture transport [17,31–33]. Thus, it is important to understand the origin of atmospheric moisture to close the atmospheric branch of the hydrological cycle. Understanding the source–sink relationships in the atmospheric water cycle is very important because of the role they play in extreme meteorological events [34]. Lagrangian approaches have been used worldwide in the last few years to estimate humidity changes along trajectories and to identify sources of moisture or sinks. Nieto et al. [35] analysed regions with different climates based on region boundaries defined in the 4th Assessment Report (AR4) of the Intergovernmental Panel on Climate Change (IPCC). Drumond et al. [32] analysed the variation in the moisture sources related to drier and wetter conditions in regions around the Mediterranean Basin for the period 2000–2005. Gomez-Hernandez et al. [31] extended the study of Drumond et al. [32] for a 21-year period, investigating the seasonal and interannual variability of the main atmospheric moisture sources over eight regions in the Mediterranean Basin. Recently, on a regional scale, Stojanovic et al. [36] investigated the anomalies in the moisture supply into the Danube River Basin during the two most severe meteorological drought episodes (1989/1990 and 2003), which they identified through the Standardised Precipitation Evapotranspiration Index (SPEI) analysis for the period 1980–2014.

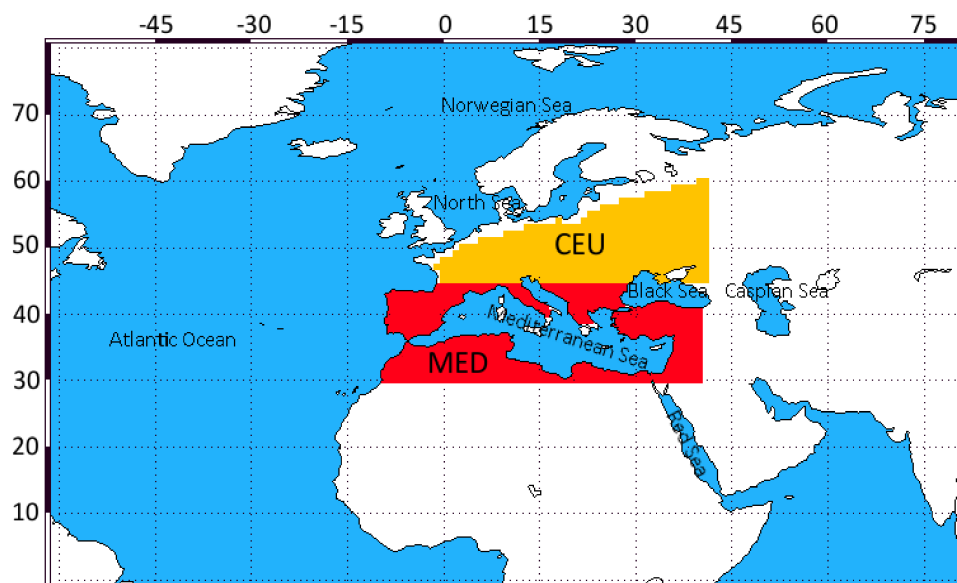


Figure 1. Central European (CEU) and Mediterranean (MED) regions. The respective boundaries were defined in the 5th Assessment Report (AR5) of the Intergovernmental Panel on Climate Change (IPCC).

In this work, our specific objectives are (1) to identify the main climatological moisture sources for CEU and MED during the period 1980–2015 by tracking the air masses that reached both regions backward in time through a Lagrangian methodology [37,38]; (2) to identify the meteorological drought events that occurred in CEU and MED over the period 1980–2015 through the SPEI [39], in order to characterise and rank the 2003 episode; and (3) to analyse the anomalies in the moisture supply in CEU and MED during the 2003 meteorological drought episode that affected most of Europe. Based on the same methodology that was applied by Stojanovic et al. [36] in their regional study for the Danube River Basin, here we focus on investigating the extension of the 2003 drought conditions across Europe on a continental scale, using a more recent Climate Research Unit (CRU) dataset, for the period 1980–2015. In this study, separate analyses were performed for two spatial domains: Central Europe and Mediterranean region, with the aim of comparing the drought conditions and anomalous moisture supply of both regions.

2. Data and Methods

2.1. Standardised Precipitation Evapotranspiration Index (SPEI)

To identify the meteorological drought episodes that occurred over CEU and MED (the boundaries of which were defined in the 5th Assessment Report (AR5) of the IPCC [6,19]) during 1980–2015, we computed the one-month SPEI (SPEI-1). The SPEI was first proposed by Vicente-Serrano et al. [39] as an improved drought index that was particularly suitable for studying the effect of global warming on droughts [40]. The SPEI follows the same conceptual approach as the Standardised Precipitation Index (SPI), but rather than concentrating on precipitation alone [9,41], it is based on a monthly climatic water balance (precipitation minus evapotranspiration). The SPEI has the advantage of combining multiscalar characteristics with the possibility of including the effects of temperature variability on the assessment of droughts. Therefore, it can point to anomalies in climatic water balance. The climatic water balance was calculated at various time scales (i.e., accumulation periods), and the resulting values were fit to a log-logistic probability distribution in order to transform the original values into standardised units that were comparable in space and time and at different SPEI time scales. The time scale over which the water deficit accumulates functionally separates meteorological, agricultural, and other types of drought. Similar to the Palmer Drought Severity Index (PDSI) [42], the SPEI

takes into account the effect of reference evapotranspiration on droughts, but its multiscalar nature allows for the identification of different types of droughts [40,43,44]. Many studies have shown that increasing temperatures affect droughts [45–47]. The role of temperature was evident in the drought in Central Europe during the summer of 2003. Extremely high temperatures over most of Europe caused the greatest damage to natural systems and increased the rates of evapotranspiration [23,24,30]. Therefore, the use of the SPEI, which includes temperature data in its formulation, is more suitable for identifying the drought episodes than indices that do not use temperature information [39,43]. Complete descriptions of the SPEI and comparisons with other indices are provided in previous studies [39,43,48–50]. For this study, the index was calculated using the Climate Research Unit (CRU) Time-Series (TS) Version 3.24.01 precipitation (PRE) and potential evapotranspiration (PET) data at an original spatial resolution of 0.5 degrees [51]. We then computed time series of PRE and PET averaged over the CEU and MED in order to calculate the SPEI-1 time series representative of each spatial domain. We chose the SPEI-1 time scale, which corresponds to the water balance for one month, because this time scale is closely related to meteorological droughts [52]. A drought episode starts when the SPEI value falls below zero, followed by a value of -1 or less, and ends when the SPEI returns to a positive value [41,53]. The criterion of McKee et al. [53] helped to classify the peak monthly value of the SPEI-1 registered during an episode, according to the four categories presented in Table 1.

Table 1. Drought classification based on the monthly Standardised Precipitation Evapotranspiration Index (SPEI-1) values and the respective time in category, according to the classification proposed by McKee et al. [53].

SPEI Values	Drought Category	Time in Category (%)
0 to -0.99	Mild	~24
-1.00 to -1.49	Moderate	9.2
-1.50 to -1.99	Severe	4.4
≤ -2.0	Extreme	2.3

2.2. Lagrangian Methodology

The Lagrangian approach that was developed by Stohl and James [37,38] was applied to identify the climatological moisture sources for CEU and MED during the period 1980–2015, and to analyse anomalies in the moisture supply over both regions during the 2003 meteorological drought. The approach was based on the FLEXible PARTicle (FLEXPART) dispersion model, which uses global data from the European Centre for Medium-Range Weather Forecasts (ECMWF): the ECMWF Re-Analysis ERA-Interim. This data set has a horizontal resolution of 1° on 61 vertical levels, ranging from 1000 to 0.1 hPa [54]. The application of the ERA-Interim reanalysis in reproducing the hydrological cycle, and in terms of water balance closure, was more realistic than the ERA-40 [55] and the newest reanalysis products, Modern Era Retrospective-Analysis for Research and Applications (MERRA) and Climate Forecast System Reanalysis (CFRS) [56]. As a result of the requirement of the FLEXPART dispersion model to use consistent, high-quality data for wind and humidity, the ERA-Interim reanalysis data were the most appropriate to be used [57].

The main advantage of this methodology was the convenience of establishing the relationship between the source and the receptor. This method was limited by the use of the time derivative of moisture; however, the use of a large number of particles and a large time period minimised the effects of unrealistic fluctuations [37,38,58]. Although other approaches, such as analytical models, box models, and physical water vapour traces (isotopes) can be used for similar purposes, the Lagrangian approach has an important advantage: it is able to calculate the path of moisture over time and enables the identification of the main moisture sources. A comparison of the methodologies and the main advantages and disadvantages of the approach applied in this study is presented in Gimeno et al. [59].

In the FLEXPART simulation, the global atmosphere was divided homogeneously into approximately 2 million particles with constant mass, transported using 3D wind fields. The changes in specific humidity (q) of each particle along its path were computed every 6 h. They could be expressed as follows: $e - p = m(dq/dt)$, where m is the mass of the particle and $e - p$ (evaporation minus precipitation) represents the freshwater flux associated with the particle. By adding $(e - p)$ for all of the particles residing in the atmospheric column over a given area, we obtained the total $(E - P)$ field. This represents the surface freshwater flux connected with the tracked particles, where (E) indicates the evaporation rate and (P) indicates the precipitation rate per unit area.

The trajectories of the particles may be traced using a backward in time analysis to determine the sources of moisture for a given region (areas where the particles obtain moisture, $(E - P) > 0$), and using a forward in time analysis to identify the sinks of the moisture transported by particles leaving a given region (areas where the particles lost moisture, $(E - P) < 0$). The particles were tracked for a period of 10 days, which is the global average residence time of water vapour in the atmosphere [60]. In this study, the trajectories of the particles that reached the CEU and MED regions were obtained by backward tracking for the period 1980–2015, and we identified the moisture sources on an annual basis. Then, the trajectories were tracked forward in time from these defined sources in order to analyse the monthly anomalies in the moisture supply to CEU and MED during the 2003 drought episode. The monthly anomaly was computed as the difference between the monthly average and the respective monthly climatological mean. Therefore, the anomaly for January 2003 is ((monthly mean January 2003) – (climatology January 1980–2015)).

3. Results and Discussion

3.1. Identification of the Major Climatological Moisture Sources for the Central European and Mediterranean Regions

To identify the major climatological moisture sources for CEU and MED, we tracked the air masses over the given regions backward in time for the period 1980–2015. The areas where evaporation exceeded precipitation in the net moisture budget ($(E - P) > 0$) represented the area of the moisture sources. In order to define the threshold that limited the spatial extent of the moisture sources, we used the 95th percentile of the positive values of $E - P$ obtained from the global climatology on an annual scale. The 95th percentile defined those regions where the air masses were likely to take up a large amount of moisture on their path to the target region.

3.1.1. Moisture Sources for Central Europe

According to the threshold of 0.06 mm/day, which corresponded to the 95th percentile of the annual averages of $(E - P) > 0$ obtained from the backward in time experiment (Figure 2a), CEU (Figure 2b) received moisture from seven different oceanic and terrestrial moisture sources: the North Atlantic (NAT), Mediterranean Sea (MDS), Baltic Sea (BAS), Black Sea (BLS), Caspian Sea (CPS), terrestrial moisture sources surrounding the region (TER), and itself (CEU). Through the forward in time analysis from these seven sources towards the CEU sink, the climatological results on an annual scale revealed that the moisture contribution came mainly from two sources: MDS (34%) and CEU (35%). During the boreal summer months, CEU was the main source, while MDS prevailed during the winter months (Figure 2c).

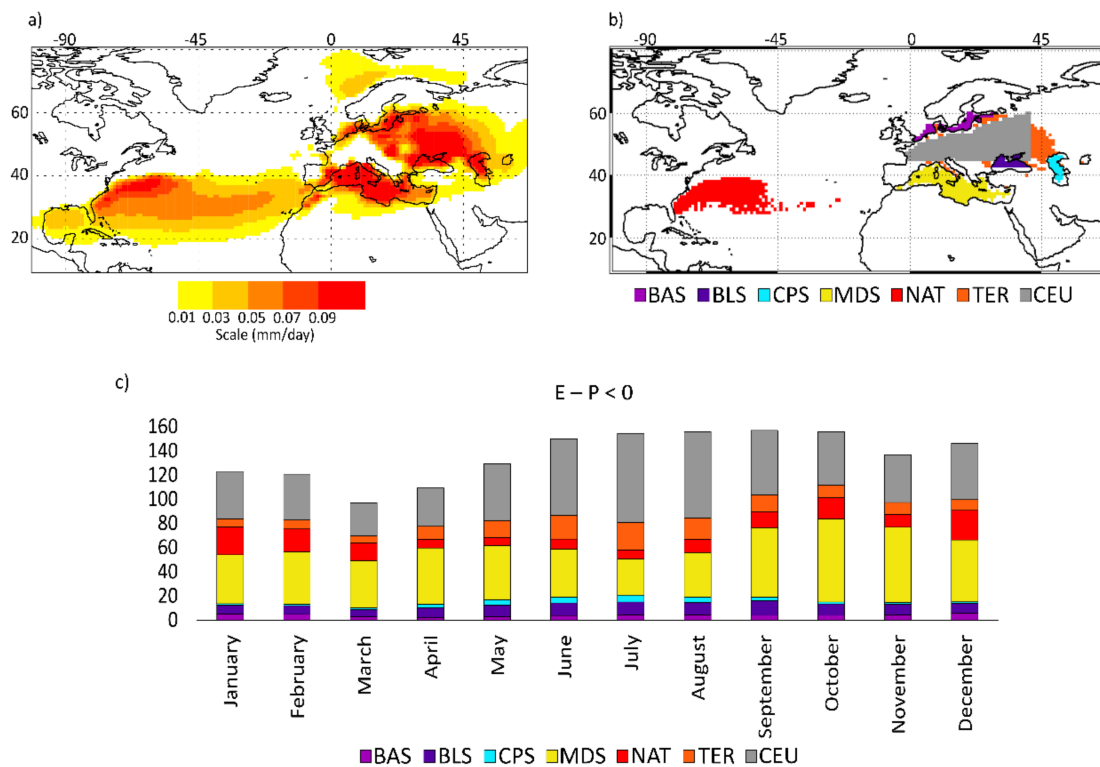


Figure 2. (a) Climatological annual (evaporation (E) – precipitation (P) > 0) values integrated backward in time over 10 days for the Central Europe region (CEU) (mm/day); (b) Schematic representation of the main moisture sources for the CEU during 1980–2015: North Atlantic (NAT), Mediterranean Sea (MDS), Baltic Sea (BAS), Black Sea (BLS), Caspian Sea (CPS), terrestrial moisture sources surrounding the region (TER), and itself (CEU); (c) Moisture contribution (E – P < 0) from the sources to CEU estimated through the forward in time experiment (mm/day).

3.1.2. Moisture Sources for the Mediterranean Region

We tracked the air masses over MED backward in time to identify the sources of moisture. The areas where $E - P > 0$ represented the areas where evaporation exceeded precipitation in the net moisture budget (Figure 3a). The main moisture sources for MED, according to the threshold of 0.04 mm/day (95th percentile of $E - P > 0$), are displayed in Figure 3b. These included the Gulf of Mexico (GMX), Gibraltar (GIB), MDS, BLS, CPS, TER, and itself (MED). Through the forward in time analysis from these sources towards the MED sink, the climatological results on an annual scale revealed that the moisture originated from two main sources: MDS (45%) and MED (33%). During the whole year, MDS appeared to be the major moisture source (Figure 3c).

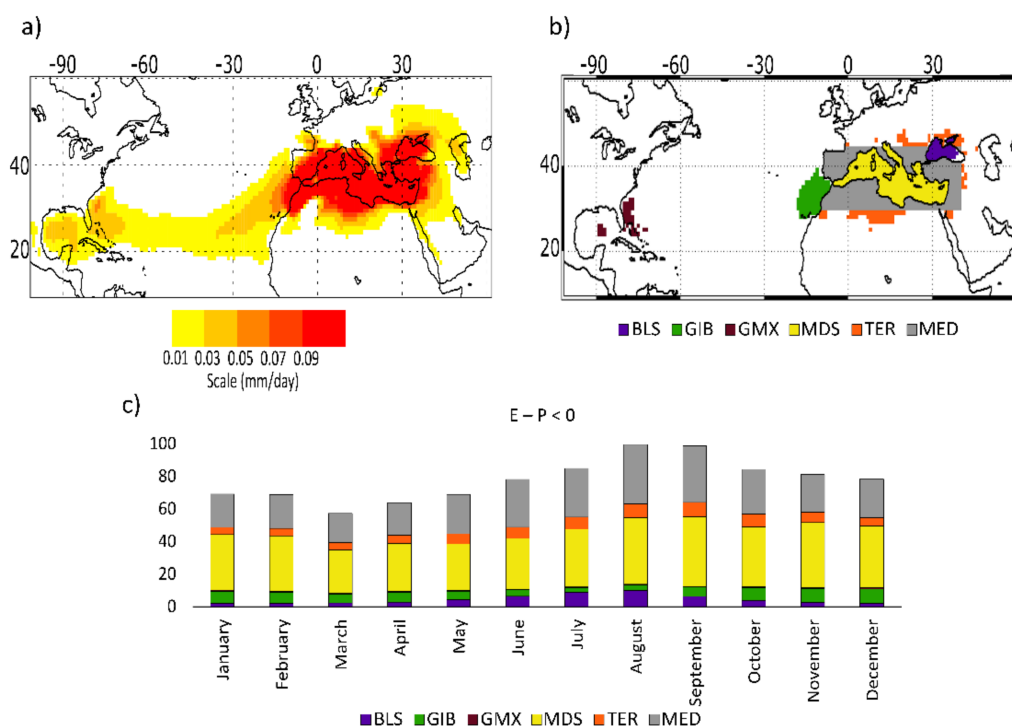


Figure 3. (a) Climatological annual ($E - P > 0$) values integrated backward in time over 10 days for the Mediterranean region (MED) (mm/day); (b) Schematic representation of the main moisture sources for the MED during 1980–2015: Gulf of Mexico (GMX), Gibraltar (GIB), Mediterranean Sea (MDS), Black Sea (BLS), terrestrial moisture sources surrounding the region (TER), and itself (MED); (c) Moisture contribution ($E - P < 0$) from the sources to the MED estimated through the forward in time experiment (mm/day).

3.2. The Extension of the Drought Conditions over Europe during 2003

The meteorological drought episodes over CEU and MED that occurred during 1980–2015 were selected using the SPEI-1 (Figure 4), which corresponded to the water balance for one month. The negative SPEI-1 values indicated dry conditions (red bars in Figure 4). Additionally, accompanying the criteria for the identification of drought episodes from McKee et al. [53], we identified 51 drought episodes that occurred over CEU and 48 that occurred over MED during the analysed period.

Some properties of the drought episodes that occurred over CEU and MED are presented in the Table 2. Severity represents the absolute value of the sum of all of the SPEI values during the episode. Therefore, for the episode that occurred over CEU, the severity was 7.10, while for the episode that occurred over MED, the severity was 7.23. Among all of the drought episodes that occurred over CEU and MED during the period 1980–2015, the 2003 episode was the most severe. A characterization of the 2003 drought episode was also conducted for each region in terms of duration (indicating the number of the months between the first and last months) and intensity (the ration between severity and duration). The number in parenthesis represents the rank occupied by the episode in comparison to the other episodes that occurred over the same region during the period 1980–2015. The 2003 drought episode for CEU lasted from February 2003 to June 2003 (five months)—the fourth longest when considering all of the episodes in the studied period. Although the 2003 episode for MED lasted from May 2003 to August 2003 (four months), it was the 10th longest event that was registered for this region. The SPEI-1 for this CEU drought episode reached a peak of -1.86 (severe), while the MED SPEI-1 reached a value of -2.71 (extreme). The MED episode was the third most intense episode (1.91) registered for this region during 1980–2015, while the CEU episode was not as intense (occupying the 11th rank) when compared to the rest of episodes over the same region. In summary, except for

the severity (both episodes were the most severe for both regions), Table 2 suggests that the 2003 episode appeared to be more significant for the MED region when compared to the rest of the episodes identified over the same region during 1980–2015. This is because it appeared between the three most important events in terms of severity, intensity, and peak SPEI-1 value.

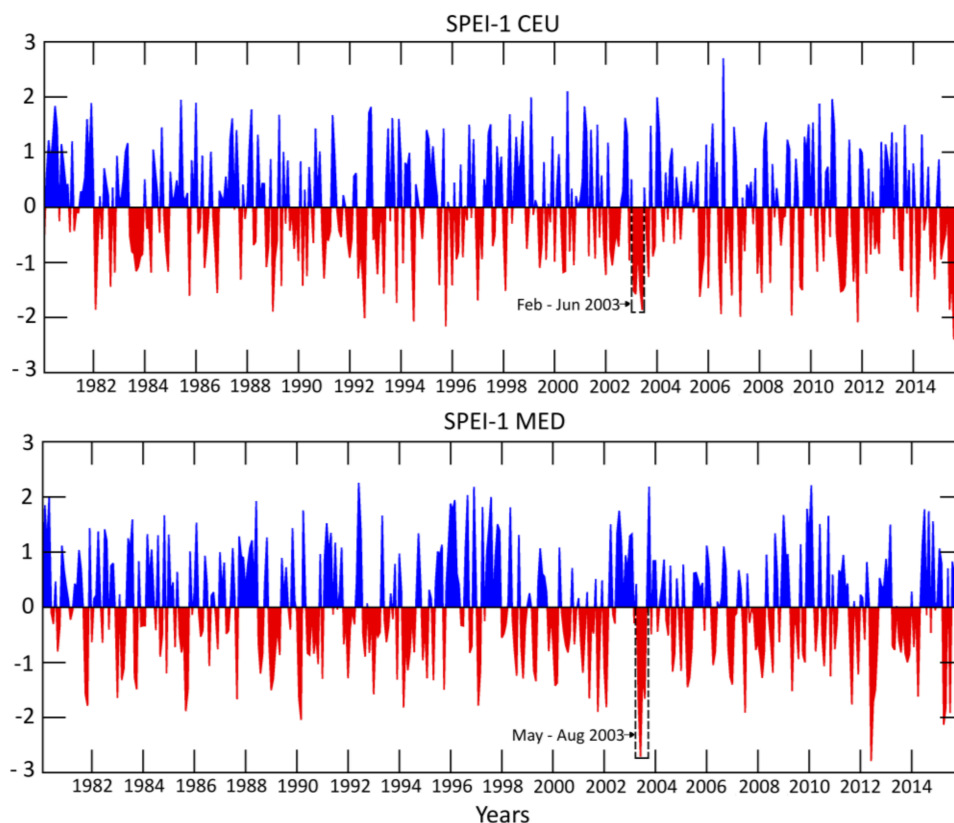


Figure 4. Time series of Standardised Precipitation Evapotranspiration Index for one month (SPEI-1) over the Central European region (**top panel**) and Mediterranean region (**bottom panel**) during 1980–2015. Positive values are in blue and negative values are in red. The black rectangles show the development of the drought episode over the Central European and Mediterranean regions during 2003.

Table 2. Characteristics of the 2003 drought episode that occurred over the Central Europe region (CEU) and the Mediterranean region (MED). The number in parenthesis indicates the rank occupied by the episode in comparison to the other episodes identified over the respective region during 1980–2015. For the peak monthly Standardised Precipitation Evapotranspiration Index for one month (SPEI-1) values, the lowest value observed in the 36-year monthly SPEI-1 time series occupies the first rank position.

Region	Drought Episode	Severity	Duration (Months)	Intensity	Peak Monthly SPEI-1 Value
CEU	February–June	7.10 (1st)	5 (4th)	1.42 (11th)	June −1.86 (11th)
MED	May–August	7.23 (1st)	4 (10th)	1.81 (3rd)	June −2.71 (2nd)

The SPEI-1 maps over Europe during 2003 are represented in Figure 5 in order to illustrate the tempo-spatial evolution of the drought conditions over the continent. In this figure, the SPEI-1 values were calculated at every grid point. The negative SPEI-1 values indicated dry conditions, while the

positive SPEI-1 values indicated wet conditions. Figure 5 shows that during January, positive values of SPEI-1 prevailed over Europe. From February (the beginning of the drought episode over CEU) to June (the end of the drought episode over CEU), the negative SPEI-1 values indicated that dry conditions extended over CEU and reached severe dry conditions in June, with a peak value of -1.86 . From July to December, the dry conditions lessened over CEU. For MED, there was an increase in dry conditions from May to August; June was the month with higher SPEI-1 values over the area of study, reaching the category of extreme drought ($\text{SPEI-1} < -2.0$).

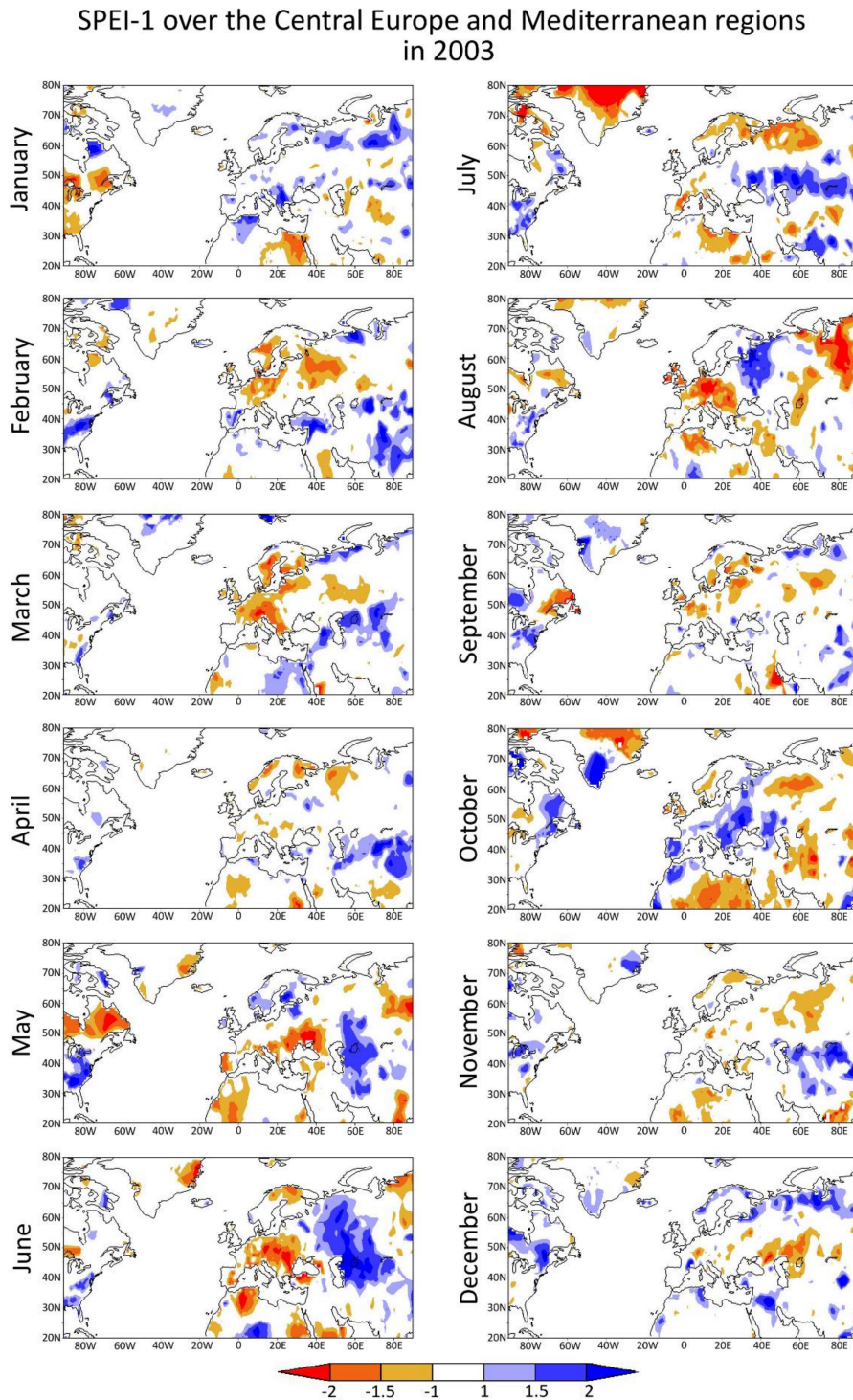


Figure 5. SPEI-1 values in 2003 over the European area.

Figure 6 shows monthly anomalies of the ERA-Interim vertically integrated moisture flux (vector) and its divergence (shaded) during 2003 to illustrate the relationship between the drought and the spatio-temporal variation of the large-scale atmospheric fields. Regions of divergence (reddish colour) prevailed over Central Europe during 2003 (with the most significant exceptions in January, April, July, and October), indicating the reduction of precipitation over this large spatial domain during the year. From April to August, those divergent conditions extended towards the Mediterranean region, prevailing over the central North Africa, Iberian Peninsula, Italy, the Balkan Peninsula, and Eastern Mediterranean. The persistence and predominance of an anomalous anticyclonic circulation over Europe during nearly the whole of 2003 (although displaced over different regions throughout the year) most likely inhibited the moisture transport that occurs climatologically from the Mediterranean towards the continent. This anomalous anticyclonic circulation appeared to be localised over Northern Europe during February and March. In May and June, it was configured over Central Europe, and it appeared centred over the British Isles in August. Between the main contributing factors that were responsible for the occurrence of this drought episode, Garcia-Herrera et al. [25] addressed the role of the northward displacement of the Azores anticyclone in enhancing the summer blocking episodes.

3.3. Anomalies during the Drought Episode That Occurred in 2003 Over Europe

3.3.1. Central Europe Drought Episode: February 2003 to June 2003

Monthly anomalies of the PRE, PET, and pressure velocity (ω) at 500 hPa, averaged over CEU during the drought episode of February to June 2003, are presented in Figure 7a. The bars in Figure 7b represent the monthly anomalies of the moisture supply ($E - P < 0$) over CEU, measured by the particles leaving the sources defined in Section 3.1 and obtained via the forward in time experiment. The lines show the PRE anomalies that were accumulated during the episode (AA-1). The two months before and after the drought episode were also plotted to observe the onset and end of the event.

For every month, bars for each source region are displayed. The height of each coloured rectangle (calculated from the difference between the upper and lower rectangle values) represents the anomalous contribution from the appropriate source. This means that larger coloured rectangles were associated with a more intense anomalous contribution. The superimposition of the anomalous moisture supply allowed us to estimate the accumulated anomalies in the moisture contribution from all of the investigated sources in a given month. The values are indicated by the green triangles.

Figure 7b shows that in February 2003—the onset of the drought episode—the moisture supply to CEU from all sources was reduced, and negative anomalies of PRE and positive anomalies of pressure velocity (indicating subsidence) prevailed (Figure 7a). From March 2003 to June 2003, there was a small increase in the moisture supply from the BAS, NAT, and CEU itself. However, the contribution from these sources was not sufficient to change the sign of the precipitation anomaly. The positive anomalies of PET and pressure velocity, and the most intense negative accumulated anomaly for PRE (AA-1), in June 2003 can be associated with the negative anomaly of PRE during the drought episode. A reduction in the moisture supply from almost all of the sources was also notable. In July 2003, the anomaly of PRE showed positive values (Figure 7a), and the accumulated loss of moisture from all of the sources was negative; the BAS, BLS, and CEU showed positive anomaly contributions. The CEU source was the most important climatological source in July, and it may have impacted the modulation of the precipitation anomalies. During August, the support of moisture from CEU increased to a point such that the sign reversed.

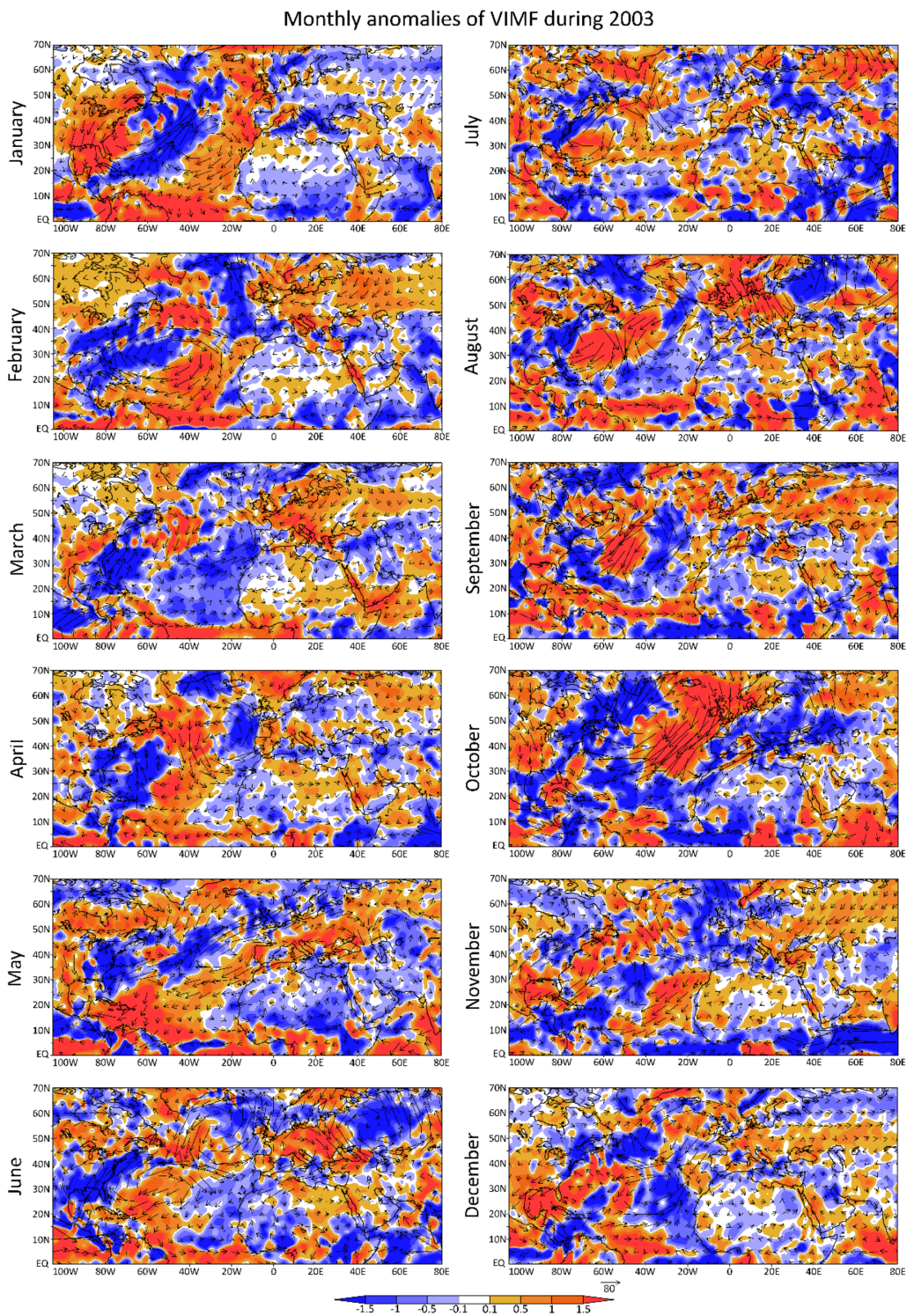


Figure 6. Monthly anomalies of the ERA-Interim vertically integrated moisture flux (VIMF) (vector, kg/(m/s)) and its divergence (shaded, mm/day) in 2003.

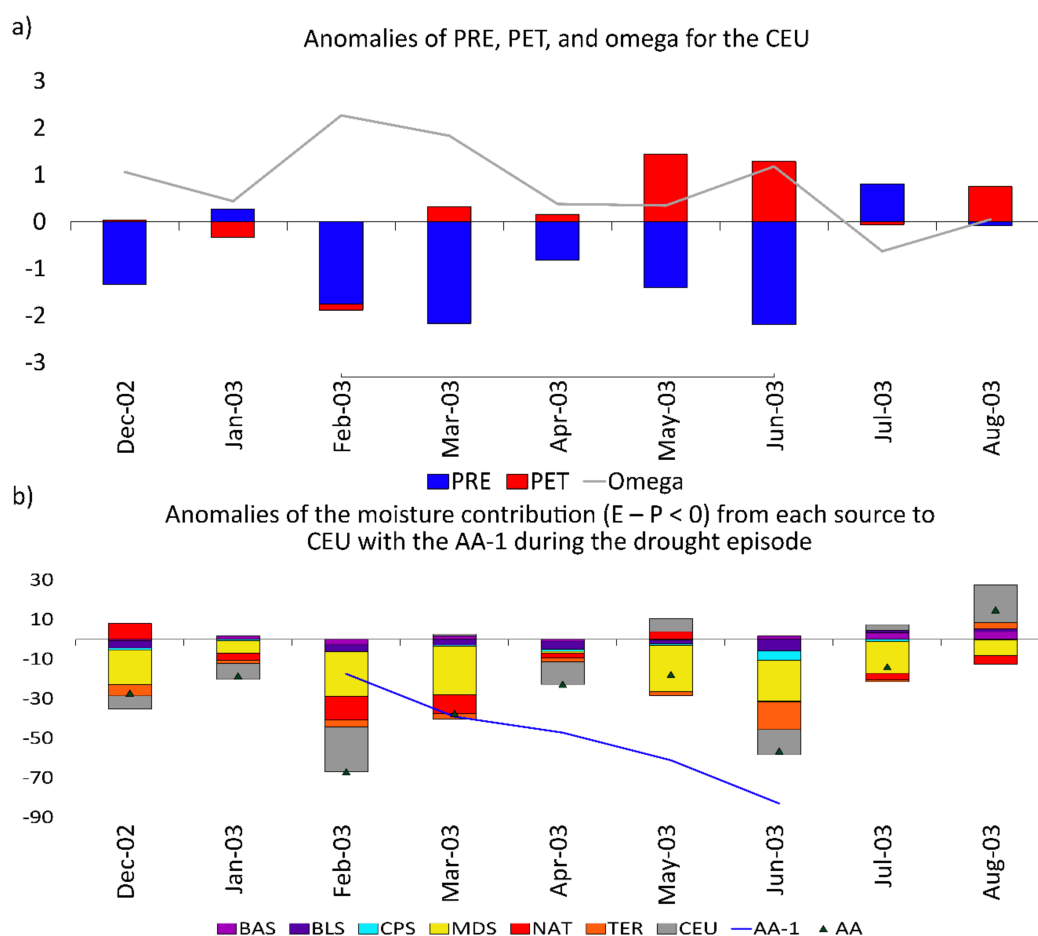


Figure 7. (a) Monthly anomalies of the precipitation (PRE, /10 mm/month), potential evapotranspiration (PET, /10 mm/month) (data from Climatic Research Unit (CRU) Time-Series (TS) 3.24.01), and average pressure velocity at 500 hPa (data from ERA-Interim) over the Central European region (CEU); and (b) Anomalies in the moisture supply ($E - P < 0$) for each source over CEU, obtained via the forward FLEXible PARTicle (FLEXPART) experiment (mm/day) with the accumulated anomaly of the supply from all of the sources (AA, mm/day) and the accumulated precipitation anomalies (AA-1, mm/month) (data from CRU 3.24.01) for the episode from February 2003 to June 2003.

The anomalies in the moisture supply from the sources to CEU that were accumulated during the February to June 2003 episode are displayed in Table 3. There was a predominance of reduced moisture supply from the studied sources. When we compared the accumulated values from the sources, the results indicated that the MDS source registered the most intense accumulated negative anomalies, followed by CEU (−91.95 and −39.42 mm/day, respectively).

Table 3. Anomalies of the moisture supply from the sources to the Central European region that were accumulated during the drought episode from February to June 2003 (mm/day). North Atlantic (NAT); Mediterranean Sea (MDS); Baltic Sea (BAS); Black Sea (BLS); Caspian Sea (CPS); terrestrial moisture sources surrounding the region (TER).

BAS	BLS	CPS	MDS	NAT	TER	CEU
−0.2	−18.2	−7.3	−91.9	−20.4	−23.9	−39.4

Table 4 shows the Pearson correlation coefficients between the time series of monthly anomalies in the moisture supply from the sources to CEU and the SPEI-1, in an attempt to reveal joint linear

variability during the period 1980–2015 (432 times). Although all of the values were positive, the BLS, CEU, MDS, and TER showed the highest annual correlation values (exceeding 0.5). This indicated that an inhibited moisture supply from these sources was linearly associated with dry conditions over CEU on the SPEI-1 scale.

Table 4. Pearson correlation coefficients between the time series of monthly anomalies in the moisture supply from the sources to the Central European region and the SPEI-1 for the period 1980–2015 (432 times). Except for the BAS, the coefficients are significant at 99.9%, according to Student’s *t*-test.

Moisture Sources	Correlation Coefficient
BLS	0.61
CEU	0.60
MDS	0.58
TER	0.57
NAT	0.44
CPS	0.30
BAS	0.04

3.3.2. The Mediterranean Region Drought Episode: May to August 2003

The drought that occurred over MED in 2003 has been investigated in previous studies [25,61–63]. This event received considerable attention because it had adverse social, economic, and environmental effects [25].

Similar to Figure 7, Figure 8a represents the monthly anomalies of the PET, PRE, and pressure velocity (ω) at 500 hPa, averaged over MED. Figure 8b represents the monthly anomalies of the moisture supply ($E - P < 0$) to the MED, measured by the particles leaving the main sources and the MED during the drought episode, together with the accumulated PRE anomalies (AA-1) and the accumulated anomalies of the moisture supply from all of the sources.

Figure 8b shows that in May 2003, the month in which the onset of the episode was observed, the moisture supply from almost all of the selected sources declined (except from the BLS and MED). In June 2003 (when the SPEI-1 value reached its peak), the moisture contribution from all of the sources declined. In July 2003, positive anomalies of moisture contribution prevailed, which were associated with some weakening in the negative anomaly of PRE. The drought episode ended in August 2003, and was associated with positive anomalies of PRE from September onwards. An intensified moisture contribution from the MDS and TER sources occurred in September 2003, while in October 2003, this intensification came mainly from the MDS, GIB, and MED.

In general, during the drought episode from May 2003 to August 2003, the contribution from the principal source of moisture—the MDS—greatly reduced, along with the negative accumulated anomaly of PRE AA-1 and positive anomalies of pressure velocity and PRE. Our findings were in agreement with those of Mariotti et al. [64], Drumond et al. [65], and Lionello et al. [63], who showed the importance of moisture transported by air masses travelling from the MDS.

The anomalies in the moisture supply from the sources to the MED accumulated during the 2003 episode are presented in Table 5, summarizing the effect of each source. In general, a reduction in the moisture supply from the studied sources prevailed during the episode, with the exception of the BLS and TER. The results also indicated that the MDS source registered the highest accumulated negative anomalies (−23.29 mm/day), followed by the GIB source (−4.82 mm/day) and the MED source (−1.82 mm/day).

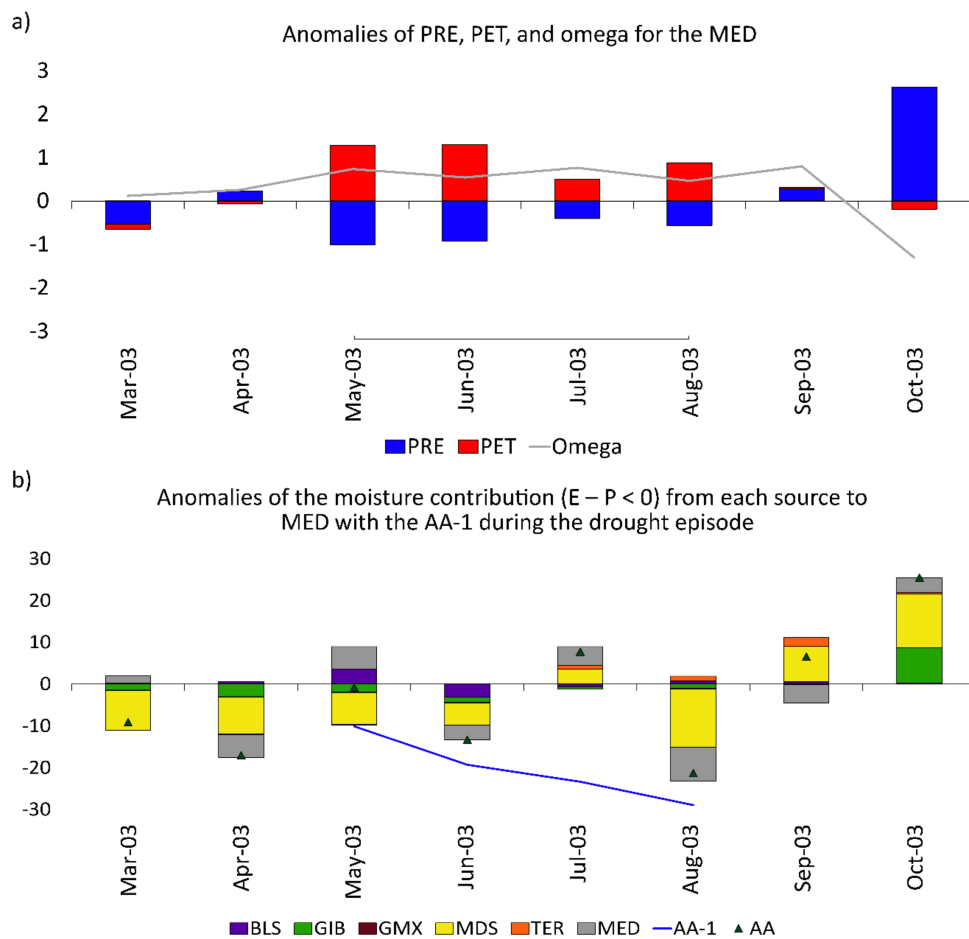


Figure 8. (a) Monthly anomalies of the precipitation (PRE, /10 mm/month), potential evapotranspiration (PET, /10 mm/month) (data from Climatic Research Unit (CRU) Time-Series (TS) 3.24.01), and average ERA-Interim pressure velocity at 500 hPa over the Mediterranean region; and (b) Anomalies in the moisture supply ($E - P < 0$) from each source over the Mediterranean region, obtained via the forward in time experiment (mm/day) with the accumulated anomaly of the supply from all of the sources (AA, mm/day) and the accumulated precipitation anomalies (data from CRU TS 3.24.01) (AA-1, mm/month) for the episode from May to August 2003.

Table 5. Anomalies of the moisture supply from the sources to the Mediterranean region accumulated during the drought episode from May to August 2003 (mm/day). Gibraltar (GIB); Gulf of Mexico (GMX).

BLS	GIB	GMX	MDS	TER	MED
0.66	-4.82	-0.27	-23.29	1.82	-1.82

Similar to Table 4, Table 6 shows the Pearson correlation coefficients between the anomalies in the moisture supply from the sources to the MED and the SPEI-1 time series for the period 1980–2015. The analysis showed that the GIB and TER had the highest correlation values (higher than 0.5), followed by the MED and MDS. Focusing on the maritime sources, this indicated that the reduction in the moisture supply from the GIB and MDS was linearly associated with dry conditions over the MED on the SPEI-1 scale. It is worth noting that although the total contribution from GIB to MED was relatively small—as shown in Figure 8 and Table 5—the correlation analysis (Table 6) reveals some important joint linear temporal variability between the moisture supply and the variability of SPEI-1 over MED.

Table 6. Pearson correlation coefficients between the time series of monthly anomalies in the moisture supply from the sources to the Mediterranean region and the SPEI-1 for the period 1980–2015 (432 times). The coefficients are significant at 99.9% for all of the sources, according to Student's *t*-test.

Moisture Sources	Correlation Coefficient
GIB	0.54
TER	0.51
MED	0.47
MDS	0.41
GMX	0.23
BLS	0.17

4. Summary

The aim of this study was to investigate the anomalies in the moisture supply observed during the meteorological drought episode that occurred over large parts of the European continent in 2003 through the Lagrangian methodology. In order to do this, we first identified the main climatological moisture sources for CEU and MED on an annual scale for the period 1980–2015, by tracking the air masses that reached the regions backward in time.

The results indicated that CEU mainly received moisture from seven different oceanic and terrestrial moisture sources. These included the NAT, MDS, BAS, BLS, CPS, TER, and CEU (itself). The main moisture sources for MED were the GMX, GIB, MDS, BLS, TER, and MED (itself). For both regions, the main climatological moisture source was MDS.

The analysis of the SPEI for CEU and MED revealed that the period from February to June 2003 (five months) for CEU, and May 2003 to August 2003 (four months) for MED, contained the most severe meteorological drought episodes in the regions during 1980–2015, according to this index calculated on a one-month time scale (SPEI-1).

The SPEI-1 for the episode from February to June 2003 (CEU) reached a peak of -1.86 , which belonged to the severe category, while the episode from May to August 2003 (MED) reached a peak of -2.71 , which is contained within the extreme category. The episode initially started in Central Europe (February 2003). For both regions, June 2003 was the month in which the SPEI-1 reached its peak value.

Except for the severity, the results suggested that the 2003 episode appeared to be more significant for the MED region when compared to the rest of the episodes identified over the same region during 1980–2015. This was because it appeared between the three most important events in terms of severity, intensity, and peak SPEI-1 value.

The analysis of the variation in the moisture supply indicated that the beginning of the drought episode over CEU was associated with a reduction in the moisture supply from all of the selected sources. This was the month in which the positive anomalies of pressure velocity reached their peak. The 2003 episode over MED (May to August 2003) was characterised by an anomalous subsidence, increased PET, and reduced PRE, which was associated with the predominance of reduced moisture supply from almost all of the detected moisture sources, with the exception of the BLS and TER. The episode that occurred over CEU ended when CEU itself began to provide moisture, while the episode that occurred over MED ended when MDS began to provide moisture.

MDS, which was the major climatological moisture contributor for CEU and MED, was the source that presented the most intense reduction in moisture supply for both regions. It appeared that the moisture advection from MDS was related to the anomalous anticyclonic circulation, localised over Europe, which inhibited the transport of moisture to the analysed regions. A linear inter-annual correlation analysis indicated that the correlation between the moisture supply from MDS and the SPEI-1 time series over the selected regions was stronger in CEU.

Previous authors have pointed to the importance of the Mediterranean Sea as the source of moisture for different regions in Europe. For example, Sodemann et al. [66] investigated the seasonal

and inter-annual variability of the moisture source for precipitation in the European Alps during 1995–2002, and showed the strong influence that the Mediterranean moisture source has for the Southern Alps. Schicker et al. [67] identified the Mediterranean Sea as an important moisture source for the Mediterranean region.

According to Levinson and Waple [15] and Ogi et al. [68], the summer of 2003 was one of the warmest, and a heat wave affected most of Europe. Two distinct periods of exceptional heat occurred. The first was in June and the second was during July–August. Across Europe, above-normal temperatures were recorded, accompanied by an almost complete absence of rainfall. Recently, Stojanovic et al. [36] found that the 2003 drought episode that occurred over the Danube River Basin was accompanied by a reduction in precipitation and an increase in potential evapotranspiration. Our findings are in agreement with these previous studies on drought. June was the month in which the most intensive negative accumulated anomalies for precipitation (PRE) were recorded across Central Europe. It was also the month in which the moisture contribution from all of the sources reduced over both regions.

Acknowledgments: Thanks for the funding by the Spanish Government and FEDER through the SETH (CGL2014-60849-JIN) project. Milica Stojanovic's Ph.D. fellowship is supported by European Commission under the Erasmus Mundus project Green-Tech-WB: Smart and Green technologies for innovative and sustainable societies in Western Balkans (551984-EM-1-2014-1-ES-ERA Mundus-EMA2). We also thank the IMDROFLOOD project financed by the Water Works 2014 co-funded call of the European Commission.

Author Contributions: Milica Stojanovic, Anita Drumond, and Luis Gimeno conceived of and designed the experiments. Milica Stojanovic performed the experiments and Milica Stojanovic, Anita Drumond, and Luis Gimeno analyzed the data. Milica Stojanovic, Anita Drumond, Raquel Nieto, and Luis Gimeno wrote the paper.

Conflicts of Interest: The authors declare no conflict of interest. The founding sponsors had no role in the design of the study; in the collection, analyses or interpretation of data; in the writing of the manuscript; nor in the decision to publish the results.

References

1. Intergovernmental Panel on Climate Change (IPCC). *Climate Change 2001: Impacts, Adaptation and Vulnerability*; Contribution of Working Group II to the Third Assessment Report of the Intergovernmental Panel on Climate Change; Cambridge University Press: Cambridge, UK, 2001.
2. Lehner, B.; Döll, P.; Alcamo, J.; Henrichs, T.; Kaspar, F. Estimating the Impact of Global Change on Flood and Drought Risks in Europe: A Continental, Integrated Analysis. *Clim. Chang.* **2006**, *75*, 273–299. [[CrossRef](#)]
3. Tsiourtis, N.X. *Drought Management Plans for the Mediterranean Region*; Water Development Department: Nicosia, Cyprus, 2001; pp. 1–19.
4. Popova, Z. Drought vulnerability estimated based on crop-yield models. In *Drought Management Centre for South-East Europe-DMCSEE—Summary of Project Results*; Slovenian Environmental Agency: Ljubljana, Slovenia, 2012; pp. 39–54.
5. Spinoni, J.; Naumann, G.; Vogt, J.; Barbosa, P. Meteorological Droughts in Europe: Events and Impacts: Past Trends and Future Projections. 2016. Available online: http://www.droughtmanagement.info/literature/EC-JRC_Report%20on%20Droughts%20in%20Europe_2016.pdf (accessed on 15 September 2017).
6. Intergovernmental Panel on Climate Change (IPCC). *Climate Change 2014: Synthesis Report*; Contribution of Working Groups I, II and III to the Fifth Assessment Report of the Intergovernmental Panel on Climate Change; Pachauri, R.K., Meyer, L.A., Eds.; IPCC: Geneva, Switzerland, 2014; 151p.
7. Wilhite, D.A.; Glantz, M.H. Understanding the Drought Phenomenon: The Role of Definitions. *Water Int.* **1985**, *10*, 111–120. [[CrossRef](#)]
8. Ionita, M.; Tallaksen, L.M.; Kingston, D.G.; Stagge, J.H.; Laaha, G.; Van Lanen, H.A.J.; Scholz, P.; Chelcea, S.M.; Haslinger, K. The European 2015 drought from a climatological perspective. *Hydrol. Earth Syst. Sci.* **2017**, *21*, 1397–1419. [[CrossRef](#)]
9. World Meteorological Organization. Drought Monitoring and Early Warning: Concepts, Progress and Future Challenges. 2006. Available online: <http://www.wamis.org/agm/pubs/brochures/WMO1006e.pdf> (accessed on 11 May 2017).

10. Dai, A. Drought under global warming: A review. *WIREs Clim. Chang.* **2010**, *2*, 45–65. [[CrossRef](#)]
11. Panu, U.S.; Sharma, T.C. Challenges in drought research: Some perspectives and future directions. *Hydrol. Sci. J.* **2002**, *47*, S19–S30. [[CrossRef](#)]
12. Tallaksen, L.M.; Van Lanen, H.A.J. Hydrological drought: Processes and estimation methods for streamflow and groundwater. In *Developments in Water Science*; Elsevier Science B.V.: Amsterdam, The Netherlands, 2004; Volume 48.
13. Rahmat, S.N. Methodology for Development of Drought Severity-Duration-Frequency (SDF) Curves. Ph.D. Thesis, RMIT University, Melbourne, Australia, 28 August 2014.
14. Goubanova, K.; Li, L. Extremes in temperature and precipitation around the Mediterranean Basin in an ensemble of future climate scenario simulation. *Glob. Planet Chang.* **2007**, *57*, 27–42. [[CrossRef](#)]
15. Levison, D.H.; Waple, A.M. State of the climate in 2003. *Bull. Am. Meteorol. Soc.* **2004**, *85*, S1–S72.
16. Luterbacher, J.; Dietrich, D.; Xoplaki, E.; Grosjean, M.; Wanner, H. European seasonal and annual temperature variability, trends, and extremes since 1500. *Science* **2004**, *303*, 1499–1503. [[CrossRef](#)] [[PubMed](#)]
17. García-Ruiz, J.M.; López-Moreno, J.I.; Vicente-Serrano, S.M.; Lasanta-Martínez, T.; Beguería, S. Mediterranean water resources in a global change scenario. *Earth Sci. Rev.* **2011**, *105*, 121–139. [[CrossRef](#)]
18. Lelieveld, J.; Hadjinicolaou, P.; Kostopoulou, E.; Chenoweth, J.; El Maayer, M.; Giannakopoulos, C.; Hannides, C.; Lange, M.A.; Tanarhte, M.; Tyrlis, E.; et al. Climate change and impacts in the Eastern Mediterranean and the Middle East. *Clim. Chang.* **2012**, *114*, 667–687. [[CrossRef](#)] [[PubMed](#)]
19. Intergovernmental Panel on Climate Change (IPCC). *Climate Change 2013: The Physical Science Basis*; Contribution of Working Group I to the Fifth Assessment Report of the Intergovernmental Panel on Climate Change; Intergovernmental Panel on Climate Change: Cambridge, UK; New York, NY, USA, 2013.
20. Andrade, C.; Leite, S.M.; Santos, J.A. Temperature extremes in Europe: Overview of their driving atmospheric patterns. *Nat. Hazards Earth Syst. Sci.* **2012**, *12*, 1671–1691. [[CrossRef](#)]
21. Carril, A.F.; Gualdi, S.; Cherchi, A.; Navarra, A. Heatwaves in Europe: Areas of homogenous variability and links with the regional to large-scale atmospheric and SSTs anomalies. *Clim. Dyn.* **2008**, *30*, 77–98. [[CrossRef](#)]
22. European Academies Science Advisory Council (EASAC). *Trends in Extreme Weather Events in Europe: Implications for National and European Union Adaptation Strategies*; EASAC Policy Report 22; European Academies Science Advisory Council: Halle, Germany, 2013.
23. Fink, A.H.; Brücher, T.; Krüger, A.; Leckebusch, G.C.; Pinto, J.G.; Ulbrich, U. The 2003 European summer heatwaves and drought-synoptic diagnosis and impacts. *Weather* **2004**, *59*, 209–216. [[CrossRef](#)]
24. Fischer, E.M.; Seneviratne, S.I.; Vidale, P.L.; Lüthi, D.; Schär, C. Soil Moisture—Atmosphere Interactions during the 2003 European Summer Heat Wave. *J. Clim.* **2007**, *20*, 5081–5099. [[CrossRef](#)]
25. Garcia-Herrera, R.; Diaz, J.; Trigo, R.M.; Luterbacher, J.; Fischer, E.M. A review of the European Summer heat wave of 2003. *Crit. Rev. Environ. Sci. Technol.* **2010**, *40*, 267–306. [[CrossRef](#)]
26. Vautard, R.; Yiou, P.; D’Andrea, F.; de Noblet, N.; Viovy, N.; Cassou, C.; Polcher, J.; Ciais, P.; Kageyama, M.; Fan, Y. Summertime European heat and drought waves induced by wintertime Mediterranean rainfall deficit. *Geophys. Res. Lett.* **2007**, *34*, L0771. [[CrossRef](#)]
27. Schär, C.; Vidale, P.L.; Lüthi, D.; Frei, C.; Haberli, C.; Liniger, M.A.; Appenzeller, C. The role of increasing temperature variability in European summer heatwaves. *Nature* **2004**, *427*, 332–336. [[CrossRef](#)] [[PubMed](#)]
28. Stefanon, M.; D’Andrea, F.; Drobinski, P. Heatwave classification over Europe and the Mediterranean region. *Environ. Res. Lett.* **2012**, *7*, 014023. [[CrossRef](#)]
29. Ciais, P.; Reichstein, M.; Viovy, N.; Granier, A.; Ogée, J.; Allard, V.; Aubinet, M.; Buchmann, N.; Bernhofer, C.; Carrara, A.; et al. Europe-wide reduction in primary productivity caused by the heat and drought in 2003. *Nature* **2005**, *437*, 529–533. [[CrossRef](#)] [[PubMed](#)]
30. Rebetez, M.; Mayer, H.; Dupont, O.; Schindler, D.; Gartner, K.; Kropp, J.P.; Menzel, A. Heat and drought 2003 in Europe: A climate synthesis. *Ann. For. Sci.* **2006**, *63*, 569–577. [[CrossRef](#)]
31. Gómez-Hernández, M.; Drumond, A.; Gimeno, L.; Garcia-Herrera, R. Variability of moisture sources in the Mediterranean region during the period 1980–2000. *Water Resour. Res.* **2013**, *49*, 6781–6794. [[CrossRef](#)]
32. Drumond, A.; Nieto, R.; Hernández, E.; Gimeno, L. A Lagrangian analysis of the variation in moisture sources related to drier and wetter conditions in regions around the Mediterranean basin. *Nat. Hazards Earth Syst. Sci.* **2011**, *11*, 2307–2320. [[CrossRef](#)]
33. Bisselink, B.; Dolman, A.J. Precipitation recycling: Moisture sources over Europe using ERA-40 Data. *J. Hydrometeorol.* **2008**, *9*, 1073–1083. [[CrossRef](#)]

34. Seneviratne, S.I.; Lüthi, D.; Litschi, M.; Schär, C. Land-atmosphere coupling and climate change in Europe. *Nature* **2006**, *443*, 205–209. [[CrossRef](#)] [[PubMed](#)]
35. Nieto, R.; Castillo, R.; Drumond, A.; Gimeno, L. A catalog of moisture sources for continental climatic regions. *Water Resour. Res.* **2014**, *50*, 5322–5328. [[CrossRef](#)]
36. Stojanovic, M.; Drumond, A.; Nieto, R.; Gimeno, L. Moisture Transport Anomalies over the Danube River Basin during Two Drought Events: A Lagrangian Analysis. *Atmosphere* **2017**, *8*, 193. [[CrossRef](#)]
37. Stohl, A.; James, P. A Lagrangian Analysis of the Atmospheric Branch of the Global Water Cycle. Part I: Method Description, Validation, and Demonstration for the August 2002 Flooding in Central Europe. *J. Hydrometeorol.* **2004**, *5*, 656–678. [[CrossRef](#)]
38. Stohl, A.; James, P. A Lagrangian analysis of the atmospheric branch of the global water cycle: Part II: Moisture Transports between Earth's Ocean Basins and River Catchments. *J. Hydrometeorol.* **2005**, *6*, 961–984. [[CrossRef](#)]
39. Vicente-Serrano, S.M.; Begueria, S.; Lopez-Moreno, A.J. A multiscalar drought index sensitive to global warming: The standardized precipitation evapotranspiration index. *J. Clim.* **2010**, *23*, 1696–1718. [[CrossRef](#)]
40. Vicente-Serrano, S.M.; Aguilar, E.; Martínez, R.; Martín-Hernández, N.; Azorin-Molina, C.; Sanchez-Lorenzo, A.; El Kenawy, A.; Tomás-Burguera, M.; Moran-Tejeda, E.; et al. The Complex influence of ENSO on droughts in Ecuador. *Clim. Dyn.* **2016**, *48*, 405–427. [[CrossRef](#)]
41. Tan, C.; Yang, J.; Li, M. Temporal-Spatial Variation of Drought Indicated by SPI and SPEI in Ningxia Hui Autonomous Region, China. *Atmosphere* **2015**, *6*, 1399–1421. [[CrossRef](#)]
42. Palmer, W.C. Meteorological Drought. 1965. Available online: <https://www.ncdc.noaa.gov/temp-and-precip/drought/docs/palmer.pdf> (accessed on 11 May 2017).
43. Vicente-Serrano, S.M.; Beguería, S.; Lorenzo-Lacruz, J.; Camarero, J.J.; López-Moreno, J.I.; Azorin-Molina, C.; Revuelto, J.; Morán-Tejeda, E.; Sanchez-Lorenzo, A. Performance of Drought Indices for Ecological, Agricultural and Hydrological Applications. *Earth Interact.* **2012**, *16*, 1–27. [[CrossRef](#)]
44. Vicente-Serrano, S.M.; Gouveia, C.; Camarero, J.J.; Beguería, S.; Trigo, R.; López-Moreno, J.I.; Azorín-Molina, C.; Pasho, E.; Lorenzo-Lacruz, J.; Revuelto, J.; et al. Response of vegetation to drought time-scales across global land biomes. *Proc. Natl. Acad. Sci. USA* **2013**, *110*, 52–57. [[CrossRef](#)] [[PubMed](#)]
45. Gornall, J.; Betts, R.; Burke, E.; Clark, R.; Camp, J.; Willett, K.; Wiltshire, A. Implications of climate change for agricultural productivity in the early twenty-first century. *Philos. Trans. R. Soc. B Biol. Sci.* **2010**, *365*, 2973–2989. [[CrossRef](#)]
46. Bitá, C.; Gerats, T. Plant tolerance to high temperature in a changing environment: Scientific fundamentals and production of heat stress tolerant crops. *Front. Plant Sci.* **2013**, *4*, 273. [[CrossRef](#)] [[PubMed](#)]
47. Adams, R.M.; Hurd, B.H.; Lenhart, S.; Leary, N. Effects of global climate change on agriculture: An interpretative review. *Clim. Res.* **1998**, *11*, 19–30. [[CrossRef](#)]
48. Vicente-Serrano, S.M.; Beguería, S.; López-Moreno, J.I. Comment on “Characteristics and trends in various forms of the Palmer Drought Severity Index (PDSI) during 1900–2008” by A. Dai. *J. Geophys. Res. Atmos.* **2011**, *116*, D19112. [[CrossRef](#)]
49. Vicente-Serrano, S.M.; Van der Schrier, G.; Beguería, S.; Azorin-Molina, C.; Lopez-Moreno, J.I. Contribution of precipitation and reference evapotranspiration to drought indices under different climates. *J. Hydrol.* **2015**, *426*, 42–54. [[CrossRef](#)]
50. Beguería, S.; Vicente-Serrano, S.M.; Reig, F.; Latorre, B. Standardized Precipitation Evapotranspiration Index (SPEI) revisited: Parameter fitting, evapotranspiration models, tools, datasets and drought monitoring. *Int. J. Climatol.* **2014**, *34*, 3001–3023. [[CrossRef](#)]
51. Harris, I.; Jones, P.D.; Osborn, T.J.; Lister, D.H. Updated high-resolution grids of monthly climatic observations—The CRU TS3.10 Dataset. *Int. J. Climatol.* **2014**, *34*, 623–642. [[CrossRef](#)]
52. Liu, Z.; Lu, G.; He, H.; Wu, Z.; He, J. Anomalous Features of Water Vapor Transport during Severe Summer and Early Fall Droughts in Southwest China. *Water* **2017**, *9*, 244. [[CrossRef](#)]
53. McKee, T.B.; Doesken, N.J.; Kleist, J. The relationship of drought frequency and duration to time scales. In Proceedings of the Eighth Conference on Applied Climatology, Anaheim, CA, USA, 17–22 January 1993; pp. 179–184.
54. Dee, D.P.; Uppala, S.M.; Simmons, A.J.; Berrisford, P.; Poli, P.; Kobayashi, S.; Andrae, U.; Balmaseda, M.A.; Balsamo, G.; Bauer, P.; et al. The ERA-Interim reanalysis: Configuration and performance of the data assimilation system. *Q. J. R. Meteorol. Soc.* **2001**, *137*, 553–597. [[CrossRef](#)]

55. Trenberth, K.E.; Fasullo, J.T.; Mackaro, J. Atmospheric moisture transports from ocean to land and global energy flows in reanalyses. *J. Clim.* **2011**, *24*, 4907–4924. [[CrossRef](#)]
56. Lorenz, C.; Kunstmann, H. The hydrological cycle in three state-of-the-art reanalyses: Intercomparison and performance analysis. *J. Hydrometeorol.* **2012**, *13*, 1397–1420. [[CrossRef](#)]
57. Gimeno, L.; Nieto, R.; Drumond, A.; Castillo, R.; Trigo, R.M. Influence of the intensification of the major oceanic moisture sources on continental precipitation. *Geophys. Res. Lett.* **2013**, *48*, 1–8. [[CrossRef](#)]
58. Gimeno, L.; Drumond, A.; Nieto, R.; Trigo, R.M.; Stohl, A. On the origin of continental precipitation. *Geophys. Res. Lett.* **2010**, *37*, L13804. [[CrossRef](#)]
59. Gimeno, L.; Stohl, A.; Trigo, R.M.; Domínguez, F.; Yoshimura, K.; Yu, L.; Drumond, A.; Durán-Quesada, A.M.; Nieto, R. Oceanic and Terrestrial Sources of Continental Precipitation. *Rev. Geophys.* **2012**, *50*, RG4003. [[CrossRef](#)]
60. Numaguti, A. Origin and recycling processes of precipitating water over the Eurasian continent: Experiments using an atmospheric general circulation model. *J. Geophys. Res. Atmos.* **1999**, *104*, 1957–1972. [[CrossRef](#)]
61. Spinoni, J.; Naumann, G.; Vogt, V.V.; Barbosa, P. The biggest drought events in Europe from 1950–2012. *J. Hydrol.* **2015**, *3*, 509–524. [[CrossRef](#)]
62. Zampieri, M.; D’Andrea, F.; Vautard, R.; Ciais, P.; de Noblet-Ducoudré, N.; Yiou, P. Hot European Summers and the Role of Soil Moisture in the Propagation of Mediterranean Drought. *J. Clim.* **2009**, *22*, 4747–4758. [[CrossRef](#)]
63. Lionello, P.; Malanotte-Rizzoli, P.; Boscolo, R.; Alpert, P.; Artale, V.; Li, L.; Luterbacher, J.; May, W.; Trigo, R.; Tsimplis, M.; et al. The Mediterranean climate: An overview of the main characteristics and issues. *Dev. Earth Environ. Sci.* **2006**, *4*, 1–26. [[CrossRef](#)]
64. Mariotti, A.; Struglia, M.V.; Zeng, N.; Lau, K.M. The Hydrological Cycle in the Mediterranean Region and Implications for the Water Budget of the Mediterranean Sea. *J. Clim.* **2002**, *15*, 1674–1690. [[CrossRef](#)]
65. Drumond, A.; Gimeno, L.; Nieto, R.; Trigo, R.M.; Vicente-Serrano, S.M. Drought episodes in the climatological sinks of the Mediterranean moisture source: The role of moisture transport. *Glob. Planet Chang.* **2017**, *151*, 4–14. [[CrossRef](#)]
66. Sodemann, H.; Zubler, E. Seasonal and inter-annual variability of the moisture sources for Alpine precipitation during 1995–2002. *Int. J. Climatol.* **2010**, *30*, 947–961. [[CrossRef](#)]
67. Schicker, I.; Radanovics, R.; Seibert, P. Origin and transport of Mediterranean moisture and air. *Atmos. Chem. Phys.* **2010**, *10*, 5089–5105. [[CrossRef](#)]
68. Ogi, M.; Yamazaki, K.; Tachibana, Y. The summer northern annular mode and abnormal summer weather in 2003. *Geophys. Res. Lett.* **2005**, *32*, L04706. [[CrossRef](#)]



© 2018 by the authors. Licensee MDPI, Basel, Switzerland. This article is an open access article distributed under the terms and conditions of the Creative Commons Attribution (CC BY) license (<http://creativecommons.org/licenses/by/4.0/>).

Article

Variations in Moisture Supply from the Mediterranean Sea during Meteorological Drought Episodes over Central Europe

Milica Stojanovic *, Anita Drumond , Raquel Nieto  and Luis Gimeno

Environmental Physics Laboratory (EPhysLab), Facultad de Ciencias, Universidad de Vigo, 32004 Ourense, Spain; anitadru@uvigo.es (A.D.); rnieto@uvigo.es (R.N.); l.gimeno@uvigo.es (L.G.)

* Correspondence: mstojanovic@uvigo.es; Tel.: +34-988-387-208

Received: 6 June 2018; Accepted: 15 July 2018; Published: 19 July 2018



Abstract: The climate in Central Europe (CEU) during the 20th century is characterized by an overall temperature increase. Severe and prolonged drought events began occurring towards the end and these have continued into the 21st century. This study aims to analyze variations in the moisture supply from the Mediterranean Sea (MDS) during meteorological drought episodes occurring over the CEU region over the last three decades. A total of 51 meteorological drought episodes (22 with summer onsets, and 29 with winter) are identified over the CEU during the period 1980–2015 through the one-month Standardized Precipitation Evapotranspiration Index (SPEI-1), and their respective indicators, including duration, severity, intensity, and peak values, are then computed. Lagrangian forward-in-time analysis reveals that negative anomalies of moisture coming from the MDS prevail in all episodes except seven. Linear regression analysis between variations in the MDS anomalies and indicators of the drought episodes shows a significant linear relationship between severity, duration, peak values (winter), and MDS anomalies, which implies that drought episodes last longer and are more severe with an increase in the negative anomaly of moisture supply from the MDS. Nevertheless, no linear relationship is found between the intensity and peak values (annual, summer) of drought episodes and anomalies in the moisture contribution from the MDS.

Keywords: drought; SPEI; Lagrangian method; Central Europe; Mediterranean Sea

1. Introduction

Hydrological cycle elements (precipitation (PRE), evaporation and moisture transport) have become some of the most important themes in current climate variability research and change evaluation [1]. Climate change influences not only average temperatures, but also the frequency of extreme events affecting natural and human systems [2]; the Intergovernmental Panel on Climate Change (IPCC) assessment report [1] on extreme events confirmed that climate change would cause changes in the intensity, severity and duration of extreme events, and would thus present severe risks to both humans and the environment. In this respect, several studies have highlighted the role of recent climate change in increasing the probability of occurrence of extreme events, such as drought [3–5]. Europe is likely to experience diverse impacts on response to climate change, such as temperature increases and variability in extreme events [6], and many European countries have experienced episodes of drought over the past 30 years that have caused significant ecological and economic damage [7]. Droughts are difficult to predict due to the complexity of contributions to their occurrence, but continuous drought monitoring is imperative.

Several authors have shown that a PRE deficit combined with high evapotranspiration typically leads to drought [8–11], and PRE deficits in some areas have been found to be related to changes in

moisture transport [8,12,13]. Therefore, it is important to examine mechanisms responsible for PRE deficits over sinks, or mechanisms related to any reduction in evaporation from the source that causes drought in certain regions.

Many drought indices have been developed to monitor, predict, and assess the severity of drought, such as the Reconnaissance Drought Index (RDI) [14], the Streamflow Drought Index (SDI) [15], the Palmer Drought Severity Index [16], the Standardized Precipitation Index (SPI) [17], the Standardized Precipitation Evapotranspiration Index (SPEI) [18], the Standardized Indices through Non-Parametric Rescaling (SINRes) [19]. Computations of the SPEI and SINRes consider both PRE and potential evapotranspiration (PET). Indirectly, temperature is taken into account, given that it is used in the computation of potential evapotranspiration. The SPEI has been extensively applied in studies around the world, such as in America [20,21], Asia [22,23], Africa [24,25] and Europe [26–30].

Several studies have investigated the relationship between sources and sinks of moisture and drought in specific regions [24,31–33]. The Lagrangian techniques have been widely utilized for identifying the sources of atmospheric moisture for continental areas (e.g., [34–37]). In comparison to the other approaches, such as the Eulerian technique “numerical water vapor tracers” [38,39], “analytical and box models” [40,41], and “physical water vapor tracers” (isotopes) [42], the Lagrangian approach [36,37,43,44] is one of the most suitable tools for establishing a source–sink relationship of the atmospheric moisture transport, as pointed out by Gimeno et al. [34].

Previous authors investigated the origin and destination of moisture over the Mediterranean region using different techniques. Fernandez et al. [45] applied a Eulerian method by integrating the vertical moisture flux over the Mediterranean Basin and Southern Europe using meteorological reanalysis from the National Centers for Environmental Prediction (NCEP). However, this method cannot provide information about the origin of moisture reaching the basin and the destination from it. Applying a Lagrangian approach over a 5-year period of data, Nieto et al. [46] and Schicker et al. [47] computed the budget of evaporation minus PRE in air masses tracked backward-in-time from the Mediterranean Basin to identify the main moisture sources; and also computed the moisture contribution from this region to surrounded continental regions by tracking forward-in-time air masses. Drumond et al. [48] extended the work of Nieto et al. [46] by focusing on the seasonal variations in moisture sources for different Mediterranean target regions during drier and wetter years. The long-term variability of the main climatological moisture sources for eight target regions in the Mediterranean Basin was investigated by Gómez-Hernández et al. [49] using the ERA-40 reanalysis dataset. Applying a different Lagrangian approach, Sodemann et al. [50] analyzed seasonal and interannual variability of the moisture sources for the Alpine PRE during 1995–2002, showing the importance of the Mediterranean as the source of moisture for PRE events.

The Mediterranean Sea (MDS) was identified as the main moisture source for Central and Eastern Europe (CEU, Figure 1) and the surrounding basin area, and changes in its moisture supply have an impact on dryness conditions in regions where moisture sinks [33,38,45,47,50–52]. Using the Lagrangian approach developed by Stohl and James [36,37], Drumond et al. [33] investigated whether severe dry conditions accumulated during the extended winter and summer seasons over the climatological moisture sinks of the MDS were associated with changes in moisture transport from the basin. Focusing on meteorological droughts, Stojanovic et al. [13] recently investigated anomalies in the moisture supply during the 2003 episode in Europe. However, further and deeper exploration is required to determine the existence of a climatological relationship between changes in the moisture supply from the MDS and meteorological drought episodes over the CEU.

The CEU region, according to the definition proposed in the 5th Assessment Report (AR5) of the IPCC [4] (Figure 1), comprises Germany, Switzerland, Liechtenstein, Austria, Poland, the Czech Republic, Slovakia, and Hungary. The climate is humid continental-type with cool summers. This is a region, where Atlantic, Mediterranean, and continental influences meet and complex orography has a significant impact on the climate and meteorology in the region [53].

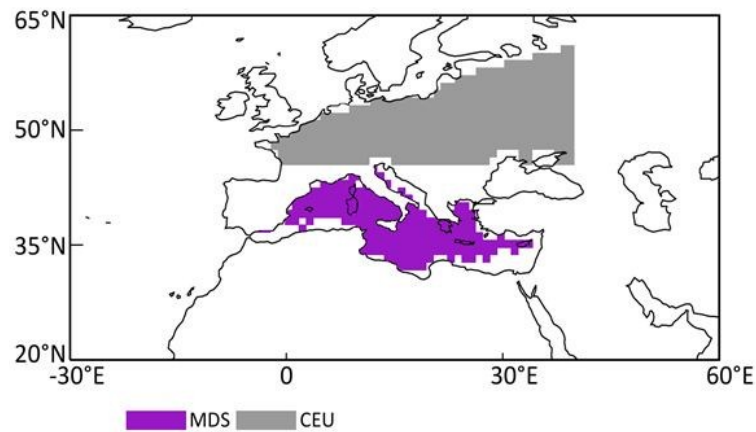


Figure 1. Central and Europe region (CEU, grey) with boundaries defined from the 5th Assessment Report (AR5) of the Intergovernmental Panel on Climate Change (IPCC), with the Mediterranean Sea (MDS, purple color) source identified using a backward-in-time experiment according to Stojanovic et al. [13].

This study therefore analyzes variations in the moisture transport from the MDS during meteorological drought episodes over the CEU (Figure 1) for the period (1980–2015), and aims to determine whether anomalies of this contribution have different effects on episodes with onsets during winter and summer seasons. The main goals are: (1) to identify meteorological drought episodes over the CEU during 1980–2015 through the one-month Standardized Precipitation Evapotranspiration Index (SPEI-1) [18]; (2) to use Lagrangian methodology to analyze the anomalous contribution from the MDS to the CEU region during drought episodes [36,37], and to check possible links between variations in moisture supply and indicators of selected episodes through linear regression analysis. This study focuses on the meteorological droughts episodes over the CEU, therefore differing from the previous analysis of dry conditions accumulated during the extended seasons over the Mediterranean sinks, which was developed by Drumond et al. [33]. Section 2 explains the data and methods; Section 3 presents results and discussion; and Section 4 provides conclusions.

2. Data and Methodology

2.1. Data

The analyses were carried out using a climatology of 36 years (1980–2015). The Lagrangian model is forced by the ERA-Interim global reanalysis dataset from the European Centre for Medium-Range Weather Forecasts (ECMWF) [54], which is available at a spatial resolution of $1^\circ \times 1^\circ$ on 61 vertical levels from the surface to 0.1 hPa. The dataset can be retrieved at (<https://www.ecmwf.int/en/forecasts/datasets/archive-datasets/reanalysis-datasets/era-interim>). Lorenz and Kunstmann [55] found that the ERA-Interim reanalysis data provide a superior performance in reproducing the hydrological cycle and a relatively reasonable closure of the terrestrial and atmospheric water balance, compared to reanalysis datasets, such as Modern Era Retrospective-Analysis for Research and Applications (MERRA) [56], and Climate Forecast System Reanalysis (CFSR) [57]. These findings thus support the use of ERA-Interim datasets for our study, since the Lagrangian model requires high-quality data for wind and humidity [58].

Datasets of PRE and PET were available at a spatial resolution of 0.5° from the Climate Research Unit (CRU) Time-Series (TS) Version 3.24.01 [59]. We calculated the time series of PRE and PET over the CEU, information required to compute the SPEI. Data are available at https://crudata.uea.ac.uk/cru/data/hrg/cru_ts_3.24.01/cruts.1701201703.v3.24.01/.

The climatological annual cycle of PRE, PET and the moisture contribution from the MDS to the CEU during 1980–2015 (Figure 2) revealed that the contribution from the MDS to the CEU was

higher from September to December. In terms of the climatological annual cycle of the freshwater flux (PET–PRE), PRE prevailed over PET during the winter season (from October to March), indicated as $(\text{PET}-\text{PRE}) < 0$, while the inverse pattern was configured as $(\text{PET}-\text{PRE}) > 0$ during summer (from April to September).

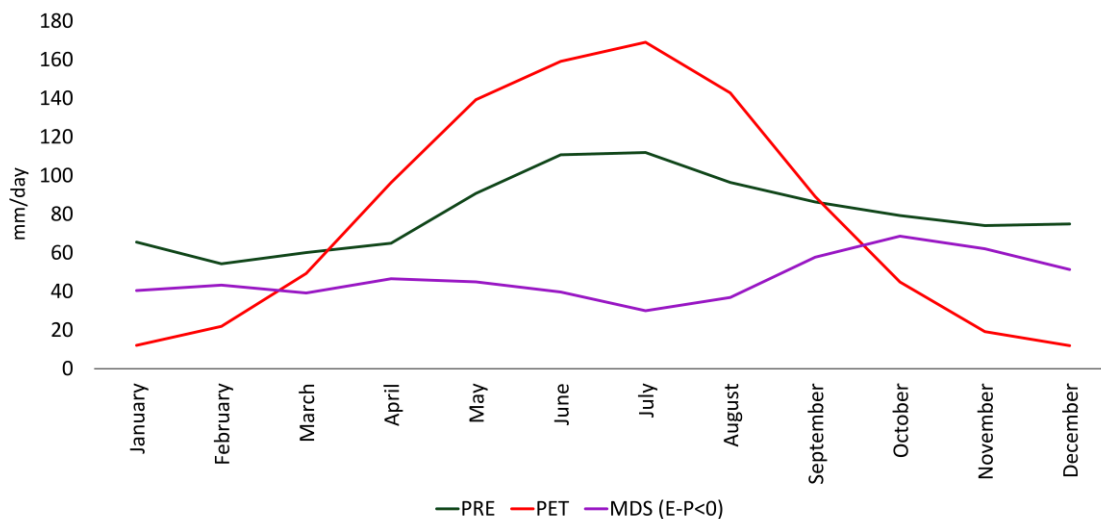


Figure 2. Climatological annual cycle of precipitation (PRE, $\times 10$ green line), potential evapotranspiration (PET, $\times 10$ red line) (data from the Climatic Research Unit (CRU) (TS3.24.01) (scale: mm/day) values integrated over the CEU), with the moisture contribution from the MDS (purple color (mm/day) values integrated over the CEU) to the CEU obtained via the forward experiment.

Evaporation data for the calculation of monthly anomalies of the evaporation rate over the MDS were obtained from the Objectively Analyzed air–sea Heat Fluxes (OAFlux) project [60], while monthly anomalies of vertical velocity (ω) at 500 hPa averaged during each meteorological drought episode identified over the CEU were calculated using the ERA-Interim dataset [54].

2.2. Standardized Precipitation Evapotranspiration Index (SPEI)

The SPEI is based on the monthly climatic water balance (PRE minus PET) calculated at various time scales (i.e., accumulation over given time intervals), and the resulting values are adjusted to a log-logistic probability distribution to convert original values to standardized units that are comparable in space and time at different SPEI timescales [18]. Other probability distributions could be applied, for instance, based on general extreme values (GEV) [61,62], but SPEI’s developers recommended the use of the first one, due to the fact that the differences between both distributions are marginal for climate analysis [63]. For the purpose of this study, the crucial advantage of SPEI over other commonly used drought indices (such as the PDSI [16] and the SPI [17]) is the role of temperature, which is considered through PET values. In addition, the multiscale characteristics of SPEI permit the identification of different types of drought [64,65], and a complete comparison of indices has been provided in previous studies [18,66,67].

This study used the one-month Standardized Precipitation Evapotranspiration Index (SPEI-1) to identify meteorological drought episodes occurring over the CEU region during the period 1980–2015. The SPEI at different timescales corresponds to different drought types, such as 1–2-month SPEI for meteorological drought (e.g., [18]). Following Liu et al. [68] the SPEI-1 was chosen in this study because we were interested in the variability of water vapor transport, which is closely related to meteorological drought. Several works used SPEI-1 or SPI-1 for the same aim of this short note over other areas, as in Southwest China [68] and Europe (e.g., [69,70]). In SPEI-1, respective values were accumulated during a one-month period, and the drought index was calculated using monthly CRUTS 3.24.01 data of PRE

and PET averaged over the CEU region. We have also calculated the SPI-1 time series for the CEU during 1980–2015 with the same CRU data. The temporal evolution of SPEI-1 and SPI-1 was similar (not shown), with a coefficient of correlation of 0.96. Although the SPI showed slightly higher peaks, the onset and dismissal of drought episodes identified through both series were the same.

Episodes were identified in concordance with the criteria of McKee et al. [17]: the start of an episode was determined when the SPEI-1 value first fell below zero followed by a value of -1 or less, and the end was decided when the SPEI-1 value returned to a positive value. After identifying events, their indicators were computed with respect to severity, duration, intensity and peak values, where severity represents the absolute value of the sum of all SPEI values during the episode, duration signifies the number of months between the first and last months of the episode, intensity is calculated as the ratio between severity and duration and peak values are the most negative values registered [71,72]. Because the purpose of this study was to analyze the relationship between the indicators of the episodes and the MDS moisture contribution under a climatological perspective, this period was classified as a drought event, even when the SPEI remained negative only for a month. The episodes were also organized into two groups according to their onset: summer (April–September) and winter (October–March).

2.3. The Lagrangian Approach

The Lagrangian FLEXible PARTicle dispersion model (FLEXPART) developed by Stohl and James [36,37] was used to investigate anomalies in the moisture supply from the MDS during drought episodes occurring over the CEU during 1980–2015.

In the FLEXPART simulation, the atmosphere is divided uniformly into approximately 2 million particles over the entire globe. A constant mass is considered for each particle as it is transported using 3D wind fields. Particles are identified every six hours, and the transport time is limited to 10 days, which reflects the mean water vapor lifetime in the global atmosphere [73]. The moisture variations presented by a particle during its trajectory can be calculated through variations in specific humidity: $e - p = m(dq/dt)$, where m is the mass of the particle and $(e - p)$ (evaporation minus PRE) represents the freshwater flux associated with the particle. Knowing the specific humidity in every time step, it is possible to identify particles that lose moisture through PRE (p), or obtain it through evaporation (e). Adding $(e - p)$ for all the particles residing in an atmospheric column over the area, it is possible to obtain the total freshwater flux ($E - P$). The trajectory of the particles can be advected using backward-in-time analysis with the aim of determining the sources of moisture for the target region ($E - P > 0$) or forward-in-time analysis to investigate where moisture sinks after being transported by particles ($E - P < 0$). More detailed information about the functionalities of FLEXPART can be found in Stohl and James [36,37] and Gimeno et al. [34].

The main advantage of the model is that it enables backward and forward tracking of air masses over time, and enables an analysis of the water balance in the atmospheric column along the trajectories. Nevertheless, this approach has two main limitations, according to Stohl and James [36,37]: the first is that it is not possible to individually diagnose E and P , and the second is that results are highly reliant on input data quality. In addition, fluctuations in specific humidity (q) along trajectories may occur for nonphysical reasons, due to the interpolation of q or trajectory errors; however, this limitation can be compensated for by the large numbers of particles that are contained in an atmospheric column over a given area. A more detailed description of backward and forward analyses can be found in a number of studies that have applied this model to estimate humidity changes along trajectories and identify sources of moisture and sinks in many different regions worldwide, such as the Danube River Basin [74], the Congo River Basin [32], Central America [75], the Mediterranean region [48], Iceland [76], the Fertile Crescent region [24] and the Indus, Ganges, and the Brahmaputra River Basin [77]. Furthermore, Stojanovic et al. [13] recently applied this method to investigate anomalies in the moisture supply during the 2003 drought episode in Europe.

In this study, we considered the MDS as the source of moisture for the CEU (Figure 1) and calculated the anomalous contribution from this source to the CEU region during drought episodes identified in the period 1980–2015. The monthly anomaly was computed as the difference of the monthly average with respect to the respective monthly climatological mean. Then, the monthly anomalies were accumulated during each episode. Forward analysis was used to calculate monthly anomalies (accumulated during each episode) from the MDS integrated over the CEU region.

2.4. Linear Regression Analysis

Using Simple Linear Regression, we calculated the coefficient of determination (R^2) with the linear regression equation, which represents the proportion of the variance in the dependent variable (severity, duration, intensity, and peak values of drought) that is predictable with respect to the independent variable (contribution from the MDS source). The linear regression analysis was conducted to verify whether variations in the contribution from the MDS to the CEU may affect the indicators of drought episodes. The student t -test and the Spearman rank correlation coefficient [78] at a 95% significance level were also applied to confirm the statistical significance of the regression coefficient.

3. Results and Discussion

3.1. Analysis of Drought

Figure 3 shows the SPEI-1 time series for the CEU during the period 1980–2015, in which the negative values (red bars) represent dry conditions and the positive ones (blue bars) represent wet conditions. We identified 51 meteorological drought episodes (22 with onsets during summer and 29 with winter onsets) and ranked these according to severity, duration, intensity and peak values. The results are shown in Table S1 in Supplementary Materials, from which it is evident that the most severe drought episode occurred from February to June 2003 (with a value of 7.1). The second most-severe event occurred in June–October 2015 (6.45), during which time the maximum peak was reached. Furthermore, the longest drought episode lasted for seven months from June to December 1983, while the most intense occurred during October 1995 (2.16) and lasted for only one month.

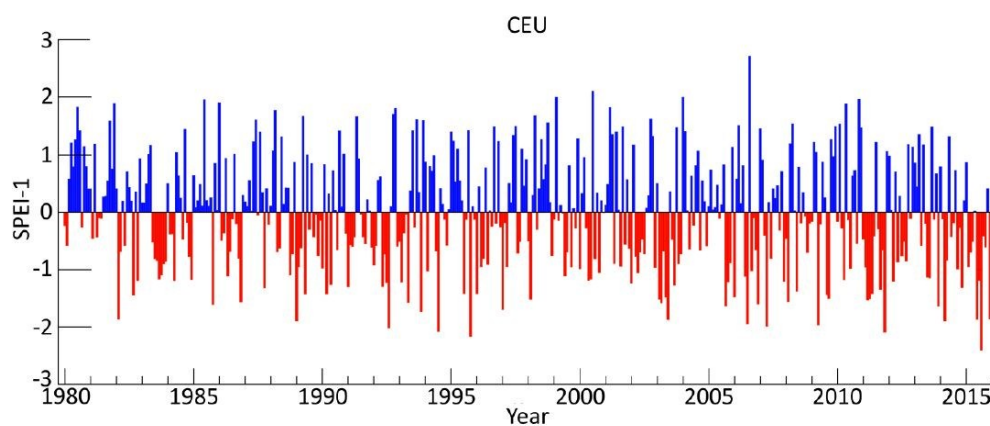


Figure 3. Time series of one-month Standardized Precipitation Evapotranspiration Index (SPEI-1) for the CEU region during 1980–2015. Blue and red bars represent positive and negative values, respectively.

3.2. Monthly Anomalies of Evaporation, Vertical Velocity (Ω) and Moisture Supply

Monthly anomalies of evaporation, vertical velocity (Ω) and moisture contribution from the MDS to the CEU region accumulated during each drought episode identified in 1980–2015 are shown in the Figure 4. Results showed that the signal of the anomalies of evaporation over the MDS

varied during the episodes, although there was a predominance of the negative anomalies (Figure 4, black line). From the 51 episodes selected, 31 events were associated with reduced evaporation over the MDS (60.8% of the cases), in contrast to the 20 events related with increasing evaporation over the MDS (39.2 % of the cases). Regarding some seasonal patterns, from the 29 drought episodes with onsets during winter, a reduction in the evaporation over the MDS was evident in 19 events, while only 10 presented increased evaporation in the basin. Nevertheless, this reduction was not so evident for the episodes with onset in summer: from the 22 events, 12 were associated with reduction in the MDS evaporation, and 10 were related with increasing evaporative conditions over the MDS.

Based on the contribution from the MDS to the CEU, we could see that with the exception of seven drought episodes (red bars) occurring in November 1982, May 1990, July–August 1995, December 1995–January 1996, October 2000, March–April 2010, and June–October 2015, negative anomalies of MDS prevailed for almost all drought episodes (blue bars). Only the episode occurring from June to October 2015 was one of the five longest and most severe episodes of all recorded, whereas the remaining six drought episodes had severity rankings between the 14 least severe episodes ever recorded in the period (Table S1, Supplementary Materials). The most intensely negative anomalies of moisture supply from the MDS occurred during January–June 2011 (103.55 mm/day), January–December 1983 (100.7 mm/day), September–December 2006 (92.08 mm/day), February–June 2003 (91.95 mm/day) and August–November 2011 (89.92 mm/day) drought episodes. These drought episodes were among the 11 longest and most severe episodes of all recorded. Except for one case with conditions associated with inhibition of local PRE (Figure 4, green line), anomalous atmospheric subsidence prevailed over the CEU during the episodes.

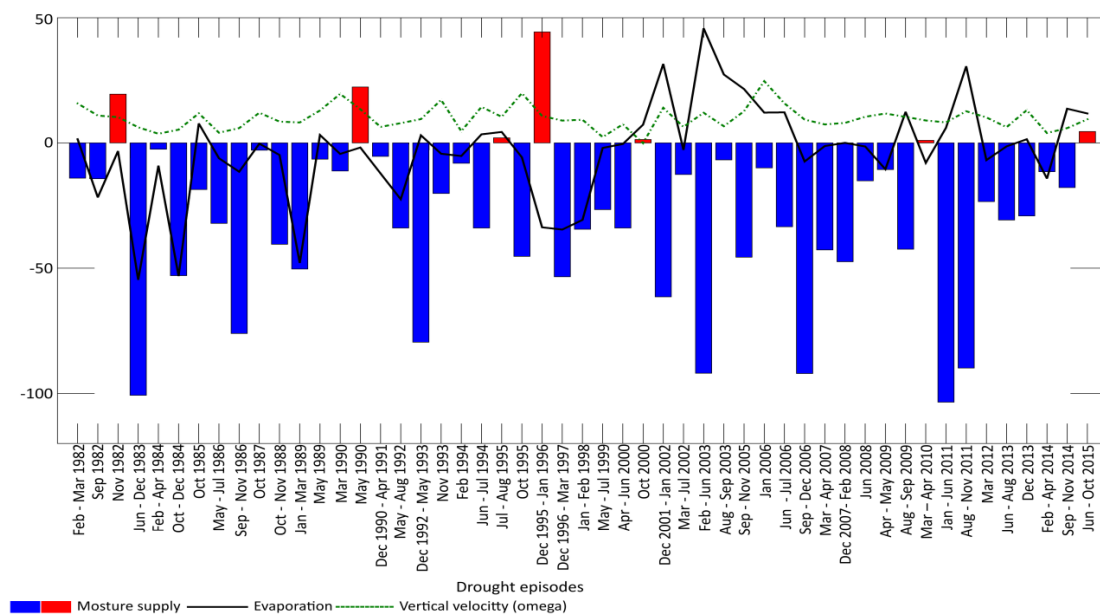


Figure 4. Monthly anomalies of the evaporation rate over the MDS ($\times 10$ mm/day, black line), the vertical velocity (omega) at 500 hPa (/1000 Pa/s, green line) and the moisture supply from the MDS (mm/day, blue and red bars) accumulated during each meteorological drought episode identified over the CEU during the period 1980–2015.

Although we were not able to verify possible alternative destinations of the moisture evaporated over the MDS from this analysis, it is evident that the moisture supply from the MDS to the CEU was reduced during the CEU meteorological episodes, which may be associated with the reduction in the MDS evaporation, particularly during the cases with onsets during winter. It is known from previous works (e.g., [33] and references therein) that the regions most affected by moisture transport from the MDS are the CEU and the Eastern Mediterranean, and it would be of further interest to analyze

how the moisture transport towards these climatological sinks was affected during the meteorological drought episodes of the CEU.

3.3. Linear Regression Analysis

To determine the existence of a linear relationship between the different indicators of drought episodes (severity, duration, intensity and peak values) and variations in contributions from the MDS, a Simple Linear Regression analysis was conducted using the Least Squares Method (Figure 5). Analysis was conducted for the entire period and was then repeated for events with onsets in winter (October–March) and in summer (April–September). The coefficient of determination was computed to determine representativeness of the analysis, and the student *t*-test at a 95% confidence interval was applied to the regression coefficient to determine statistical significance. Table 1 shows the significance (a significance level of 95%), slope, intercept and coefficient of determination (R^2) for the severity, duration, intensity and peak values with MDS anomalies on annual, winter and summer scales.

According to the student *t*-test statistic applied here, a significant linear relationship was shown to exist between the severity, duration, peak value (winter season) and the MDS anomalies. This implied that episodes, which were more severe and longer, and had peaks that were more intensive, were associated with more intensively negative moisture supply anomalies from the MDS (accumulated during the episode). However, no linear relationship was determined between the intensity and peak value of drought episodes (the whole period, summer season) and moisture contribution anomalies from the MDS. The highest coefficient values of determination (R^2) occurred between severity and MDS anomalies during winter (0.53), which meant that 53% of variability in the severity of drought episodes could be explained by variations in moisture supply anomalies from the MDS. Although R^2 for the severity of drought episodes for the whole period (0.38) and severity of episodes beginning during summer (April–September) (0.22) were less than those for episodes beginning in winter (October–March), the analysis showed a significant linear relationship. The duration of episodes was also associated with variations in MDS supply anomalies with R^2 of 0.35 for the entire period; R^2 was increased slightly to 0.39 for episodes with summer onsets only; and R^2 was reduced to 0.31 for winter episodes. Results from a Spearman's rank correlation analysis (not shown) corroborated the regression analysis presented here through a non-parametric approach [79].

The Simple Linear Regression analysis was repeated after classifying droughts as a short and a medium terms based on duration (duration less than or equal to 3 months is a short-term episode, while duration greater than 3 months corresponds to a medium-term event), and also as mild and severe/extreme based on peaks (peaks that are less intensive than -1.5 are mild, and peaks that are more intensive than -1.5 are severe/extreme [17]), and results are shown in Tables S2 and S3 of Supplementary Materials. Although the occurrence of medium-term episodes prevailed over the short-term ones (40 and 11, respectively), the linear association between the severity and moisture supply was mainly preserved for the short-term episodes. Only the severity of the medium-term episodes with onsets in winter was linearly associated with the variability in the moisture supply. The linear association between the duration and moisture supply was preserved for all short-term episodes observed during the year, and also for the short-term ones with onsets in summer. For the remaining properties of the episodes (intensity and peak), only the intensity of the medium-term episodes with onsets in summer was linearly associated with variations in the moisture supply from the MDS. Concerning the episodes classified based on peaks, the occurrence of severe/extreme episodes prevailed over the mild ones (39 and 12, respectively), and the linear association between the severity, as well as duration, and moisture supply persisted only for the severe/extreme episodes, given all severe episodes, as well as the ones with onsets during winter were considered.

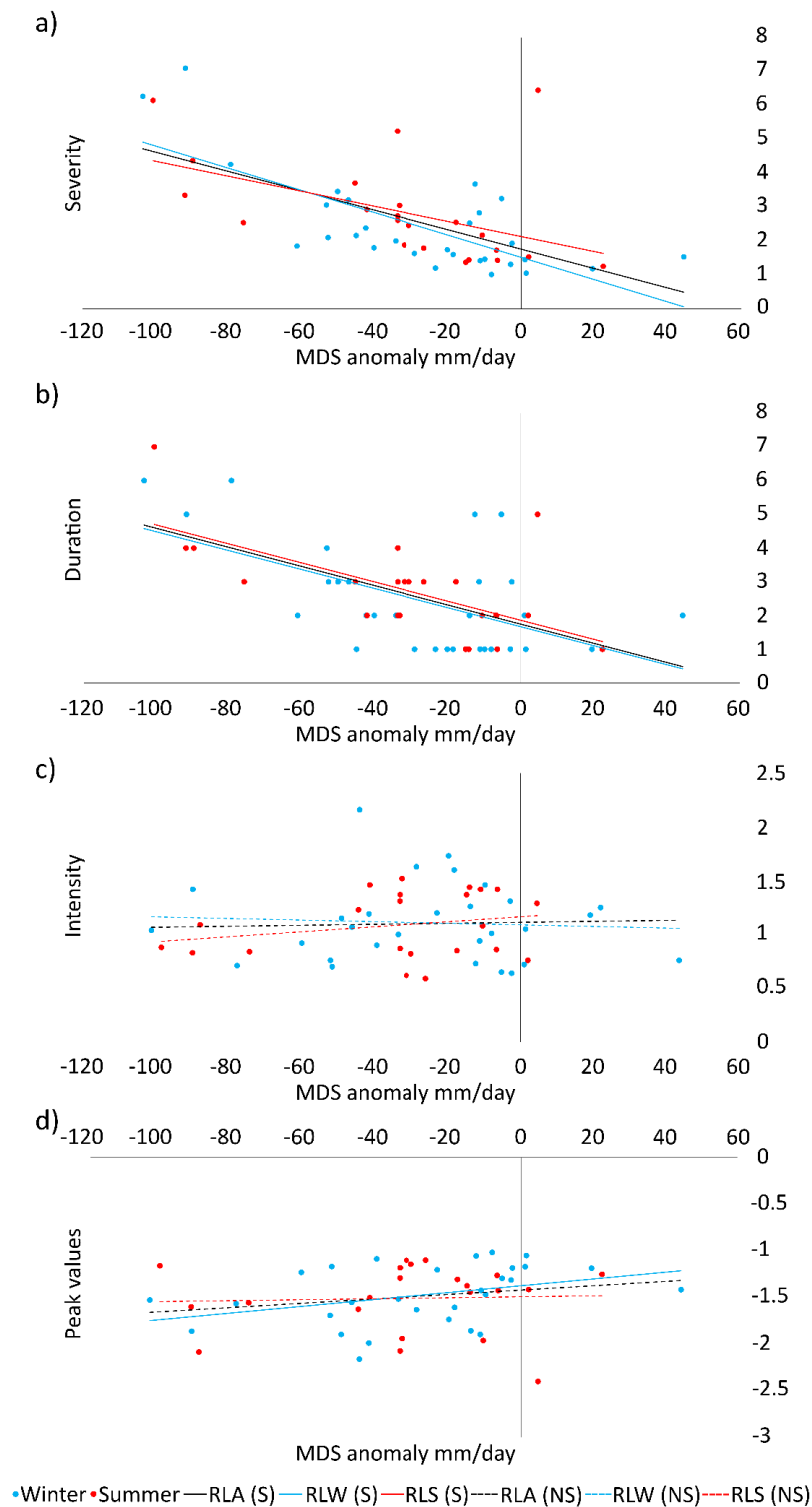


Figure 5. Scatterplot: moisture supply anomalies from the MDS (x-axis, mm/day) and the severity (a); duration (b); intensity (c) and peak values (d) of drought episodes at the annual (entire period shown by both blue and red dots), onsets in winter (March–October) (blue dots) and summer (April–September) (red dots) scales. Corresponding regression lines are also shown: RLA (S) represents Regression Line Annual Significant; RLW (S) represents Regression Line Winter Significant; RLS (S) represents Regression Line Summer Significant; RLA (NS) represents Regression Line Annual Nonsignificant; RLW (NS) represents Regression Line Winter Nonsignificant; and RLS (NS) represents Regression Line Summer Nonsignificant.

Table 1. The significance (a significance level of 95%), slope, intercept and coefficient of determination (R^2) for severity, duration, intensity and peak values with respect to MDS anomaly on annual, winter and summer scales. Underlined bold numbers represent a significant linear relationship with MDS anomaly.

	Annual			Winter			Summer		
	Slope	Intercept	R^2	Slope	Intercept	R^2	Slope	Intercept	R^2
Severity × MDS anomaly	<u>−0.0286</u>	<u>1.7580</u>	<u>0.3860</u>	<u>−0.0328</u>	<u>1.5150</u>	<u>0.5314</u>	<u>−0.0222</u>	<u>2.1310</u>	<u>0.2276</u>
Duration × MDS anomaly	<u>−0.0284</u>	<u>1.7420</u>	<u>0.3508</u>	<u>−0.0281</u>	<u>1.6650</u>	<u>0.3167</u>	<u>−0.00282</u>	<u>1.8570</u>	<u>0.3987</u>
Intensity × MDS anomaly	0.0004	1.1120	0.0018	−0.0007	1.0890	0.0044	0.0023	1.1640	0.0520
Peak values × MDS anomaly	0.0023	−1.4200	0.0487	<u>0.0036</u>	<u>−1.3730</u>	<u>0.1354</u>	0.0005	−1.4920	0.0020

4. Conclusions

This study investigated the relationship between moisture supply anomalies from the MDS and the severity, duration, intensity, and peak values of meteorological drought episodes occurring over the CEU during the period 1980–2015.

A total of 51 drought episodes were identified through the one-month SPEI-1 (22 episodes with onsets during summer (April–September) and 29 events in winter (October–March)). Winter was climatologically characterized by a surplus of PRE in comparison to PET in the freshwater flux and by a peak in the moisture contribution from the MDS into the CEU.

Lagrangian forward analysis was used to investigate possible changes in the moisture contribution from the MDS to the CEU during these drought episodes. The accumulated monthly moisture supply anomaly was calculated for each drought episode, and the results obtained showed that a contribution from the MDS to the CEU for 44 cases out of the 51 episodes analyzed was negative.

A Simple Linear Regression analysis was then conducted to determine the existence of any dependent relationship between different drought episodes indicators (severity, duration, intensity, and peak values) and the contribution from the MDS. Results indicated a significant linear relationship between severity, duration, peak values (winter season), and MDS anomalies. This implied that episodes that were longer, more severe, and had a peak that was more intensive, might be associated with intensification in the moisture supply deficit from the MDS during such episodes. The highest coefficient of determination (R^2) was found between severity of a drought episode and MDS anomalies, particularly for episodes with onsets in winter, the season when (climatologically) PRE prevailed over PET. These results showed that the severity of episodes might be modulated by variations in the moisture supply from the MDS. Nevertheless, no linear relationship was determined between the intensity and peak values (the whole period, summer season) of drought episodes and moisture contribution anomalies from the MDS.

Our findings are in agreement with previous studies that identified the MDS as the important moisture source for Europe and showed that changes in its moisture supply have an impact on dryness conditions over the region in regions where moisture sinks [33,47,50]. Focusing on the six-month accumulation period instead of the one-month applied here, Drumond et al. [33] have also verified a significant reduction in the moisture contribution from the MDS towards its climatological sinks (including the CEU region) during the summer and winter dry periods. In their results, anomalies in MDS evaporation presented seasonal contrasts, i.e., a reduction in winter and an increase in summer dry conditions.

The approach applied here is generally suitable for identification of linear relationships between the variability of the moisture contribution of MDS and the characteristics of the meteorological drought episodes over the CEU, which consists with the aim of this study. However, if one looks for a more realistic relationship model (e.g., for prediction purposes), it is interesting to check whether a

non-linear relationship would fit better, as well as to consider the contribution of other sources besides the MDS.

It is important to state that for this climatological analysis, we focused on the domain-scale episodes affecting the CEU, a climatically homogeneous region defined by the IPCC, and on the impact of the MDS contribution (as a whole) for the CEU. The approach of deriving the SPEI from data averaged over the entire domain for climatological large-scale studies has been satisfactorily applied in some past studies (e.g., [33,69,79]). However, because each drought event is unique in terms of its temporal and spatial development, a grid point analysis would reveal not only areas more affected by dry conditions during a particular episode, but also regions particularly prone to the MDS moisture contribution. Thus, considering the intra-domain variability would be more appropriated for a detailed spatial–temporal analysis of a case.

Supplementary Materials: The following are available online at <http://www.mdpi.com/2073-4433/9/7/278/s1>, Table S1: Drought events that occurred over Central Europe during 1980–2015; Table S2: The significance (a significance level of 95%), slope, intercept and coefficient of determination (R^2) for severity, duration, intensity and peak values with respect to MDS anomaly on annual, winter and summer scales of episodes classified based on duration; Table S3: The significance (a significance level of 95%), slope, intercept and coefficient of determination (R^2) for severity, duration, intensity and peak values with respect to MDS anomaly on annual, winter and summer scales of episodes classified based on peaks.

Author Contributions: M.S., A.D. and L.G. conceived and designed experiments. M.S. conducted experiments, and M.S., A.D. and L.G. analyzed the data. M.S., A.D., R.N. and L.G. wrote the paper.

Funding: We are grateful to the financial support from the Spanish Government (Ministerio de Economía, Industria y Competitividad) and the European Regional Development Fund of the European Commission (in Spanish, FEDER) through the SETH project (CGL2014-60849-JIN). The PhD. Fellowship of Milica Stojanovic is supported by the European Commission under the Erasmus Mundus project Green-Tech-WB: Smart and Green technologies for innovative and sustainable societies in Western Balkans (551984-EM-1-2014-1-ES-ERA Mundus-EMA2). This work was partially supported by Xunta de Galicia under Project ED431C 2017/64-GRC “Programa de Consolidación e Estruturação de Unidades de Investigación Competitivas (Grupos de Referencia Competitiva)”. We would also like to thank the IMDROFLOOD project financed by the Water Works 2014 co-funded call of the European Commission.

Conflicts of Interest: The authors declare no conflicts of interest. The founding sponsors had no role in the design of the study, or in the collection, analysis or interpretation of data, or in the writing of the manuscript, or in the decision to publish the results.

References

1. Intergovernmental Panel on Climate Change (IPCC). *Climate Change 2001: Impacts, Adaptation and Vulnerability; Contribution of Working Group II to the Third Assessment Report of the Intergovernmental Panel on Climate Change*; Cambridge University Press: Cambridge, UK, 2001. Available online: http://hcl.harvard.edu/collections/ipcc/docs/27_WGIITAR_FINAL.pdf (accessed on 9 July 2018).
2. Field, C.B.; Barros, V.; Stocker, T.F.; Dahe, Q. *Managing the Risks of Extreme Events and Disasters to Advance Climate Change Adaptation: A Special Report of Working Groups I and II of the Intergovernmental Panel on Climate Change*; Cambridge University Press: Cambridge, UK, 2012; Available online: https://www.ipcc.ch/pdf/special-reports/srex/SREX_Full_Report.pdf (accessed on 9 July 2018).
3. Lehner, B.; Döll, P.; Alcamo, J.; Henrichs, T.; Kaspar, F. Estimating the Impact of Global Change on Flood and Drought Risks in Europe: A Continental, Integrated Analysis. *Clim. Chang.* **2006**, *75*, 273–299. [CrossRef]
4. Intergovernmental Panel on Climate Change (IPCC). *Climate Change 2014: Synthesis Report; Contribution of Working Groups I, II and III to the Fifth Assessment Report of the Intergovernmental Panel on Climate Change*; Pachauri, R.K., Meyer, L.A., Eds.; IPCC: Geneva, Switzerland, 2014; 151p. Available online: https://www.ipcc.ch/pdf/assessment-report/ar5/syr/SYR_AR5_FINAL_full_wcover.pdf (accessed on 9 July 2018).
5. Seneviratne, S.I.; Lüthi, D.; Litschi, M.; Schär, C. Land-atmosphere coupling and climate change in Europe. *Nature* **2006**, *443*, 205–209. [CrossRef] [PubMed]
6. Spinoni, J.; Vogt, J.V.; Naumann, G.; Barbosa, P.; Dosio, A. Will drought events become more frequent and severe in Europe? *J. Climatol.* **2017**, *38*, 1718–1736. [CrossRef]
7. Spinoni, J.; Naumann, G.; Vogt, V.V.; Barbosa, P. The biggest drought events in Europe from 1950–2012. *J. Hydrol.* **2015**, *3*, 509–524. [CrossRef]

8. García-Ruiz, J.M.; López-Moreno, J.I.; Vicente-Serrano, S.M.; Lasanta-Martínez, T.; Beguería, S. Mediterranean water resources in a global change scenario. *Earth Sci. Rev.* **2011**, *105*, 121–139. [[CrossRef](#)]
9. Bates, B.C.; Kundzewicz, Z.W.; Wu, S.; Palutikof, J.P. *Technical Paper of the Intergovernmental Panel on Climate Change: Climate Change Water*; IPCC Secretariat: Geneva, Switzerland, 2008. Available online: <https://www.ipcc.ch/pdf/technical-papers/climate-change-water-en.pdf> (accessed on 9 July 2018).
10. Ionita, M.; Tallaksen, L.M.; Kingston, D.G.; Stagge, J.H.; Laaha, G.; Van Lanen, H.A.J.; Scholz, P.; Chelcea, S.M.; Haslinger, K. The European 2015 drought from a climatological perspective. *Hydrol. Earth Syst. Sci.* **2017**, *21*, 1397–1419. [[CrossRef](#)]
11. Tallaksen, L.M.; Van Lanen, H.A.J. *Hydrological Drought: Processes and Estimation Methods for Streamflow and Groundwater*; Developments in Water Science; Elsevier Science B.V.: Amsterdam, The Netherlands, 2004; Volume 48.
12. Bisselink, B.; Dolman, A.J. Precipitation recycling: Moisture sources over Europe using ERA-40 Data. *J. Hydrometeorol.* **2008**, *9*, 1073–1083. [[CrossRef](#)]
13. Stojanovic, M.; Drumond, A.; Nieto, R.; Gimeno, L. Anomalies in Moisture Supply during the 2003 Drought Event in Europe: A Lagrangian Analysis. *Water* **2018**, *10*, 467. [[CrossRef](#)]
14. Tsakiris, G.; Pangalou, D.; Vangelis, H. Regional drought assessment based on the Reconnaissance Drought Index (RDI). *Water Resour. Manag.* **2007**, *21*, 821–833. [[CrossRef](#)]
15. Nalbantis, I.; Tsakiris, G. Assessment of Hydrological Drought Revisited. *Water Resour. Manag.* **2009**, *23*, 881–897. [[CrossRef](#)]
16. Palmer, W.C. *Meteorological Drought*; White, R.M., Ed.; U.S. Weather Bureau: Washington, DC, USA, 1965. Available online: <https://www.ncdc.noaa.gov/temp-and-precip/drought/docs/palmer.pdf> (accessed on 9 July 2018).
17. McKee, T.B.; Doesken, N.J.; Kleist, J. The relationship of drought frequency and duration to time scales. In Proceedings of the Eighth Conference on Applied Climatology, Boston, MA, USA, 17–22 January 1993; pp. 179–184.
18. Vicente-Serrano, S.M.; Begueria, S.; Lopez-Moreno, J.I. A multiscalar drought index sensitive to global warming: The Standardized Precipitation Evapotranspiration Index. *J. Clim.* **2010**, *23*, 1696–1718. [[CrossRef](#)]
19. Onyutha, C. On Rigorous Drought Assessment Using Daily Time Scale: Non-Stationary Frequency Analyses, Revisited Concepts, and a New Method to Yield Non-Parametric Indices. *Hydrology* **2017**, *4*, 48. [[CrossRef](#)]
20. Sordo-Ward, A.; Dolores Bejarano, M.; Iglesias, A.; Asenjo, V.; Garrote, L. Analysis of Current and Future SPEI Droughts in the La Plata Basin Based on Results from the Regional Eta Climate Model. *Water* **2017**, *9*, 857. [[CrossRef](#)]
21. Meza, F.J. Recent trends and ENSO influence on droughts in Northern Chile: An application of the standardized precipitation evapotranspiration index. *Weather Clim. Extrem.* **2013**, *1*, 51–58. [[CrossRef](#)]
22. Mathbout, S.; Lopez-Bustins, J.A.; Martin-Vide, J.; Bech, J.; Rodrigo, F.S. Spatial and temporal analysis of drought variability at several time scales in Syria during 1961–2012. *Atmos. Res.* **2018**, *200*, 153–168. [[CrossRef](#)]
23. Wang, R.; Peng, W.; Liu, X.; Wu, W.; Chen, X.; Zhang, S. Responses of Water Level in China’s Largest Freshwater Lake to the Meteorological Drought Index (SPEI) in the Past Five Decades. *Water* **2018**, *10*, 137. [[CrossRef](#)]
24. Salah, Z.; Nieto, R.; Drumond, A.; Gimeno, L.; Vicente-Serrano, S.M. A Lagrangian analysis of the moisture budget over the Fertile Crescent during two intense drought episodes. *J. Hydrol.* **2018**, *560*, 382–395. [[CrossRef](#)]
25. Hassanein, M.K.; Kahlil, A.A.; Essa, Y.H. Assessment of drought impact in Africa using Standard Precipitation Evapotranspiration Index. *Nat. Sci.* **2013**, *11*, 75–81. Available online: <https://www.researchgate.net/publication/283615625> (accessed on 9 July 2018).
26. Potop, V.; Boroneant, C.; Stepanek, P.; Skalac, P.; Mozný, M. Observed spatiotemporal characteristics of drought on various time scales over the Czech Republic. *Theor. Appl. Climatol.* **2013**, *115*, 563–581. [[CrossRef](#)]
27. Paulo, A.A.; Rosa, R.D.; Pereira, L.S. Climate trends and behaviour of drought indices based on precipitation and evapotranspiration in Portugal. *Nat. Hazards Earth Syst. Sci.* **2012**, *12*, 1481–1491. [[CrossRef](#)]

28. Vicente-Serrano, S.M.; López-Moreno, J.I.; Lorenzo-Lacruz, J.; El Kenawy, A.; Azorin-Molina, C.; Morán-Tejeda, E.; Pasho, E.; Zabalza, J.; Begueria, S.; Angulo-Martinez, M. The NAO impact on droughts in the Mediterranean region. In *Hydrological, Socioeconomic and Ecological Impacts of the North Atlantic Oscillation in the Mediterranean Region—Advances in Global Change Research*; Springer: Rotterdam, The Netherlands, 2011; Volume 46, pp. 23–40. [[CrossRef](#)]
29. Potopová, V.; Boroneat, C.; Boincean, B.; Soukup, J. Impact of agricultural drought on main crop yields in the Republic of Moldova. *Int. J. Climatol.* **2016**, *36*, 2063–2082. [[CrossRef](#)]
30. Spinoni, J.; Naumann, G.; Vogt, J.V.; Barbosa, P. European drought climatologies and trends based on a multi-indicator approach. *Glob. Planet. Chang.* **2015**, *127*, 50–57. [[CrossRef](#)]
31. Peterson, T.C.; Hoerling, M.P.; Stott, P.A.; Herring, S.C. (Eds.) Explaining Extreme Events of 2012 from a Climate Perspective. *Bull. Am. Meteorol. Soc.* **2013**, *94*, S1–S74. [[CrossRef](#)]
32. Sori, R.; Nieto, R.; Vicente-Serrano, S.M.; Drumond, A.; Gimeno, L. A Lagrangian perspective of the hydrological cycle in the Congo River Basin. *Earth Syst. Dyn.* **2017**, *8*, 653–675. [[CrossRef](#)]
33. Drumond, A.; Gimeno, L.; Nieto, R.; Trigo, R.M.; Vicente-Serrano, S.M. Drought episodes in the climatological sinks of the Mediterranean moisture source: The role of moisture transport. *Glob. Planet. Chang.* **2017**, *151*, 4–14. [[CrossRef](#)]
34. Gimeno, L.; Stohl, A.; Trigo, R.M.; Domínguez, F.; Yoshimura, K.; Yu, L.; Drumond, A.; Durán-Quesada, A.M.; Nieto, R. Oceanic and Terrestrial Sources of Continental Precipitation. *Rev. Geophys.* **2012**, *50*, RG4003. [[CrossRef](#)]
35. Gimeno, L.; Drumond, A.; Nieto, R.; Trigo, R.M.; Stohl, A. On the origin of continental precipitation. *Geophys. Res. Lett.* **2010**, *37*, L13804. [[CrossRef](#)]
36. Stohl, A.; James, P. A Lagrangian Analysis of the Atmospheric Branch of the Global Water Cycle. Part I: Method Description, Validation, and Demonstration for the August 2002 Flooding in Central Europe. *J. Hydrometeorol.* **2004**, *5*, 656–678. [[CrossRef](#)]
37. Stohl, A.; James, P. A Lagrangian analysis of the atmospheric branch of the global water cycle: Part II: Moisture Transports between Earth's Ocean Basins and River Catchments. *J. Hydrometeorol.* **2005**, *6*, 961–984. [[CrossRef](#)]
38. Mariotti, A.; Struglia, M.V.; Zeng, N.; Lau, K.M. The Hydrological Cycle in the Mediterranean Region and Implications for the Water Budget of the Mediterranean Sea. *J. Clim.* **2002**, *15*, 1674–1690. [[CrossRef](#)]
39. Bosilovich, M.G.; Schubert, S.D. Water vapor tracers as diagnostics of the regional hydrologic cycle. *J. Hydrometeorol.* **2002**, *3*, 149–165. [[CrossRef](#)]
40. Brubaker, K.L.; Entekhabi, D.; Eagleson, P. Estimation of continental precipitation recycling. *J. Clim.* **1993**, *6*, 1077–1089. [[CrossRef](#)]
41. Dominguez, F.; Kumar, P.; Liang, X.-Z.; Ting, M. Impact of atmospheric moisture storage on precipitation recycling. *J. Clim.* **2006**, *19*, 1513–1530. [[CrossRef](#)]
42. Coplen, T.B.; Neiman, P.J.; White, A.B.; Landwehr, J.M.; Ralph, F.M.; Dettinger, M.D. Extreme changes in stable hydrogen isotopes and precipitation characteristics in a landfalling Pacific storm. *Geophys. Res. Lett.* **2008**, *35*, L21808. [[CrossRef](#)]
43. Sodemann, H.; Schwierz, C.; Wernli, H. Interannual variability of Greenland winter precipitation sources: Lagrangian moisture diagnostic and North Atlantic Oscillation influence. *J. Geophys. Res.* **2008**, *113*, D03107. [[CrossRef](#)]
44. Dirmeyer, P.A.; Brubaker, K.L. Characterization of the global hydrologic cycle from a back-trajectory analysis of atmospheric water vapor. *J. Hydrometeorol.* **2007**, *8*, 20–37. [[CrossRef](#)]
45. Fernandez, J.; Saenz, J.; Zorita, E. Analysis of winter time atmospheric moisture transport and its variability over Southern Europe in the NCEP-reanalyses. *Clim. Res.* **2003**, *23*, 195–215. [[CrossRef](#)]
46. Nieto, R.; Gimeno, L.; Drumond, A.; Hernandez, E. A Lagrangian identification of the main moisture 344 sources and sinks affecting the Mediterranean area. *WSEAS Trans. Environ. Dev.* **2010**, *6*, 1790–5079. Available online: http://ephyslab.uvigo.es/publica/documents/file_23740-A%20Lagrangian%20identification%20of%20the%20main%20moisture%20sources%20and%20sinks%20affecting%20the%20Mediterranean%20area-WSEAS-2010.pdf (accessed on 9 July 2018).
47. Schicker, I.; Radanovics, R.; Seibert, P. Origin and transport of Mediterranean moisture and air. *Atmos. Chem. Phys.* **2010**, *10*, 5089–5105. [[CrossRef](#)]

48. Drumond, A.; Nieto, R.; Hernández, E.; Gimeno, L. A Lagrangian analysis of the variation in moisture sources related to drier and wetter conditions in regions around the Mediterranean basin. *Nat. Hazards Earth Syst. Sci.* **2011**, *11*, 2307–2320. [[CrossRef](#)]
49. Gómez-Hernández, M.; Drumond, A.; Gimeno, L.; Garcia-Herrera, R. Variability of moisture sources in the Mediterranean region during the period 1980–2000. *Water Resour. Res.* **2013**, *49*, 6781–6794. [[CrossRef](#)]
50. Sodemann, H.; Zubler, E. Seasonal and inter-annual variability of the moisture sources for Alpine precipitation during 1995–2002. *Int. J. Climatol.* **2010**, *30*, 947–961. [[CrossRef](#)]
51. Lionello, P.; Malanotte-Rizzoli, P.; Boscolo, R.; Alpert, P.; Artale, V.; Li, L.; Luterbacher, J.; May, W.; Trigo, R.; Tsimplis, M.; et al. The Mediterranean climate: An overview of the main characteristics and issues. *Dev. Earth Environ. Sci.* **2006**, *4*, 1–26. [[CrossRef](#)]
52. Ciric, D.; Nieto, R.; Losada, L.; Drumond, A.; Gimeno, L. The Mediterranean Moisture Contribution to Climatological and Extreme Monthly Continental Precipitation. *Water* **2018**, *4*, 519. [[CrossRef](#)]
53. Kyselý, J.; Beranová, R. Climate-change effects on extreme precipitation in central Europe: Uncertainties of scenarios based on regional climate models. *Theor. Appl. Climatol.* **2009**, *95*, 361–374. [[CrossRef](#)]
54. Dee, D.P.; Uppala, S.M.; Simmons, A.J.; Berrisford, P.; Poli, P.; Kobayashi, S.; Andrae, U.; Balmaseda, M.A.; Balsamo, G.; Bauer, P.; et al. The ERA-Interim reanalysis: Configuration and performance of the data assimilation system. *Q. J. R. Meteorol. Soc.* **2001**, *137*, 553–597. [[CrossRef](#)]
55. Lorenz, C.; Kunstmann, H. The hydrological cycle in three state-of-the-art reanalyses: Intercomparison and performance analysis. *J. Hydrometeorol.* **2012**, *13*, 1397–1420. [[CrossRef](#)]
56. Rienecker, M.; Suarez, M.; Gelaro, R.; Todling, R.; Bacmeister, J. Co-authors, 2011: MERRA: NASA's Modern Era Retrospective Analysis for Research and Applications. *J. Clim.* **2014**, *24*, 3624–3648. [[CrossRef](#)]
57. National Center for Atmospheric Research Staff (Ed.) Last modified 08 November 2017. "The Climate Data Guide: Climate Forecast System Reanalysis (CFSR)". Available online: <https://climatedataguide.ucar.edu/climate-data/climate-forecast-system-reanalysis-cfsr> (accessed on 9 July 2018).
58. Gimeno, L.; Nieto, R.; Drumond, A.; Castillo, R.; Trigo, R.M. Influence of the intensification of the major oceanic moisture sources on continental precipitation. *Geophys. Res. Lett.* **2013**, *40*, 1443–1450. [[CrossRef](#)]
59. Harris, I.; Jones, P.D.; Osborn, T.J.; Lister, D.H. Updated high-resolution grids of monthly climatic observations—The CRU TS3.10 Dataset. *Int. J. Climatol.* **2014**, *34*, 623–642. [[CrossRef](#)]
60. Yu, L.; Jin, X.; Weller, R.A. *Multidecade Global Flux Datasets from the Objectively Analyzed Air-Sea Fluxes (OAFlux) Project: Latent and Sensible Heat Fluxes, Ocean Evaporation, and Related Surface Meteorological Variables*; OAFlux Project Tech. Rep. OA-2008-01; Woods Hole Oceanographic Institution: Woods Hole, MA, USA, 2008; 64p. Available online: http://oafux.whoi.edu/pdfs/OAFlux_TechReport_3rd_release.pdf (accessed on 9 July 2018).
61. Stagge, J.A.; Tallaksen, L.M.; Gudmundsson, L.; Van Loon, A.F.; Stahle, K. Candidate distributions for climatological drought indices (SPI and SPEI). *Int. J. Climatol.* **2015**, *35*, 4027–4040. [[CrossRef](#)]
62. Stagge, J.A.; Tallaksen, L.M.; Gudmundsson, L.; Van Loon, A.F.; Stahle, K. Short communication response to comment on Candidate Distributions for Climatological Drought Indices (SPI and SPEI). *Int. J. Climatol.* **2016**, *36*, 2132–2138. [[CrossRef](#)]
63. Vicente-Serrano, S.M.; Beguería, S. Short communication comment on "candidate distributions for climatological drought indices (SPI and SPEI)" by James H. Stagge et al. *Int. J. Climatol.* **2016**, *36*, 2120–2131. [[CrossRef](#)]
64. Vicente-Serrano, S.M.; Gouveia, C.; Camarero, J.J.; Beguería, S.; Trigo, R.; López-Moreno, J.I.; Azorín-Molina, C.; Pasho, E.; Lorenzo-Lacruz, J.; Revuelto, J.; et al. Response of vegetation to drought time-scales across global land biomes. *Proc. Natl. Acad. Sci. USA* **2013**, *110*, 52–57. [[CrossRef](#)] [[PubMed](#)]
65. Vicente-Serrano, S.M.; Aguilar, E.; Martínez, R.; Martín-Hernández, N.; Azorin-Molina, C.; Sanchez-Lorenzo, A.; El Kenawy, A.; Tomás-Burguera, M.; Moran-Tejeda, E.; López-Moreno, J.I.; et al. The Complex influence of ENSO on droughts in Ecuador. *Clim. Dyn.* **2016**, *48*, 405–427. [[CrossRef](#)]
66. Vicente-Serrano, S.M.; Beguería, S.; López-Moreno, J.I. Comment on "Characteristics and trends in various forms of the Palmer Drought Severity Index (PDSI) during 1900–2008" by A. Dai. *J. Geophys. Res. Atmos.* **2011**, *116*, D19112. [[CrossRef](#)]
67. Beguería, S.; Vicente-Serrano, S.M.; Reig, F.; Latorre, B. Standardized Precipitation Evapotranspiration Index (SPEI) revisited: Parameter fitting, evapotranspiration models, tools, datasets and drought monitoring. *Int. J. Climatol.* **2014**, *34*, 3001–3023. [[CrossRef](#)]

68. Liu, Z.; Lu, G.; He, H.; Wu, Z.; He, J. Anomalous Features of Water Vapor Transport during Severe Summer and Early Fall Droughts in Southwest China. *Water* **2017**, *9*, 244. [[CrossRef](#)]
69. Stojanovic, M.; Drumond, A.; Nieto, R.; Gimeno, L. Moisture Transport Anomalies over the Danube River Basin during Two Drought Events: A Lagrangian Analysis. *Atmosphere* **2017**, *8*, 193. [[CrossRef](#)]
70. Brázdil, R.; Raška, P.; Trnka, M.; Zahradníček, P.; Valášek, H.; Dobrovolný, P.; Řezníčková, L.; Tremml, P.; Stachoň, Z. The central European drought of 1947: Causes and consequences, with particular reference to the Czech Lands. *Clim. Res.* **2016**, *70*, 161–178. [[CrossRef](#)]
71. Tan, C.; Yang, J.; Li, M. Temporal-Spatial Variation of Drought Indicated by SPI and SPEI in Ningxia Hui Autonomous Region, China. *Atmosphere* **2015**, *6*, 1399–1421. [[CrossRef](#)]
72. Spinoni, J.; Naumann, G.; Carrao, H.; Barbosa, P.; Vogt, J. World drought frequency, duration, and severity for 1951–2010. *Int. J. Climatol.* **2014**, *34*, 2792–2804. [[CrossRef](#)]
73. Numaguti, A. Origin and recycling processes of precipitating water over the Eurasian continent: Experiments using an atmospheric general circulation model. *J. Geophys. Res. Atmos.* **1999**, *104*, 1957–1972. [[CrossRef](#)]
74. Ciric, D.; Stojanovic, M.; Drumond, A.; Nieto, R.; Gimeno, L. Tracking the Origin of Moisture over the Danube River Basin Using a Lagrangian Approach. *Atmosphere* **2016**, *7*, 162. [[CrossRef](#)]
75. Duran-Quesada, A.M.; Gimeno, L.; Amador, J.A.; Nieto, R. Moisture sources for Central America: Identification of moisture sources using a Lagrangian analysis technique. *J. Geophys. Res.* **2010**, *115*, D05103. [[CrossRef](#)]
76. Nieto, R.; Gimeno, L.; Gallego, D.; Trigo, R.M. Contributions to the moisture budget of airmasses over Iceland. *Meteorol. Z.* **2007**, *16*, 37–44. [[CrossRef](#)]
77. Sori, R.; Nieto, R.; Drumond, A.; Vicente-Serrano, S.M.; Gimeno, L. The atmospheric branch of the hydrological cycle over the Indus, Ganges, and Brahmaputra river basins. *Hydrol. Earth Syst. Sci.* **2017**, *21*, 6379–6399. [[CrossRef](#)]
78. Zar, J.H. Significance testing of the Spearman rank correlation. *J. Am. Stat. Assoc.* **1972**, *67*, 578–580. [[CrossRef](#)]
79. Drumond, A.; Nieto, R.; Gimeno, L. A Lagrangian approach for investigating anomalies in the moisture transport during drought episodes. *Cuadernos de Investigación Geográfica* **2016**, *42*, 113–125. [[CrossRef](#)]



© 2018 by the authors. Licensee MDPI, Basel, Switzerland. This article is an open access article distributed under the terms and conditions of the Creative Commons Attribution (CC BY) license (<http://creativecommons.org/licenses/by/4.0/>).

Bridging Anomalous Moisture Transport and Drought Episodes in the IPCC Reference Regions

Anita Drumond ^{1*}, Milica Stojanovic¹, Raquel Nieto¹, Sergio Martin Vicente-Serrano², Luis Gimeno¹

1 Environmental Physics Laboratory (UVIGO-CSIC Associated Unit), Universidade de Vigo, Ourense 32004, Spain

2 Instituto Pirenaico de Ecología, Consejo Superior de Investigaciones Científicas (IPE-CSIC), Campus de Aula Dei, Zaragoza 50059, Spain

(*) Corresponding author's e-mail: anitadru@uvigo.es

Capsule (max 30 words):

Catalogue of the drought episodes in the IPCC reference regions from 1980 to 2015, available online, with an analysis of a few moisture budget components during significant meteorological drought episodes

Keywords: moisture transport, IPCC, Lagrangian approach, droughts, SPEI

Abstract

Changes in moisture transport are often the cause of extreme precipitation events; deviations from the “normal” can lead to droughts when the moisture supply is diminished or interrupted. Significant research has been completed to characterise precipitation in the IPCC reference regions (RRs) but a systematic analysis of the changes in atmospheric transport linked to drought episodes is missing. This article describes a catalogue in which the most important drought episodes around the world over the past few decades are identified, and some components of the moisture budget during significant meteorological drought episodes are analysed. For each of the 27 RRs defined in the 5th IPCC Assessment Report, drought episodes during 1980-2015 were identified at different scales through the Standardized Precipitation Evapotranspiration Index (SPEI). SPEI values were computed using time series of the monthly precipitation and Atmospheric Evaporative Demand (AED) averaged over each RR. The approach, which was applied to both identify the climatological moisture sources and sinks for each RR and to investigate anomalies in moisture transport during the most severe meteorological drought episode, is based on the Lagrangian model FLEXPART, integrated with the ERA-Interim data. For each RR, the following components were analysed: a) evaporative conditions over the respective sources; b) partial moisture budget over sources (considering only particles travelling from the sources towards the RR); c) moisture supply from the sources into the RR; and d) moisture supply from the RR into its sink. The results are organized in a webpage available to the scientific community and stakeholders.

Introduction

Understanding hydroclimatological processes is incredibly important, given the number of scientific disciplines involved and their association with several economic, social and ecological impacts (Allen and Ingram, 2002). Climate change is driving global temperature changes and affecting hydroclimatic processes via alterations to circulation (Vecchi and Soden, 2007) and thermodynamic processes (Hirschi et al., 2011). Changes to both these process groups may increase aridity in large regions as a consequence of decreasing moisture supply to continental areas (Sherwood and Fu, 2014). These changes could increase the severity and duration of extreme hydroclimatic events such as droughts (Vicente-Serrano, 2016).

Droughts are extremely complex, with varied definitions causing problems in the conceptualization of the phenomenon (Lloyd-Hughes, 2013). In general, drought is a temporal anomaly in relation to the long-term climate conditions (Wilhite and Pulwarthy, 2017) and is characterised by water availability below normal levels such that it cannot supply the existing demand (Redmond, 2002). Drought is one of the most complex natural hazards to be identified, analysed, monitored, and managed (Wilhite, 1985). However, identifying the physical factors that trigger a drought, which can be extremely complex, involve different mechanism (e.g., García-Herrera et al., 2007), and differ among drought episodes (Marengo and Espinoza, 2015), is also challenging.

There are a number of studies that have linked drought with atmospheric circulation mechanisms, and also with thermodynamic processes related to soil water availability, latent and sensible fluxes, and hot weather (e.g. Feng et al., 2010; Miralles et al, 2018). Nevertheless, no studies have analysed the contribution of moisture sources and moisture transport processes to trigger drought episodes in depth at the global scale. The variations in moisture transport are usually related to a precipitation deficit over an area and, in some cases, to the drought occurrence (Liu et al., 2017).

Gimeno et al. (2012) reviewed the different techniques that may be applied in the investigation of sources of moisture, including “analytical and box models”, “physical water vapour tracers” (isotopes), and “numerical water vapour tracers” (including Lagrangian and Eulerian approaches). Among them, the Lagrangian approach enables the tracking of air parcels, allowing source–receptor relationships to be established in a realistic way (Gimeno et al., 2012). For this reason, this method has been extensively applied in studies of the origin of the water that precipitates over a given region (e.g. Stohl and James, 2004, 2005; Dirmeyer and Brubaker, 2007; Sodemann et al. 2008; Knippertz et al., 2013) and in the characterisation of moisture transport worldwide (e.g. Drumond et al., 2008; Gomez-Hernandez et al., 2013; Sori et al., 2017; Drumond et al., 2016; Salah et al, 2018).

Applying the Lagrangian approach developed by Stohl and James (2004, 2005), Gimeno et al. (2010, 2012, 2013) investigated moisture transport from the major oceanic sources to continental regions. Moreover, Nieto et al. (2014) identified the major climatic sources of moisture during 1980-2012 for two sets of continental climatic regions: one based on regions with similar late 20th century mean climates and similar projected late 21st century precipitation changes, and the other based on the 21 Reference Regions (RRs) defined in the 4th Assessment Report (AR4) of the Intergovernmental Panel on Climate Change (IPCC). They also analysed the interannual variability of these sources and the role

of some climate variability modes (including ENSO and the Northern and Southern Annular Modes (NAM and SAM, respectively)).

Despite the abundance of studies regarding moisture transportation, relatively few studies have analysed the contribution of moisture sources and moisture transport to drought episodes at the regional scale (e.g. Drumond et al., 2016; 2017; Stojanovic et al, 2018a, 2018b; Salah et al., 2018). While it has been proven that the absence of moisture transport from the sources towards the continents may even contribute to the persistence of droughts (Trigo et al., 2013), a systematic analysis of droughts and the associated moisture transport at the global scale is still missing from the literature. Pioneer studies at the regional scale, cited above, have suggested that droughts are strongly affected by anomalies in the moisture source regions and also during moisture transport to the target region. This makes a global assessment of these processes a real priority to determine drought mechanisms, with implications for drought early warning systems, monitoring and forecasting.

This study describes an analysis that may be organized into two major goals: a) identification of the drought episodes at different SPEI time scales (1, 3, 6, 12, 24) over the terrestrial areas of 27 RRs defined in the 5th Assessment Report (AR5) of the IPCC (IPCC, 2014) during 1980-2015, and (b) a Lagrangian analysis of the associated changes in atmospheric moisture transport for the most severe meteorological drought event registered for each RR during the covered period. This global analysis considers the RRs defined at http://www.ipcc-data.org/guidelines/pages/ar5_regions.html and shown in Figure 1a. The results for all the regions are provided in an open catalogue (<http://ephyslab.uvigo.es/seth/>).

The South-eastern South America (SSA) region is analysed in more detail as the only example of a full catalogue in all of the RRs. The SSA comprises Argentina, Uruguay, southern Brazil, and central-southern Paraguay, where a large part of the population and the economic activities of the continent are located. Most of the SSA belongs to the La Plata Basin (LPB), the second largest basin in South America, with economic and ecological significance, as well as increasing demands as a water resource and a source of hydropower (Barros et al., 2006). Pampas, one of the world's richest grasslands in terms of size and biodiversity, and a major agricultural resource, is also located in LPB (Viglizzo and Frank, 2006). The SSA is affected by the South American Monsoon System (Nogués-Paegle et al., 2002), and both continental and ocean surface conditions (Pacific, Indian and Atlantic Oceans) may affect precipitation over the SSA (e.g. Drumond et al., 2008; Sörensson and Menéndez, 2011; Cherchi et al., 2013; Nieto et al., 2014). Droughts are a recurrent phenomenon in areas of the SSA, with impacts including the reduction of crop yields, streamflow deficiencies, and consequent problems for hydropower generation (Carbone et al, 2004; Rivera and Penalba, 2014).

The specific analyses covered in this catalogue for each RR are (a) moisture sources and sinks, (b) the climatic annual cycle of different freshwater budget components, (c) drought episodes at different time scales during the period 1980-2015, (d) anomalies of some freshwater budget components for the most severe meteorological drought episode registered during the period analysed, and (e) the linear correlation between the components of the moisture budget and the SPEI-1 time series.

Method

Lagrangian approach for analysis of moisture transport

The investigation of moisture transport in this study is based on the method developed by Stohl and James (2004, 2005), which made use of the Lagrangian FLEXible PARTicle dispersion model (FLEXPART) (Stohl et al., 2005). In the FLEXPART model, the atmosphere is divided homogeneously into 3-D finite elements (hereafter ‘particles’) that are advected using three-dimensional wind data. The particle positions (latitude, longitude, and altitude) and specific humidity (q) are recorded every 6 hours. The change in the specific moisture of each particle (of mass m) along its trajectory is proportional to the freshwater flux in the particle (the difference between the evaporation e and precipitation p , $e-p$) and can be expressed as: $e - p = m \, dq/dt$. By summing ($e-p$) for all the particles residing in the atmospheric column over a given area, the freshwater flux connected with the tracked particles ($E-P$) is obtained, where E and P are the evaporation and precipitation rate per unit area, respectively.

A complete review of this method, and its advantages and disadvantages with respect to other approaches for moisture transport analysis, is presented in Gimeno et al. (2012). The main advantage of this approach is establishing the relationship between the source and the receptor. This method is limited by the use of the time derivative of moisture, in which unrealistic fluctuations can be interpreted as moisture fluxes. Nevertheless, the presence of a large number of particles in an atmospheric column minimises the effects of such random errors (Stohl and James, 2004, 2005; Gimeno et al., 2010).

The FLEXPART V9.0 particle dispersion model was fed with the ERA-Interim global reanalysis data set from the European Centre for Medium-Range Weather Forecasts (ECMWF) (Dee et al., 2011), with a horizontal resolution of 1° on 61 vertical levels, ranging from 1000 to 0.1 hPa. Since FLEXPART requires high-quality data for wind and humidity, the ERA-Interim reanalysis data is the most appropriate to feed the model (Gimeno et al., 2013) because it reproduces the hydrological cycle in a more realistic way than the ERA-40 data and other reanalysis products, such as the Modern Era Retrospective-Analysis for Research and Applications (MERRA) and Climate Forecast System Reanalysis (CFRS) (Trenberth et al., 2011; Lorenz and Kunstmann, 2012) data.

The analysis covered the period from 1980 to 2015. Because the FLEXPART model requires high-quality data for wind and humidity, the restriction of using reanalysis data post-1979 is justified by the inclusion of satellite information, which contributed to minimize the errors in both variables (Gimeno et al., 2013). Other sources of error in this Lagrangian approach are the limited resolution, uncertainties, and the interpolation of the input data (Scarchilli et al., 2011).

For this work, the outputs of FLEXPART came from a global simulation in which the atmosphere was divided into approximately 2 million ‘particles’. The changes in specific moisture were computed every 6 hours (00:00, 06:00, 12:00 and 18:00 UTC). The particles were tracked for a period of 10 days, which is the global average residence time of water vapour in the atmosphere (Numaguti, 1999). The analysis of the E-P field averaged over the 10-d period reveals the main sources and sinks of moisture for a given region. The moisture sources are identified through backwards time analysis, and

comprised areas where evaporation exceeded precipitation ($E - P > 0$) when only considering trajectories towards the target area. The forward-tracking analysis identifies those points at which the moisture budget of the air particles shows a contribution of moisture to the atmosphere along trajectories from a given region, i.e. the region's moisture sinks (areas where precipitation exceeded evaporation, $E - P < 0$). In addition, a forward analysis may be conducted from the sources to estimate their moisture supply (negative values of $E - P$) for a target region. In order to be consistent with the resolution of the Era-Interim data, the outputs from the Lagrangian approach were re-arranged in a 1° horizontal resolution grid. All the remaining fields analysed in this work were also interpolated to a 1° resolution (where they were originally available in a different resolution) before proceeding with the calculations.

Drought identification and analysis

Given the difficulties in quantification, several indices have been developed to identify drought and to establish its severity (Heim, 2002; Mishra and Singh, 2010; Mukherjee et al., 2018). The World Meteorological Organization (WMO) recommends the use of the Standardized Precipitation Index (SPI) for operative monitoring purposes (Hayes et al., 2011), a standard methodology to calculate this index already exists (WMO, 2012). The main advantage of this index is the ability to calculate it on different time scales, which is essential when adapting the different response times of usable water sources to precipitation variability (McKee et al., 1993), with implications for the accurate identification of hydrological, agricultural and environmental impacts (Lorenzo-Lacruz et al., 2013; Vicente-Serrano et al., 2013; Peña-Gallardo et al., 2018). The main problem with the SPI is that calculation is exclusively based on precipitation, but other meteorological variables also affect drought occurrence and severity. Among these variables, the Atmospheric Evaporative Demand (AED) is essential to determine drought severity and intensification processes, which is stressed in recent “flash drought” episodes in which drought has evolved in few weeks as a consequence of a strong AED (Otkin et al., 2017).

For this reason, in this study, drought severity is identified by the Standardized Precipitation Evapotranspiration Index (SPEI) (Vicente-Serrano et al., 2010). The SPEI follows the same conceptual approach as the SPI, being calculated at various time scales, but also includes the AED in calculations by means of a simple climatic balance (precipitation minus AED). The SPEI is equally sensitive to precipitation and the AED (Vicente-Serrano et al., 2015) and is advantageous in relation to other indices which can identify drought severity and impacts worldwide (e.g. Vicente-Serrano et al., 2012). Details of the SPEI calculation can be found in Vicente-Serrano et al., 2010; Beguería et al., 2014 and Vicente-Serrano and Beguería, 2016.

1-, 3-, 6-, 12-, and 24-month SPEI time scales for 1980-2015 were calculated for each RR through time series of monthly precipitation (PRE) and AED, averaged over the region, in order to identify the drought episodes at different time scales. The data comes from the Climate Research Unit (CRU) Time-Series (TS) Version 3.24.01 (Harris et al., 2014), available with a horizontal resolution of 0.5 degrees. A modified version of the Penman-Monteith Reference Evapotranspiration (ET_o) equation is used in the CRU dataset as a metric of the AED. This ET_o can be associated with the AED since resistance factors are not temporally and spatially variable and only depend on the four main

meteorological drivers of AED (i.e. air temperature, radiation, atmospheric humidity and wind speed, as is the case for FAO-56 crop reference evaporation (Allen et al., 1998)).

The identification of drought episodes during 1980-2015 follows the criteria of McKee et al. (1993), in which an episode starts when the SPEI value first falls below zero (month included), followed by a value of -1 or less, and ends when the SPEI returns to a positive value (month not included). Some variables for the different drought episodes were then computed: severity, duration, intensity and peak value (Spinoni et al., 2014; Tan et al., 2015). The severity represents the absolute sum of all SPEI values during the episode; duration signifies the number of months between the first and last month of the episode; intensity is calculated as the ratio between the severity and duration; and the peak value is the most negative value registered during the event.

Description of the Catalogue

Item 1: Climatological Annual Cycle of Precipitation and Atmospheric Evaporative Demand over the RR

The 1980-2015 monthly averages of the PRE and AED integrated over the RR illustrates the climatological annual cycle of both fields necessary for the computation of the SPEI index. Figure 1b shows an example for the SSA region.

Item 2: Climatological Annual Cycle of Selected Freshwater Budget Components Associated with the Moisture Sources and Sinks of the RR

The major moisture sources have been identified through the tracking of air masses over a given region backwards through time. A percentile criterion was applied to define a threshold delimiting the spatial extent of the sources and sinks of moisture (Drumond et al., 2014). The 95th percentile of the climatological annual global positive E-P field returns the grid points in which 5% of the highest positive (E-P) values are found, and indicates those regions where the air masses take up a large amount of moisture on their path to the target region. For the example given here, the main moisture sources for the SSA RR, according to the threshold of 0.15 mm/day (95th percentile of E-P > 0 values obtained for the globe, indicated as a blue contour line in Figure 2a), are displayed in Figure 2b. According to the analysis, there are three remote major moisture sources for the SSA RR (grey region in Figure 2b): namely the South Atlantic Ocean (SAT, dark blue), the South Pacific Ocean (SPO, light blue), and a terrestrial source (TER, orange). For consistency between figures for different RRs, the remote terrestrial sources are given in orange and the RR itself appears in grey.

The annual climatological cycle of some moisture budget components associated with each RR is displayed in this item. The evaporation rate, integrated over the maritime and terrestrial sources, was computed using data from the Objectively Analysed air-sea Heat Fluxes (OAFlux, available at a horizontal resolution of 1°) (Yu et al., 2008) and the Global Land Evaporation Amsterdam Model (GLEAM v3.1a, available at a horizontal resolution of 0.25°) (Miralles et al., 2011) projects, respectively (Figures 2c and d for the SSA RR). GLEAM data was applied for remote terrestrial areas only, and over the RR itself (sources identified as orange and grey in Figure 2, respectively). For the remaining maritime sources, evaporation was computed from the OAFLUX. The source-sink relationship

obtained through the Lagrangian analysis is illustrated in the moisture uptake ($E-P > 0$, backward run from the RR) integrated over the sources (Figures 2e and f for the SSA RR), and the moisture supply ($E-P < 0$, forward run) from the sources and integrated over the RR (Figures 2g and h for the SSA RR). The 1980-2015 monthly averages for the sources analysed are superposed on a histogram, and the annual values in percentage terms are summarized in a pie chart.

Analysing the SSA RR as an example (Figure 2) of the interpretation of the results, the evaporation rates (Figures 2c and d), the moisture uptake (Figures 2e and f) and the moisture supply (Figures 2g and h) associated with the selected sources show a similar annual pattern, with minimum values during June-August (Austral Winter), reaching a maximum during November-March (Austral Summer). Comparing the evaporation over the sources, evaporation over the maritime SAT prevails throughout the year and is particularly strong from April to June. Evaporation over the SSA RR itself is also significant through the year, particularly from October to March (Figures 2c and d). The moisture uptake by particles travelling towards the SSA RR prevails over the SSA itself and TER regions (Figures 2e and f). The annual cycle of moisture supply from the sources for the SSA (the moisture from these sources left over the SSA RR by particles) shows that the terrestrial supply (TER) prevailed throughout the year, even when reduced in the Austral Winter months (Figure 2g).

On one hand, although the SAT is the most evaporative source, it is interesting to note that its relevance for the SSA RR decreases in terms of moisture uptake when considering only the particles travelling from the SAT towards the SSA RR, what means that the moisture evaporated over the SAT may be transported towards other regions instead of the SSA RR. Moreover, the moisture supplied by the SAT to the SSA RR is minimal in comparison with other sources, suggesting that this source is not as effective in generating precipitation over the SSA RR when compared to the SSA RR and TER. On the other hand, although not as evaporative, the moisture transport from the TER source is more relevant for the SSA RR, seen in the increase in the relative importance of moisture uptake over the source and, mainly, through the predominance of the supply of moisture from the TER in the annual cycle.

The importance of the RR as a source of moisture for remote continental areas has also been investigated. The identification of remote moisture sinks is based on the tracking of air masses over the RR forward in time. The 99th percentile of the negative values of $E-P$ (areas where precipitation exceeded evaporation), obtained from the global climate on an annual scale, defined the spatial extent of these sinks, and indicates regions where the air masses lose a large amount of moisture on their path from the RR. For the SSA RR, the main continental moisture sink, according to the threshold of -0.34 mm/day (99th percentile of $E-P < 0$ values obtained for the globe, indicated as a red contour line in Figure 3a), constitutes a small portion west of the RR (TER, orange region in Figure 3b).

To illustrate how the moisture transport from the RR may affect remote continental precipitation, the annual cycle of PRE over its sink is plotted together with the moisture contribution ($E-P < 0$ from the forward run) from the RR to its sink (Figure 3c for the SSA RR). All values are the total over an area. Figure 3c exemplifies the results for the SSA RR, and the 1980-2015 annual cycle reveals that the RR contribution (moisture supply to the SSA RR, grey line) and the PRE over the sink (PRE, blue line) follow a similar evolution, with a maximum during the Austral Summer, and a minimum during the

Austral Winter months, which suggests that the RR significantly influences precipitation regime of its moisture sink.

Item 3: Standardized Precipitation Evapotranspiration Index (SPEI) Time Series and Drought Episodes Identified Over the RR at Different Scales during 1980-2015

The time series of the SPEI on the scale of 1, 3, 6, 12, and 24 months over the RR are plotted to show the evolution of the index on different time scales. Figure 4 shows the time series of the SPEI over the SSA RR, with positive values in blue indicating wet periods, and negative values in red showing dry conditions.

A figure illustrating the drought episodes identified in each RR over the five times scales between 1980-2015 is included on the webpage (Figure 5 provides an example for the SSA RR), together with a list of the episodes and their respective indicators (Table 1 shows the SSA RR drought episodes at SPEI-1, SPEI-3, SPEI-6, SPEI-12, and SPEI-24 time scales).

Item 4: Anomalies of Some Freshwater Budget Components for the Most Severe Meteorological Drought Episode Over the RR Identified through SPEI-1 during 1980-2015

It is known that precipitation deficit over an area are usually related to changes in moisture transport, which can lead to drought (Liu et al., 2017). Thus, it is important to analyse how a meteorological drought episode may be associated with changes in the freshwater budget. For this purpose, a case study regarding the anomalies of some freshwater budget components during the most severe meteorological drought episodes identified for each RR during 1980-2015 were analysed.

The SPEI-1 time scale, which corresponds to the climatic water balance for one month, was chosen to select the episodes because it is closely related to meteorological droughts (Liu et al., 2017). The most severe SPEI-1 episode selected for each RR is taken from the list provided in Item 3. For the SSA RR, the selected episode was from Sep/2008 to Jun/2009, with a ten month-long duration, a severity of 11.75, an intensity of 1.18, and a peak of -2.48. Previous studies state that the drought of 2008/2009 in the SSA RR, accompanied by warmer temperatures and inhibited precipitation over the region, was among the most significant in terms of both intensity and extent, causing significant economic losses due to a reduction in crop yields and water supply deficiencies (Marengo et al., 2009, 2010; Aceituno et al., 2009; Bidegain et al., 2010; D'Ambrosio et al., 2013; Carbone et al, 2015, Müller et al., 2014). This episode occurred during a prolonged 2007/2009 La Niña event, which favoured dry conditions over the region (e.g. Diaz et al., 1998).

Monthly anomalies of the following fields for the most severe meteorological drought episode selected over each RR are plotted in a similar way, shown in Figure 6 for the SSA RR:

a) PRE (blue bars, Figure 6a) and AED (red bars, Figure 6a) integrated over the RR, together with the precipitation anomalies accumulated during the episode (orange line, Figure 6a) using the CRU dataset. The scale is in mm/day.

b) Evaporation integrated over the oceanic and terrestrial sources identified in Item 2, as shown as for the SSA RR case in Figure 6b. For this example, the bars show the anomalies over four different moisture sources (the South Atlantic (SAT) (dark blue), South Pacific (SPO) (light blue), terrestrial moisture sources surrounding the region (TER), and the region itself (SSA)). For each month, the bars for each source region are superimposed to avoid cluttering. The height of each bar represents the magnitude of the anomalies from the respective source. For each month, a triangle indicates the total accumulated anomaly from all the sources. The scale is in mm/day, and the maritime evaporation data comes from OAFLUX, while the terrestrial is from GLEAM.

c) Moisture uptake ($E-P > 0$) integrated over the sources, as well as the accumulated anomaly from all the sources. The structure of the graphic is similar to that of b). The values are obtained via the backwards-in-time Lagrangian analysis from the RR, and the scale is in mm/day.

d) Moisture supply ($E-P < 0$) from each source and integrated over RR, and the accumulated anomaly of the supply from all the sources. The structure of the graphic also follows b) and c). The values are obtained via the forward Lagrangian analysis from each source, and the scale is in mm/day.

e) Moisture supply ($E-P < 0$) from the RR integrated over its climatic sink (identified in Item 2), and the PRE integrated over the sink (Figure 6e, bars and contour line for PRE and supply, respectively). The values of the supply are obtained via the forward Lagrangian analysis from the RR and integrated over the sink, while the PRE is obtained from CRU data. The scale is in mm/day for both fields.

In all the graphics, the first and last month are determined considering an interval of two months before the onset and after the dismissal of the episode. This information is also provided in the list of the episodes available in Item 3.

Taking the 2008/2009 episode over the SSA RR as an example of this analysis, Figure 6a shows the predominance of negative PRE anomalies over the SSA RR during the event, reaching a peak in April 2009. Positive AED anomalies prevailed over the SSA RR during the episode, being more intense in November 2008. The total evaporation over the sources (Figure 6b) reduced from September 2008 to March 2009, in particular over the SSA RR and TER. In April 2009, increased evaporation over the SAT coincided with the month in which the evaporation over this source became climatically significant (Figure 2c). The moisture uptake over the sources (Figure 6c) reduced from September to November 2008, mainly over the SSA RR. However, it increased from December 2008 to April 2009. The moisture supply accumulated from all sources for the SSA RR reduced during the episode, particularly from the TER and SSA RR up to April 2009 (Figure 6d). Results from Figure 6 suggest that April 2009 was a key month for this episode, when the most intense negative anomalies of PRE occurred over the SSA RR, associated with the most negative moisture supply values (mainly from the TER and SSA). However, evaporation over the SAT increased in April 2009, and the anomalies in the moisture uptake and supply reduced in May.

Figure 6e shows how the moisture transport from the SSA RR, to its sink, was affected during this episode. Reduced moisture supply from the SSA RR and negative precipitation anomalies prevailed over the sink from January 2009 onwards, and the peak in both anomalies occurred in February 2009.

Item 5: Correlation Analysis between the Anomalies of Selected Freshwater Budget Components and the SPEI-1 Time Series for the RR during 1980-2015

In this item, a climatological perspective of the relationship between meteorological droughts over the RRs and the components of the freshwater budget is provided. The joint linear variability between the SPEI-1 time series for the RR and anomalies of the components analysed in Item 4 is investigated through Pearson correlation analysis for 1980-2015.

The results are shown in two tables, as illustrated here for the SSA RR example, and the values significant at the 99% confidence level, according to the Student's t-test, are emphasised in italics.

The Pearson correlation coefficients between the evaporation and moisture uptake anomalies over the sources, as well as in the moisture supply from the sources to the RR, and the SPEI-1 for RR, are shown in the first table of Item 5. With regard to the SSA RR (Table 2), results show a higher joint linear temporal variability between the SPEI-1 and the moisture supply from both terrestrial sources (local SSA RR and external TER) with coefficients higher than 0.5.

The second table in this item shows the Pearson correlation coefficients between the time series of moisture supply from the RR to its remote terrestrial sink, as well as PRE over sink. For the SSA RR (Table 3), the coefficient is 0.28.

Final Remarks

The purpose of the catalogue described in this paper is to contribute towards a deeper understanding of the climate regions defined in the IPCC and considered as reference, particularly in climate change studies, by the scientific community, not only by the identification of drought episodes on several time-scales during the last three decades, but also by a detailed analysis of different components of the associated moisture budget. The moisture analysis, developed through a Lagrangian approach, is organised in two parts: the first highlights the role of the region as a receptor and source of moisture under a climatic perspective, while the second one analyses variations in the moisture budget components during a case study of a significative meteorological drought. Although performed for just one case, this analysis serves as an attempt to illustrate which components of the moisture budget most significantly impact the region during extreme conditions. Knowing the effective moisture source-sink relationships is useful to elucidate how sensitive precipitation of a given region may be to changes in the moisture budget associated with a remote area, and this information is of key importance to both present and future climate studies.

Acknowledgements

We are grateful to the financial support from the Spanish Government (Ministerio de Economía, Industria y Competitividad) and the European Regional Development Fund of the European Commission (in Spanish, FEDER) through the SETH project (CGL2014-60849-JIN). The PhD. Fellowship of Milica Stojanovic is supported by the European Commission under the Erasmus Mundus project Green-Tech-WB: Smart and Green technologies for innovative and sustainable societies in Western Balkans (551984-EM-1-2014-1-ES-ERA Mundus-EMA2). This work was partially supported by Xunta de Galicia under Project ED431C 2017/64-GRC “Programa de Consolidación e Estruturación de Unidades de Investigación Competitivas (Grupos de Referencia Competitiva)”. We would also like to thank the IMDROFLOOD project financed by the Water Works 2014 co-funded call of the European Commission.

References

- Aceituno P., M. Bidegain, J. Quintana, M. Skansi, and M. Rusticucci, 2009: Southern South America [in “State of the Climate in 2008”]. *Bull. Amer. Meteor. Soc.*, **90** (8), S136–S137
- Allan, M. R., and W. J. Ingram, 2002: Constrains on future changes in climate and the hydrological cycle, *Nature*, 409, 224-232, <http://dx.doi.org/10.1038/nature01092>.
- Allen, R.G., L.S. Pereira, D. Raes, and M. Smith, 1998: FAO Irrigation and Drainage Paper No. 56; Food and Agriculture Organization of the United Nations: Rome, Italy.
- Barros, V., R. Clarke, and P.S. Dias (Eds), 2006: Climate Change in the La Plata Basin, Publication of the Inter-American Institute for Global Change Research (<http://www.iai.int/>).
- Beguiría, S., S.M. Vicente-Serrano, F. Reig, and B. Latorre, 2014: Standardized Precipitation Evapotranspiration Index (SPEI) revisited: Parameter fitting, evapotranspiration models, tools, datasets and drought monitoring. *Int. J. Climatol.*, **34**, 3001–3023, <https://doi.org/10.1002/joc.3887>.
- Bidegain M., M. Skansi, O. Penalba, J. Quintana, and P. Aceituno, 2010: Southern South America [in “State of the Climate in 2009”]. *Bull. Amer. Meteor. Soc.*, **91** (7), S150–S152.
- Carbone M.E., M.C. Piccolo, and B.V. Scian, 2004: Análisis de los periodos secos y húmedos en la cuenca del Arroyo Claromecó, Argentina. *Papeles de Geografía* **40**, 25-36.
- Cherchi, A., A. Carril, C. Menéndez, and L. Zamboni, 2014: La Plata Basin precipitation variability in spring: Role of remote SST forcing as simulated by GCM experiments. *Climate Dyn.*, **42**, 219–236, [doi:https://doi.org/10.1007/s00382-013-1768-y](https://doi.org/10.1007/s00382-013-1768-y).
- Carbone, M.E., C.F. Fornerón, and M.C. Piccolo, 2015: Impacto de los eventos de sequía en la región de la cuenca hidrográfica de la laguna Sauce Grande (Provincia de Buenos Aires, Argentina). *Investigaciones Geográficas*, **63**, 131-142, DOI: 10.14198/INGEO2015.63.09.

D'Ambrosio, G. T., V.Y. Bohn, and M.C. Piccolo, 2013: Evaluación de la sequía 2008-2009 en el oeste de la Región Pampeana. *Cuadernos Geográficos*, **52**, 29-45.

Dee, D.P., and Coauthors, 2011: The ERA-Interim reanalysis: configuration and performance of the data assimilation system. *Q. J. Roy. Meteorol. Soc.*, **137**, 553– 597, doi:10.1002/qj.828.

Diaz, A.F., C.D. Studzinski and C.R. Mechoso, 1998: Relationships between precipitation anomalies in Uruguay and southern Brazil and sea surface temperature in the Pacific and Atlantic oceans. *J. Climate*, **11**, 251-271, DOI: 10.1175/1520-0442(1998)011<0251:RBPAlU>2.0.CO;2.

Dirmeyer, P. A., and K. L. Brubaker, 2007: Characterization of the global hydrologic cycle from a back-trajectory analysis of atmospheric water vapor, *J. Hydrometeorol.*, **8**, 20–37, doi:10.1175/JHM557.1.

Drumond, A., R. Nieto, L. Gimeno, and T. Ambrizzi, 2008: A Lagrangian identification of major sources of moisture over central Brazil and La Plata Basin, *J. Geophys. Res.*, **113**, D14128, doi:10.1029/2007JD009547.

Drumond, A., J. Marengo, T. Ambrizzi, R. Nieto, L. Moreira, and L. Gimeno, 2014: The role of the Amazon Basin moisture in the atmospheric branch of the hydrological cycle: A Lagrangian analysis. *Hydrol. Earth Syst. Sci.*, **18**, 2577–2598, <https://doi.org/10.5194/hess-18-2577-2014>.

Drumond, A., R. Nieto, and L. Gimeno, 2016: A Lagrangian approach for investigating anomalies in the moisture transport during drought episodes. *Cuadernos de Investigación Geográfica*, **42** (1), 113–125, doi:10.18172/cig.2925.

Drumond, A., L. Gimeno, R. Nieto, R.M. Trigo, and S.M. Vicente-Serrano, 2017: Drought episodes in the climatological sinks of the Mediterranean moisture source: The role of moisture transport. *Glob. Planet. Chang.*, **2017**, 151, 4–14, <https://doi.org/10.1016/j.gloplacha.2016.12.004>.

Feng, S., Q. Hu, , J. Robert, 2010: Influence of Atlantic sea surface temperatures on persistent drought in North America. *Clim. Dyn* , **37** (3-4), 569-586, <http://dx.doi.org/10.1007/s00382-010-0835-x>.

García-Herrera R., D. Paredes, R. M. Trigo, I. F. Trigo, E. Hernandez, D. Barriopedro, and M. A. Mendes, 2007: The outstanding 2004/05 drought in the Iberian Peninsula: associated atmospheric circulation. *J. Hydrometeorol.*, **8**, 483–498, <https://doi.org/10.1175/JHM578.1>.

Gimeno, L., A. Drumond, R. Nieto, R.M. Trigo, and A. Stohl, 2010: On the origin of continental precipitation. *Geophys. Res. Lett.*, **37**, L13804. <https://doi.org/10.1029/2010GL043712>.

Gimeno, L., and Coauthors, 2012: Oceanic and terrestrial sources of continental precipitation. *Rev. Geophys.*, **50**, RG4003, doi:10.1029/2012RG000389.

Gimeno, L., R. Nieto, A. Drumond, R. Castillo, and R.M. Trigo, 2013: Influence of the intensification of the major oceanic moisture sources on continental precipitation, *Geophys. Res. Lett.*, **40**, 1443–1450, doi:10.1002/grl.50338.

- Gómez-Hernández, M., A. Drumond, L. Gimeno, and R. Garcia-Herrera, 2013: Variability of moisture sources in the Mediterranean region during the period 1980–2000. *Water Resour. Res.* **49**, 6781–6794, <https://doi.org/10.1002/wrcr.20538>.
- Harris, I., P.D. Jones, T.J. Osborn, and D.H. Lister, 2014: Updated high-resolution grids of monthly climatic observations—The CRU TS3.10 Dataset. *Int. J. Climatol.*, **34**, 623–642, <https://doi.org/10.1002/joc.3711>.
- Hayes, M., M. Svoboda, N. Wall, and M. Widhalm, 2011: The Lincoln Declaration on Drought Indices: Universal meteorological drought index recommended. *Bull. Amer. Meteor. Soc.*, **92**, 485–488, <https://doi.org/10.1175/2010BAMS3103.1>.
- Heim, R.R., 2002: A Review of Twentieth-Century Drought Indices Used in the United States. *Bull. Amer. Meteor. Soc.*, **83**, 1149–1165, DOI: 10.1175/1520-0477(2002)083<1149:AROTDI>2.3.CO;2.
- Hirschi, M., and Coauthors, 2011: Observational evidence for soil-moisture impact on hot extremes in southeastern Europe. *Nat. Geosci.*, **4**, 17–21, <https://www.nature.com/articles/ngeo1032>.
- Intergovernmental Panel on Climate Change (IPCC). Climate Change 2014: Synthesis Report; Contribution Of Working Groups I, II and III to the Fifth Assessment Report of the Intergovernmental Panel on Climate Change; Pachauri, R.K., Meyer, L.A., Eds.; IPCC: Geneva, Switzerland, 2014; 151p.
- Knippertz P., H. Wernli, and G. Gläser, 2013: A Global Climatology of Tropical Moisture Exports. *J. Clim.*, **26**, 3031–3045, <https://doi.org/10.1175/JCLI-D-12-00401.1>.
- Liu, Z., G. Lu, H. He, Z. Wu, and J. He, 2017: Anomalous Features of Water Vapor Transport during Severe Summer and Early Fall Droughts in Southwest China. *Water*, **9**, 244, <https://doi.org/10.3390/w9040244>.
- Lloyd-Hughes, B., 2013: The impracticality of a universal drought definition, *Theor. Appl. Climatol.*, **117**(3-4), 607–611, doi:10.1007/s00704-013-1025-7.
- Lorenz C., and H. Kunstmann, 2012: The Hydrological Cycle in Three State-of-the-Art Reanalyses: Intercomparison and Performance Analysis. *J. Hydrometeorol.*, **13**, 1397– 1420, doi: 10.1175/jhm-d-11-088.1.
- Lorenzo-Lacruz, J., S.M. Vicente-Serrano, J.C. Gonzalez-Hidalgo, J.L. López-Moreno, and N. Cortesi, 2013: Hydrological drought response to meteorological drought in the Iberian Peninsula. *Clim. Res.*, **58** (2), 117–131, <http://dx.doi.org/10.3354/cr01177>.
- Marengo, J.A., J. Baez, and J. Ronchail, 2009: Tropical South America East of the Andes [in “State of the Climate in 2008”]. *Bull. Amer. Meteor. Soc.*, **90** (8), S134–S136.

- Marengo, J.A., J. Ronchail, J. Baez, L.M. Alves, 2010: Tropical South America East of the Andes [in “State of the Climate in 2009”]. *Bull. Amer. Meteor. Soc.*, **91** (7), S148–S150.
- Marengo, J.A., and J.S. Espinoza, 2015: Extreme Seasonal Droughts and Floods in Amazonia: Causes, Trends and Impacts. *Int J. Climatol.*, **36**, 1033-1050, <https://doi.org/10.1002/joc.4420>.
- McKee, T.B., N.J. Doesken, and J. Kleist, 1993: The relationship of drought frequency and duration to time scales. In *Proceedings of the Eighth Conference on Applied Climatology*, 17–22 January 1993, Anaheim, CA, USA, 179–184.
- Miralles, D. G., T.R.H. Holmes, R.A.M. De Jeu, J.H. Gash, A.G.C.A. Meesters, and A.J. Dolman, 2011: Global land-surface evaporation estimated from satellite-based observations, *Hydrol. Earth Syst. Sci.*, **15**, 453–469, <https://doi.org/10.5194/hess-15-453-2011>.
- Gonzalez Miralles, D., P. Gentine, S. I. Seneviratne, and A. J. Teuling. 2018: Land–atmospheric Feedbacks During Droughts and Heatwaves: State of the Science and Current Challenges”, *Ann. N.Y. Acad. Sci.*, <https://doi.org/10.1111/nyas.13912>
- Mishra, A.K., and V.P. Singh, 2010: A review of drought concepts. *J. Hydrol.*, **391**, 202–216, <https://doi.org/10.1016/j.jhydrol.2010.07.012>.
- Mukherjee, S., A. Mishra, and K.E. Trenberth, 2018: Climate Change and Drought: a Perspective on Drought Indices. *Curr Clim Change Rep.*, **4**, 145-163, <https://doi.org/10.1007/s40641-018-0098-x>.
- Müller, O. V., E. H. Berbery, D. Alcaraz-Segura, and M. B. Ek, 2014: Regional model simulations of the 2008 drought in southern South America using a consistent set of land surface properties. *J. Climate*, **27**, 6754–6778, doi:<https://doi.org/10.1175/JCLI-D-13-00463.1>.
- Nieto, R., R. Castillo, A. Drumond, and L. Gimeno 2014: A catalog of moisture sources for continental climatic regions. *Water Resour. Res.*, **50**, 5322–5328, doi:10.1002/2013WR013901.
- Nogués-Paegle J., C.R. Mechoso, R. Fu, E.H. Berbery, W.C. Chao, T.C. Chen, K. Cook, A.F. Diaz, D. Enfield, R. Ferreira, A.M. Grimm, V. Kousky, B. Liebmann, J. Marengo, K. Mo, J.D. Neelin, J. Paegle, A.W. Robertson, A. Seth, C.S. Vera, J. Zhou, 2002: Progress in Pan American CLIVAR research: understanding the South American monsoon. *Meteorologica*, **27**, 3–32
- Numaguti, A., 1999: Origin and recycling processes of precipitating water over the Eurasian continent: Experiments using an atmospheric general circulation model. *J. Geophys. Res.*, **104**, 1957–1972, <https://doi.org/10.1029/1998JD200026>.
- Otkin, J.A., M. Svoboda, E.D. Hunt, T.W. Ford, M.C. Anderson, C. Hain, and B. Basara, 2017: Flash Droughts: A Review and Assessment of the Challenges Imposed by Rapid-Onset Droughts in the United States. *Bull. Amer. Meteor. Soc.*, 911-919, <https://doi.org/10.1175/BAMS-D-17-0149.1>

- Redmond, K. T., 2002: The depiction of drought: A commentary. *Bull. Amer. Meteor. Soc.*, **83**, 1143–1147, [https://doi.org/10.1175/1520-0477\(2002\)0832.3.CO;2](https://doi.org/10.1175/1520-0477(2002)0832.3.CO;2).
- Rivera, J.A., and O.C. Penalba, 2014: Trends and Spatial Patterns of Drought Affected Area in Southern South America. *Climate*, **2**, 264-278, <https://doi.org/10.3390/cli2040264>.
- Salah, Z., R. Nieto, A. Drumond, L. Gimeno, and S.M. Vicente-Serrano, 2018: A Lagrangian analysis of the moisture budget over the Fertile Crescent during two intense drought episodes. *J. Hydrol.*, **560**, 382–395. <https://doi.org/10.1016/j.jhydrol.2018.03.021>
- Scarchilli, C., M. Frezzotti, and P.M. Ruti, 2011: Snow precipitation at four ice core sites in East Antarctica: Provenance, seasonality and blocking factors. *Clim. Dyn.*, **37**, 2107–2125, DOI: 10.1007/s00382-010-0946-4.
- Sherwood, S., and Q. Fu, 2014: A drier future?, *Science*, **343**, 737–739, DOI: 10.1126/science.1247620.
- Sodemann, H., C. Schwierz, and H. Wernli, 2008: Interannual variability of Greenland winter precipitation sources: Lagrangian moisture diagnostic and North Atlantic Oscillation influence, *J. Geophys. Res.*, **113**, D03107, doi:10.1029/2007JD008503.
- Sörensson, A.A., and C.G. Menéndez, 2011: Summer soil-precipitation coupling in South America. *Tellus A.*, **63A**, 56–68, doi: 10.1111/j.1600-0870.2010.00468. x.
- Sorí, R., R. Nieto, S.M. Vicente-Serrano, A. Drumond, and L. Gimeno, 2017: A Lagrangian perspective of the hydrological cycle in the Congo River basin, *Earth Syst. Dynam.*, **8**, 653-675, <https://doi.org/10.5194/esd-8-653-2017>.
- Spinoni, J., G. Naumann, H. Carrao, P. Barbosa, and J. Vogt, 2014: World drought frequency, duration, and severity for 1951–2010. *Int. J. Climatol.*, **34**, 2792–2804, doi:10.1002/joc.3875.
- Stohl A., and P. James 2004: A Lagrangian analysis of the atmospheric branch of the global water cycle. Part I: Method description, validation, and demonstration for the August 2002 flooding in central Europe. *J. Hydrometeorol.*, **5**, 656–678, [https://doi.org/10.1175/1525-7541\(2004\)005<0656:ALAOTA>2.0.CO;2](https://doi.org/10.1175/1525-7541(2004)005<0656:ALAOTA>2.0.CO;2),
- Stohl A., and P.A. James 2005: A Lagrangian analysis of the atmospheric branch of the global water cycle. Part II: Moisture transports between Earth's ocean basins and river catchments. *J. Hydrometeorol.*, **6**, 961–984, <https://doi.org/10.1175/JHM470.1>.
- Stohl, A., C. Forster, A. Frank, P. Seibert, and G. Wotawa 2005: Technical Note : The Lagrangian particle dispersion model FLEXPART version 6.2. *Atmos. Chem. Phys.* **5**, 2461-2474.
- Stojanovic, M., A. Drumond, R. Nieto, and L. Gimeno, 2018a: Anomalies in Moisture Supply during the 2003 Drought Event in Europe: A Lagrangian Analysis. *Water*, **10**(4), 467.

- Stojanovic, M., A. Drumond, R. Nieto, and L. Gimeno, 2018b: Variations in Moisture Supply from the Mediterranean Sea during Meteorological Drought Episodes over Central Europe. *Atmosphere*, **9**(7), 278, doi:10.3390/atmos9070278.
- Tan, C., J. Yang, and M. Li, 2015: Temporal-Spatial Variation of Drought Indicated by SPI and SPEI in Ningxia Hui Autonomous Region, China. *Atmosphere*, **6**, 1399–1421, doi:10.3390/atmos6101399.
- Trenberth, K. E., J. T. Fasullo, and J. Mackaro, 2011: Atmospheric moisture transports from ocean to land and global energy flows in reanalyses, *J. Clim.*, **24**, 4907–4924, doi:10.1175/2011JCLI4171.1.
- Trigo, R.M., and Coauthors, 2013: The record Winter drought of 2011-12 in the Iberian Peninsula, in Explaining Extreme Events of 2012 from a Climate Perspective. *Bull. Amer. Meteor. Soc.*, **94**(9), S41-S45.
- Vecchi, G. A., and B. J. Soden, 2007: Global warming and the weakening of the tropical circulation. *J. Climate*, **20**(17), 4316–4340, <https://doi.org/10.1175/JCLI4258.1>.
- Vicente-Serrano, S.M., S. Begueria, and A.J. Lopez-Moreno, 2010: A multiscalar drought index sensitive to global warming: The standardized precipitation evapotranspiration index. *J. Clim.*, **23**, 1696–1718.
- Vicente-Serrano, S.M., and Coauthors, 2012: Performance of Drought Indices for Ecological, Agricultural and Hydrological Applications. *Earth Interact.*, **16**, 1–27, <https://doi.org/10.1175/2012EI000434.1>.
- Vicente-Serrano, S.M., and Coauthors, 2013: Response of vegetation to drought time-scales across global land biomes. *Proc. Natl. Acad. Sci. USA.*, **110**, 52–57, doi: 10.1073/pnas.1207068110.
- Vicente-Serrano, S.M., G. Van der Schrier, S. Beguería, C. Azorin-Molina, and J.I. Lopez-Moreno, 2015: Contribution of precipitation and reference evapotranspiration to drought indices under different climates. *J. Hydrol.*, **426**, 42–54.
- Vicente-Serrano, S.M., 2016: Foreword: Drought complexity and assessment under climate change conditions. *Cuadernos de Investigación Geográfica*, **42**(1), 7-11, doi:<http://dx.doi.org/10.18172/cig.2961>.
- Vicente-Serrano, S.M., and S. Beguería, 2016: Short communication comment on “candidate distributions for climatological drought indices (SPI and SPEI)” by James H. Stagge et al. *Int. J. Climatol.*, **36**, 2120–2131, <https://doi.org/10.1002/joc.4474>.
- Viglizzo E.F. and F.C. Frank, 2006: Ecological interactions, feedbacks, thresholds and collapses in the Argentine Pampas in response to climate and farming during the last century. *Quaternary International*, **158** (1), 122-126, <https://doi.org/10.1016/j.quaint.2006.05.022>
- Wilhite, D. A., and M. H. Glantz, 1985: Understanding the drought phenomenon: The role of definitions. *Water Int.*, **10**, 111–120, <https://doi.org/10.1080/02508068508686328>.

Wilhite, D., and R. Pulwarty, 2017: Drought and Water Crises, Boca Raton: CRC Press, 542 pp.

World Meteorological Organization, 2012: Standardized Precipitation Index User Guide (M. Svoboda, M. Hayes and D. Wood). (WMO-No. 1090), Geneva.

Yu, L., X. Jin, and R.A. Weller, 2008: Multidecadeglobal flux datasets from the objectively analyzed air-sea fluxes (OAFlux) Project: Latent and sensible heat fluxes, ocean evaporation, and related surface meteorological variables OAFlux Project Tech. Rep. OA-2008-01, 64pp., Woods Hole Oceanographic Institution, Woods Hole, Mass.

Tables:

Table 1: SPEI drought events at 1, 3, 6, 12 and 24-month time scales over the SSA RR between 1980-2015. D - duration, S - severity; I - intensity; P - peak.

SPEI- 1						SPEI- 3					
<i>inidate</i>	<i>findate</i>	<i>D</i>	<i>S</i>	<i>I</i>	<i>P</i>	<i>inidate</i>	<i>findate</i>	<i>D</i>	<i>S</i>	<i>I</i>	<i>P</i>
1/1980	3/1980	3	2.26	0.75	-1.61	2/1980	3/1980	2	1.24	0.62	-1.03
9/1980	9/1980	1	1.10	1.10	-1.10	4/1981	5/1982	14	10.73	0.77	-1.79
3/1981	3/1981	1	1.48	1.48	-1.48	11/1985	3/1986	5	4.52	0.90	-1.42
5/1981	10/1981	6	5.51	0.92	-1.51	2/1988	7/1989	18	21.28	1.18	-2.06
12/1981	1/1982	2	1.67	0.83	-1.64	10/1989	1/1990	4	2.66	0.67	-1.23
4/1982	5/1982	2	1.90	0.95	-1.12	3/1993	5/1993	3	2.39	0.80	-1.35
5/1985	6/1985	2	1.54	0.77	-1.18	5/1995	2/1996	10	9.29	0.93	-1.38
10/1985	2/1986	5	3.75	0.75	-1.34	5/1996	9/1996	5	5.32	1.06	-1.80
6/1987	6/1987	1	1.17	1.17	-1.17	3/1997	6/1997	4	3.43	0.86	-1.41
9/1987	10/1987	2	2.08	1.04	-1.25	8/1999	1/2000	6	6.27	1.05	-1.68
2/1988	2/1988	1	1.17	1.17	-1.17	5/2003	11/2003	7	6.55	0.94	-1.19
4/1988	8/1988	5	5.03	1.01	-1.54	1/2004	5/2004	5	4.97	0.99	-2.01
10/1988	5/1989	8	9.67	1.21	-2.05	8/2004	11/2004	4	3.43	0.86	-1.43
10/1989	11/1989	2	2.58	1.29	-1.68	2/2005	4/2005	3	2.87	0.96	-1.18
2/1991	3/1991	2	2.07	1.04	-1.41	11/2005	11/2006	13	15.34	1.18	-1.86
2/1993	4/1993	3	2.90	0.97	-1.59	6/2007	1/2008	8	6.41	0.80	-1.12
7/1993	9/1993	3	1.49	0.50	-1.23	3/2008	8/2009	18	22.31	1.24	-2.22
8/1994	9/1994	2	1.62	0.81	-1.08	10/2010	1/2011	4	4.23	1.06	-1.44
4/1995	9/1995	6	5.54	0.92	-1.33	3/2011	7/2011	5	3.59	0.72	-1.37
11/1995	12/1995	2	2.19	1.09	-1.29	9/2011	9/2012	13	9.61	0.74	-1.66
5/1996	8/1996	4	4.80	1.20	-1.75	1/2013	10/2013	10	6.40	0.64	-1.60
3/1997	5/1997	3	3.15	1.05	-1.64	12/2013	2/2014	3	2.93	0.98	-1.11
8/1999	1/2000	6	5.37	0.89	-1.69	SPEI- 6					
4/2003	11/2003	8	5.29	0.66	-1.04	<i>inidate</i>	<i>findate</i>	<i>D</i>	<i>S</i>	<i>I</i>	<i>P</i>
1/2004	3/2004	3	4.59	1.53	-1.71	7/1981	6/1982	12	10.78	0.90	-1.58
8/2004	10/2004	3	2.87	0.96	-1.40	10/1985	5/1986	8	4.12	0.51	-1.13
12/2004	2/2005	3	2.43	0.81	-1.65	1/1988	3/1990	27	27.22	1.01	-2.28

7/2005	7/2005	1	1.39	1.39	-1.39	5/1995	5/1996	13	8.97	0.69	-1.51
11/2005	9/2006	11	11.20	1.02	-2.04	9/1999	4/2000	8	6.48	0.81	-1.38
6/2007	6/2007	1	2.15	2.15	-2.15	6/2003	7/2005	26	18.90	0.73	-1.43
3/2008	7/2008	5	5.12	1.02	-1.40	11/2005	12/2006	14	17.25	1.23	-2.03
9/2008	6/2009	10	11.75	1.18	-2.48	8/2007	9/2009	26	33.63	1.29	-2.38
6/2010	6/2010	1	1.40	1.40	-1.40	10/2010	11/2012	26	19.89	0.76	-1.40
8/2010	8/2010	1	1.11	1.11	-1.11	1/2013	3/2014	15	9.78	0.65	-1.35
10/2010	12/2010	3	3.43	1.14	-1.75	<i>SPEI- 12</i>					
3/2011	5/2011	3	3.28	1.09	-1.69	<i>inidate</i>	<i>findate</i>	<i>D</i>	<i>S</i>	<i>I</i>	<i>P</i>
9/2011	9/2011	1	1.88	1.88	-1.88	7/1981	8/1982	14	9.10	0.65	-1.23
11/2011	1/2012	3	3.71	1.24	-1.75	4/1988	3/1990	24	30.81	1.28	-2.11
3/2012	3/2012	1	1.15	1.15	-1.15	5/1995	11/1996	19	12.02	0.63	-1.06
7/2012	7/2012	1	1.13	1.13	-1.13	10/2003	4/2007	43	37.45	0.87	-1.85
9/2012	9/2012	1	1.15	1.15	-1.15	12/2007	1/2010	26	34.51	1.33	-2.17
11/2012	11/2012	1	1.18	1.18	-1.18	12/2010	4/2014	41	34.66	0.85	-1.47
1/2013	5/2013	5	4.47	0.89	-1.88	<i>SPEI- 24</i>					
11/2013	1/2014	3	2.01	0.67	-1.90	<i>inidate</i>	<i>findate</i>	<i>D</i>	<i>S</i>	<i>I</i>	<i>P</i>
8/2014	8/2014	1	1.38	1.38	-1.38	8/1988	12/1990	29	35.07	1.21	-1.86
10/2014	10/2014	1	1.23	1.23	-1.23	3/2004	2/2011	84	81.10	0.97	-2.07
3/2015	4/2015	2	2.10	1.05	-1.20	11/2011	12/2014	38	34.92	0.92	-1.48

Table 2: Pearson correlation coefficients between the time series of SPEI-1 and evaporation, moisture uptake and moisture supply over the SSA RR. Values significant at the 99% confidence level, according to the Student's t-test, are given in italics and are with red colour. Data sources: GLEAM 3.1a for terrestrial evaporation, OAFLUX for oceanic evaporation, moisture uptake and supply from the Lagrangian analysis.

SPEI-1 x	SAT	SPO	TER	SSA
Evaporation	<i>-0.224</i>	<i>0.131</i>	<i>0.269</i>	<i>0.309</i>
Moisture uptake	0.001	<i>0.167</i>	<i>0.306</i>	<i>-0.450</i>
Moisture supply	<i>0.336</i>	0.092	<i>0.605</i>	<i>0.510</i>

Table 3: Pearson correlation coefficient between the time series of moisture supply from the SSA RR to its remote terrestrial sink, and PRE over its sink. The value is significant at the 99% confidence level according to the Student's t-test. Data sources: CRU TS 3.24.01 for PRE, and moisture supply from the Lagrangian analysis.

	PRE sink
Moisture supply	<i>0.280</i>

Figure Captions:

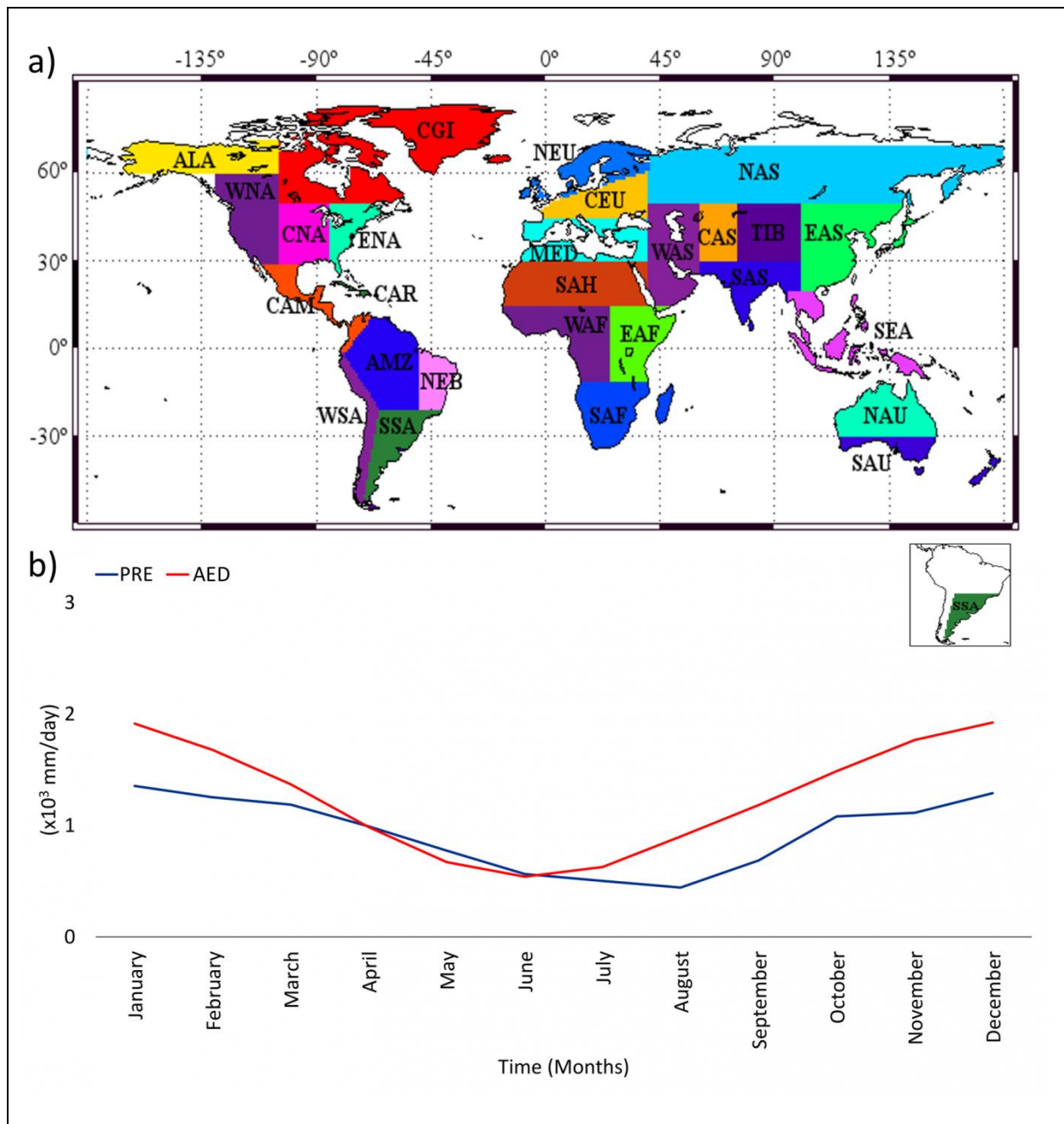


Figure 1 (a) Continental Reference Regions (RRs) based on the geographical domains defined in the IPCC 5th Assessment Report. The south-eastern South America (SSA) region is shown in dark green color; (b) The annual climatological precipitation cycle (PRE, blue line) and atmospheric evaporative demand (AED, red line) integrated over the SSA RR for 1980–2015. Data from the Climatic Research Unit (CRU TS3.24.01). Scale in mm/day.

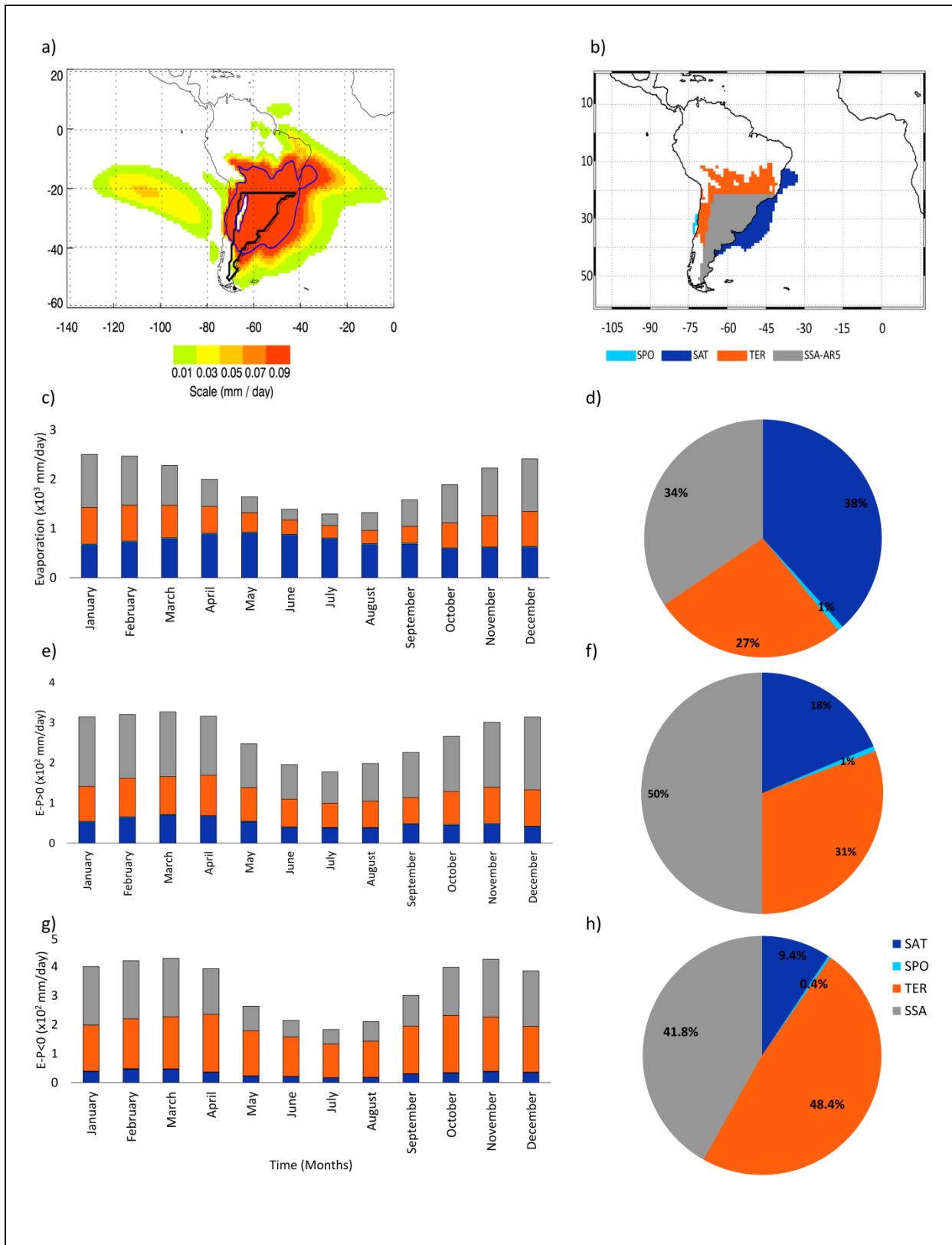


Figure 2 (a) Annual climatological (evaporation (E) - precipitation (P) > 0) values integrated backwards in time over 10 days for the SSA RR (mm/day). The blue line delimits the moisture source areas selected using the 95th percentile of the (E-P) > 0 values (i.e., 0.15 mm/day); (b) Schematic representation of the main moisture sources for the SSA RR between 1980–2015: South Pacific Ocean (SPO), South Atlantic (SAT), terrestrial moisture sources surrounding the region (TER), and the region itself (SSA-AR5); (c) The annual climatological cycle of evaporation rate integrated over the sources for

the SSA RR and (d) the contribution of each source toward the total annual value; (e) and (f), same as (c) and (d), but for moisture uptake ($E - P > 0$) integrated over the sources obtained from backward analysis for the SSA RR; (g) and (h), same as (c) and (d), but for moisture contribution ($E - P < 0$) integrated from the sources to the SSA RR, estimated through the forward analysis. Scale: mm/day

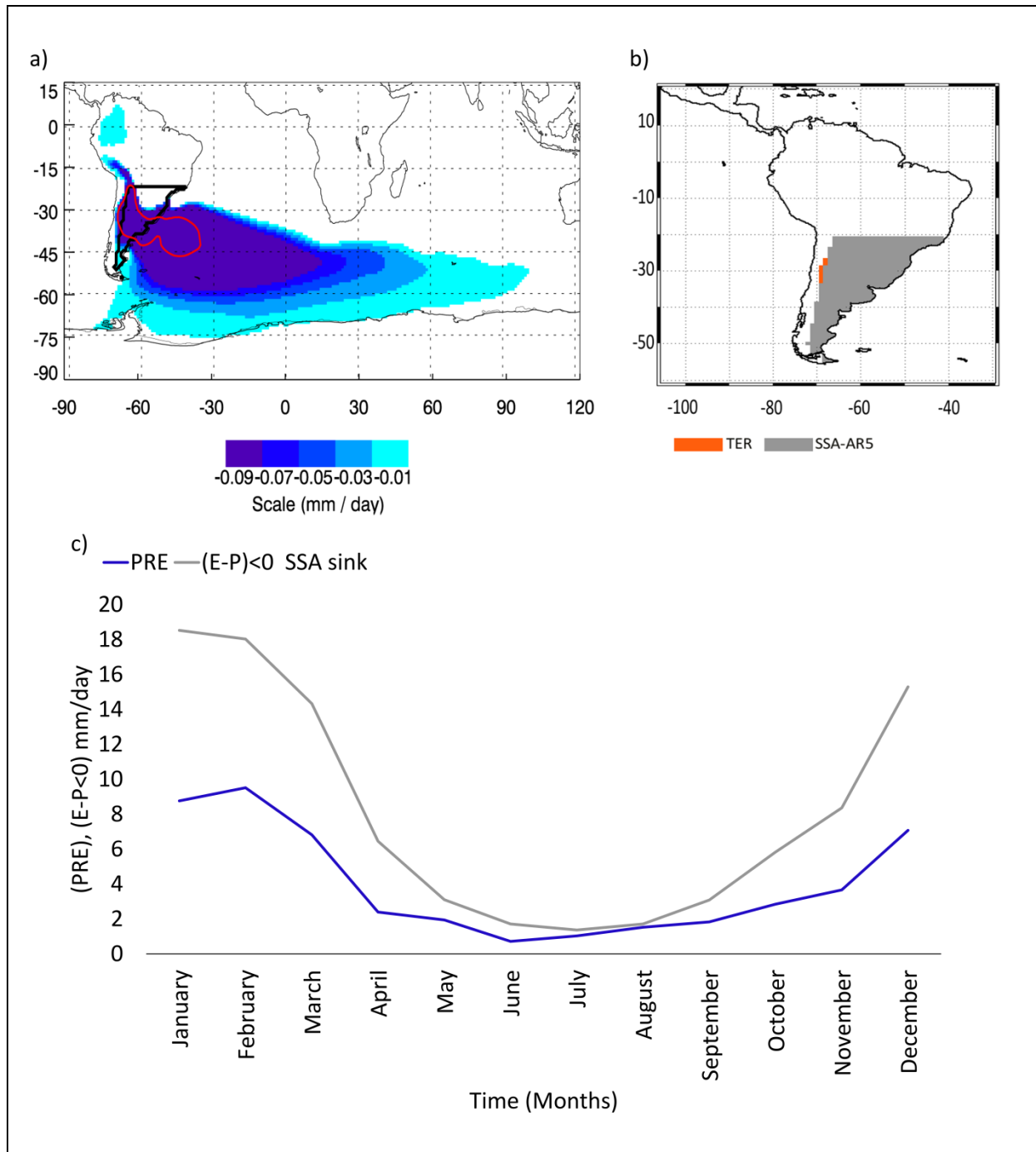


Figure 3 (a) Annual climatological (evaporation (E) - precipitation (P) < 0) values integrated forward in time over 10 days from the SSA RR (mm/day). The red line delimits the moisture sink areas selected using the 99th percentile of the ($E - P$) < 0 values (i.e., -0.34 mm/day); (b) Schematic representation of the remote terrestrial moisture sink (TER, orange) for the SSA RR; (c): The annual climatological cycle of precipitation (blue line) and moisture supply (grey line) for the SSA sinks. Scale in mm/day.

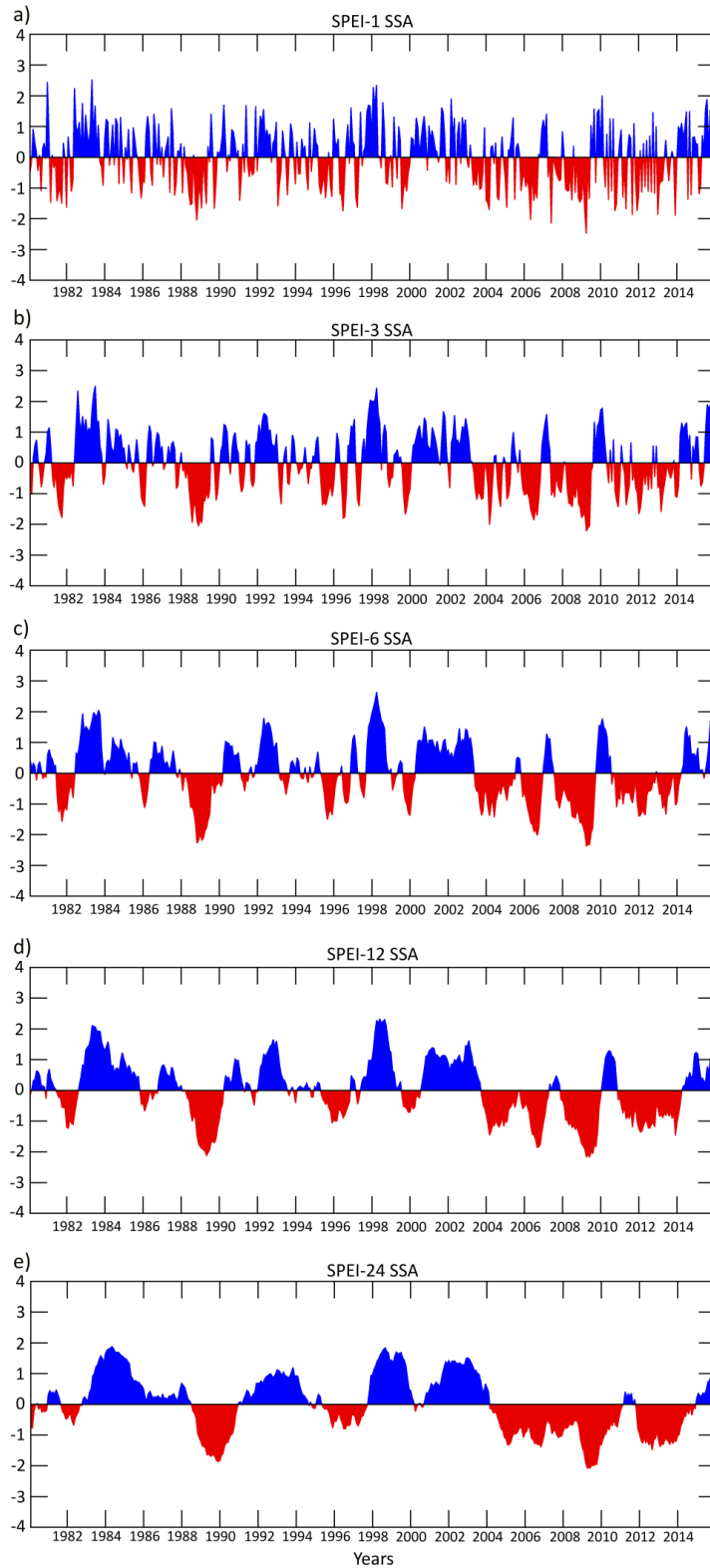


Figure 4 Time series of SPEI-1, SPEI-3, SPEI-6, SPEI-12, and SPEI-24 for the SSA RR during 1980-2015. Data from the Climatic Research Unit (CRU TS3.24.01).

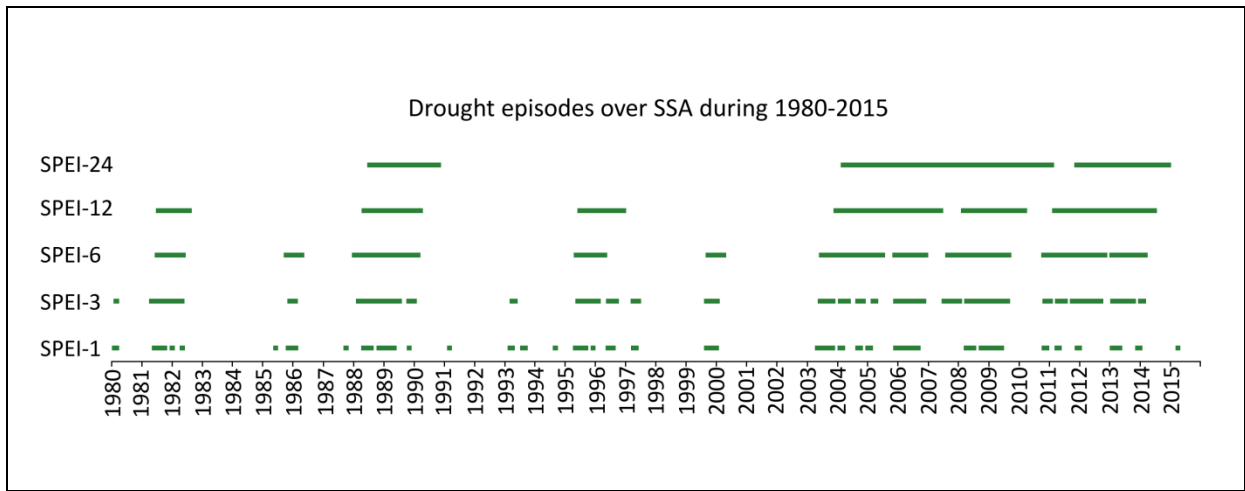


Figure 5 SPEI-1, SPEI-3, SPEI-6, SPEI-12, and SPEI-24 drought episodes which occurred over the SSA RR during 1980-2015

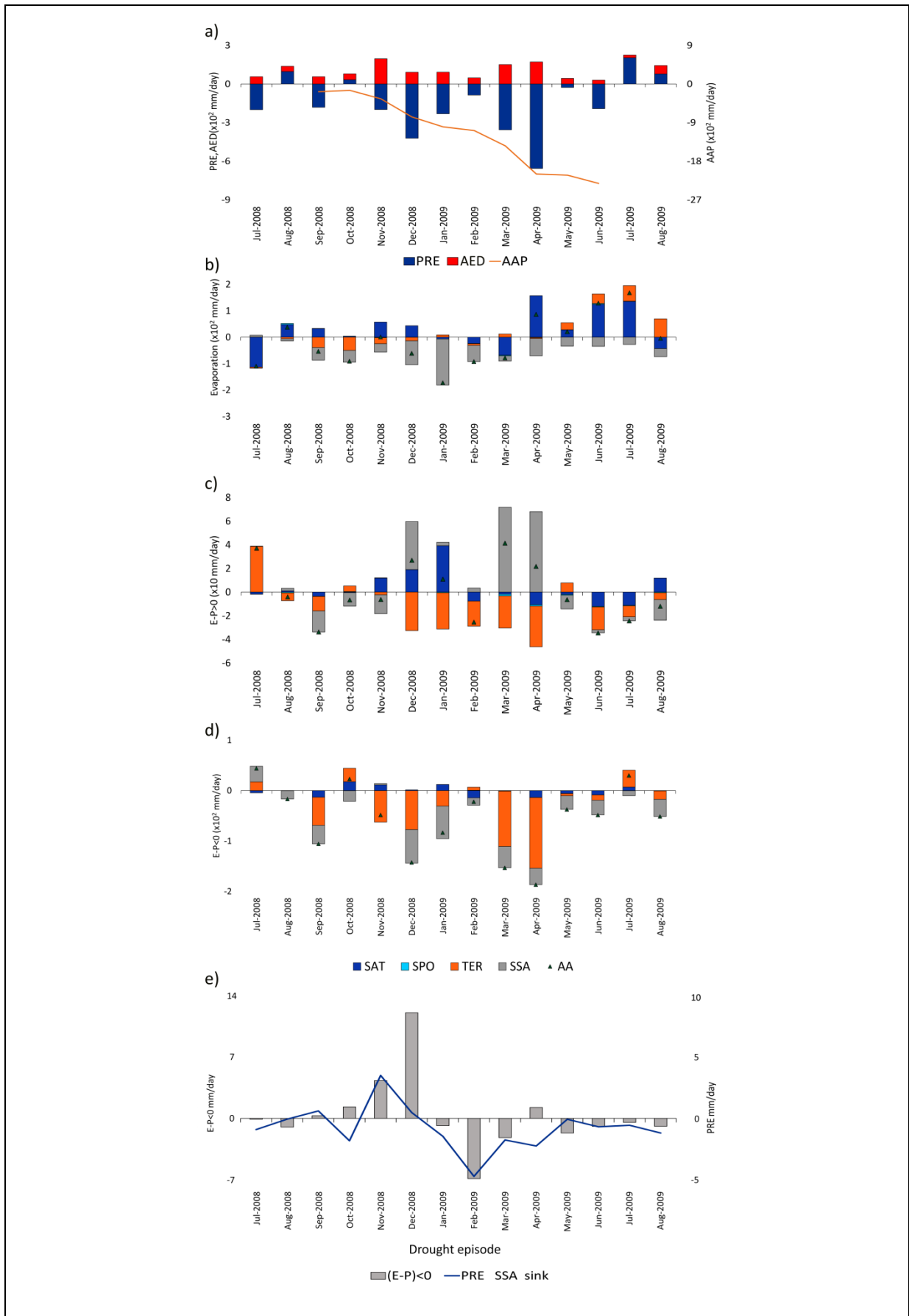


Figure 6 (a) Monthly anomalies of precipitation (PRE), atmospheric evaporative demand (AED) and accumulated precipitation anomalies (AAP) (data from CRUTS 3.24.01) during the most severe

drought episode that occurred over the SSA RR; (b) Same as (a), but for evaporation over the oceanic sources (OAFUX) and terrestrial sources (GLEAM) with the accumulated evaporation anomaly from all of the sources (AA); (c) Same as (a), but for moisture uptake ($E - P > 0$) over the sources with the accumulated anomaly of the sources (AA); (d) Same as (a), but for moisture supply ($E - P < 0$) from each source over the SSA RR with the accumulated anomaly of the supply from all of the sources (AA); (e) Monthly anomalies of the moisture supply from the SSA RR to its remote terrestrial sink and PRE over the sink accumulated during the drought episode. Scale in mm/day.

5

Summary, conclusions, and further research

The general aim of this thesis was to analyse anomalies in moisture transport during meteorological drought episodes. For this purpose, the most severe meteorological drought episodes that occurred around the world during the period from 1980-2015 were investigated. The initial analysis focused on a regional perspective and subsequent investigations expanded towards a global scale.

In order to analyse droughts, a climatological overview of each region of interest is necessary. The main climatological sources of moisture for the drought areas were determined and their respective moisture contributions were estimated. The One Month Standardised Precipitation Evapotranspiration Index (SPEI-1), an index that is sensitive to precipitation and temperature, was used to identify the meteorological drought episodes over each region of interest and to compute their respective drought indicators. The moisture transport analysis was based on a Lagrangian model (FLEXPART), which is widely used to study the transport of moisture in the atmosphere. This approach enabled the source-sink relationship in the atmospheric water cycle to be established.

Looking for commonalities between the papers within this thesis, the main conclusions drawn are pointed out below:

Analysis of the relationships between anomalies in moisture contribution from the Mediterranean Sea and severity, duration, intensity, and peak values.

In order to determine the link between diverse drought indicators and the Mediterranean Sea, which is the principal moisture source for Central Europe, 51 drought episodes identified over Central Europe were ranked with respect to severity, duration, intensity, and peak values. Of these 51 drought episodes, 22 started during the summer (April–September) and 29 started during the winter (October–March).

Results show that an important linear connection exists between anomalies in moisture transport from the Mediterranean Sea and the duration, severity, and peak values (during the winter season). This means that episodes that were longer, more severe, and with more intense peak (winter season), could be related to anomalies in moisture contribution from the Mediterranean Sea. The highest coefficient of determination (R^2) was discovered between the severity of drought episodes and MDS anomalies, which means that variability in the severity of drought may be modulated by fluctuations in the contribution of moisture from the MDS.

No linear connections were identified between anomalies in moisture supply from the Mediterranean Sea and the peak values of the whole year, the peak values of the summer season, and the intensity of drought episodes.

The year 2003: The most severe meteorological drought episodes over three regions in Europe (Danube River Basin, Central Europe, and the Mediterranean region)

The analyses of the meteorological droughts over these three specific regions revealed the impact of the 2003 meteorological drought event across the European

continent, providing some information about the spatial extension of the affected areas and the temporal evolution of the drought event. Using the SPEI, different characteristics of the drought episode were able to be compared to the spatial and temporal progression of the drought over the continent.

On a regional scale, of the 50 drought episodes that occurred over Danube River Basin during 1980-2014, the episode from February to August 2003 was the most severe during the spring and summer seasons.

Extending the analysis towards a continental scale, the most severe meteorological drought episodes during 1980-2015 were from February to June 2003 in Central Europe and from May 2003 to August 2003 in the Mediterranean region.

The onset of the 2003 drought was initially identified in Central Europe and the Danube River Basin in February 2003; it appears that the drought conditions extended southwards and the drought was last registered in the Mediterranean region. Comparing the drought indicators associated with each one of the three regions, results show that the episode was longer and more severe over the Danube River Basin.

The SPEI-1 for the drought episode from February to June 2003 achieved a peak of -1.86 in Central Europe, which categorises it as severe. The episodes in the Danube River Basin from February to August 2003 and in the Mediterranean region from May to August 2003 had peaks equal to -2.09 and -2.71 , respectively, which placed them in the extreme category. For all three areas, June 2003 was the month when the SPEI-1 reached its peak value and the month in which the positive anomalies of potential evapotranspiration and negative anomalies of precipitation prevailed.

Location of the principal climatological moisture sources for three regions in Europe (Danube River Basin, Central Europe, and the Mediterranean region)

The main moisture sources that are common sources for all three regions are the North Atlantic Ocean, the Mediterranean Sea, the Black Sea, the Caspian Sea, and

terrestrial moisture sources that surround the region. On an annual scale, the climatological analysis demonstrated that the moisture contribution to all three regions primarily came from the Mediterranean Sea and terrestrial moisture sources that surround the region together with own regions. During the summer months, the main moisture sources were the own regions and terrestrial moisture sources, while the Mediterranean Sea seemed to be the major moisture source during the winter months.

During the 2003 drought episode, the most intense reductions in moisture resulted from reduced moisture transport from the Mediterranean Sea to Central Europe and the Mediterranean region, and reduced moisture contribution to the Danube River Basin from the Mediterranean Sea and terrestrial sources surrounding region.

Analysis of anomalies in moisture transport during the most severe meteorological drought episode of 2003 that occurred over three regions in Europe

For all three regions, results show that precipitation and moisture contribution from the source to precipitation predominantly weakened throughout the drought episodes. The decreases in moisture contribution and precipitation occurred alongside the onset of the drought episodes; the episodes ended when the Mediterranean Sea, the major climatological moisture contributor for the regions, began to provide moisture to all analysed regions. The drought episodes were characterized by anomalous subsidence, increased evapotranspiration, and decreased precipitation caused by reduced moisture contribution from almost all sources.

Maps of the monthly anomalies in vertically integrated moisture flux (VIMF) and its divergence from ERA-Interim show that an anomalous, anticyclonic circulation pattern was observed across Europe during 2003. This circulation pattern is responsible for preventing moisture transport from the Mediterranean Sea to the three regions being studied.

Anomalies in moisture transport during the most severe meteorological drought episodes worldwide

For each of the 27 RRs defined in the 5th Assessment Report of the IPCC, a systematic analysis of the changes in atmospheric transport linked to drought episodes was performed. These analyses were compiled into a catalogue that identifies the drought episodes around the world during 1980-2015 and discusses some components of the moisture budget during the most severe meteorological drought episodes over each region. This catalogue will be freely available here: <http://ephyslab.uvigo.es/seth/>.

The catalogue contains five items that may be used to interpret current climate in terms of the variations in moisture transport:

- Item 1: Climatological Annual Cycle of Precipitation and Atmospheric Evaporative Demand over the RRs.
- Item 2: Climatological Annual Cycle of Selected Freshwater Budget Components Associated with the Moisture Sources and Sinks of the RRs.
- Item 3: SPEI Time Series and Drought Episodes Identified Over the RRs at Different Scales during 1980-2015.
- Item 4: Anomalies of Some Freshwater Budget Components of the Most Severe Meteorological Drought Episode Over the RRs Identified by the SPEI-1 during 1980-2015.
- Item 5: Correlation Analysis between the Anomalies of Selected Freshwater Budget Components and the SPEI-1 Time Series for the RRs during 1980-2015.

The purpose of this catalogue is to contribute to a deeper understanding of the climate regions defined in the IPCC; ideally, it will be considered as reference by the scientific community, particularly for climate change studies. In addition, the results

presented in the catalogue may be used to plan hydrological policies in regions that are more sensitive to water resources.

Limitations of the study and suggestions for further work

Identification and characterization of drought episodes and analysis of anomalies in moisture transport will be an important component of regional and global climate assessments in the coming years. This study suggests some interesting perspectives on future research. The studies in this thesis investigated meteorological drought; however, future research may investigate how moisture transport indirectly affects other categories of drought, such as hydrological and agricultural drought. Of particular interest may be a more detailed study between drought episodes and the main modes of climate variability, such as the North Atlantic Oscillation (NAO), the El Niño-Southern Oscillation (ENSO), and the East Atlantic pattern (EA). These modes vary over a large range of space and time scales, and their fluctuations can affect variations in global and regional temperatures.

It is important to note that this investigation concentrated on the domain-scale episodes that influence the studied regions. Nevertheless, because each episode is singular in terms of its temporal and spatial expansion, a grid point analysis would identify regions that are more affected by dry conditions during a specific episode. Therefore, detailed spatial-temporal studies should consider the intra-domain variability.

APPENDIX A: SUPPLEMENTARY MATERIAL

Table 1. Drought events that occurred over Central Europe during 1980-2015

	Drought (CEU)	Severity	Drought (CEU)	Duration	Drought (CEU)	Intensity	Drought (CEU)	Peak value
1	Feb – Jun 2003	7.1	Jun – Dec 1983	7	Oct –Oct 1995	2.16	Jun – Oct 2015	-2.40
2	Jun – Oct 2015	6.45	Jan – Jun 2011	6	Nov – Nov 1993	1.73	Oct –Oct 1995	-2.16
3	Jan – Jun 2011	6.27	Dec 1992 – May 1993	6	Dec – Dec 2013	1.63	Aug – Nov 2011	-2.08
4	Jun – Dec 1983	6.15	Feb – Jun 2003	5	Oct –Oct 1985	1.6	Jun – Jul 1994	-2.07
5	May – Aug 1992	5.24	Jun – Oct 2015	5	Jun – Jul 2006	1.52	Mar - Apr 2007	-1.99
6	Aug – Nov 2011	4.37	Mar – Jul 2002	5	Aug – Sep 2009	1.46	Apr - May 2009	-1.96
7	Dec 1992 – May 1993	4.26	Dec 1990 – Apr 1991	5	Jan – Jan 2006	1.46	Jun – Jul 2006	-1.94
8	Sep – Nov 2005	3.71	May – Aug 1992	4	Sep – Sep 1982	1.44	Feb - Apr 2014	-1.90
9	Mar – Jul 2002	3.68	Aug – Nov 2011	4	May – May 1989	1.42	Jan – Mar 1989	-1.89
10	Jan – Mar 1989	3.46	Sep – Dec 2006	4	May – May 1990	1.42	Feb – Jun 2003	-1.86
11	Sep – Dec 2006	3.35	Dec 1996 – Mar 1997	4	Feb – Jun 2003	1.42	Feb - Mar 1982	-1.86
12	Dec 1990 – Apr 1991	3.25	Feb – Apr 1984	3	Jun – Jun 2008	1.37	Nov – Nov 1993	-1.74
13	Dec 2007 – Feb 2008	3.21	Oct – Dec 1984	3	Jun – Jul 1994	1.37	Dec 1996 – Mar 1997	-1.69
14	Dec 1996 – Mar 1997	3.06	May – Jul 1986	3	Oct – Oct 1987	1.31	Dec – Dec 2013	-1.63
15	Jun – Jul 2006	3.05	Sep – Nov 1986	3	May – Aug 1992	1.31	Sep – Nov 2005	-1.63
16	Aug - Sep 2009	2.93	Jan – Mar 1989	3	Jun – Oct 2015	1.29	Oct –Oct 1985	-1.61
17	Feb - Apr 2014	2.83	May – Jul 1999	3	Feb - Mar 1982	1.26	Sep – Dec 2006	-1.60
18	Jun – Jul 1994	2.74	Apr - Jun 2000	3	Mar – Mar 1990	1.25	Dec 1992 – May 1993	-1.57
19	Apr - Jun 2000	2.61	Sep – Nov 2005	3	Sep – Nov 2005	1.23	Sep – Nov 1986	-1.56
20	Sep – Nov 2014	2.55	Dec 2007 – Feb 2008	3	Mar – Mar 2012	1.2	Dec 2007 – Feb 2008	-1.55
21	Sep – Nov 1986	2.54	Jun – Aug 2013	3	Mar - Apr 2007	1.19	Jan – Jun 2011	-1.53
22	Feb - Mar 1982	2.53	Feb - Apr 2014	3	Nov – Nov 1982	1.18	Jan – Feb 1998	-1.52
23	Jun – Aug 2013	2.46	Sep – Nov 2014	3	Jan – Mar 1989	1.15	Aug - Sep 2009	-1.50
24	Mar - Apr 2007	2.38	Feb - Mar 1982	2	Aug – Nov 2011	1.09	Jan – Jan 2006	-1.47
25	Apr - May 2009	2.17	Oct – Nov 1988	2	Apr - May 2009	1.08	Sep – Sep 1982	-1.44
26	Oct –Oct 1995	2.16	Jun – Jul 1994	2	Dec 2007 – Feb 2008	1.07	May – May 1989	-1.43
27	Oct – Dec 1984	2.1	Jan – Feb 1998	2	Oct – Oct 2000	1.05	Mar – Mar 1990	-1.42
28	Jan – Feb 1998	2	Jul – Aug 1995	2	Jan – Jun 2011	1.04	Dec 1995 – Jan 1996	-1.42
29	Feb – Apr 1984	1.93	Dec 1995 – Jan 1996	2	Feb – Feb 1994	1.01	Jul – Aug 1995	-1.42
30	May – Jul 1986	1.88	Dec 2001 – Jan 2002	2	Jan – Feb 1998	1	Jun – Jun 2008	-1.37
31	Dec 2001 – Jan 2002	1.85	Aug – Sep 2003	2	Feb - Apr 2014	0.94	Oct – Oct 1987	-1.31
32	Oct – Nov 1988	1.8	Jun – Jul 2006	2	Dec 2001 – Jan 2002	0.92	Sep – Nov 2014	-1.31
33	May – Jul 1999	1.79	Mar - Apr 2007	2	Oct – Nov 1988	0.9	Dec 1990 – Apr 1991	-1.30
34	Nov – Nov 1993	1.74	Apr - May 2009	2	Jun – Dec 1983	0.88	May – Aug 1992	-1.29
35	Aug – Sep 2003	1.73	Aug - Sep 2009	2	Apr - Jun 2000	0.87	Aug – Sep 2003	-1.26
36	Dec – Dec 2013	1.63	Mar – Apr 2010	2	Aug – Sep 2003	0.86	May – May 1990	-1.25
37	Oct –Oct 1985	1.6	Sep – Sep 1982	1	Sep – Nov 2014	0.85	Dec 2001 – Jan 2002	-1.23
38	Jul – Aug 1995	1.53	Nov – Nov 1982	1	Sep – Nov 1986	0.84	Mar – Mar 2012	-1.20
39	Dec 1995 – Jan 1996	1.53	Oct –Oct 1985	1	Sep – Dec 2006	0.83	Nov – Nov 1982	-1.19
40	Jan – Jan 2006	1.46	Oct – Oct 1987	1	Jun – Aug 2013	0.82	Feb – Apr 1984	-1.18
41	Mar – Apr 2010	1.45	May – May 1989	1	Jul – Aug 1995	0.76	Apr - Jun 2000	-1.18
42	Sep – Sep 1982	1.44	Mar – Mar 1990	1	Dec 1995 – Jan 1996	0.76	Mar – Apr 2010	-1.17
43	May – May 1989	1.43	May – May 1990	1	Dec 1996 – Mar 1997	0.76	Oct – Dec 1984	-1.17
44	Mar – Mar 1990	1.42	Nov – Nov 1993	1	Mar – Jul 2002	0.73	Jun – Dec 1983	-1.16
45	Jun – Jun 2008	1.37	Feb – Feb 1994	1	Mar – Apr 2010	0.72	Jun – Aug 2013	-1.14
46	Oct – Oct 1987	1.31	Oct –Oct 1995	1	Dec 1992 – May 1993	0.71	May – Jul 1986	-1.10
47	May – May 1990	1.25	Oct – Oct 2000	1	Oct – Dec 1984	0.7	May – Jul 1999	-1.10
48	Mar – Mar 2012	1.2	Jan – Jan 2006	1	Dec 1990 – Apr 1991	0.65	Oct – Nov 1988	-1.09
49	Nov – Nov 1982	1.18	Jun – Jun 2008	1	Feb – Apr 1984	0.64	Mar – Jul 2002	-1.06
50	Oct – Oct 2000	1.05	Mar – Mar 2012	1	May – Jul 1986	0.62	Oct – Oct 2000	-1.05
51	Feb – Feb 1994	1.01	Dec – Dec 2013	1	May – Jul 1999	0.59	Feb – Feb 1994	-1.02

Table 2. The significance (a significance level of 95%), slope, intercept and coefficient of determination (R^2) for severity, duration, intensity and peak values with respect to the MDS anomaly on annual, winter and summer scales of episodes classified based on duration. Underlined bold numbers represent significant linear relationship with MDS anomaly.

		Annual			Winter			Summer		
		Slope	Intercept	R2	Slope	Intercept	R2	Slope	Intercept	R2
Severity × MDS anomaly	Short – term	<u>-0.0176</u>	<u>1.6215</u>	<u>0.3629</u>	<u>-0.0141</u>	<u>1.5798</u>	<u>0.2908</u>	<u>-0.0226</u>	<u>1.6521</u>	<u>0.4964</u>
	Medium – term	-0.009	4.2931	0.0648	<u>-0.032</u>	<u>2.7559</u>	<u>0.6163</u>	0.015	6.0493	0.2896
Duration × MDS anomaly	Short – term	<u>-0.015</u>	<u>1.5987</u>	<u>0.1871</u>	-0.0098	1.55431	0.0929	<u>-0.023</u>	<u>1.632</u>	<u>0.393</u>
	Medium – term	-0.0068	4.5944	0.078	-0.0084	4.6806	0.2137	-0.0057	4.4436	0.0402
Intensity × MDS anomaly	Short – term	-0.001	1.1126	0.0044	-0.0018	0.8774	0.0116	0.0012	1.1214	0.0052
	Medium – term	-0.005	0.9437	0.0057	-0.0012	1.1206	0.0345	<u>0.0042</u>	<u>1.3481</u>	<u>0.7477</u>
Peak values × MDS anomaly	Short – term	0.0035	-1.386	0.0679	0.0039	-1.3889	0.0901	0.0027	-1.3865	0.039
	Medium – term	-0.00004	-1.5967	0.00001	0.0053	-1.1958	0.5746	-0.0058	-2.067	0.2519

Table 3. The significance (a significance level of 95%), slope, intercept and coefficient of determination (R²) for severity, duration, intensity and peak values with respect to MDS anomaly on annual, winter and summer scales of episodes classified based on peaks. Underlined bold numbers represent significant linear relationship with MDS anomaly.

		Annual			Winter			Summer		
		Slope	Intercept	R2	Slope	Intercept	R2	Slope	Intercept	R2
Severity × MDS anomaly	Severe	<u>-0.0240</u>	<u>2.1100</u>	<u>0.2735</u>	<u>-0.0297</u>	<u>1.7805</u>	<u>0.4408</u>	-0.0162	2.5511	0.1200
	Mild	-0.0029	1.2859	0.0628	-0.0020	1.2517	0.0191	-0.0043	1.3578	0.7671
Duration × MDS anomaly	Severe	<u>-0.0228</u>	<u>2.1700</u>	<u>0.2442</u>	<u>-0.0219</u>	<u>2.1442</u>	<u>0.2006</u>	-0.0218	2.3201	0.2800
	Mild	-0.0074	1.1233	0.0912	0.0048	1.1453	0.0287	Episodes lasted 1 month each one		
Intensity × MDS anomaly	Severe	-0.0060	1.0349	0.0027	-0.0015	1.0382	0.0145	0.0005	1.0345	0.0030
	Mild	-0.0047	1.2173	0.0831	-0.0008	1.1475	0.0031	0.0026	1.4425	0.1120
Peak values × MDS anomaly	Severe	0.0007	-1.5298	0.0036	0.0170	-1.5038	0.0337	-0.0007	-1.5672	0.0032
	Mild	0.0037	-1.2632	0.1021	0.0033	-1.2153	0.0652	0.0044	-1.3591	0.7949

References

Ayantobo, O. O., Li, Y., Song, S. and Yao, N. (2017). Spatial Comparability of Drought Characteristics and Related Return Periods in Mainland China Over 1961–2013. *J. Hydrol.*, 550, 549–567. <https://doi.org/10.1016/j.jhydrol.2017.05.019>.

Beniston, M., Stephenson, D., Christensen, O., Ferro, C., Frei, C., Goyette, S., Halsnaes, K., Holt, T., Jylhä, K., Koffi, B., Palutikof, J., Schöll, R., Semmler, T., and Woth, K. (2007). Future extreme events in European climate: an exploration of regional climate model projections. *Clim. Chang.*, 81, 71–95. doi: 10.1007/s10584-006-9226-z.

Bisselink, B. and Dolman, A.J. (2008). Precipitation recycling: Moisture sources over Europe using ERA-40 Data. *J. Hydrometeorol.*, 9, 1073–1083. <https://doi.org/10.1175/2008JHM962.1>

Bosilovich, M.G. and Schubert, S.D. (2002). Water vapor tracers as diagnostics of the regional hydrologic cycle. *J. Hydrometeorol.*, 3(2), 149–165, doi: 10.1175/1525-7541(2002)003h0149:WVTADOi2.0.CO;2.

Briffa, K.R., Van Der Schrier, G. and Jones, P.D. (2009). Wet and dry summers in Europe since 1750: evidence of increasing drought. *Int. J. Climatol.*, 29(13): 1894. doi: 10.1002/joc.1836.

Brubaker, K L., Dirmeyer, P.A. Sudradjat, A. Levy, B.S. and Bernal, F. (2001). A 36-yr climatological description of the evaporative sources of warm-season precipitation in the Mississippi River basin. *J. Hydrometeorol.*, 2(6), 537–557, doi: 10.1175/1525-7541(2001)002h0537:AYCDOTi2.0.CO;2.

Brubaker, K.L., Entekhabi, D., and Eagleson, P.S. (1993). Estimation of Continental Precipitation Recycling. *J. Climate.*, 6, 1077–1089. [https://doi.org/10.1175/1520-0442\(1993\)006<1077:EOCPR>2.0.CO;2](https://doi.org/10.1175/1520-0442(1993)006<1077:EOCPR>2.0.CO;2).

Budyko, M. J. (1974). *Climate and life*. Academic Press. N.Y. 508.

Burke, E. J. and Brown, S. J. (2008). Evaluating uncertainties in the projection of future drought. *J. Hydrometeorol.*, 9(2), 292–299. <https://doi.org/10.1175/2007JHM929.1>

Ciric, D., Nieto, R., Losada, L., Drumond, A. and Gimeno, L. (2018). The Mediterranean Moisture Contribution to Climatological and Extreme Monthly Continental Precipitation. *Water*, 4, 519. <https://doi.org/10.3390/w10040519>.

Cook, B. I., Ault, T. R. and Smerdon, J. E. (2015). Unprecedented 21st century drought risk in the American Southwest and Central Plains. *Sci. Adv.*, 1, e1400082, <https://doi.org/e1400082>.

Coplen, T.B., Neiman, P.J. White, A.B. Landwehr, J.M. Ralph, F.M. and Dettinger, M.D. (2008). Extreme changes in stable hydrogen isotopes and precipitation characteristics in a landfalling Pacific storm. *Geophys. Res. Lett.*, 35(L21808), doi: 10.1029/2008GL035481.

D'Abreton, P.C., and Tyson, P.D. (1995). Divergent and non-divergent water vapor transport over southern Africa during wet and dry conditions. *Meteorol. Atmos. Phys.*, 55(1–2), 47–59. doi:10.1007/BF01029601.

Dai, A. (2010). Drought under global warming: a review. *Wiley Inter disc. Rev. Clim.Change*, 2(1), 45–65. <https://doi.org/10.1002/wcc.81>.

Dai, A. (2013). Increasing drought under global warming in observations and models. *Nature Clim. Change*, 3, 52–58, <https://doi.org/10.1038/nclimate1633>, 2012.

Dee, D.P., Uppala, S.M., Simmons, A.J., Berrisford, P., Poli, P., Kobayashi, S., Andrae, U., Balmaseda, M.A., Balsamo, G., Bauer, P., et al. (2011). The ERA-Interim

reanalysis: Configuration and performance of the data assimilation system. *Q. J. R. Meteorol. Soc.*, 137, 553–597. <https://doi.org/10.1002/qj.828>

Dirmeyer, P.A. and Brubaker, K.L. (1999). Contrasting evaporative moisture sources during the drought of 1988 and the flood of 1993. *J. Geophys. Res.*, 104(D16), 19383–19397, doi:10.1029/1999JD900222.

Dirmeyer, P.A. and Brubaker, K.L. (2006). Evidence for trends in the Northern Hemisphere water cycle. *Geophys. Res. Lett.*, 33(L14712), doi:10.1029/2006GL026359.

Dirmeyer, P.A., Brubaker, K.L. and DelSole, T. (2009). Import and export of atmospheric water vapor between nations. *J. Hydrol.*, 365, 11–22. doi: 10.1016/j.jhydrol.2008.11.016.

Dominguez, F., Kumar, P., Liang, X.-Z. and Ting, M. (2006). Impact of atmospheric moisture storage on precipitation recycling. *J. Clim.*, 19(8), 1513–1530, doi: 10.1175/JCLI3691.1.

Dominguez, F., Villegas, J. C. and Breshears, D. D. (2009). Spatial extent of the North American Monsoon: Increased cross-regional linkages via atmospheric pathways, *Geophys. Res. Lett.*, 36, L07401. doi:10.1029/2008GL037012.

Donat, M.G., Pitman, A. J. and Seneviratne, S. I. (2017). Regional warming of hot extremes accelerated by surface energy fluxes. *Geophys. Res. Lett.*, 44, 7011-7019. <https://doi.org/10.1002/2017GL073733>.

Drumond, A., Gimeno, L., Nieto, R., Trigo, R.M. and Vicente-Serrano, S.M. (2017). Drought episodes in the climatological sinks of the Mediterranean moisture source: The role of moisture transport. *Glob. Planet. Chang.*, 151, 4–14. <https://doi.org/10.1016/j.gloplacha.2016.12.004>.

Drumond, A., Marengo, J., Ambrizzi, T., Nieto, R., Moreira, L. and Gimeno, L. (2014). The role of the Amazon Basin moisture in the atmospheric branch of the hydrological cycle: a Lagrangian analysis, *Hydrol. Earth Syst. Sci.*, 18, 2577–2598, <https://doi.org/10.5194/hess-18-2577-2014>.

Drumond, A., Nieto, R. and Ambrizzi, T. (2008). A Lagrangian identification of major sources of moisture over Central Brazil and La Plata Basin. *J. Geophys. Res.*, 113, D14128, doi:10.1029/2007JD009547.

Drumond, A., Nieto, R., and Gimeno, L. (2011). Sources of moisture for China and their variations during drier and wetter conditions in 2000–2004: a Lagrangian approach, *Clim. Res.*, 50, 215–225. <https://doi.org/10.3354/cr01043>, 2011.

Drumond, A., Nieto, R. and Gimeno, L. (2016). A Lagrangian approach for investigating anomalies in the moisture transport during drought episodes, *Cuadernos de Investigación Geográfica*, 42, 113–125, <https://doi.org/10.18172/cig.2925>.

Drumond, A., Nieto, R., Hernández, E. and Gimeno, L. (2011). A Lagrangian analysis of the variation in moisture sources related to drier and wetter conditions in regions around the Mediterranean basin. *Nat. Hazards Earth Syst. Sci.*, 11, 2307–2320. doi: 10.5194/nhess-11-2307-2011.

Durán-Quesada, A. M., Gimeno, L., Amador, J.A. and Nieto, R. (2010). Moisture sources for Central America: Identification of moisture sources using a Lagrangian analysis technique. *J. Geophys. Res.*, 115, D05103. doi:10.1029/2009JD012455.

Emanuel, K., and Zivkovic-Rothman, M. (1999). Development and Evaluation of a Convection Scheme for Use in Climate Models. *J. Atmos. Sci.*, 56, 1766- 1782. [https://doi.org/10.1175/1520-0469\(1999\)056<1766:DAEOAC>2.0.CO;2](https://doi.org/10.1175/1520-0469(1999)056<1766:DAEOAC>2.0.CO;2).

Fischer, E., Seneviratne, S., Lüthi, D. and Schär, C. (2007). Contribution of land-atmosphere coupling to recent European summer heat waves. *Geophys. Res. Lett.*, 34, L06707. <https://doi.org/10.1029/2006GL029068>.

Forzieri, G., Feyen, L., Rojas, R., Flörke, M., Wimmer, F. and Bianchi, A. (2014). Ensemble projections of future streamflow droughts in Europe. *Hydrol. Earth Syst. Sci.*, 18(1), 85 – 108. <https://doi.org/10.5194/hess-18-85-2014>.

García-Ruiz, J.M., López-Moreno, J.I., Vicente-Serrano, S.M., Lasanta-Martínez, T. and Beguería, S. (2011). Mediterranean water resources in a global change scenario. *Earth Sci. Rev.*, 105, 121–139. <https://doi.org/10.1016/j.earscirev.2011.01.006>.

Gat, J. and Carmi I. (1970). Evolution of the isotopic composition of atmospheric waters in the Mediterranean Sea area. *J. Geophys. Res.*, 75(15), 3039 – 3048, doi:10.1029/JC075i015p03039.

Gibbs, W. J. and Maher, J. V. (1967). Rainfall deciles as drought indicators. Bureau of Meteorology Bulletin No 48. Commonwealth of Australia, Melbourne <https://trove.nla.gov.au/version/25447946>.

Gimeno, L., Dominguez, F., Nieto, R., Trigo, R.M., Drumond, A., Reason, C., Taschetto, A.S., Ramos, A.M., Kumar, R. and Marengo, J. (2016). Major Mechanisms of Atmospheric Moisture Transport and Their Role in Extreme Precipitation Events. *Annu. Rev. Environ. Resour.*, 41, 117–141. Doi: 10.1146/annurev-environ-110615-085558.

Gimeno, L., Drumond, A., Nieto, R., Trigo, R. M. and Stohl, A. (2010). On the origin of continental precipitation. *Geophys. Res. Lett.*, 37, L13804. doi:10.1029/2010GL043712.

Gimeno, L., Nieto, R., Drumond, A., Castillo, R. and Trigo, R.M. (2013). Influence of the intensification of the major oceanic moisture sources on continental precipitation. *Geophys. Res. Lett.*, 40, 1–8. <https://doi.org/10.1002/grl.50338>.

Gimeno, L., Stohl, A., Trigo, R. M., Dominguez, F., Yoshimura, K., Yu, L., Drumond, A., Durán-Quesada, A. M. and Nieto, R. (2012). Oceanic and terrestrial sources of continental precipitation, *Rev. Geophys.*, 50, RG4003, <https://doi.org/10.1029/2012RG000389>.

Gómez-Hernández, M., Drumond, A., Gimeno, L. and Garcia-Herrera, R. (2013). Variability of moisture sources in the Mediterranean region during the period 1980–2000. *Water Resour. Res.*, 49, 6781–6794. <https://doi.org/10.1002/wrcr.20538>.

- Gudmundsson, L. and Seneviratne, S.I. (2015). European drought trends. *Hydrol. Sci.*, 369, 75 – 79. doi: 10.5194/piahs-369-75-2015.
- Hanel, M., Rakovec, O., Markonis, Y., Máca, P., Samaniego, L., Kysely, J. and Kumar, R. (2018). Revisiting the recent European droughts from a long-term perspective. *Sci. Rep.*, 8, 9499. doi:10.1038/s41598-018-27464-4.
- Hanna, S.R. (1982). Applications in Air Pollution Modeling, in F. T. M. Nieuwstadt and H. van Dop (eds.), Atmospheric Turbulence and Air Pollution Modelling. D. Reidel Publishing Company, Dordrecht.
- Hao, Z., AghaKouchak, A. and Phillips, T.J. (2013). Changes in concurrent monthly precipitation and temperature extremes. *Environ. Res. Lett.*, 8(3), 034014. <http://dx.doi.org/10.1088/1748-9326/8/3/034014>.
- Hao, Z., Yuan, X., Xia, Y., Hao, F. and Singh, V. (2017). An overview of drought monitoring and prediction systems at regional and global scales. *Bull. Amer. Meteor. Soc.*, 98(9), 1879–1896. <https://doi.org/10.1175/BAMS-D-15-00149.1>.
- Harris, I., Jones, P. D., Osborn, T. J. and Lister, D. H. (2014). Updated high-resolution grids of monthly climatic observations – the CRU TS3.10 Dataset, *Int. J. Climatol.*, 34, 623–642, <https://doi.org/10.1002/joc.3711>.
- Hassanein, M.K., Kahlil, A.A. and Essa, Y.H. (2013). Assessment of drought impact in Africa using Standard Precipitation Evapotranspiration Index. *Nat. Sci.*, 11, 75–81.
- Heim, R. R. Jr. (2002). A review of twentieth-century drought indices used in the United States. *Bull. Amer. Meteor. Soc.*, 83, 1149–1165, [https://doi.org/10.1175/1520-0477\(2002\)0832.3.CO;2](https://doi.org/10.1175/1520-0477(2002)0832.3.CO;2).

Hoerling, M., Eischeid, J., Perlwitz, J., Quan, X., Zhang, T. and Pegion, P. (2012). On the increased frequency of Mediterranean drought. *J. Clim.*, 25(6), 2146 – 2161. <https://doi.org/10.1175/JCLI-D-11-00296.1>.

Hoerling, M. P. and Kumar, A. (2003). The perfect ocean for drought. *Science*, 299, 691–694, doi:10.1126/science.1079053.

Homdee, T., Pongput, K. and Kanae, S. (2016). A comparative performance analysis of three standardized climatic drought indices in the Chi River basin, Thailand. *Agric. Nat. Resour.*, 50, 211–219. <https://doi.org/10.1016/j.anres.2016.02.002>.

Ionita, M., Tallaksen, L.M., Kingston, D.G., Stagge, J.H., Laaha, G., Van Lanen, H.A.J., Scholz, P., Chelcea, S.M. and Haslinger, K. (2017). The European 2015 drought from a climatological perspective. *Hydrol. Earth Syst. Sci.*, 21, 1397–1419. <https://doi.org/10.5194/hess-21-1397-2017>, 2017.

IPCC, 2013: Climate Change 2013: The Physical Science Basis. Contribution of Working Group I to the Fifth Assessment Report of the Intergovernmental Panel on Climate Change. In, Stocker TF, Qin D, Plattner GK, Tignor M, Allen SK, Boschung J, Nauels A, Xia Y, Bex V, Midgley PM (eds). Cambridge University Press: Cambridge, UK and New York, NY, 1535 pp.

IPCC, 2014a: Climate Change 2014: Synthesis Report. Contribution of Working Groups I, II and III to the Fifth Assessment Report of the Intergovernmental Panel on 155 Climate Change [Core Writing Team, R.K. Pachauri and L.A. Meyer (eds.)]. IPCC, Geneva, Switzerland, 151 pp.

IPCC, 2014b: Climate Change 2014: Impacts, Adaptation and Vulnerability: Part B: Regional Aspects: Working Group II Contribution to the IPCC Fifth Assessment Report, Cambridge: Cambridge University Press, <https://doi.org/10.1017/CBO9781107415386>.

Jones, P. D. and Moberg, A. (2003). Hemispheric and large-scale surface air temperature variations: An extensive revision and an update to 2001. *J. Climate*, 16, 206–223, [https://doi.org/10.1175/1520-0442\(2003\)0162.0.CO;2](https://doi.org/10.1175/1520-0442(2003)0162.0.CO;2).

Joussaume, S., Sadourny, R. and Jouzel, J. (1984). A general circulation model of water isotope cycles in the atmosphere. *Nature*, 311(5981), 24–29, doi: 10.1038/311024a0.

Khalili, D., Farnoud, T., Jamshidi, H., Kamgar-Haghighi, A.A. and Zand-Parsa, S. (2011). Comparability analyses of the SPI and RDI meteorological drought indices in different climatic zones. *Water Resour. Manag.*, 25, 1737–1757. doi: 10.1007/s11269-010-9772-z.

Koster, R., Jouzel, J., Suozzo, R., Russell, G., Broecker, W., Rind, D. and Eagleson, P. (1986). Global sources of local precipitation as determined by the NASA/GISS GCM. *Geophys. Res. Lett.*, 13(2), 121–124, doi:10.1029/GL013i002p00121.

Kuchment, L.S. (2004). The hydrological cycle and human impact on it. In *Water Resour. Manag (EOLSS)*, Developed under the Auspices of the UNESCO; Hoekstra, A.Y., Savenije, H.H.G., Eds.; Eolss Publishers: Oxford, UK.

Leelaruban, N. and Padmanabhan, G. (2017). Drought Occurrences and Their Characteristics across Selected Spatial Scales in the Contiguous United States. *Geosciences*, 7, 59. doi:10.3390/geosciences7030059.

Lehner, B., Döll, P., Alcamo, J., Henrichs, T. and Kaspar, F. (2006). Estimating the Impact of Global Change on Flood and Drought Risks in Europe: A Continental, Integrated Analysis. *Clim. Change*, 75, 273–299. doi: 10.1007/s10584-006-6338-4.

Lehner, B. and Grill, G. (2013). Global river hydrography and network routing: baseline data and new approaches to study the world's large river systems. *Hydrol. Process.* 27, 2171–2186. <https://doi.org/10.1002/hyp.9740>.

Lelieveld, J., Hadjinicolaou, P., Kostopoulou, E., Chenoweth, J., El Maayer, M., Giannakopoulos, C., Hannides, C., Lange, M.A., Tanarhte, M., Tyrlis, E. and Xoplaki, E. (2012). Climate change and impacts in the Eastern Mediterranean and the Middle East. *Clim. Chang.*, 114, 667–687. doi: 10.1007/s10584-012-0418-4.

Levison, D.H. and Waple, A.M. (2004). State of the climate in 2003. *Bull. Am. Meteorol. Soc.*, 85, S1–S72. doi: 10.1175/BAMS-85-6-Levinson.

Liu, Z., Lu, G., He, H., Wu, Z. and He, J. (2017). Anomalous Features of Water Vapor Transport during Severe Summer and Early Fall Droughts in Southwest China. *Water*, 9, 244. <https://doi.org/10.3390/w9040244>.

Lloyd-Hughes, B. (2013). The impracticality of a universal drought definition. *Theor. Appl. Climatol.*, 117(3-4), 607–611. doi:10.1007/s00704-013-1025-7.

Luterbacher, J., Dietrich, D., Xoplaki, E., Grosjean, M. and Wanner, H. (2004). European seasonal and annual temperature variability, trends, and extremes since 1500. *Science*, 303, 1499–1503. doi: 10.1126/science.1093877.

Mariotti, A., Struglia, M. V. Zeng, N. and Lau, K.M. (2002). The hydrological cycle in the Mediterranean region and implications for the water budget of the Mediterranean Sea. *J. Climate*, 15, 1674-1690. [https://doi.org/10.1175/1520-0442\(2002\)015<1674:THCITM>2.0.CO;2](https://doi.org/10.1175/1520-0442(2002)015<1674:THCITM>2.0.CO;2).

Masih, I., Maskey, S., Mussá, F. and Trambauer, P. (2014). A review of droughts on the African continent: a geospatial and long-term perspective. *Hydrol. Earth Syst. Sci.*, 18(9), 3635–3649. <https://doi.org/10.5194/hess-18-3635-2014>.

Massacand, A.C., Wernli, H. and Davies, H.C. (1998). Heavy precipitation on the alpine southside: An upper-level precursor. *Geophys. Res. Lett.*, 25(9), 1435–1438, doi:10.1029/98GL50869.

Mathbout, S., Lopez-Bustins, J.A., Martin-Vide, J., Bech, J. and Rodrigo, F.S. (2018). Spatial and temporal analysis of drought variability at several time scales in Syria during 1961–2012. *Atmos. Res.*, 200, 153–168. <https://doi.org/10.1016/j.atmosres.2017.09.016>.

Mazdiyasn, O. and AghaKouchak, A. (2015). Substantial increase in concurrent droughts and heatwaves in the United States. *Proc. Natl. Acad. Sci.*, 112(37), 11484–11489. doi:10.1073/pnas.1422945112.

McKee, T.B., Doesken, N.J. and Kleist, J. (1993). The relationship of drought frequency and duration to time scales. In: *Proceedings of the Eighth Conference on Applied Climatology*. Anaheim, CA, USA, 17–22 January, pp. 179–184.

Mdee, O.J., Kimambo, C.Z., Nielson, T.K. and Kihedu, J. (2018). Measurement methods for hydropower resources: a review. *Water Utility Journal*, 18, 21–38.

Meza, F.J. (2013). Recent trends and ENSO influence on droughts in Northern Chile: an application of the standardized precipitation evapotranspiration index. *Weather Clim. Extremes*, 1, 51–58. <https://doi.org/10.1016/j.wace.2013.07.002>

Miralles, D.G., Gentile, P., Seneviratne, S.I. and Teuling, A.J. (2018). Land–atmospheric feedbacks during droughts and heatwaves: state of the science and current challenges. *Ann. N. Y. Acad. Sci.*, Special Issue: Climate Sciences, 1–17, <https://doi.org/10.1111/nyas.13912>.

Miralles, D.G., Holmes, T.R.H., De Jeu, R.A.M., Gash, J.H., Meesters, A.G.C.A. and Dolman, A.J. (2011). Global land-surface evaporation estimated from satellite-based observations. *Hydrol. Earth Syst. Sci.*, 15, 453–469, doi: 10.5194/hess-15-453-2011.

Miralles, D.G., Teuling, A.J., Van Heerwaarden, C.C. and de Arellano, J.V-G. (2014). Mega-heatwave temperatures due to combined soil desiccation and atmospheric heat accumulation. *Nat. Geosci.*, 7, 345–349. doi: 10.1038/ngeo2141.

Mishra, A.K. and Singh, V.P. (2010). A review of drought concepts. *J. Hydrol.*, 391, 202–216. <https://doi.org/10.1016/j.jhydrol.2010.07.012>.

Nalbantis, I. and Tsakiris, G. (2009). Assessment of Hydrological Drought Revisited. *Water Resour. Manag.*, 23(5), 881-897. doi:10.1007/s11269-008-9305-1.

Naumann, G., Alfieri, L., Wyser, K., Mentaschi, L., Betts, R. A., Carrao, H., Spinoni, J., Vogt, J. and Feyen, L. (2018). Global changes in drought conditions under different levels of warming. *Geophys. Res. Lett.*, 45. <https://doi.org/10.1002/2017GL076521>.

Naumann, G., Spinoni, J., Vogt, J. V. and Barbosa, P. (2015). Assessment of drought damages and their uncertainties in Europe. *Environ. Res. Lett.*, 10(12), 124013. <https://doi.org/10.1088/1748-9326/10/12/124013>.

Nieto, R., Durán -Quesada, A. M., and Gimeno, L. (2010). Major sources of moisture for Antarctic ice-core sites identified through a Lagrangian approach. *Clim. Res.*, 40, 45–49, doi:10.3354/cr00842.

Nieto, R., Gimeno, L., Drumond, A. and Hernandez, E. A. (2010). Lagrangian identification of the main moisture sources and sinks affecting the Mediterranean area. *WSEAS Trans. Environ. Dev.*, 6, 1790–5079.

Nieto, R., Gimeno, L., Gallego, D. and Trigo, R. (2007). Contributions to the moisture budget of airmasses over Iceland. *Meteorol. Z.*, 16, 37–44. doi: 10.1127/0941-2948/2007/0176.

Nieto, R., Gimeno, L. and Trigo, R.M. (2006). A Lagrangian identification of major sources of Sahel moisture. *Geophys. Res. Lett.*, 33, L18707. doi:10.1029/2006GL027232.

Numaguti, A. (1999). Origin and recycling processes of precipitating water over the Eurasian continent: Experiments using an atmospheric general circulation model. *J. Geophys. Res.*, 104, 1957–1972. Doi:10.1029/1998JD200026.

Oki, T. (2005), The hydrologic cycles and global circulation, in Encyclopedia of Hydrological Sciences, edited by M. G. Anderson and J. McDonnell, pp. 13–22, John Wiley, New York.

Otkin, J.A., Svodoba, M., Hunt, E.D., Ford, T.W., Anderson, M.C., Hain, C. and Basara, B. (2017). Flash Droughts: A Review and Assessment of the Challenges Imposed by Rapid-Onset Droughts in the United States. *Bull. Amer. Meteor. Soc.*, 911-919. <https://doi.org/10.1175/BAMS-D-17-0149.1>

Palmer, W.C. (1965). Meteorological Drought. Res. Paper No.45, 58pp., Dept. of Commerce, Washington, D.C.

Paulo, A.A., Rosa, R.D. and Pereira, L.S. (2012). Climate trends and behavior of drought indices based on precipitation and evapotranspiration in Portugal. *Nat. Hazards Earth Syst. Sci.*, 12, 1481–1491. doi:10.5194/nhess-12-1481-2012.

Peixoto, J.P. and Oort, A.H. (1992), Physics of climate, 520 pp., American Institute of Physics, New York.

Potop, V. (2011). Evolution of drought severity and its impact on corn in the Republic of Moldova. *Theor. Appl. Climatol.*, 105, 1–15, doi:10.1007/s00704-011-0403-2, 2011.

Potop, V., Boroneant, C., Možný, M., Štěpánek, P. and Skalák, P. (2013). Observed spatiotemporal characteristics of drought on various time scales over the Czech Republic. *Theor Appl Climatol.*, 115, 563-581. doi:10.1007/s00704-013-0908-y.

Qian, W.H., Shan, X.L. and Zhu, Y.F. (2011). Ranking regional drought events in China for 1960–2009. *Adv. Atmos. Sci.*, 28(2), 310–321. <https://doi.org/10.1007/s00376-009-9239-4>.

Redmond, K. T. (2002). The depiction of drought: A commentary. *Bull. Amer. Meteor. Soc.*, 83, 1143–1147. [https://doi.org/10.1175/1520-0477\(2002\)0832.3.CO;2](https://doi.org/10.1175/1520-0477(2002)0832.3.CO;2).

Rozanski, K., Sonntag, C. and Munnich, K. (1982). Factors controlling stable isotope composition of European precipitation. *Tellus*, 34(2), 142–150, [doi:10.1111/j.2153-3490.1982.tb01801.x](https://doi.org/10.1111/j.2153-3490.1982.tb01801.x).

Salah, Z., Nieto, R., Drumond, A., Gimeno, L. and Vicente-Serrano, S.M. (2018). A Lagrangian analysis of the moisture budget over the Fertile Crescent during two intense drought episodes. *J. Hydrol.*, 560, 382–395. <https://doi.org/10.1016/j.jhydrol.2018.03.021>

Salati, E., Dall'Olio, A., Matsui, E. and Gat, J.R. (1979). Recycling of water in the Amazon basin: An isotopic study. *Water Resour. Res.*, 15(5), 1250–1258, [doi:10.1029/WR015i005p01250](https://doi.org/10.1029/WR015i005p01250).

Schicker, I., Radanovics, R. and Seibert, P. (2010). Origin and transport of Mediterranean moisture and air. *Atmos. Chem. Phys.*, 10, 5089–5105. [doi:10.5194/acp-10-5089-2010](https://doi.org/10.5194/acp-10-5089-2010).

Seneviratne, S.I. et al. (2012). Changes in Climate Extremes and their Impacts on the Natural Physical Environment. In *Managing the Risks of Extreme Events and Disasters to Advance Climate Change Adaptation*. C.B. Field et al., Eds.: 109–230. Cambridge University Press.

Seneviratne, S. I., Lüthi, D., Litschi, M. and Schär, C. (2006). Land– atmosphere coupling and climate change in Europe. *Nature*, 443, 205–209. [doi: 10.1038/nature05095](https://doi.org/10.1038/nature05095).

Sheffield, J. and Wood, E. F. (2008). Projected changes in drought occurrence under future global warming from multimodel, multi-scenario, IPCC AR4 simulations. *Clim. Dynam.*, 31(1), 79–105. <https://doi.org/10.1007/s00382-007-0340-z>.

Sheffield, J., Wood, E. F. and Roderick, M. L. (2012). Little change in global drought over the past 60 years. *Nature*, 491(7424), 435–438. <https://doi.org/10.1038/nature11575>.

Smakhtin, V.U. and Schipper, E.L. (2008). Droughts: the impact of semantics and perceptions. *Water Policy*, 10, 131-143. <https://doi.org/10.2166/wp.2008.036>.

Sodemann, H., Schwierz, C. and Wernli, H. (2008). Interannual variability of Greenland winter precipitation sources: Lagrangian moisture diagnostic and North Atlantic Oscillation influence, *J. Geophys. Res.*, 113, D03107, doi: 10.1029/2007JD008503.

Sodemann, H. and Zubler, E. (2010). Seasonal and inter-annual variability of the moisture sources for Alpine precipitation during 1995–2002. *Int. J. Climatol.*, 30, 947–961. doi: 10.1002/joc.1932.

Solomon, S., Qin, D., Manning, M., Chen, Z., Marquis, M., Averyt, K., et al. (Eds.) (2007). *Climate change 2007 - The physical science basis*, Working Group I Contribution to the Fourth Assessment Report of the IPCC (pp. 996). Cambridge, UK: Cambridge University Press.

Sordo-Ward, A., Dolores Bejarano, M., Iglesias, A., Asenjo, V. and Garrote, L. (2017). Analysis of Current and Future SPEI Droughts in the La Plata Basin Based on Results from the Regional Eta Climate Model. *Water*, 9(11), 857 <https://doi.org/10.3390/w9110857>.

Sorí, R., Marengo, J., Nieto, R., Drumond, A. and Gimeno, L. (2018). The Atmospheric Branch of the Hydrological Cycle over the Negro and Madeira River Basins in the Amazon Region, *Water*, 10(6), 738. <https://doi.org/10.3390/w10060738>

Sori, R., Nieto, R., Vicente-Serrano, S.M., Drumond, A. and Gimeno, L. (2017). A Lagrangian perspective of the hydrological cycle in the Congo River Basin. *Earth Syst. Dyn.*, 2017, 8, 653–675. <https://doi.org/10.5194/esd-8-653-2017>.

Spinoni, J., Antofie, T., Barbosa, P., Bihari, Z., Lakatos, M., Szalai, S., Szentimrey, T. and Vogt, J. (2013). An overview of drought events in the Carpathian Region in 1961–2010. *Adv. Sci. Res.*, 10(1), 21 – 32. <https://doi.org/10.5194/asr-10-21-2013>.

Spinoni, J., Lakatos, M., Szentimrey, T., Bihari, Z., Szalai, S., Vogt, J. and Antofie, T. (2015a). Heat and cold waves trends in the Carpathian region from 1961 to 2010. *Int. J. Climatol.*, 35(14), 4197 – 4209. doi: 10.1002/joc.4279.

Spinoni, J., Naumann, G., Carrao, H., Barbosa, P. and Vogt, J. (2014). World drought frequency, duration, and severity for 1951–2010. *Int. J. Climatol.*, 34, 2792–2804. <https://doi.org/10.1002/joc.3875>.

Spinoni, J., Naumann, G., Vogt, J. and Barbosa, P. (2016). Meteorological droughts in Europe: events and impacts—past trends and future projections. Publications Office of the European Union, Luxembourg, EUR 27748 EN. doi: 10.2788/450449.

Starr, V.P. and Peixoto, J.P. (1958). On the global balance of water vapor and the hydrology of deserts. *Tellus*, 10(2), 188–194, doi:10.1111/j.2153-3490.1958.tb02004.x.

Stohl, A., Forster, C., Eckhardt, S., Spichtinger, N., Huntrieser, H., Heland, J., Schlager, H., Wilhelm, S., Arnold, F. and Cooper, O. (2003). A backward modeling study of intercontinental pollution transport using aircraft measurements. *J. Geophys. Res. Atmos.*, 108, 4370. <https://doi.org/10.1029/2002JD002862>.

Stohl A. and James, P. (2004). A Lagrangian analysis of the atmospheric branch of the global water cycle. Part I: Method description, validation, and demonstration for the August 2002 flooding in central Europe. *J. Hydrometeorol.*, 5, 656–678. doi:10.1175/1525-7541(2004)005<0656: ALAOTA>2.0.CO;2.

Stohl, A. and James, P. (2005). A Lagrangian analysis of the atmospheric branch of the global water cycle. Part II: Moisture transports between the Earth's ocean basins and river catchments. *J. Hydrometeorol.*, 6, 961–984. <https://doi.org/10.1175/JHM470.1>.

Stohl, A., and Seibert, P. (1998). Accuracy of trajectories as determined from the conservation of meteorological tracers. *Q. J. R. Meteorol. Soc.*, 124, 1465-1484. doi: 10.1002/qj.49712454907.

Stojanovic, M., Drumond, A., Nieto, R. and Gimeno, L. (2017). Moisture Transport Anomalies over the Danube River Basin during Two Drought Events: A Lagrangian Analysis. *Atmosphere*, 8, 193. <https://doi.org/10.3390/atmos8100193>.

Tallaksen, L.M. and Van Lanen, H.A. (2004). Hydrological Drought: Processes and Estimation Methods for Streamflow and Groundwater. Vol. 48, Elsevier, Amsterdam.

Tan, C., Yang, J. and Li, M. (2015). Temporal-Spatial Variation of Drought Indicated by SPI and SPEI in Ningxia Hui Autonomous Region, China. *Atmosphere*, 6, 1399–1421. <https://doi.org/10.3390/atmos6101399>.

Touma, D., Ashfaq, M., Nayak, M. A., Kao, S-C. and Diffenbaugh, N. S. (2015). A multi-model and multi-index evaluation of drought characteristics in the 21st century. *J. Hydrol.*, 526, 196–207. <https://doi.org/10.1016/j.jhydrol.2014.12.011>.

Trenberth, K.E. (2011). Changes in precipitation with climate change. *Clim. Res.*, 47 (1), 123. doi: 10.3354/cr00953.

Trenberth, K. E., Dai, A., Van Der Schrier, G., Jones, P. D., Barichivich, J., Briffa, K. R. and Sheffield, J. (2014). Global warming and changes in drought. *Nature Clim. Change*, 4(1), 17–22. <https://doi.org/10.1038/nclimate2067>.

Trenberth, K.E. and Guillemot, C.J. (1998). Evaluation of the atmospheric moisture and hydro-logical cycle in the NCEP/NCAR reanalysis. *Clim. Dynam.*, 14, 213–231. <http://dx.doi.org/10.1007/s003820050219>.

Trenberth, K.E., Fasullo, J.T. and Shepherd, T.G. (2015). Attribution of climate extreme events. *Nature Clim. Change* 5, 725–730. doi: 10.1038/nclimate2657.

Trigo, R.M., Anel, J., Barriopedro, D., Garcia-Herrera, R., Gimeno L., Nieto, R., Castillo, R., Allen, M.R. and Massey, N. (2013). The record winter drought of 2011–12 in the Iberian Peninsula, in explaining extreme events of 2012 from a climate perspective. *Bull. Amer. Meteor. Soc.*, 94(9), S41–S45.

Tsakiris, G., and Vangelis, H. (2005). Establishing a drought index incorporating evapotranspiration. *European Water.*, 9(10), 3–11.

Tsiourtis, N. X. (2001). Drought management plans for the Mediterranean region. Report of the Water Development Department, Nicosia, Cyprus.

Vázquez, M., Nieto, R., Drumond, A. and Gimeno, L. (2017). Extreme Sea Ice Loss over the Arctic: An Analysis Based on Anomalous Moisture Transport. *Atmosphere*, 8, 32. doi: 10.3390/atmos8020032.

Vicente-Serrano, S.M., Aguilar, E., Martínez, R., Martín-Hernández, N., Azorin-Molina, C., Sanchez-Lorenzo, A., El Kenawy, A., Tomás-Burguera, M., Moran-Tejeda, E., López-Moreno, J.I., Revuelto, J., Beguería, S., Nieto, J.J., Drumond, A., Gimeno, L. and Nieto, R. (2016). The Complex influence of ENSO on droughts in Ecuador. *Clim. Dyn.*, 48, 405–427. doi: 10.1007/s00382-016-3082-y.

Vicente-Serrano, S.M., Beguería, S., Lorenzo-Lacruz, J., Camarero, J.J., López-Moreno, J.I., Azorin-Molina, C., Revuelto, J., Morán-Tejeda, E. and Sanchez-Lorenzo, A. (2012). Performance of Drought Indices for Ecological, Agricultural, and Hydrological Applications. *Earth Interact.*, 16, 1–27. <https://doi.org/10.1175/2012EI000434.1>.

Vicente-Serrano, S. M., Lopez-Moreno, J. I., Beguería, S., Lorenzo-Lacruz, J., Sanchez-Lorenzo, A., García-Ruiz, J. M., Azorin-Molina, C., Morán-Tejeda, E., Revuelto, J., Trigo, R., Coelho, F. and Espejo, F. (2014). Evidence of increasing drought severity caused by temperature rise in southern Europe. *Environ. Res. Lett.*, 9(4), 044001. <https://doi.org/10.1088/1748-9326/9/4/044001>.

Vicente-Serrano, S.M., Beguería, S., and López-Moreno, J.I. (2010a). A Multiscalar Drought Index Sensitive to Global Warming: The Standardized Precipitation Evapotranspiration Index. *J. Climate*, 23, 1696–1718. <https://doi.org/10.1175/2009JCLI2909.1>.

Vicente-Serrano, S.M., Beguería, S., López-Moreno, J.I., Angulo, M. and El Kenawy, A. (2010b). A new global 0.5° gridded dataset (1901-2006) of a multiscalar drought index: comparison with current drought index datasets based on the Palmer Drought Severity Index. *J. Hydrometeorol.*, 11: 1033–1043. doi: 10.1175/2010JHM1224.1.

Vicente-Serrano, S.M., Van der Schrier, G., Beguería, S., Azorin-Molina, C. and Lopez-Moreno, J.I. (2015). Contribution of precipitation and reference evapotranspiration to drought indices under different climates. *J. Hydrol.*, 426, 42–54. <https://doi.org/10.1016/j.jhydrol.2014.11.025>.

Wang, R., Peng, W., Liu, X., Wu, W., Chen, X. and Zhang, S. (2018). Responses of Water Level in China's Largest Freshwater Lake to the Meteorological Drought Index (SPEI) in the Past Five Decades. *Water*, 10, 137. <https://doi.org/10.3390/w10020137>.

Wang, Z., Li, J., Lai, C., Zeng, Z., Zhong, R., Chen, X., Zhou, X. and Wang, M. (2017). Does drought in China show a significant decreasing trend from 1961 to 2009? *Sci. Total Environ.*, 579, 314–324. <https://doi.org/10.1016/j.scitotenv.2016.11.098>.

Wells, N., Goddard, S. and Hayes, M.J. (2004). A self-calibrating Palmer Drought Severity Index. *J. Clim.*, 17, 2335-2351. [https://doi.org/10.1175/1520-0442\(2004\)017<2335:ASPDSI>2.0.CO;2](https://doi.org/10.1175/1520-0442(2004)017<2335:ASPDSI>2.0.CO;2).

Wernli, H. (1997). A lagrangian-based analysis of extratropical cyclones, II: A detailed case study. *Q. J. R. Meteorol. Soc.*, 123(542), 1677-1706, doi:10.1002/qj.49712354211.

Wilhite, D. A. (1993), Understanding the phenomenon of drought, *Hydro Rev.*, 12(5), 136 – 148.

Wilhite, D. A. and Glantz, M. H. (1985) Understanding the drought phenomenon: The role of definitions. *Water Int.*, 10, 111–120. doi.org/10.1080/02508068508686328.

Wilhite, D. A. (2000). Drought as a natural hazard: Concepts and definitions. *Drought: A Global Assessment*, D. A. Wilhite, Ed., Routledge, 3-18.

Wilhite, D.A., Sivakumar M.V.K. and Pulwarty, R. (2014). Managing drought risk in a changing climate: The role of national drought policy. *Weather Clim. Extrem.*, 3, 4–13. <https://doi.org/10.1016/j.wace.2014.01.002>.

Wilks, D. S. (2006). Statistical methods in the atmospheric sciences, in: no. v. 91 in International geophysics series, 2nd Edn., Academic Press, Amsterdam, Boston, 2006.

WMO, 2006: Drought Monitoring and Early Warning: Concepts, Progress, and Future Challenges (D. Wilhite). Pub. No 1006. Geneva, Switzerland 26 pp. Available online at <http://www.wamis.org/agm/pubs/brochures/WMO1006e.pdf>.

WMO Report 385. International Glossary of Hydrology. 2012. ISBN 978-92-63-03385-8.

Yu, L., Jin, X. and Weller, R.A. (2008). Multidecade global flux datasets from the objectively analyzed air-sea fluxes (OAFlux) Project: Latent and sensible heat fluxes,

ocean evaporation, and related surface meteorological variables OAFflux Project Tech. Rep. OA-2008-01, 64 pp., Woods Hole Oceanographic Institution, Woods Hole, Mass.

Yu, M., Li, Q., Hayes, M.J., Svoboda, M. D. and Heim, R. R. (2013). Are droughts becoming more frequent or severe in China based on the Standardized Precipitation Evapotranspiration Index: 1951–2010? *Int. J. Climatol.*, 34, 545-558. doi:10.1002/joc.3701.

Zar, J.H. (1972). Significance testing of the Spearman rank correlation. *J. Am. Stat. Assoc.*, 67, 578–580. doi: 10.1080/01621459.1972.10481251.

Zargar, A., Sadiq, R., Naser, B. and Khan, F.I. (2011). A review of drought indices. *Environ. Rev.*, 19 333–49. <https://doi.org/10.1139/a11-013>.

Zhao, T. and Dai, A. (2016). Uncertainties in historical changes and future projections of drought. Part II: model-simulated historical and future drought changes. *Clim. Change*, 144(3), 535–548. <https://doi.org/10.1007/s10584-016-1742-x>.

Zscheischler, J. and Seneviratne, S.I. (2017). Dependence of drivers affects risks associated with compound events. *Sci. Adv.*, 3, e1700 263. doi: 10.1126/sciadv.1700263.

Zscheischler, J., Westra, S., van den Hurk, B. J. J.M., Seneviratne, S.I., Ward, P.J., Pitman, A., AghaKouchak, A., Bresch, D.N., Leonard, M., Wahl, T. and Zhang, X. (2018). Future climate risk from compound events, *Nat. Clim. Change*, 8, 469–477, <https://doi.org/10.1038/s41558-25018-0156-3>.